

**STUDY OF RELATION BETWEEN ENVIRONMENT AND
INTENSITY OF TROPICAL CYCLONES FORMED IN THE BAY
OF BENGAL DURING 2000-2011**

*A dissertation submitted to the Department of Physics,
Bangladesh University of Engineering and Technology (BUET), Dhaka in
partial fulfillment of the requirements for the degree of
MASTER OF PHILOSOPHY IN PHYSICS*

Submitted by

Suman Saha

Roll No.: 0412143018F

Session: April/2012



DEPARTMENT OF PHYSICS

**BANGLADESH UNIVERSITY OF ENGINEERING AND
TECHNOLOGY (BUET), DHAKA-1000, BANGLADESH**

October, 2016

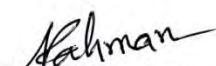
BANGLADESH UNIVERSITY OF ENGINEERING AND TECHNOLOGY, DHAKA
DEPARTMENT OF PHYSICS

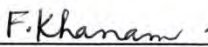



CERTIFICATION OF THESIS

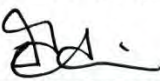
The thesis titled “STUDY OF RELATION BETWEEN ENVIRONMENT AND INTENSITY OF TROPICAL CYCLONES FORMED IN THE BAY OF BENGAL DURING 2000-2011”, submitted by **Suman Saha**, Roll No: 0412143018F Session: **April/2012**, has been accepted as satisfactory in partial fulfillment of the requirement for the degree of **Master of Philosophy (M.Phil.) in Physics** on **18 October, 2016**.


BOARD OF EXAMINERS

1. 

Dr. Nasreen Akter
Associate Professor
Department of Physics, BUET, Dhaka.
(Supervisor) **Chairman**
2. 

Prof. Fahima Khanam
Head
Department of Physics, BUET, Dhaka. **Member (Ex-Officio)**
3. 

Dr. Md. Abu Hashan Bhuiyan
Professor
Department of Physics, BUET, Dhaka. **Member**
4. 

Dr. Md. Rafi Uddin
Professor
Department of Physics, BUET, Dhaka. **Member**
5. 

Mrs. Mehrun Nessa
Chief Scientific Officer (CSO), SPARRSO
Ministry of Defence, Mohakash Biggyan Bhaban
Agargaon, Sher-E-Bangla Negar, Dhaka. **Member (External)**

Dedicated
To
My Beloved Parents

CONTENTS

	Page No.
List of Table	viii
List of Figures	ix
Abbreviations	xvii
Acknowledgement	xviii
Abstract	xix
CHAPTER 1: INTRODUCTION	1-4
1.1 Prelude	1
1.2 Objectives of the Research	4
CHPATER 2: LITERATURE REVIEW	5-39
2.1 Previous Work	5
2.2 Overview of the Study	8
2.2.1 Cyclone	8
2.2.2 Detail of Tropical Cyclone	9
2.2.2.1 Understanding of Tropical Cyclone	9
2.2.2.2 Tropical Cyclone Basins	10
2.2.2.2.1 North Indian Ocean	10
2.2.2.2.2 Arabian Sea	11
2.2.2.2.3 Bay of Bengal	11
2.2.2.3 Classifications of Tropical Cyclone Intensity	12
2.2.2.4 Physical Structure of Tropical Cyclone	14
2.2.2.4.1 Wind Field	14
2.2.2.4.2 Eye and Center	15
2.2.2.5 Formation Process of Cyclone	17
2.2.2.5.1 Secondary Circulation	17
2.2.2.5.2 Primary Circulation	18
2.2.2.6 Required Environment for the Formation of cyclone	20
2.2.2.7 Movement and Dissipation of Tropical Cyclone	22
2.2.2.8 Observation and Forecasting of TC	23
2.2.3 Environmental Parameters	26
2.2.3.1 Dynamic Parameters	26
2.2.3.1.1 Vertical Wind Shear (VWS)	26
2.2.3.1.2 Relative vorticity	27

2.2.3.1.3 Divergence	29
2.2.3.1.4 Moisture Flux	30
2.2.3.2 Thermodynamic Parameters	32
2.2.3.2.1 Relative Humidity	32
2.2.3.2.2 Sea Surface Temperature	33
2.2.3.2.3 Convective Available Potential Energy	34
2.2.3.2.4 Convective Inhibition (CIN)	35
2.2.3.2.5 Geopotential Height	37
2.2.3.2.6 Mean Sea Level Pressure (MSLP)	38
CHAPTER 3: DATA AND METHODOLOGY	40-59
3.1 Data Sources	40
3.2 Study Area	43
3.3 Scale Used for Cyclone Intensity	44
3.4 Cyclones in the study periods	45
3.5 Used Environmental Data	57
3.6 Study Method	58
3.6.1 Environmental Data collection Method	59
3.6.2 Grid Analysis and Display System (GrADS)	59
CHAPTER 4: RESULTS & DISCUSSION	60-155
4.1 Dynamic parameters	60-96
4.1.1 Low level relative vorticity	60
4.1.2 Mid-tropospheric relative vorticity	70
4.1.3 Low level vertical wind shear	79
4.1.4 Low level moisture flux	88
4.2 Thermodynamic parameters	97-155
4.2.1 Mid-tropospheric relative humidity	97
4.2.2 Convective available potential energy	105
4.2.3 Convective inhibition	114

4.2.4 Precipitable water	122
4.2.5 Sea surface temperature	130
4.2.6 Geopotential Thickness	138
4.2.7 Mean sea level pressure	146

CHAPTER 5: CONCLUSIONS **156-159**

REFERENCES **160-166**

List of Tables

No.	Captions	Page No.
Table 1.	Tropical cyclone classifications	13
Table 2.	Tropical Cyclone Intensity Scale according to IMD	44
Table 3.	Summary of studied Cyclones information	56
Table 4.	Characteristic of low level relative vorticity for pre- monsoon cyclones	64
Table 5.	Characteristic of low level relative vorticity for post- monsoon cyclones	68
Table 6.	Characteristic of mid-trosposhperic relative vorticity for pre- monsoon cyclones	74
Table 7.	Characteristics of mid-tropospheric relative vorticity for post- monsoon cyclones	77
Table 8.	Characteristics of low level VWS for pre-monsoon cyclones	83
Table 9.	Characteristic of low level VWS for post-monsoon cyclones	86
Table 10.	Characteristic of low level moisture flux for pre-monsoon Cyclones	91
Table 11.	Characteristic of low level moisture flux for post-monsoon Cyclones	95
Table 12.	Characteristic of mid-tropospheric relative humidity for pre- monsoon cyclones	100
Table 13.	Characteristic of mid-tropospheric relative humidity for post- monsoon cyclones	103
Table 14.	Characteristic of CAPE for pre-monsoon cyclones	108
Table 15.	Characteristic of CAPE for post-monsoon cyclones	112
Table 16.	Characteristic of CIN for pre-monsoon cyclones	117
Table 17.	Characteristic of CIN for post-monsoon cyclones	120
Table 18.	Characteristic of PW for pre-monsoon cyclones	125

Table 19. Characteristic of PW for post-monsoon cyclones	128
Table 20. Characteristic of SST for pre-monsoon cyclones	133
Table 21. Characteristic of SST for post-monsoon cyclones	136
Table 22. Characteristic of geopotential thickness for pre-monsoon Cyclones	141
Table 23. Characteristic of geopotential thickness for post-monsoon Cyclones	144
Table 24. Characteristic of MSLP for pre-monsoon cyclones	150
Table 25. Characteristic of MSLP for post-monsoon cyclones	153

List of Figures

No.	Captions	Page No.
Fig 1.1.	Location of the Bay of Bengal	02
Fig 2.1.	Tropical Cyclone basins	10
Fig 2.2.	Location of Indian Ocean	11
Fig 2.3.	Tropical cyclone formation over the Bay of Bengal during 1990–2009	12
Fig 2.4.	Schematic view of a typical tropical cyclone	14
Fig 2.5.	A cross section diagram of a mature tropical cyclone	16
Fig 2.6.	Overturning circulation of tropical cyclone	18
Fig 2.7.	Waves in the trade winds	22
Fig 2.8.	Radar and satellite image tropical cyclone	24
Fig 2.9.	Forecast track of tropical cyclone (Sidr)	25
Fig 2.10.	Height (m) vs mean wind speed (m/s) graph	26

Fig 2.11. Effects of VWS on Tropical Cyclone	27
Fig 2.12. Earth vorticity	28
Fig 2.13. Cyclonic and anticyclonic phase of vorticity	29
Fig 2.14. Convergence and Divergence process of tropical Cyclone	30
Fig 2.15. Surface moisture flux Convergence over NIO	31
Fig 2.16. Relationship between relative humidity and the humidity Parameter	32
Fig 2.17. Seasonal peaks of tropical cyclone activity worldwide in terms of SST	33
Fig 2.18. CAPE and wind speed at height 2.25 km	35
Fig 2.19. A Skew-T thermodynamic diagram	37
Fig 2.20. 1000-700 mb thickness as first-order partial predictor	38
Fig 2.21. Typical MSLP analysis	39
Fig 3.1. Location map of study area	43
Fig 3.2. Total number of TCs over BoB during 2000-2011	45
Fig 3.3. Track of Cyclone-2004	46
Fig 3.4: Track of Cyclone Mala-2006	47
Fig 3.5. Track of Cyclone Akash-2007	48
Fig 3.6: Track of Cyclone Nargis-2008	49
Fig 3.7. Track of Cyclone Aila-2009	50
Fig 3.8. Track of Cyclone Laila-2010	51
Fig 3.9. Track of Cyclone-2000	52
Fig 3.10. Track of Cyclone Sidr-2007	53
Fig 3.11. Track of Cyclone Giri-2010	54
Fig 3.12. Track of Cyclone Thane-2011	55

Fig 3.13. Example for extracting method for environmental data	58
Fig 4.1. Spatial distribution of averaged low level relative vorticity during cyclone period of each post-monsoon cyclone	61
Fig 4.2. Relative vorticity (1000-850 hpa) for individual pre-monsoon Cyclone	62
Fig 4.3. Low level relative vorticity for pre-monsoon cyclones	63
Fig 4.4. Spatial distribution of average low level relative vorticity during cyclone period of each post-monsoon cyclone	65
Fig 4.5. Relative vorticity (1000-850hPa) for individual post-monsoon cyclone	66
Fig 4.6. Low level relative vorticity for post-monsoon cyclones	66
Fig 4.7. Average value of low level relative vorticity	69
Fig 4.8. Average increment per intensity level of relative vorticity (%) low level for all studied cyclones	69
Fig 4.9. Spatial distribution of mid level relative vorticity during cyclone period of each pre-monsoon cyclone	71
Fig 4.10. Relative vorticity for individual pre-monsoon cyclone	72
Fig 4.11. Mid-tropospheric relative vorticity for pre-monsoon cyclones	73
Fig 4.12. Spatial distribution of mid level relative vorticity during cyclone periods of each post-monsoon cyclones	75
Fig 4.13. Relative vorticity for individual post-monsoon cyclone	76
Fig 4.14. Mid-tropospheric relative vorticity for post-monsoon cyclones	76
Fig 4.15. Average value of mid level relative vorticity	78

Fig 4.16. Average increment per intensity level of relative vorticity (%) at mid level cyclone for all cyclones	78
Fig 4.17. Spatial distribution of average low level VWS during cyclone period of each pre-monsoon cyclone	80
Fig 4.18. Low level VWS for individual pre-monsoon cyclone	80
Fig 4.19. Low level VWS for pre-monsoon cyclones	82
Fig 4.20. Spatial distribution of average low level VWS during cyclone period of each post-monsoon cyclone	84
Fig 4.21. Low-level VWS for individual post-monsoon cyclone	85
Fig 4.22. Low level VWS for post-monsoon cyclones	85
Fig 4.23. Average value of low level VWS during cyclones period	87
Fig 4.24. Average increment per intensity level of VWS (%) at low level	87
Fig 4.25. Spatial distribution of average low level moisture flux during cyclone period of each cyclone	88
Fig 4.26. Low level moisture flux for individual pre-monsoon cyclone cyclone	89
Fig 4.27. Low level moisture flux for pre-monsoon cyclones	90
Fig 4.28. Spatial distribution of average low level moisture flux during cyclone period of each post-monsoon cyclone	92
Fig 4.29. Low level moisture flux for individual post-monsoon cyclones	93
Fig 4.30. Low level moisture flux for post-monsoon cyclones	93
Fig 4.31. Average value of low level moisture flux during cyclones period	96
Fig 4.32. Average increment per intensity level of moisture flux (%) at low level level	96
Fig 4.33. Spatial distribution of average mid-tropospheric relative humidity during cyclone period of each cyclone	97
Fig 4.34. Mid-tropospheric relative humidity for individual pre-monsoon cyclone	98
Fig 4.35. Mid-level relative humidity for pre-monsoon cyclones	99

Fig 4.36. Spatial distribution of average mid-tropospheric relative humidity during cyclone period of each post-monsoon cyclone	101
Fig 4.37. Mid-tropospheric relative humidity for individual post-monsoon cyclones	102
Fig 4.38. Mid-tropospheric relative humidity for post-monsoon cyclones	102
Fig 4.39. Average value of relative humidity at 500 hPa during cyclones period	104
Fig 4.40. Average increment per intensity level of relative humidity (%) at 500 hPa	105
Fig 4.41. Spatial distribution of average CAPE during cyclone period of each pre-monsoon cyclone	106
Fig 4.42. CAPE for individual pre-monsoon cyclones	107
Fig 4.43. CAPE for all pre-monsoon cyclones	108
Fig 4.44. Spatial distribution of average CAPE during cyclone period of each post-monsoon cyclone	109
Fig 4.45. CAPE for individual post-monsoon cyclones	110
Fig 4.46. CAPE for all post-monsoon cyclones	111
Fig 4.47. Average value of CAPE during cyclones period	113
Fig 4.48. Average increment per intensity level of CAPE at surface	113
Fig 4.49. Spatial distribution of average CIN during cyclone period of each pre-monsoon cyclone	114
Fig 4.50. CIN for individual each pre-monsoon cyclone	115
Fig 4.51. CIN for all post-monsoon cyclone	116
Fig 4.52. Spatial distribution of average CIN during cyclone period of each post-monsoon cyclone	118

Fig 4.53. CIN for individual post-monsoon cyclone	119
Fig 4.54. CIN for all post-monsoon cyclones	119
Fig 4.55. Average value of CIN during cyclones period	121
Fig 4.56. Average increment per intensity level of CIN (%) at surface	121
Fig 4.57. Spatial distribution of average PW during cyclone period of each pre-monsoon cyclone	123
Fig 4.58. PW for individual pre-monsoon cyclone	124
Fig 4.59. PW for all pre-monsoon cyclones	125
Fig 4.60. Spatial distribution of average PW during cyclone period of each post-monsoon cyclone	126
Fig 4.61. PW for individual post-monsoon cyclone	127
Fig 4.62. PW for all post-monsoon cyclone	128
Fig 4.63. Average value of PW during cyclones period	129
Fig 4.64. Average increment per intensity level of PW (%)	129
Fig 4.65. Spatial distribution of average SST during cyclone period of each pre-monsoon cyclone	131
Fig 4.66. SST for all individual pre-monsoon cyclones	132
Fig 4.67. SST for all pre-monsoon cyclones	133
Fig 4.68. Spatial distribution of average SST during cyclone period of each post-monsoon cyclone	134
Fig 4.69. SST for individual post-monsoon cyclones	135

Fig 4.70. SST for all post-monsoon cyclones	136
Fig 4.71. Average value of SST during cyclones period	137
Fig 4.72. Average increment per intensity level of SST (%).	137
Fig 4.73. Spatial distribution of average geopotential thickness during cyclone period of each pre-monsoon cyclone	139
Fig 4.74. Geopotential thickness (1000-200 hPa) for individual pre-monsoon cyclones	140
Fig 4.75. Geopotential thickness for all pre-monsoon cyclones	141
Fig 4.76. Spatial distribution of average geopotential thickness during cyclone period of each post-monsoon cyclone	142
Fig 4.77. Geopotential thickness for individual post-monsoon cyclone	143
Fig 4.78. Geopotential thickness for all post-monsoon cyclones	143
Fig 4.79. Average value of geopotential thickness during cyclones period	145
Fig 4.80. Average increment per intensity level of geopotential thickness (%)	146
Fig 4.81. Spatial distribution of average MSLP during cyclone period of each pre-monsoon cyclone	147
Fig 4.82. MSLP for individual pre-monsoon cyclone	148
Fig 4.83. MSLP for all pre-monsoon cyclones	149
Fig 4.84. Spatial distribution of average MSLP during cyclone period of each post-monsoon cyclone	151
Fig 4.85. MSLP for individual post-monsoon cyclone	152

Fig 4.86. MSLP for all post-monsoon cyclones	152
Fig 4.87. Average value of MSLP during cyclones period	154
Fig 4.88. Average increment per intensity level of MSLP (%)	154
Fig 4.89. Dry line for 2000-2011 during the pre-monsoon	155

Abbreviations

TC	: Tropical cyclone
NIO	: North Indian Ocean
BoB	: Bay of Bengal
IMD	: Indian Meteorological Department
VWS	: Vertical Wind Shear
RH	: Relative Humidity
CAPE	: Convective Available Potential Energy
CIN	: Convective Inhibition
PW	: Precipitable Water
SST	: Sea Surface Temperature
MSLP	: Mean Sea Level Pressure
RI	: Rapid Intensification
WISHE	: Wind Induced Surface Heat Exchange
JTWC	: Joint Typhoon Warning Center
NCEP	: National Centers for Environmental Prediction
CFSR	: Climate Forecast System Reanalysis
RTG_SST	: Real-Time Global, Sea Surface Temperature
GrADS	: Grid Analysis and Display System
Dep	: Depression
DDep	: Deep depression
CS	: Cyclonic Storm
SCS	: Severe Cyclonic Storm
VSCS	: Very Severe Cyclonic Storm
SuperSC	: Super Cyclonic Storm
R ²	: Co-efficient of Determination
MCS	: Mesoscale Convective System

Acknowledgment

All praises are due to the Almighty God who has enabled me to complete this thesis for the M.Phil. degree.

I would like to express my gratitude and appreciation to my supervisor Dr. Nasreen Akter, Associate Professor, Department of Physics, Bangladesh University of Engineering and Technology (BUET) for her guidance and fruitful criticism throughout the entire period of research works and during preparation of the manuscript of this thesis.

I am grateful to Prof. Fahima Khanam, Head, Department of Physics, Bangladesh University of Engineering and Technology (BUET) to support and to allow me to do this research. I am very much thankful to Dr. Md. Rafi Uddin, Professor, Department of Physics (BUET) for his kind cooperation and valuable suggestions about my research.

I would also like to extend my indebtedness to Assistant Professor A.T.M. Shafiul Azam, Department of Physics, Bangladesh University of Engineering and Technology (BUET), for his suggestions that helped quite a great extent in writing of this thesis.

I would like to thank Atmospheric Laboratory and Department of Physics (BUET) to provide the facilities for the study.

I express my cordial thanks to Nayan Chanda Ghosh, Mamun Ar Rahid and Josna Saha for their endless inspiration during study period.

Lastly but not the least, I express my profound gratitude to my beloved parents and my younger brother Rajan Saha Raju for their inspiration, encouragement and endless love to complete my study.

The Author

ABSTRACT

Tropical cyclones (TCs) are one of the most dangerous natural hazards which are responsible for considerable loss of life and do immense damage to property. Due to the position in the tropical region and the funnel shaped structure, Bay of Bengal (BoB) is favorable for the formation of the strongest and deadliest TCs in the world. The BoB, which is the important branch of the North Indian Ocean, is located in the northeastern part of the Indian Ocean between latitudes 5° N to 22° N and longitudes 80° E to 100° E. During the study period from 2000 to 2011, a total number of 44 active TCs were formed in the BoB, which were bimodal in distribution during pre- and post-monsoon seasons. Within these cyclones, 6 pre-monsoon cyclones named as Cyclone(2004), Mala (2006), Akash (2007), Nargis (2008), Aila (2009) and Laila (2010) and 4 post-monsoon cyclones named as Cyclone (2000), Sidr (2007), Giri (2010) and Thane (2011) were considered for this study because they have sustainable maximum wind speed of 64kt ($\geq 33\text{m/s}$) or more. The change in intensity of each TC was correlated with the environmental condition. The dynamic and thermodynamic environmental parameters, namely, relative vorticity at low level (1000-850 hPa) and mid level (850-500 hPa), low level vertical wind shear (VWS), low level moisture flux, relative humidity at 500 hPa, convective available potential energy (CAPE), convective inhibition (CIN), precipitable water (PW), sea surface temperature (SST), geopotential thickness and mean sea level pressure (MSLP) were analyzed for this purpose. Joint Typhoon Warning Center best-track data, the National Centers for Environmental Prediction Climate Forecast System Reanalysis 6-hourly data with horizontal resolution of 0.5° x 0.5° and Real-Time, Global, Sea Surface Temperature with a 0.5° x 0.5° resolution data were used in this study.

Intensity of TCs is directly related with the decrease of MSLP. In this study, MSLP was found to be decreased with an average value of 2 hPa per intensity level for pre-monsoon cyclones, whereas, it was approximately 1 hPa for post-monsoon cyclones. The values of CAPE were also noticed as decreasing with the cyclone intensity. The average decreasing values per intensity level of TC were 10% and 5%, respectively for all pre- and post-monsoon cyclones. In case of pre-monsoon cyclones CAPE and MSLP were 4.5% and 0.1% higher than in post-monsoon cyclones. The values of low

and mid- level relative vorticity, moisture flux, CIN, and geopotential thickness were found to be increased with the change of cyclone intensity and averaged increasing value per intensity level were approximately 18%, 21%, 16%, 44% and 0.07%, respectively for all pre-monsoon cyclones. For all post-monsoon cyclones the values were increased approximately 9%, 14%, 7%, 42% and 0.01%, respectively per intensity level, however, the values were almost half than that in the pre-monsoon cases. Average value of mid-tropospheric relative humidity for all cyclones was calculated more than 75%, however, no particular value was significant for the intensity of cyclones. Similarly, Precipitable water and SST remained almost constant with the change of cyclone intensity. In all cases Precipitable water values were found greater than 60 kg/m². Average value of SST was more than 26 °C for all cases and found 3 °C higher in the pre-monsoon period than that in the post-monsoon.

Chapter One

Introduction

1.1 Preamble

A tropical cyclone (TC) is a rotating, organized system of clouds and thunderstorms that originates over tropical or subtropical waters and has a closed low-level circulation. Tropical cyclones rotate counterclockwise in the Northern Hemisphere and clockwise in the Southern Hemisphere [1]. Depending on its location and strength, a tropical cyclone is referred as cyclonic storm, severe and super tropical storm. However, cyclone classification also depends on location.

In general, TC formation areas in the world are divided into seven basins in which North Indian Ocean (NIO) is one of them. It has two wings, the Arabian Sea and the Bay of Bengal (BoB). The BoB is the largest bay in the world, which is located in the northeastern part of the Indian Ocean between latitudes 5° N to 22° N and longitudes 80° E to 100° E. The location of BoB is shown in figure 1.1. Roughly, it is triangular in shape, bordered mostly by India and Sri Lanka to the west, Bangladesh to the north, and Myanmar and the Andaman and Nicobar Islands to the east. The BoB occupies an area of about 2.2 million sq km and the average depth is 2,600 m with a maximum depth of 5,258 m.

A unique feature of the BoB is the extreme variability of its physical properties. Temperature in the offshore areas, however, is warm and markedly uniform at all seasons. The mean annual temperature of the surface water is about 28° C [2]. Surface movements of the waters change direction with the seasons, the northeast monsoon (Jan-Feb) giving them a clockwise circulation, the southwest monsoon (June-Sep) a counterclockwise circulation. The southern BoB experiences the southwest monsoon in early May. The maximum annual sea surface temperature (SST) in the central BoB and the northward-propagating deep convection phase of the intraseasonal oscillations (ISOs) trigger an earlier monsoon onset in the BoB than in India. The BoB is not only significant for the Asian monsoon onset but also offers a unique setting for TC activities.



Fig 1.1: Location of the Bay of Bengal

The position of the BoB in the tropical region is suitable as a playground of tropical cyclones and as a result, several cyclonic storms hit its coastal area every year. According to global cyclone statistics, only 7% of TC occur in the North Indian Ocean, but five to six times as many occur in the BoB as in the Arabian Sea [3]. The TCs over the BoB are confined within the monsoon transition periods, with a maximum frequency in October–November and a second maximum in May. However, Cyclones occurring in the funnel shaped BoB are particularly deadly, by name Sidr (November 2007), Nargis (April 2008), Aila (May 2009) and Giri (October 2010), Phailin (October 2013) and Hudhud (October 2014) in the Bay of Bengal are recent strong, destructive storms which causes severe flooding of the densely populated low-lying coasts of Bangladesh, India, and Myanmar.

The working and maintenance of the TC is still a puzzle. Its genesis and development is being pondered by atmospheric scientists from many years. The climatological conditions under which tropical cyclone processes that are poorly understood. Cyclone formation is normally correlated with the seasonally averaged values of six parameters [4-5]: three dynamic variables (low-level relative vorticity, inverse of the tropospheric vertical wind shear, and the Coriolis parameter) and three thermodynamic variables (ocean thermal energy extending to a sufficient depth, moist static instability, and mid-tropospheric relative humidity). Variability in tropical cyclone intensity originates from two sources: internal variability and environmental interactions. Most researches on tropical cyclone intensity have focused on the interactions between tropical cyclones and the influence of their atmospheric environment. An important aspect of environmental interaction is the coupling between the storm and the underlying ocean [6].

The substantial impact of SST on the genesis and intensification of tropical cyclones has long been recognized. It is found that tropical cyclones are driven by turbulent heat fluxes from the ocean. Tropical cyclones develop only over warm oceans with SSTs of 26 °C or higher [7]. Emanuel developed a theory of the tropical cyclone intensity in which a storm is treated as a Carnot heat engine. In this theory, the maximum intensity increases rapidly for increasing SST [8].

Vertical wind shear (VWS) is one of the most important dynamical parameters of the large-scale environment related to tropical cyclone (TC) formation, as well as its structure and intensity changes [9]. It is generally believed that strong VWS is unfavorable for TC genesis and intensification [10]. TC intensity change and vertical wind shear are generally negatively correlated, indicating the overall negative effect of vertical wind shear on TC intensity. The strong, slow moving, and low latitude TCs are strongly affected by vertical wind shear in a deep layer, while the weak, fast moving, and high latitude TCs are subject to strong effect by vertical wind shear in the mid-level troposphere [11-13].

It is well observed that TC intensity directly related to the magnitude of low level tropospheric relative vorticity. Tropical cyclones form only in regions of large positive low level vorticity. The larger this low level vorticity, the greater appears the

potential for cyclone genesis [14]. The monsoon trough additionally promotes the organization of the tropical disturbances which are essential for cyclogenesis.

For cyclone formation, mid-tropospheric relative humidity greater than 65% is favorable [14]. Also Convective available potential energy (CAPE) helps to the formation of a tropical deep convection. In the BoB during the pre-monsoon season (Mar-May), the potential for convection was highest, with surface-based CAPE values of more than $2,500 \text{ J kg}^{-1}$ and during the post-monsoon (Oct-Dec) CAPE value less than $1,500 \text{ J kg}^{-1}$. Also Convective inhibition (CIN) that measures the strength of stable layer, have important effects on cyclogenesis over the BoB [14]. However, it is still unknown how these parameters relates with the cyclone intensity. To our knowledge these parameters are not yet correlated with the TC intensification in any basin including NIO.

1.2 Objectives of the Research

The objectives of this research work are to

- i. Find out the cyclone frequency from 2000 to 2011 over the BoB.
- ii. Study the positions and intensities of TCs over the BoB during pre and post monsoon.
- iii. Study the characteristics of dynamic and thermodynamics environmental parameters at different location of TC.
- iv. Analyze the relation between different environmental parameters with TC intensity change.

These results of the research work may help to draw relation how the environmental parameters are effects the intensity over the BoB. This study will help to forecast TC intensity more accurately by analyzing the pre-environmental conditions over the BoB.

Chapter Two

Literature Review

2.1 Previous Work

Tropical cyclones (TCs) are the intense atmospheric vortices that develop over the warm tropical oceans. The working and maintenance of the TC is still a puzzle. Its genesis and development is being pondered by atmospheric scientists from many years. The climatological conditions under which tropical cyclone processes that are poorly understood. There are multi-scale interactions related to TC development, motion, and structure and intensity changes. While the motion is mostly controlled by the steering flow associated with the large-scale environment, as well as the beta-gyres and the upper-tropospheric negative potential vorticity anomalies [15]. The structure and intensity changes are affected at any time by large and complex arrays of physical processes that govern the inner core structure and the interaction between the storm and both the underlying ocean and its atmospheric environment [16]. As a result, understanding and forecasting of TC structure and intensity changes are much more difficult than those TC track.

The effect of vertical wind shear (VWS) between different pressure levels on TC intensity change is statistically analyzed based on the best track data of TCs in the Western North Pacific from the Joint Typhoon Warning Center (JTWC) and the ECMWF interim reanalysis data during 1981–2013. Results show that the commonly used VWS measure between 200 and 850 hPa is less representative of the attenuating deep-layer shear effect than that between 300 and 1000 hPa. Moreover, scientist find that the low-level shear between 850 (or 700) and 1000 hPa is more negatively correlated with TC intensity change than any deep-layer shear during the active typhoon season, whereas deep-layer shear turns out to be more influential than low-level shear during the remaining less active seasons. Further analysis covering all seasons exhibits that a TC has a better chance to intensify than to decay when the deep-layer shear is lower than $7\text{--}9\text{ ms}^{-1}$ and the low-level shear is below 2.5 ms^{-1} . The

Probability for TCs to intensify and undergo rapid intensification (RI) increases with decreasing VWS and increasing SST. TCs moving at slow translational speeds (less than 3 ms^{-1}) intensify under relatively weaker VWS than TCs moving at intermediate translational speeds. The probability of RI becomes lower than that of rapid decaying when the translational speed is larger than 8 ms^{-1} . Most TCs tend to decay when the translational speed is larger than 12 m s^{-1} regardless of the shear condition [17].

A relationship between wind shear and intensity change is documented by investigating the impact of environmental wind shear on the intensity change of hurricane-strength tropical cyclones in the Australian region. Correlations between wind shear and intensity change to 36 h are of the order of 0.4. Typically a critical wind shear value of $\sim 10 \text{ ms}^{-1}$ represents a change from intensification to dissipation. Wind shear values of less than $\sim 10 \text{ ms}^{-1}$ favor intensification, with values between ~ 2 and 4 ms^{-1} favoring rapid intensification. Shear values greater than $\sim 10 \text{ ms}^{-1}$ are associated with weakening, with values greater than 12 ms^{-1} favoring rapid weakening. There appears to be a time lag between the onset of increased vertical wind shear and the onset of weakening, typically between 12 and 36 h [18].

The influence of various environmental factors on tropical cyclone intensity is explored using a simple coupled ocean–atmosphere model. It is first demonstrated that this model is capable of accurately replicating the intensity evolution of storms that move over oceans whose upper thermal structure is not far from monthly mean climatology and that are relatively unaffected by environmental wind shear. A parameterization of the effects of environmental wind shear is then developed and shown to work reasonably well in several cases for which the magnitude of the shear is relatively well known. When used for real-time forecasting guidance, the model is shown to perform better than other existing numerical models while being competitive with statistical methods. In the context of a limited number of case studies, the model is used to explore the sensitivity of storm intensity to its initialization and to a number of environmental factors, including potential intensity, storm track, wind shear, upper-ocean thermal structure, bathymetry, and land surface characteristics. All of these factors are shown to influence storm intensity, with their relative contributions varying greatly in space and time. Accurate forecasts of tropical cyclone intensity require not only good forecasts of environmental winds but good knowledge of upper-ocean thermal structure. Shear in suppressing storm intensity,

also suppresses ocean feedback; the sudden cessation of shearing can then lead to more rapid intensification and, briefly, to greater intensity than could have been reached had shear been absent altogether. The importance of tropical cyclone intensity prediction justifies the inclusion of upper-ocean temperature and salinity measurements in routine airborne reconnaissance missions [19].

A statistical model for predicting intensity changes of Atlantic tropical cyclones at 12, 24, 36, 48, and 72 h is described. The model was developed using a standard multiple regression technique with climatological, persistence, and synoptic predictors. The model developmental sample includes all of the named Atlantic tropical cyclones from 1989 to 1992. The four primary predictors are 1) the difference between the current storm intensity and an estimate of the maximum possible intensity determined from the sea surface temperature, 2) the vertical shear of the horizontal wind, 3) persistence, and 4) the flux convergence of eddy angular momentum evaluated at 200 mb. The sea surface temperature and vertical shear variables are averaged along the track of the storm during the forecast period. The sea surface temperatures along the storm track are determined from monthly climatological analyses linearly interpolated to the position and date of the storm. The vertical shear values along the track of the storm are estimated using the synoptic analysis at the beginning of the forecast period. All other predictors are evaluated at the beginning of the forecast period [20].

Determining the proper relation between the mean sea level pressure and maximum sustained winds in tropical cyclones has been a long-standing problem. The major obstacle has been the lack of sufficient ground truth i.e. actual measurements of maximum wind speeds in tropical cyclones with a wide range of central pressures. A new relationship is developed based on maximum wind observation recorded at island and coastal stations in the western north pacific area during cyclone passes during a 28-year period [21].

The intensity of tropical cyclones is sensitive to the rates at which enthalpy and momentum are transferred between sea and air in the high-wind core of the storm. When a spray droplet is ejected from the ocean, it remains airborne long enough to cool to a temperature below the local air temperature but not long enough to evaporate an appreciable fraction of its mass. The spray droplet thus gives up sensible heat and returns to the sea before it has time to extract back from the

atmosphere the heat necessary to continue its evaporation. Microphysical modeling, combined with data from the Humidity Exchange over the Sea Experiment, makes it possible to derive an expression for the net enthalpy transfer of re-entrant spray. This spray enthalpy flux is roughly cubic in wind speed. When this relation is used in a numerical simulation of a hurricane, the spray more than compensates for the observed increase in the ratio of drag and enthalpy transfer coefficients with wind speed. The momentum flux associated with sea spray is an important energy sink that moderates the effects of this spray enthalpy flux. Including a parameterization for this momentum sink along with wave drag and spray enthalpy transfer in the hurricane simulation produces results that are similar to ones based on equal transfer coefficients [22].

Little work is done on establishing relation between other environmental parameters like CAPE, CIN, Relative vorticity, moisture flux and Geopotential thickness etc with TCs intensity change rather than cyclogenesis.

From above found that, most of previous work is done on other basin like Pacific Ocean, Atlantic Ocean, very few work is done on BoB and its environment.

2.2 Overview of the Study

2.2.1 Cyclone

In meteorology, cyclone is a large-scale atmospheric wind and pressure system characterized by low pressure at its center and by circular wind motion, counterclockwise in the Northern Hemisphere, clockwise in the Southern Hemisphere [23].

Most large-scale cyclonic circulations are centered on areas of low atmospheric pressure. The largest low-pressure systems are cold-core polar cyclones and extratropical cyclones which lie on the synoptic scale. Mesocyclones, tornadoes and dust devils lie within the small mesoscale. Upper level cyclones can exist without the presence of a surface low, and can pinch off from the base of the tropical upper tropospheric trough during the summer months in the Northern Hemisphere. Cyclones have also been seen on extraterrestrial planets, such as Mars and Neptune [24]. Cyclogenesis describes the process of cyclone formation and intensification. Extratropical cyclones form as waves in large regions of enhanced

mid-latitude temperature contrasts called baroclinic zones. On the other hand, TCs form in a uniform temperature region.

2.2.2 Detail of Tropical Cyclone

2.2.2.1 Understanding of Tropical Cyclone

A TC is a rapidly rotating storm system characterized by a low-pressure center, strong winds, and a spiral arrangement of thunderstorms that produce heavy rain. The term "tropical" refers to the geographical origin of these systems, which form almost exclusively over tropical seas. The term "cyclone" refers to their cyclonic nature, with wind blowing counterclockwise in the Northern Hemisphere and clockwise in the Southern Hemisphere. The opposite direction of circulation is due to the Coriolis effect. TCs originate about 5° away from the equator. Depending on its location and strength, a TC is referred to by many other names such as in the North Atlantic and eastern North Pacific regions it is called "hurricanes", in the western North Pacific "typhoons" [25].

TCs form over large bodies of relatively warm water and usual diameter in between 100 and 4,000 km (62 and 2,485 mi). They derive their energy through the evaporation of water from the ocean surface, which ultimately recondenses into clouds and rain when moist air rises and cools to saturation. The strong rotating winds of a TCs are a result of the conservation of angular momentum imparted by the Earth's rotation as air flows inwards toward the axis of rotation. As a result, they rarely form within 5° of the equator [26]. Due to strong winds and rain, TCs are capable of generating high waves, damaging storm surge, and tornadoes. TC weaken rapidly over land where they are cut off from their primary energy source. For this reason, coastal regions are particularly vulnerable to damage from a TC as compared to inland regions. Heavy rains, however, can cause significant flooding inland, and storm surges can produce extensive coastal flooding up to 40 kilometers (25 mi) from the coastline. Though their effects on human populations are often devastating TC relieve drought conditions. They also carry heat energy away from the tropics and transport it toward temperate latitudes, which may play an important role in modulating regional and global climate.

2.2.2.2 Tropical Cyclone Basins

TC formation area are divided into seven basins shown in fig 2.1. These include the North Atlantic Ocean, the eastern and western parts of the northern Pacific Ocean, the southwestern Pacific, the southwestern and southeastern Indian Oceans, and the North Indian Ocean (Arabian Sea and Bay of Bengal).

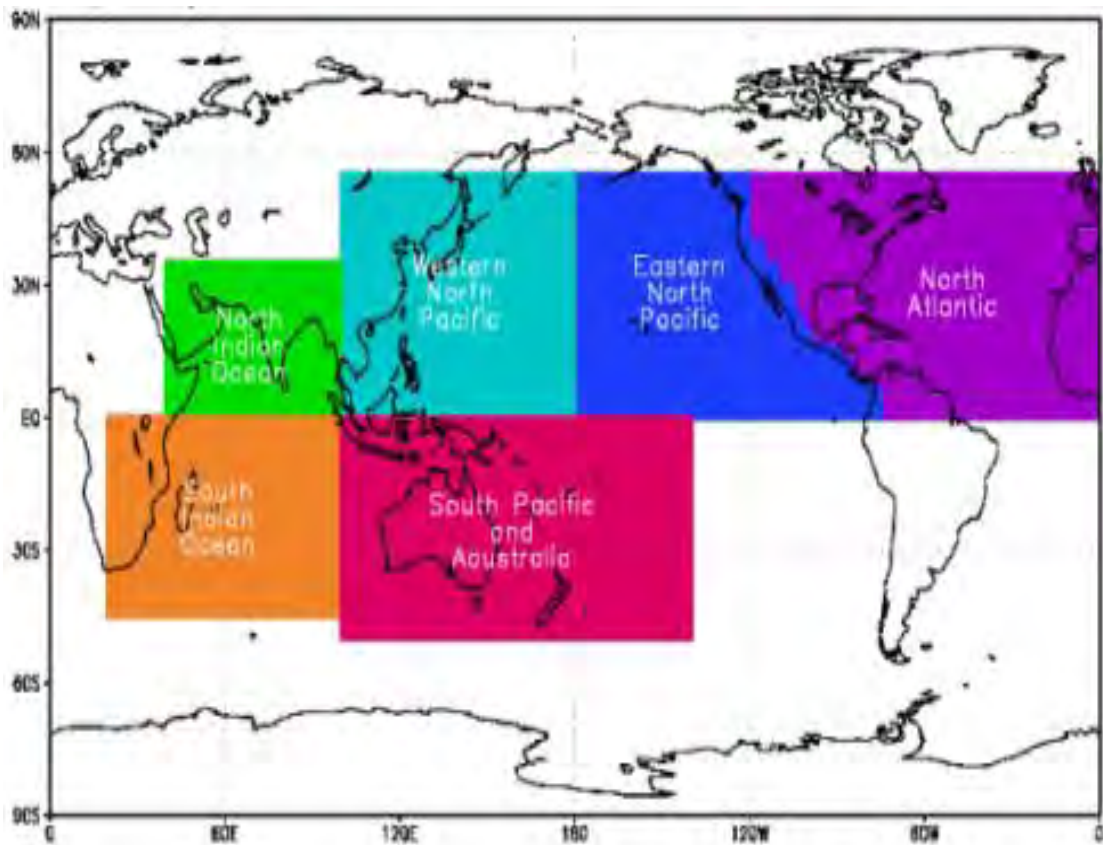


Fig 2.1: Tropical Cyclone basins [27].

2.2.2.2.1 North Indian Ocean

Figure 2.2 shows the North Indian Ocean is divided into two part: the Bay of Bengal and the Arabian Sea. This basin is the most inactive worldwide, with only 4 to 6 storms per year. This basin's season has a double peak: one in April and May, before the onset of the monsoon, and another in October and November, just after. Although it is an inactive basin, the deadliest tropical cyclones in the world have formed here.



Fig 2.2: Location of Indian Ocean [28].

2.2.2.2.2 Arabian Sea

The Arabian Sea is a sea located to the north of the Indian Ocean. The Arabian Sea's coast is shared among India, Yemen, Oman, Iran, Pakistan, Sri Lanka, Maldives and Somalia. Cyclones are very rare in the Arabian Sea, but the basin can produce strong tropical cyclones. Super Cyclonic Storm Gonu was the strongest recorded tropical cyclone in the basin.

2.2.2.2.3 Bay of Bengal

The BoB, located north of the Indian Ocean. The BoB's coast is shared among India, Bangladesh, Myanmar, Sri Lanka and western part of Thailand. In the BoB, a distinctly bimodal cyclone season is observed: March-May (pre-monsoon) and October-December (post-monsoon). Synoptic-scale movements of air toward the BoB can create environments favorable for the initiation of cyclogenesis during the pre- and post-monsoon. The primary peak in cyclone frequency over BoB is in November, and the secondary peak is in May, figure 2.3 shows the annual cyclone occurrence frequency over BoB.

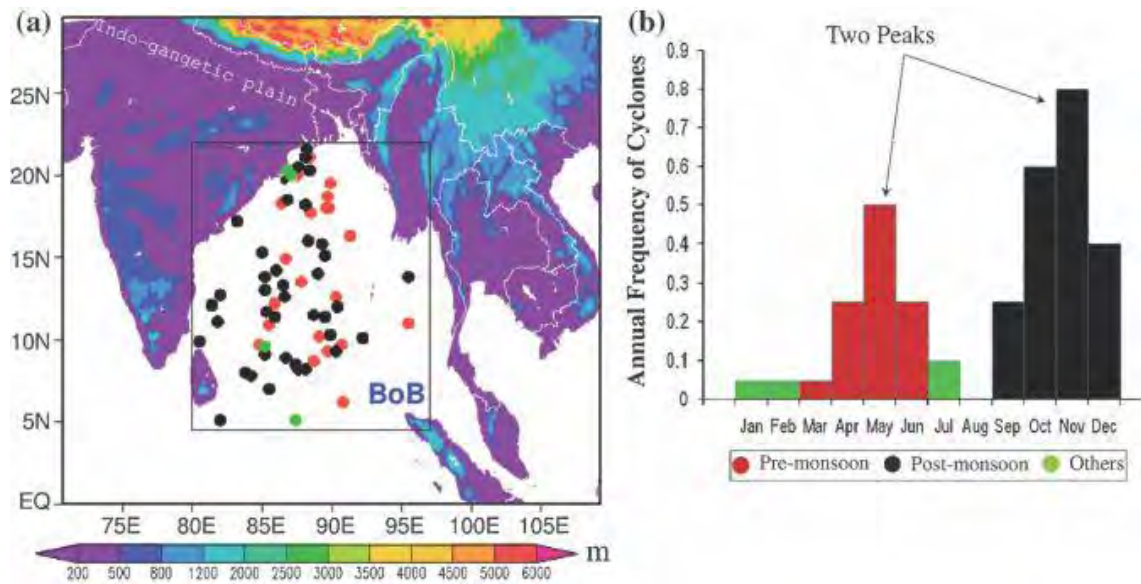


Fig 2.3: (a) Tropical cyclone formation over the Bay of Bengal (BoB) during 1990–2009 (dots): red pre- monsoon; black post-monsoon; green other. (b) Annual cyclone occurrence frequency [14].

The BoB is responsible for the formation of some of the strongest and deadliest tropical cyclones in the world. Between 100,000 and 500,000 residents of Bangladesh were killed because of the 1970 Bhola cyclone formed over the BoB [29].

2.2.2.3 Classifications of Tropical Cyclone Intensity

Tropical cyclones are classified into three main groups, based on intensity: tropical depressions, tropical storms, and a third group of more intense storms, whose name depends on the region. As indicated in the table 1, each basin uses a separate system of terminology, which can make comparisons between different basins. If a tropical storm in the Northwestern Pacific reaches hurricane-strength winds on the Beaufort scale, it is referred to as a typhoon; if a tropical storm passes the same benchmark in the Northeast Pacific Basin, or in the North Atlantic, it is called a hurricane. Neither "hurricane" nor "typhoon" is used in either the Southern Hemisphere or the Indian Ocean. In these basins, storms of a tropical nature are referred to as either tropical cyclones, severe tropical cyclones or very intense tropical cyclones.

According to the Indian Meteorological Department (IMD) Tropical cyclone scale as mentioned in table 1 tropical disturbance in the BoB are classified in to 7 categories

based on the maximum sustainable wind speed. We used IMD tropical cyclone scale for classifying tropical cyclone intensities over BoB [30-31].

Table 1: Tropical cyclone classifications [30-31].

Tropical Cyclone Classifications (all winds are 10-minute averages)									
Beaufort scale	10-minute sustained winds (knots)	N Indian Ocean IMD	SW Indian Ocean MF	Australia BOM	SW Pacific FMS	NW Pacific JMA	NW Pacific JTWC	NE Pacific & N Atlantic NHC & CPHC	
0-6	<28	Depression	Trop. Disturbance	Tropical Low	Tropical Depression	Tropical Depression	Tropical Depression	Tropical Depression	
7	28-29	Deep Depression	Depression					Tropical Storm	Tropical Storm
	30-33			Tropical Storm					
8-9	34-47	Cyclonic Storm	Moderate Tropical Storm	Trop. Cyclone (1)	Tropical Cyclone	Typhoon	Typhoon	Tropical Storm	
10	48-55	Severe Cyclonic Storm	Severe Tropical Storm	Tropical Cyclone (2)				Severe Tropical Storm	Severe Tropical Storm
11	56-63	Storm	Storm	Storm				Storm	Storm
12	64-72	Very Severe Cyclonic Storm	Tropical Cyclone	Severe Tropical Cyclone (1)	Tropical Cyclone	Typhoon	Typhoon	Hurricane (1)	
	73-85			Severe Tropical Cyclone (2)				Hurricane (2)	
	86-89			Severe Tropical Cyclone (3)				Hurricane (3)	
	90-99		Intense Tropical Cyclone	Major Hurricane (4)					
	100-106		Intense Tropical Cyclone	Major Hurricane (5)					
	107-114		Very Intense Tropical Cyclone	Super Typhoon					
	115-119		Very Intense Tropical Cyclone	Super Typhoon					
	>120	Super Cyclonic Storm	Very Intense Tropical Cyclone	Super Typhoon				Major Hurricane (5)	

2.2.2.4 Physical Structure of Tropical Cyclone

A mature TC typically consist of warm core vertical circulation, cyclonic in lower and anticyclonic in upper troposphere, with a core of intense wind and precipitation. The vertical perturbation winds upon the mean environment may extend outward well over 1000 km from the storm center. At the core there is typically an eye of 5-50 km radius with warm, calm and deep convection surrounded with eye wall. A schematic diagram of idealized mature TC is shown in fig 2.4 [32].

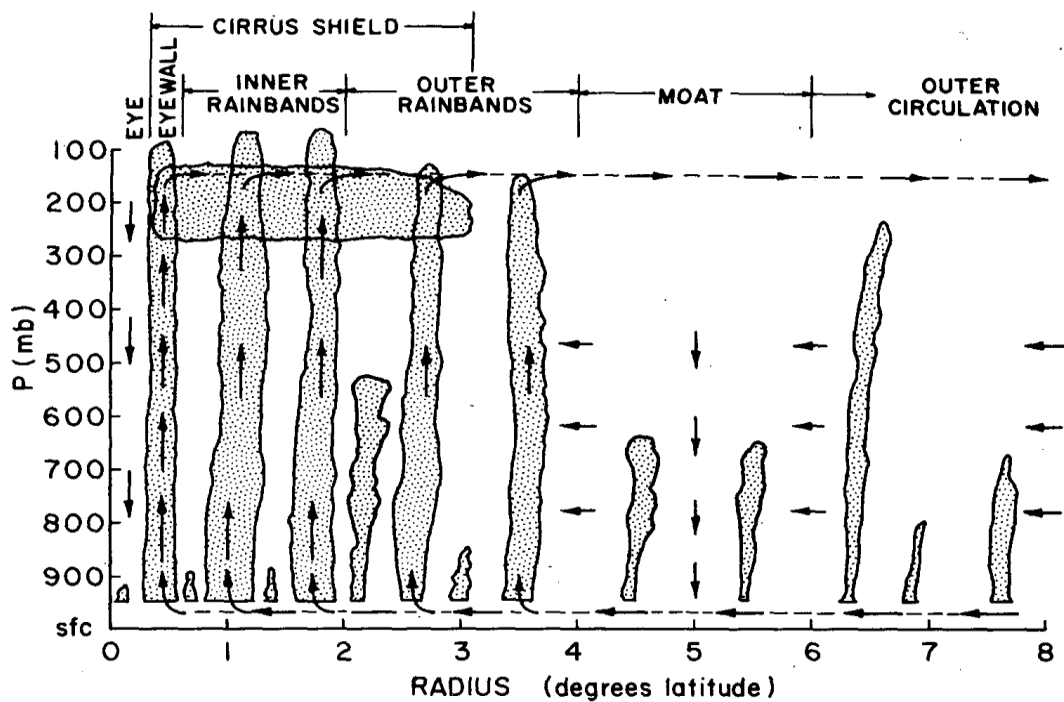


Fig 2.4: Schematic view of a typical tropical cyclone [23].

2.2.2.4.1 Wind Field

A wind field of tropical Cyclone is nearly axisymmetric. The near-surface wind field of a tropical cyclone is characterized by air rotating rapidly around a centre of circulation while also flowing radially inwards. Due to the Earth's rotation, the air has non-zero absolute angular momentum. As air flows radially inward, it begins to rotate cyclonically (counter-clockwise in the Northern Hemisphere, and clockwise in the Southern Hemisphere) in order to conserve angular momentum. At an inner radius, air begins to ascend to the top of the troposphere. This radius is typically coincident with the inner radius of the eyewall, and has the strongest near-surface winds of the storm; consequently, it is known as the radius of maximum winds [33].

Wind speeds are low at the centre, increase rapidly moving outwards to the radius of maximum winds, and then decay more gradually with radius to large radii. The wind field often exhibits additional spatial and temporal variability due to the effects of localized processes, such as thunderstorm activity and horizontal flow instabilities.

2.2.2.4.2 Eye and Center

The main parts of a tropical cyclone are the rainbands, the eye, and the eyewall. The environment near the center of tropical cyclones is warmer than the surroundings at all altitudes, thus they are characterized as "warm core" systems [34]. At the center of a mature tropical cyclone, air sinks rather than rises. For a sufficiently strong storm, air may sink over a layer deep enough to suppress cloud formation, thereby creating a clear "eye". A typical tropical cyclone will have an eye of approximately 30–65 km (20–40 mi) across, usually situated at the geometric center of the storm. Weather in the eye is normally calm and free of clouds, although the sea may be extremely violent. An eye will usually develop when the maximum sustained wind speeds go above 74 mph (119 km/h) and is the calmest part of the storm. The cause of eye formation is still not fully understood. It probably has to do with the combination of "the conservation of angular momentum" and centrifugal force. The conservation of angular momentum means is objects will spin faster as they move toward the center of circulation. So air increases its speed as it heads toward the center of the tropical cyclone. As the speed increases, an outward-directed force, called the centrifugal force, occurs because the wind's momentum wants to carry the wind in a straight line. Since the wind is turning about the center of the tropical cyclone, there is a pull outward. The sharper the curvature, and/or the faster the rotation, the stronger is the centrifugal force.

Around 74 mph (119 km/h) the strong rotation of air around the cyclone balances inflow to the center, causing air to ascend about 10-20 miles (16-32 km) from the center forming the eyewall. This strong rotation also creates a vacuum of air at the center, causing some of the air flowing out the top of the eyewall to turn inward and sink to replace the loss of air mass near the center. This sinking air suppresses cloud formation, creating a pocket of generally clear air in the center [35]. Figure 2.5 shows the cross sectional diagram of a mature tropical cyclone indicating Eye, Eyewall and rainbands position. The eyewall typically expands outward with height, resembling an

arena football stadium; this phenomenon is sometimes referred to as the stadium effect. Eyewalls are typically circular; however, distinctly polygonal shapes ranging from triangles to hexagons occasionally occur.

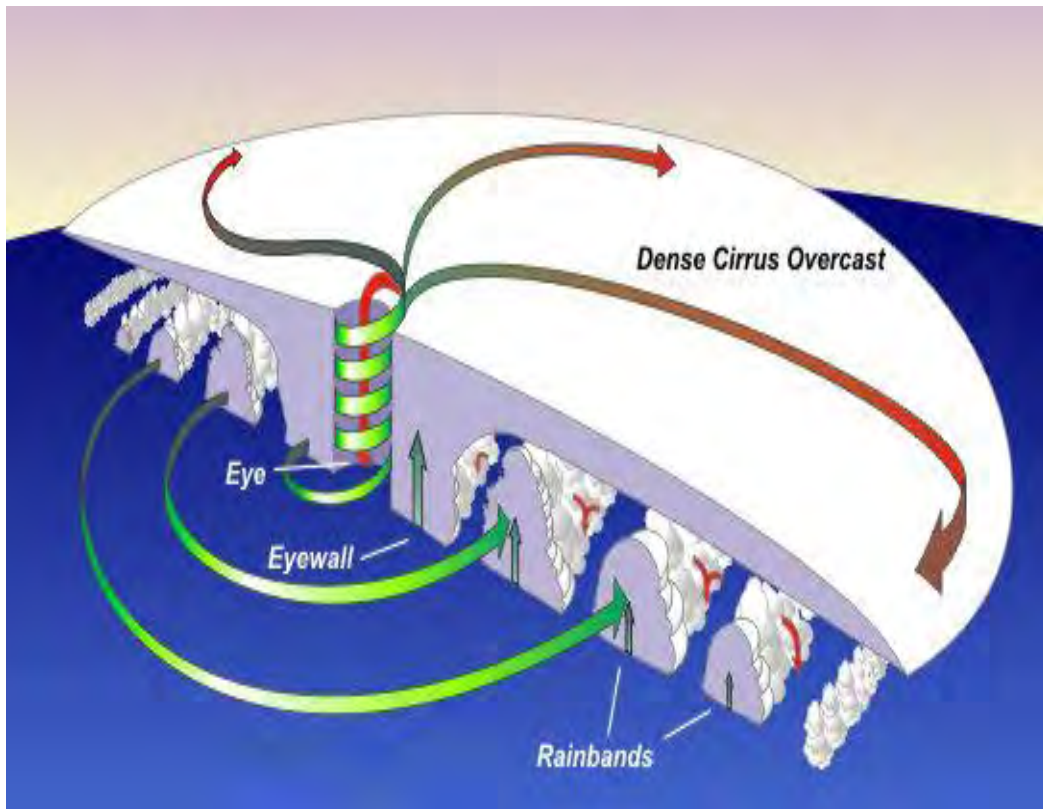


Fig 2.5: A cross section diagram of a mature tropical cyclone.

The eyewall consists of a ring of tall thunderstorms that produce heavy rains and usually the strongest winds. The heaviest wind damage occurs where a tropical cyclone's eyewall passes over land. The eyewall may vary over time in the form of eyewall replacement cycles, particularly in intense tropical cyclones. When tropical cyclone intensity become greater than 185 km/h (115 mph) and the eyewall contracts or is already sufficiently small. Some of the outer rainbands may strengthen and organize into a ring of thunderstorms-an outer eyewall-that slowly moves inward and robs the inner eyewall of its needed moisture and angular momentum. Since the strongest winds are located in a cyclone's eyewall, the tropical cyclone usually weakens during this phase, as the inner wall is "choked" by the outer wall. Eventually the outer eyewall replaces the inner one completely, and the storm can re-intensify. Eyewall mesovortices are most common during periods of intensification in tropical

cyclones. Eyewall mesovortices are a significant factor in the formation of tornadoes after tropical cyclone landfall [36].

2.2.2.5 Formation Process of Cyclone

The three-dimensional wind field in a tropical cyclone can be separated into two components: a "primary circulation" and a "secondary circulation". The primary circulation is the rotational part of the flow; it is purely circular. The secondary circulation is the overturning (in-up-out-down) part of the flow; it is in the radial and vertical directions. The primary circulation has the strongest winds and is responsible for the majority of the damage a storm causes, while the secondary circulation is slower but governs the energetics of the storm.

2.2.2.5.1 Secondary Circulation

Tropical cyclones form when the energy released by the condensation of moisture in rising air causes a positive feedback loop over warm ocean waters. A tropical cyclone's primary energy source is the evaporation of water from the ocean surface, which ultimately recondenses into clouds and rain when moist air rises and cools to saturation. The energetics of the system may be idealized as an atmospheric Carnot heat engine [37]. Figure 2.6 shows the overturning circulation of Tropical Cyclone where air inflows at low levels near the surface, rises in thunderstorm clouds, and outflows at high levels near the tropopause.

First, inflowing air near the surface acquires heat primarily via evaporation of water (i.e. latent heat) at the temperature of the warm ocean surface. Second, air rises and cools within the eyewall while conserving total heat content (latent heat is simply converted to sensible heat during condensation). Third, air outflows and loses heat via infrared radiation to space at the temperature of the cold tropopause. Finally, air subsides and warms at the outer edge of the storm while conserving total heat content. The first and third legs are nearly isothermal, while the second and fourth legs are nearly isentropic. This in-up-out-down overturning flow is known as the secondary circulation. The Carnot perspective provides an upper bound on the maximum wind speed that a storm can attain.

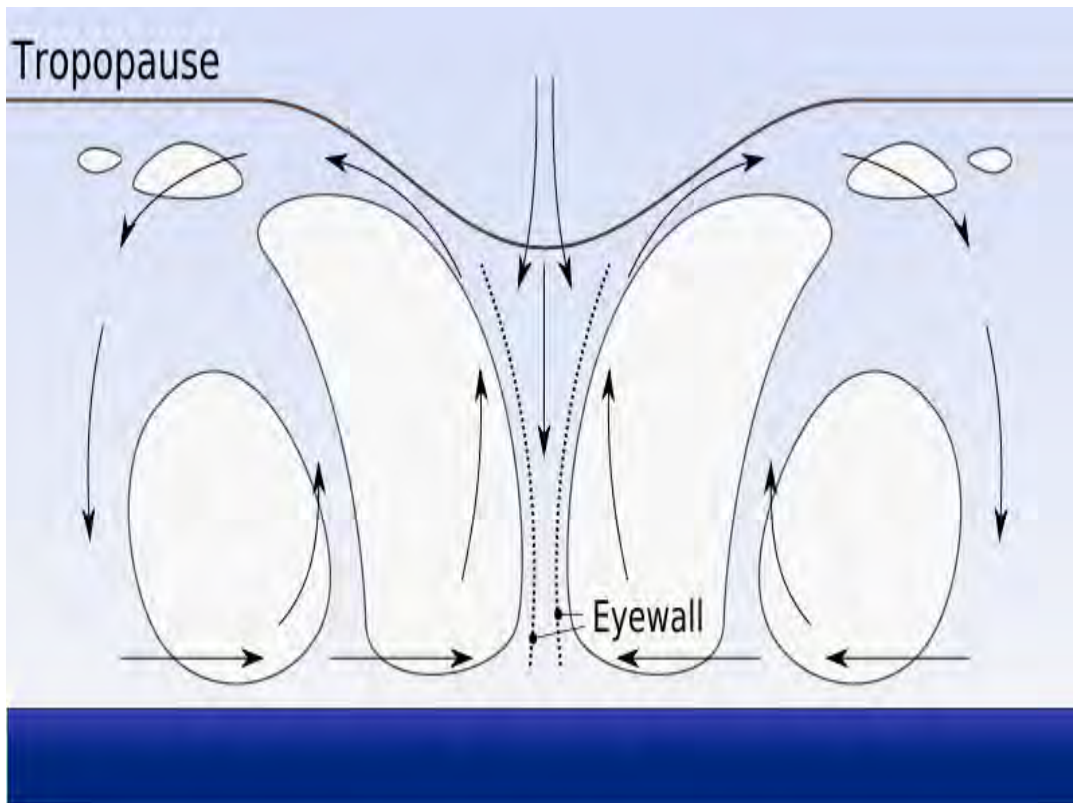


Fig 2.6: Overturning circulation of tropical cyclone [38].

Scientists estimate that a tropical cyclone releases heat energy at the rate of 50 to 200 exajoules (10^{18} J) per day, equivalent to about 1 PW (10^{15} watt). This rate of energy release is equivalent to 70 times the world energy consumption of humans and 200 times the worldwide electrical generating capacity, or to exploding a 10-megaton nuclear bomb every 20 minutes [39].

2.2.2.5.2 Primary Circulation

The primary rotating flow in a tropical cyclone results from the conservation of angular momentum by the secondary circulation. Absolute angular momentum on a rotating planet M is given by

$$M = \frac{1}{2}fr^2 + vr$$

where f is the Coriolis parameter, v is the azimuthal (i.e. rotating) wind speed, and r is the radius to the axis of rotation. The first term on the right hand side is the component of planetary angular momentum that projects onto the local vertical (i.e.

the axis of rotation). The second term on the right hand side is the relative angular momentum of the circulation itself with respect to the axis of rotation. Because the planetary angular momentum term vanishes at the equator (where $f=0$), tropical cyclones rarely form within 5° of the equator [40]. As air flows radially inward at low levels, it begins to rotate cyclonically in order to conserve angular momentum. Similarly, as rapidly rotating air flows radially outward near the tropopause, its cyclonic rotation decreases and ultimately changes sign at large enough radius, resulting in an upper-level anti-cyclone. The result is a vertical structure characterized by a strong cyclone at low levels and a strong anti-cyclone near the tropopause, this corresponds to a system that is warmer at its center than in the surrounding environment at all altitudes [41].

The inflow only partially conserves angular momentum, due to surface friction. Thus, the sea surface lower boundary acts as both a source (evaporation) and sink (friction) of energy for the system. This fact leads to the existence of a theoretical upper bound on the strongest wind speed that a tropical cyclone can attain. Because evaporation increases linearly with wind speed, there is a positive feedback on energy input into the system known as the Wind-Induced Surface Heat Exchange (WISHE) feedback. This feedback is offset when frictional dissipation, which increases with the cube of the wind speed, becomes sufficiently large. This upper bound is called the "maximum potential intensity" v_p , and is given by

$$v_p^2 = \frac{C_k T_s - T_o}{C_d T_o} \Delta k$$

Where T_s is the temperature of the sea surface, T_o is the temperature of the outflow ([K]), Δk is the enthalpy difference between the surface and the overlying air ([J/kg]), and C_k and C_d are the surface exchange coefficients (dimensionless) of enthalpy and momentum, respectively. The surface-air enthalpy difference is taken as $\Delta k = K_s^* - k$, where K_s^* is the saturation enthalpy of air at sea surface temperature and sea-level pressure and k is the enthalpy of boundary layer air overlying the surface [42].

The maximum potential intensity is predominantly a function of the background environment alone (i.e. without a tropical cyclone), and thus this quantity can be used to determine which regions on Earth can support tropical cyclones of a given intensity, and how these regions may evolve in time [43].

The passage of a tropical cyclone over the ocean causes the upper layers of the ocean to cool substantially, which can influence subsequent cyclone development. This cooling is primarily caused by wind-driven mixing of cold water from deeper in the ocean with the warm surface waters. This effect results in a negative feedback process that can inhibit further development or lead to weakening. Additional cooling may come in the form of cold water from falling raindrops (this is because the atmosphere is cooler at higher altitudes). Cloud cover may also play a role in cooling the ocean, by shielding the ocean surface from direct sunlight before and slightly after the storm passage. All these effects can combine to produce a dramatic drop in sea surface temperature over a large area in just a few days [44].

2.2.2.6 Required Environment for the Formation of Cyclone

The formation of tropical cyclones is the topic of extensive ongoing research and is still not fully understood. Seasonal tropical cyclone frequency can be directly related to a combination of six environmental parameters which will henceforth be referred to as primary genesis parameters. These parameters are:

- i. Low level relative vorticity (ζ_r)
- ii. Coriolis Parameter (**f**)
- iii. The inverse of the vertical shear S_z of the horizontal wind between the lower and upper troposphere or ($1/S_z$)
- iv. Ocean thermal energy or sea temperature above 26 o C to a depth of 60 m (**E**).
- v. Vertical gradient of θ_e between the surface and 500 mb ($\partial\theta_e / \partial p$).
- vi. Middle troposphere relative humidity (**RH**).

It will be shown that seasonal cyclone genesis frequency is well related to the adjusted seasonal magnitude of the product of these six parameters, or

$$\text{(Seasonal Genesis Frequency)} \propto (\zeta_r) \times (f) \times (1/S_z) \times (E) \times (\partial\Theta_e / \partial p) \times (RH)$$

It is believed cyclone genesis is dependent on the magnitude of all of these parameters. In most situations, water temperatures of at least 26.5 °C (79.7 °F) are needed down to a depth of at least 50 m (160 ft). Waters of this temperature cause the overlying atmosphere to be unstable enough to sustain convection and thunderstorms. Another factor is rapid cooling with height, which allows the release of the heat of condensation that powers a tropical cyclone. High humidity is needed, especially in the lower-to-mid troposphere; when there is a great deal of moisture in the atmosphere, conditions are more favorable for disturbances to develop. Low amounts of wind shear are needed, as high shear is disruptive to the storm's circulation. Tropical cyclones generally need to form more than 555 km (345 mi) or five degrees of latitude away from the equator, allowing the Coriolis effect to deflect winds blowing towards the low pressure center and creating a circulation. Lastly, a formative tropical cyclone needs a pre-existing system of disturbed weather. Tropical cyclones will not form spontaneously. Low-latitude and low-level westerly wind bursts associated with the Madden-Julian oscillation can create favorable conditions for tropical cyclogenesis by initiating tropical disturbances [4, 45].

Figure 2.7 shows the areas of converging winds that move along the same track as the prevailing wind-create instabilities in the atmosphere that may lead to the formation of cyclone.

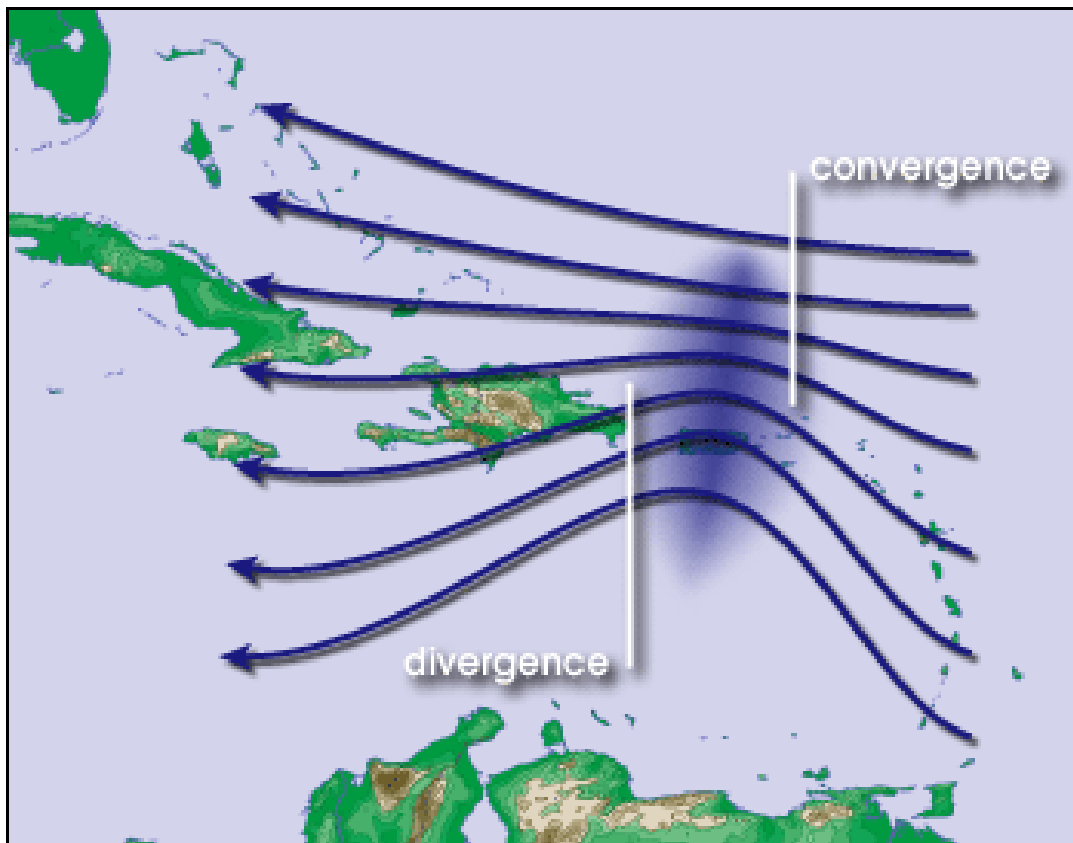


Fig 2.7: Waves in the trade winds.

2.2.2.7 Movement and Dissipation of Tropical Cyclone

The movement of a tropical cyclone (i.e. its "track") is typically approximated as the sum of two terms: "steering" by the background environmental wind and "beta drift". Environmental steering represents the movement of the storm with the background environment. The flow field in the vicinity of a tropical cyclone may be decomposed into two parts: the flow associated with the storm itself, and the large-scale background flow of the environment in which the storm is embedded. This environmental flow is termed the "steering flow". In the Indian Ocean tropical cyclogenesis is influenced the seasonal movement of the Intertropical Convergence Zone and the monsoon trough. Tropical Cyclone motion can be influenced by transient weather systems, such as extratropical cyclones [46]. In addition to environmental steering, a tropical cyclone will tend to drift slowly poleward and westward, a motion known as "beta drift". This motion is due to the superposition of a vortex, such as a tropical cyclone, onto an environment in which the Coriolis force varies with latitude, such as on a sphere or beta plane. It is induced indirectly by

the storm itself, the result of a feedback between the cyclonic flow of the storm and its environment. A tropical cyclone typically moves from east to west in the tropics, its track may be recurve i.e. shift poleward and eastward if it interacts with the mid-latitude flow, such as the jet stream or an extratropical cyclone.

A tropical cyclone can cease to have tropical characteristics in several different ways. One such way is if it moves over land, thus depriving it of the warm water it needs to power itself, quickly losing strength. Most strong storms lose their strength very rapidly after landfall and become disorganized areas of low pressure within a day or two, or evolve into extratropical cyclones. A tropical cyclone can dissipate when it moves over waters significantly below 26.5 °C (79.7 °F). This will cause the storm to lose its tropical characteristics, such as a warm core with thunderstorms near the center, and become a remnant low-pressure area which may persist for up to several days before losing their identity [47]. Weakening or dissipation can occur if it experiences vertical wind shear, causing the convection and heat engine to move away from the center; this normally ceases development of a tropical cyclone. A cyclone can also merge with another area of low pressure, becoming a larger area of low pressure. This can strengthen the resultant system, although it may no longer be a tropical cyclone. In addition, its interaction with the main belt of the Westerlies, by means of merging with a nearby frontal zone, can cause tropical cyclones to evolve into extratropical cyclones. This transition can take 1–3 days. Even after a tropical cyclone is said to be extratropical or dissipated, it can still have tropical storm force (or occasionally hurricane/typhoon force) winds and drop several inches of rainfall.

2.2.2.8 Observation and Forecasting of TC

Intense tropical cyclones pose a particular observation challenge, as they are a dangerous oceanic phenomenon. Tropical cyclone observation has been carried out over the past couple of centuries in various ways. The passage of typhoons, hurricanes, as well as other tropical cyclones have been detected by word of mouth from sailors recently coming to port or by radio transmissions from ships at sea, from sediment deposits in near shore estuaries, to the wiping out of cities near the coastline. Advances in technology have included using planes to survey the ocean basins, satellites to monitor the world's oceans from outer space using a variety of methods, radars to monitor their progress near the coastline, and recently the introduction of

unmanned aerial vehicles to penetrate storms. In general, surface observations are available only if the storm is passing over an island or a coastal area, or if there is a nearby ship. Real-time measurements are usually taken in the periphery of the cyclone, where conditions are less catastrophic and its true strength cannot be evaluated. For this reason, there are teams of meteorologists that move into the path of tropical cyclones to help evaluate their strength at the point of landfall. On site measurements, in real-time, can be taken by sending specially equipped reconnaissance flights into the cyclone. Tropical cyclones far from land are tracked by weather satellites capturing visible and infrared images from space, usually at half-hour to quarter-hour intervals. As a storm approaches land, it can be observed by land-based Doppler weather radar. Radar plays a crucial role around landfall by showing a storm's location and intensity every several minutes [48]. Figure 2.8 shows the radar and satellite images of cyclone and different stages of cyclone.

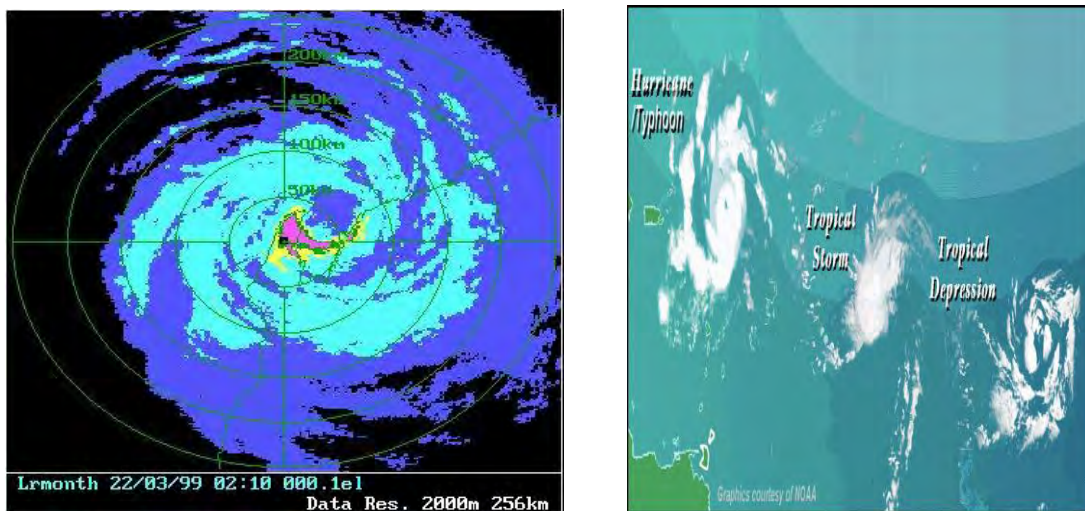


Fig 2.8 (a): Radar image of tropical cyclone (b): satellite image tropical cyclone

Tropical cyclone track forecasting involves predicting where a tropical cyclone is going to track over the next five days, every 6 to 12 hours as shown in figure 2.9. The history of tropical cyclone track forecasting has evolved from a single station approach to a comprehensive approach which uses a variety of meteorological tools and methods to make predictions. The weather of a particular location can show signs of the approaching tropical cyclone, such as increasing swell, increasing cloudiness, falling barometric pressure, increasing tides, squalls, and heavy rainfall. Accurate track predictions depend on determining the position and strength of high and low

pressure areas, and predicting how those areas will migrate during the life of a tropical system.

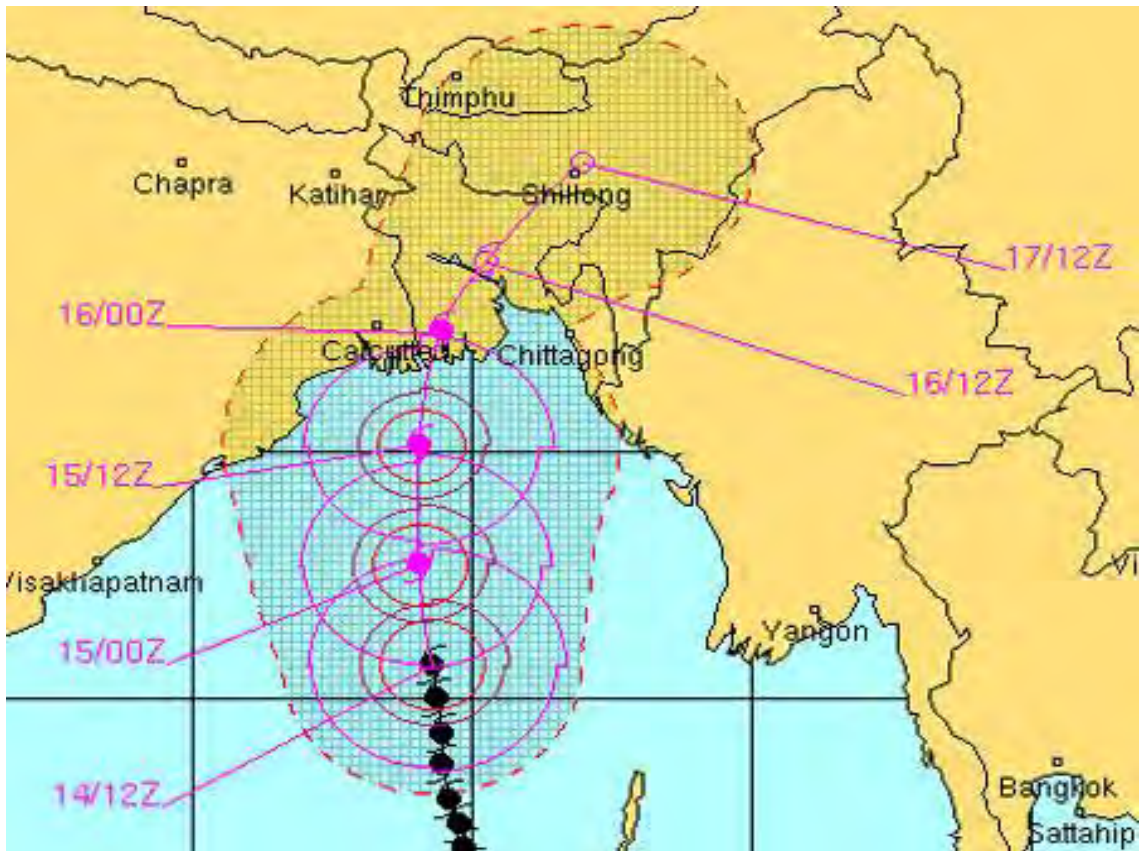


Fig 2.9: Forecast track of tropical cyclone (Sidr)

The deep layer mean flow, or average wind through the depth of the troposphere, is considered the best tool in determining track direction and speed. If storms are significantly sheared, use of wind speed measurements at a lower altitude, such as at the 70 kPa pressure surface (3,000 metres or 9,800 feet above sea level) will produce better predictions. High-speed computers and sophisticated simulation software allow forecasters to produce computer models that predict tropical cyclone tracks based on the future position and strength of high- and low-pressure systems. Combining forecast models with increased understanding of the forces that act on tropical cyclones, as well as with a wealth of data from Earth-orbiting satellites and other sensors, scientists have increased the accuracy of track forecasts over recent decades [49].

2.2.3 Environmental Parameters

Environment that can be responsible for formation and intensification of tropical cyclone are divided into dynamic and thermodynamic parameters. The details of these parameters are described below:

2.2.3.1 Dynamic Parameters

2.2.3.1.1 Vertical Wind Shear (VWS)

Wind shear or wind gradient is a difference in wind speed and direction over a relatively short distance in the atmosphere. Wind shear can be broken down into vertical and horizontal components. According to figure 2.10, VWS can be described by the change of mean large-scale horizontal wind with height. VWS is commonly measured as the horizontal wind difference (magnitude and direction) between 200 - 850 hPa averaged within a given radius.

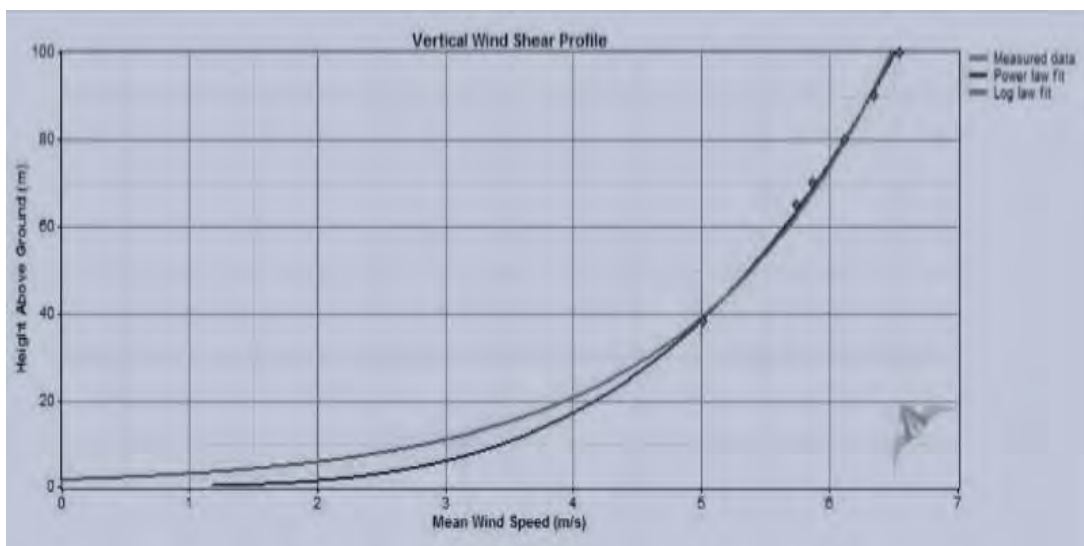


Fig 2.10: Height (m) vs mean wind speed (m/s) graph

VWS is one of the most important dynamical parameters of the large-scale environment related to TC formation, as well as its structure and intensity change. VWS is considered as one of the major predictors in several statistical TC intensity prediction. VWS is the major factors that can lead to strong convective asymmetries in the core of a TC. Scientist showed that the strong, slow-moving, and low-latitude (south of 35°N) TCs are strongly affected by VWS over a deep layer, while the weak, fast-moving, and high-latitude TCs (north of 35°N) are strongly affected by VWS in

the mid- to lower troposphere. It is generally believed that strong VWS is unfavorable for TC genesis and intensification and reduces TC maximum intensity.

The low level VWS is negatively correlated with TC intensity change [17, 50]. Figure 2.11 shows the effect of VWS on TC. TC development requires relatively low values of vertical wind shear so that their warm core can remain above their surface circulation center, thereby promoting strengthening. Vertical wind shear tears up the "machinery" of the heat engine causing it to break down. Strongly sheared tropical cyclones weaken as the upper circulation is blown away from the low level center. When the wind shear is weak, the storms that are part of the cyclone grow vertically, and the latent heat from condensation is released into the air directly above the storm, aiding in development. When there is stronger wind shear, this means that the storms become more slanted and the latent heat release is dispersed over a much larger area [51].

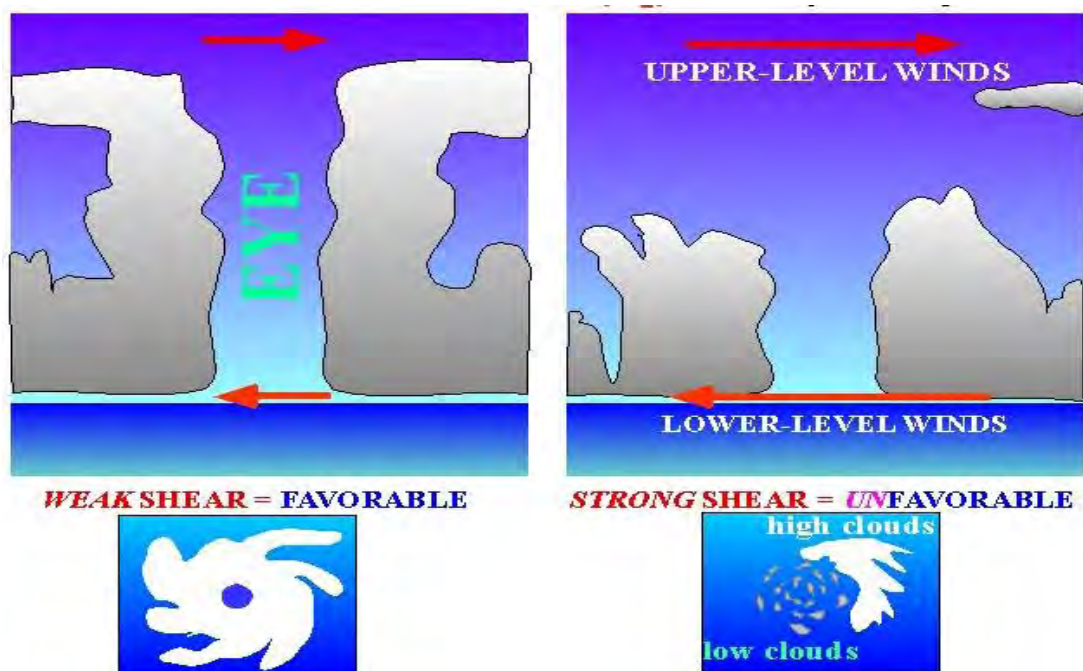


Fig 2.11: Effects of VWS on Tropical Cyclone

2.2.3.1.2 Relative vorticity

Vorticity is the tendency for elements of the fluid to spin. Vorticity is defined as twice the angular rate of rotation of an object about a vertical axis. The vorticity is

a pseudo vector field $\vec{\omega}$, defined as the curl (rotational) of the flow velocity \mathbf{u} vector. The definition can be expressed by the vector analysis formula:

$$\vec{\omega} = \nabla \times \vec{u}$$

Figure 2.12 shows the present of vorticity. The spin imparted to the air by the rotating Earth (rotation around a local vertical) called Earth vorticity.

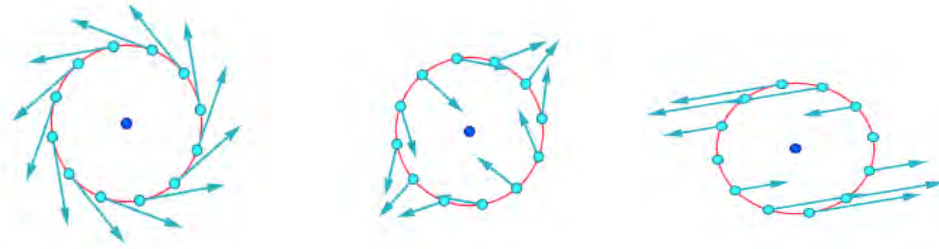


Fig 2.12: Vorticity $\neq 0$

Vorticity $\neq 0$

Vorticity = 0

The relative vorticity is the vorticity of the air velocity field relative to the Earth. This is often modeled as a two-dimensional flow parallel to the ground, so that the relative vorticity vector is generally perpendicular to the ground, and can then be viewed as a scalar quantity, positive when the vector points upward, negative when it points downwards. Figure 2.13 shows the positive and negative nature of vorticity. Vorticity is positive when the wind turns counter-clockwise (looking down onto the Earth's surface). In the Northern Hemisphere, positive vorticity is called cyclonic rotation, and negative vorticity is anticyclonic rotation; the nomenclature is reversed in the Southern Hemisphere. Parcels acquire relative vorticity when they encounter curved flow and horizontal differences in wind speeds. The large magnitude of low level relative vorticity is play an important role in determining regions of high tropical cyclone genesis frequency. It is well observed that tropical cyclones form only in regions of large positive low level vorticity. The larger this low level vorticity, the greater appears the potential for cyclone genesis. Other conditions being favorable and remaining constant, tropical cyclone genesis should be directly related to the magnitude of low level tropospheric relative vorticity [52].

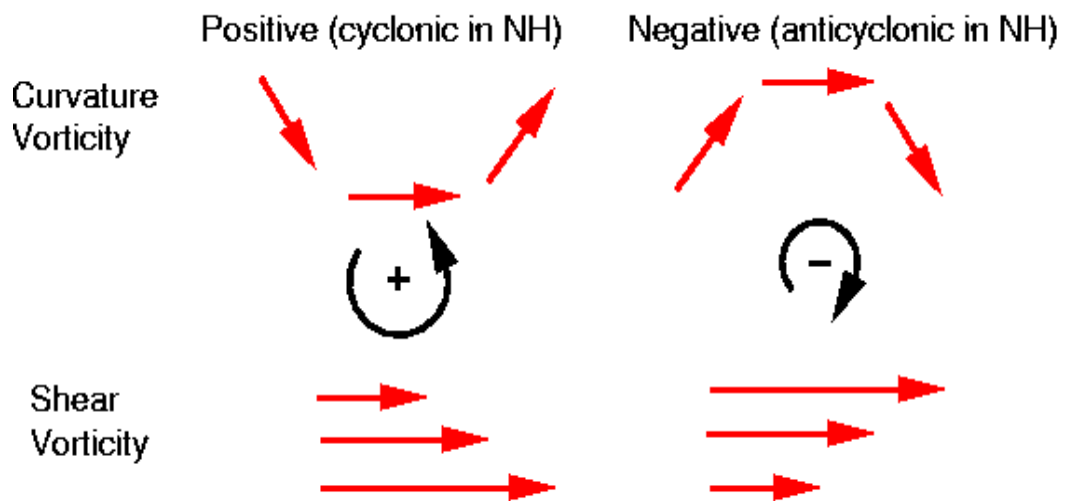


Fig 2.13: Cyclonic and anticyclonic phase of vorticity

2.2.3.1.3 Divergence

Divergence is the motion that results in neighboring air parcels at a given level "spreading apart." Weather is directly affected by the vertical motion of air which, in turn, is influenced by horizontal convergence and divergence. In the atmosphere, the distribution of horizontal convergence and divergence of air is rather complicated. During tropical cyclone formation convergence occurs at the low level and divergence appears aloft. Inflowing air near the ocean surface acquires heat primarily via evaporation of water at the temperature of the warm ocean surface then air rises and cools within the eyewall while conserving total heat content finally air outflows and loses heat via infrared radiation to space at the temperature of the cold tropopause. In the most cyclones strong convergence occurs in the 850-300 mb inflow level and divergence occurs in the 300-100 mb outflow level. Figure 2.14 shows the convergence and divergence process during tropical cyclone formation.

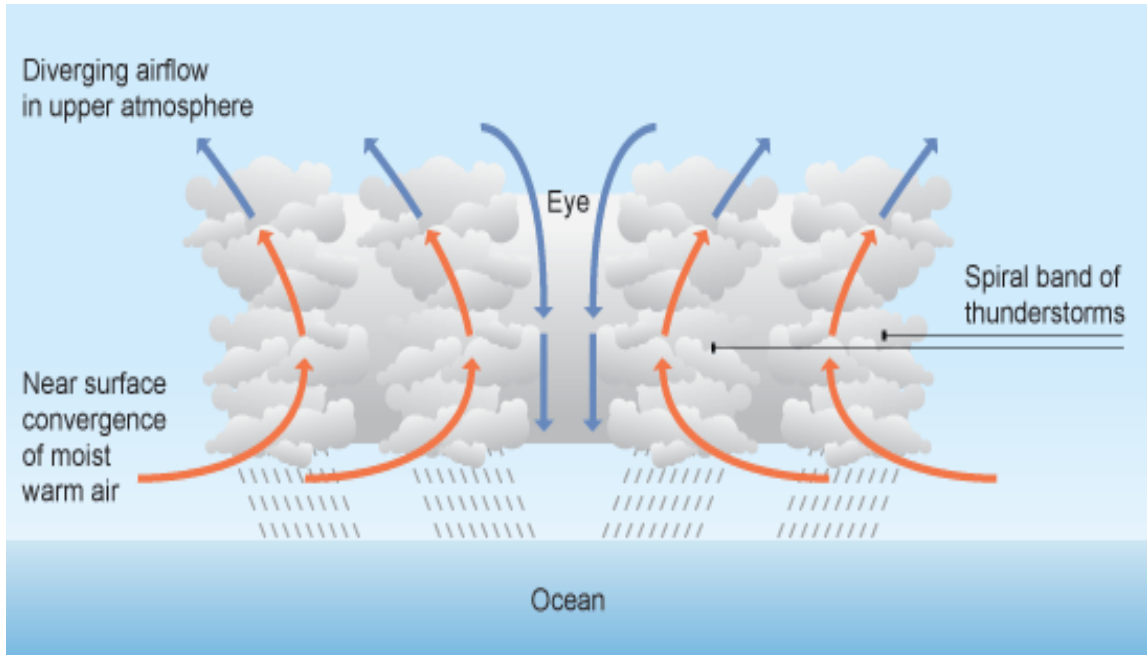


Fig 2.14: Convergence and Divergence process of tropical Cyclone

2.2.3.1.4 Moisture Flux

Moisture advection is the horizontal transport of water vapor by the wind. In terms of mixing ratio, horizontal transport/advection can be represented in terms moisture flux:

$$\mathbf{f} = q\mathbf{V}$$

in which q is the mixing ratio. The value can be integrated throughout the atmosphere to total transport of moisture through the vertical:

$$\mathbf{F} = \int_0^{\infty} \rho \mathbf{f} dz = - \int_P^0 \frac{\mathbf{f}}{g} dp$$

Where ρ is the density of air, P is pressure at the ground surface.

From the perspective of water budget, moisture flux convergence was dominant and contributed ~70% of the moisture for TC precipitation over the ocean and almost all over the land, especially inside the TC circulation. TC precipitation was mainly controlled by the water vapor supply from the environment over ocean. TC size is relevant to the moisture content in the environment. Moisture flux convergence is

related to the intensity of TC. Moisture flux convergence can be divided into two parts: wind convergence and moisture advection. Moisture flux convergence was mostly due to wind convergence, which was dominant in the southwestern quadrants of the TCs. Figure 2.15 shows the moisture flux advection over BoB. Moisture advection was located in the northern area, and becomes relatively important when the TCs approached the land. The moisture flux convergence and its two parts varied during TC movement, with strengthening and contraction of moisture convergence present near landfall. The vertical structure of most of the TC indicated that the moisture convergence was mainly confined to the lower atmosphere under 800 hPa and a weak divergence region was present in the middle troposphere around 550 hPa [53].

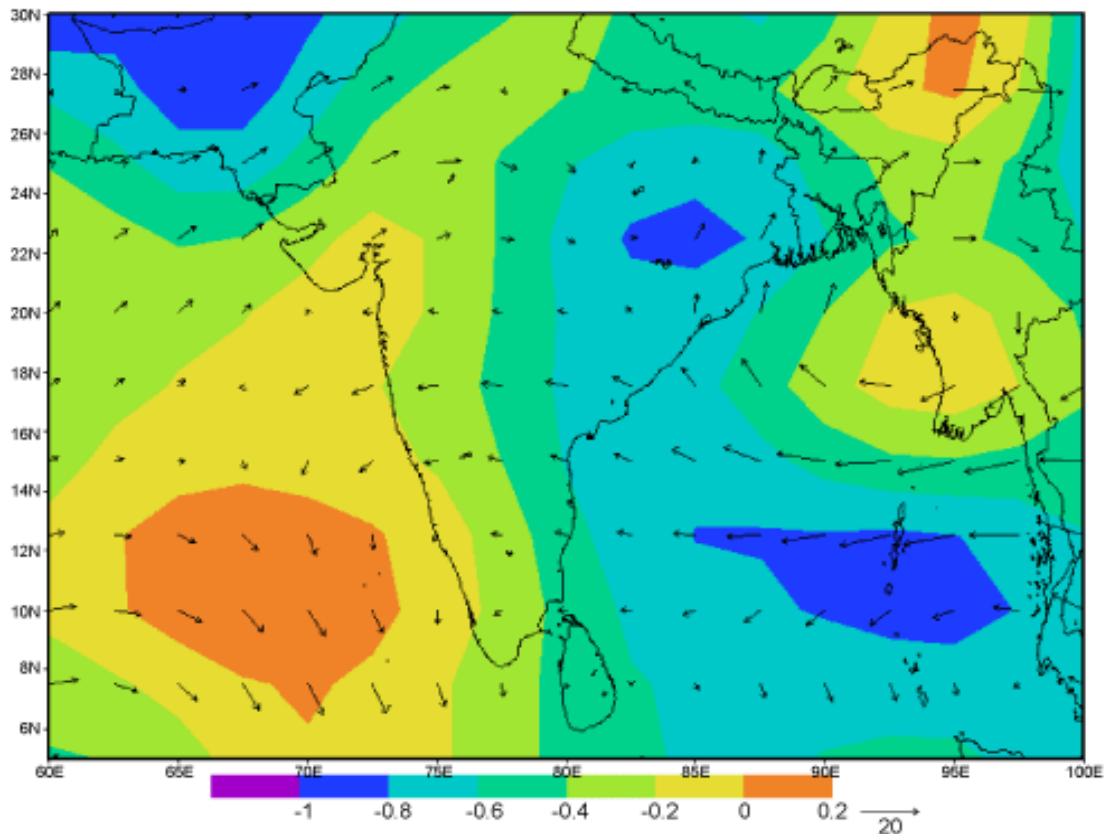


Fig 2.15: Surface moisture flux Convergence over NIO

2.2.3.2 Thermodynamic Parameters

2.2.3.2.1 Relative Humidity

Humidity is the amount of water vapor in the air. The relative humidity (ϕ) of an air-water mixture is defined as the ratio of the partial pressure of water vapor (e_w) in the mixture to the equilibrium vapor pressure of water (e_w^*) at a given temperature.

Relative humidity is normally expressed as a percentage and is calculated by using the following equation

$$\phi = e_w / e_w^* \times 100 \%$$

It is observed that Tropical Cyclone genesis is directly related to the high average of 500 and 700 mb relative humidity (Fig 2.16). Tropical Cyclone development is not possible if seasonal 500-700 mb relative humidity is less than 40 percent. This factor increases linearly to 1 for seasonal 700-500 mb humidity equal to or greater than 70 percent.

Humidity Parameter = $(RH - 40)/30$ if RH is between 40 and 70%.

The relationship between middle level moisture and cyclone genesis is expressed by the above humidity parameter.

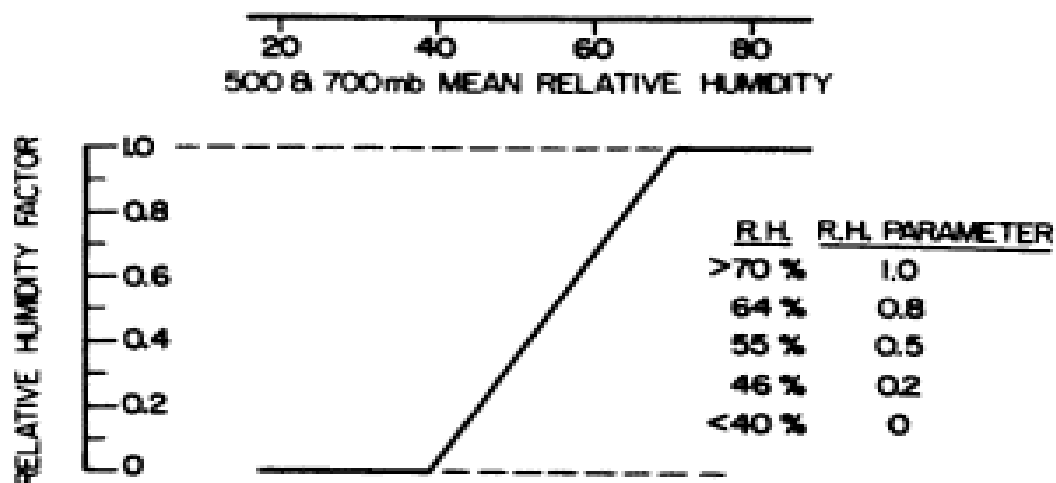


Fig 2.16: Relationship between average 500 to 700 mb seasonal relative humidity and the humidity Parameter

Environmental relative humidity (ERH) above the boundary layer generally decreases with time as TCs evolve. Near the surface, ERH stays approximately constant. ERH generally increases with increasing TC intensity and intensification rate [4, 54].

2.2.3.2.2 Sea Surface Temperature

Sea surface temperature (SST) is the water temperature close to the ocean's surface. The distribution of SST exceeding 26°C is one of the primary factors explaining the seasonal distribution and frequency of tropical cyclones over the oceans. Waters of this temperature cause the overlying atmosphere to be unstable enough to sustain convection and thunderstorms and maintain the warm core that fuels tropical systems. The temperature of the underlying water is the dominant factor in tropical cyclone intensification. Increasingly warmer water would enable progressively stronger tropical storm to form [55]. The formation of SCS, VSCS and SC starts after 27.50°C and increases with increasing SST but discontinuously. The intensity of cyclone has a step-like rather than continuous relationship with SST. Figure 2.17 shows the seasonal peaks of tropical cyclone activity worldwide in terms of SST. SST alone is an adequate predictor of tropical cyclone intensity.

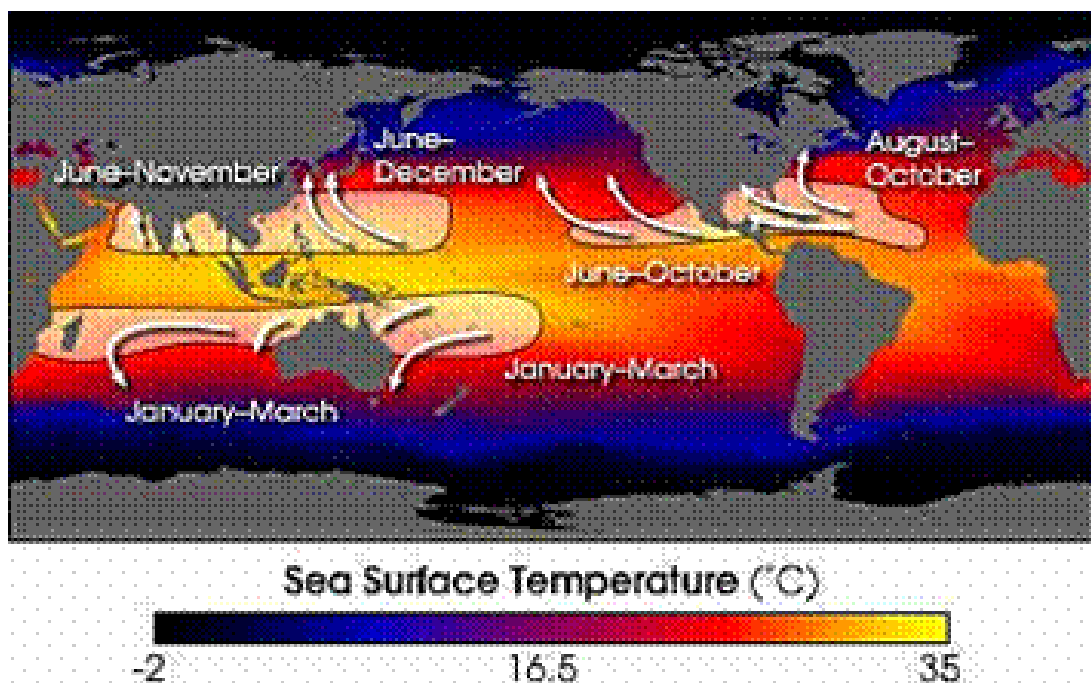


Fig 2.17: Seasonal peaks of tropical cyclone activity worldwide in terms of SST

2.2.3.2.3 Convective Available Potential Energy (CAPE)

In meteorology, convective available potential energy (CAPE), sometimes, simply, available potential energy (APE), is the amount of energy a parcel of air would have if lifted a certain distance vertically through the atmosphere. CAPE is effectively the positive buoyancy of an air parcel and is an indicator of atmospheric instability, which makes it very valuable in predicting severe weather. CAPE exists within the conditionally unstable layer of the troposphere, the free convective layer, where an ascending air parcel is warmer than the ambient air. CAPE is measured in joules per kilogram of air (J/kg). Any value greater than 0 J/kg indicates instability and the possibility of thunderstorms. Generic CAPE is calculated by integrating vertically the local buoyancy of a parcel from the level of free convection to the equilibrium level :

$$\text{CAPE} = \int_{z_f}^{z_n} g \left(\frac{T_{v,\text{parcel}} - T_{v,\text{env}}}{T_{v,\text{env}}} \right) dz$$

Where Z_f is the height of the level of free convection and Z_n is the height of the equilibrium level(neutral buoyancy), where $T_{v, \text{parcel}}$ is the virtual temperature of the specific parcel, where $T_{v, \text{env}}$ is the virtual temperature of the environment, and where g is the acceleration due to gravity [56].

CAPE is an indicator of the environmental potential for formation of a tropical deep convection or MCS and tropical cyclone formation and intensification. High CAPE is favorable for high convection. In the Bay of Bengal during the Pre-monsoon season, the potential for convection was highest, with surface-based CAPE values of more than 2,500 J kg^{-1} and during post-monsoon mostly less than 1,500 J kg^{-1} . According to the WISHE theory for tropical cyclogenesis (WISHE = Wind Induced Surface Heat Exchange), the existence of CAPE is not required in the intensification process [4, 57]. The presence of CAPE plays a significant role in enhancing the cyclogenesis, especially in the earlier stages, when compared to the process in the later stages when the cyclone is achieving equilibrium. CAPE was high in the initial stages of development but as the cyclone intensified, CAPE decreased in the inner

core region. Figure 2.18 shows the intensification rate in the axisymmetric tropical cyclone is highly influenced by CAPE and thus changes in the way the cyclone intensifies [58].

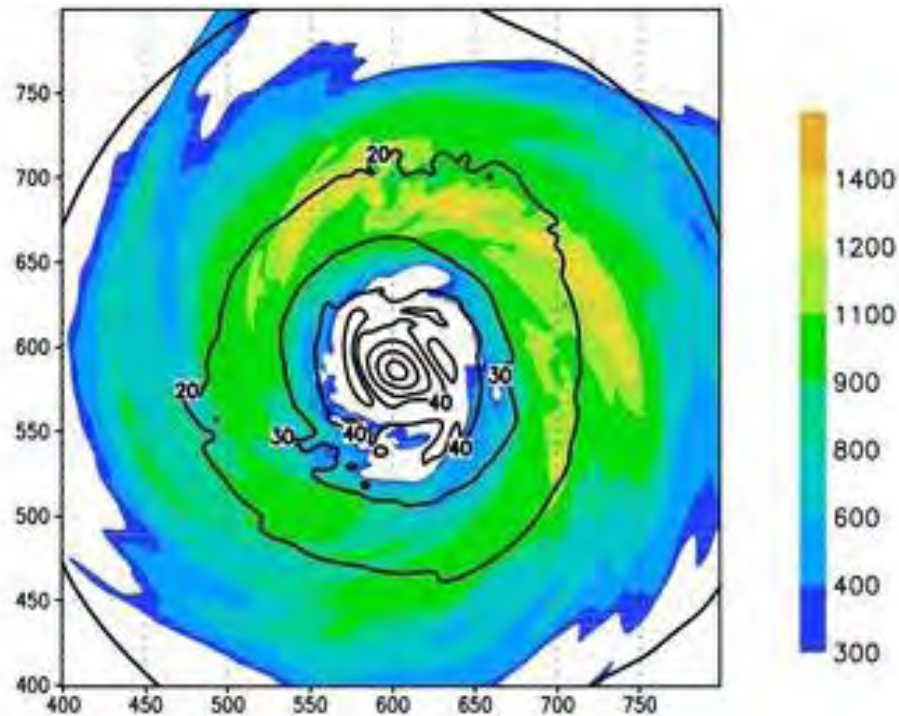


Figure 2.18: CAPE (coloured shadings, J/kg) and wind speed at height 2.25 km (isolines, m/s) of a CM1 tropical cyclogenesis simulation at the time of maximum intensification. [59]

2.2.3.2.4 Convective Inhibition (CIN)

Convective inhibition (CIN or CINH) is a numerical measure in meteorology that indicates the amount of energy that will prevent an air parcel from rising from the surface to the level of free convection. CIN is the amount of energy required to overcome the negatively buoyant energy the environment exerts on an air parcel. In most cases, when CIN exists, it covers a layer from the ground to the level of free convection (LFC). The negatively buoyant energy exerted on an air parcel is a result of the air parcel being cooler (denser) than the air which surrounds it, which causes the air parcel to accelerate downward. The situation in which convective inhibition is measured is when layers of warmer air are above a particular region of air [60]. The effect of having warm air above a cooler air parcel is to prevent the

cooler air parcel from rising into the atmosphere. This creates a stable region of air. Figure 2.19 shows the area of convergence positive/negative buoyancy as well as the lifted condensation level, level of free convection, and equilibrium level. Convective inhibition indicates the amount of energy that will be required to force the cooler packet of air to rise. This energy comes from fronts, heating, moistening, or mesoscale convergence boundaries such as outflow and sea breeze boundaries, or orographic lift. Typically, an area with a high convection inhibition number is considered stable and has very little likelihood of developing a thunderstorm. Conceptually, it is the opposite of CAPE. CIN is strengthened by low altitude dry air advection and surface air cooling. Surface cooling causes a small capping inversion to form aloft allowing the air to become stable. Incoming weather fronts and short waves influence the strengthening or weakening of CIN. CIN is an energy per unit mass and the units of measurement are joules per kilogram (J/kg). CIN is measured as

$$CIN = \int_{SFC}^{LFC} R_d (T_{ve} - T_{vp}) d \ln(p).$$

Where T_{ve} and T_{vp} are the ambient virtual temperature of the environment and that of the specific parcel, respectively, and R_d is the gas constant of dry air.

CIN can limit convection even when CAPE is very large. The larger the CIN value the stronger the „cap“ is that suppresses convection. Above a CIN value of 50 J kg^{-1} , convection is strongly prevented, unless some other mechanism initiates the convection. The frequency of cyclone formation is inversely related to the environmental CIN [14, 61].

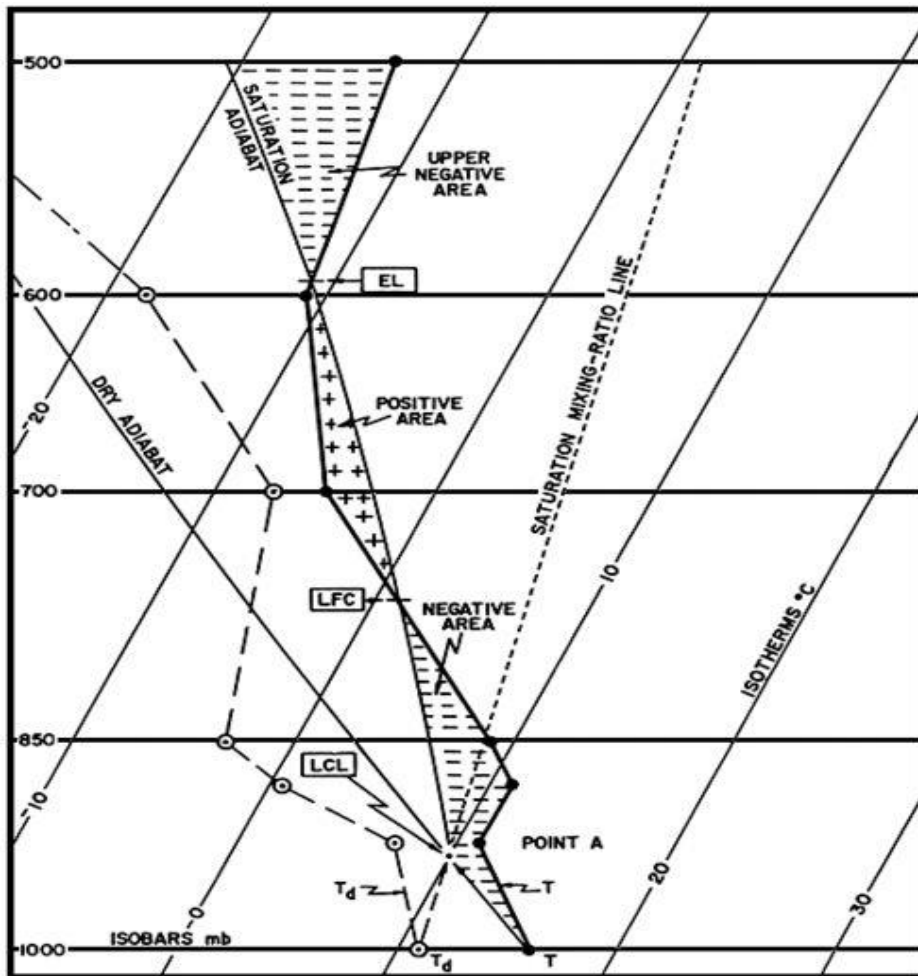


Fig 2.19: A Skew-T thermodynamic diagram showing areas of positive/negative buoyancy as well as the lifted condensation level, level of free convection, and equilibrium level [source: https://en.wikipedia.org/wiki/Convective_inhibition]

2.2.3.2.5 Geopotential Height

The difference in the geopotential height of two constant-pressure surfaces in the atmosphere, proportional to the appropriately defined mean air temperature between the two surfaces:

$$\Delta\phi = -R \int_{p_1}^{p_2} T \frac{dp}{p} = RT_m \ln \left(\frac{p_1}{p_2} \right)$$

Where $\Delta\phi$ is the geopotential thickness; R the gas constant for air; p_1 and p_2 the pressure at the lower and upper isobaric surface, respectively; the T Kelvin temperature and T_m the mean temperature [62].

Geopotential height is a vertical coordinate referenced to Earth's mean sea level an adjustment to geometric height (elevation above mean sea level) using the variation of gravity with latitude and elevation. Thus it can be considered a "gravity-adjusted height". One usually speaks of the geopotential height of a certain pressure level, which would correspond to the geopotential height necessary to reach the given pressure. Geopotential Thickness is use as a good predictor of tropical cyclone motion and intensity change. Geopotential Thickness data is used in the statistical prediction of tropical cyclone intensity change. Figure 2.20 indicated that the 1000-700 mb in the vicinity of cyclone in the poleward and eastward quadrant is a significant predictor of 24 hours intensity change, even when combined with climatology and persistence [63].

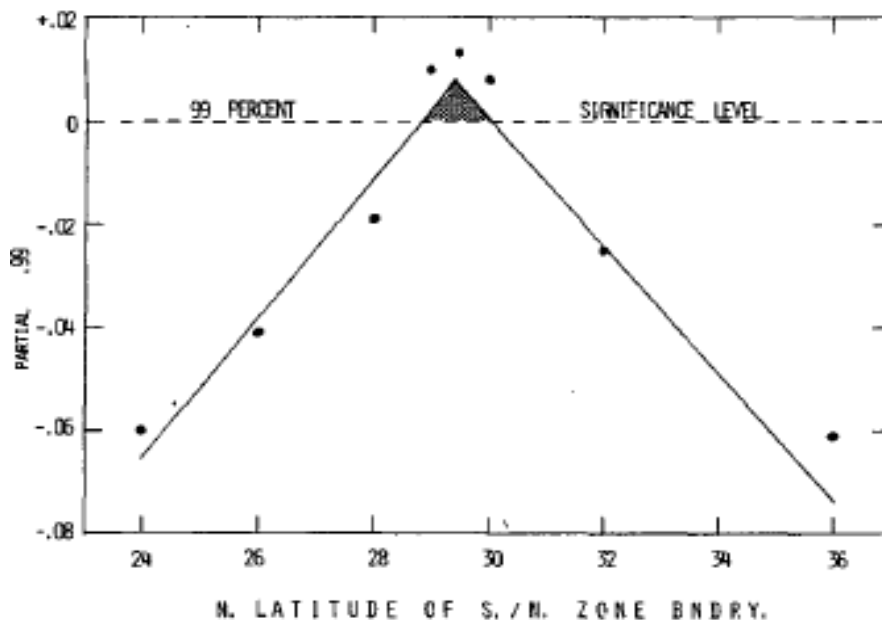


Fig 2.20: 1000-700 mb thickness as first-order partial predictor of 24 hour maximum wind change in south zone. Shading depicts area of significant at 99% level. [63]

2.2.3.2.6 Mean Sea Level Pressure (MSLP)

The maximum sustained surface wind in tropical cyclone is a function of the local maximum pressure gradient. Determining the proper relationship between the minimum sea level pressures and maximum sustained winds in tropical cyclones has been a long-standing problem. The major obstacle has been the lack of sufficient

ground truth, i.e., actual measurements of maximum wind speeds in tropical cyclones with a wide range of central pressures [64]. The nonlinear equation

$$V_m = 6.7(1010 - P_e)^{0.644}$$

Where V_m is the maximum surface wind speed (kt) and P_e is the MSLP (mb).

A mean sea level pressure chart shows the direct relationship between isobar spacing (pressure gradient) and orientation, and the strength and direction of surface winds.

The most obvious features of the MSLP analyses shown in Fig 2.21 are the patterns of high and low pressure, and the barbed lines identifying cold fronts. Friction over the earth's surface causes the winds to be deflected slightly inwards towards low pressure centers, and slightly outwards from high pressure systems. Wind strength is inversely proportional to the distance between isobars-the closer the lines, the stronger the winds. The general rule is that winds are strongest where the isobars are closest together. Thus the strongest winds are usually experienced near low pressure systems. Winds are normally light near high pressure systems where the isobars are widely spaced. Tropical cyclones are low pressure systems in the tropics which, in the southern hemisphere, have well defined clockwise circulations with mean surface winds (averaged over ten minutes) exceeding gale force (63 kilometers per hour) surrounding the center. The pressure gradient is very steep towards the cyclone's center and wind speeds on the nearby coast in this case would have been about 110 kilometers per hour with gusts 50 per cent or more above this mean wind speed [65].

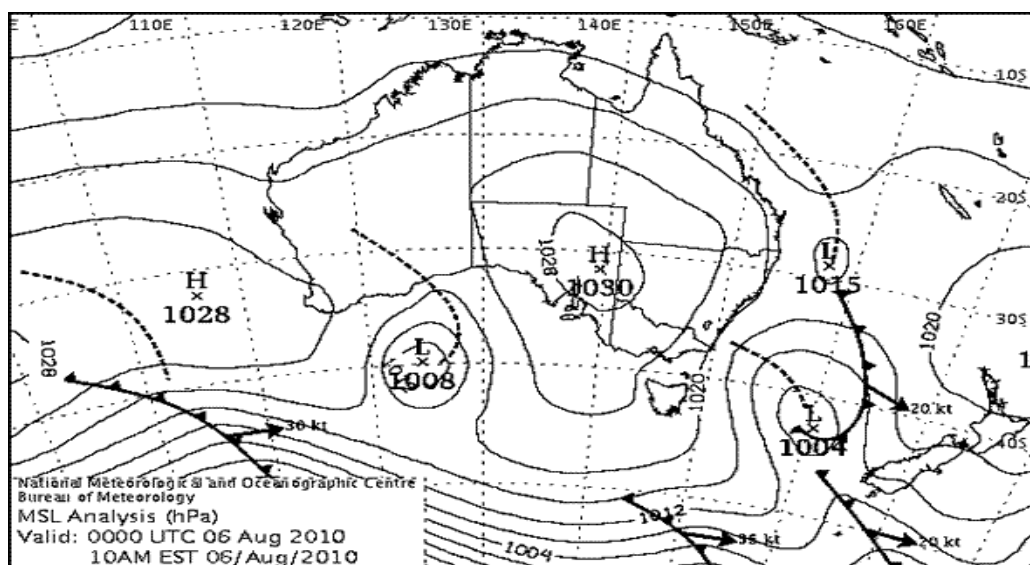


Fig 2.21: Typical MSLP analysis (source: www.bom.gov.au/Interpreting_MSLP)

Chapter Three

Data and Methods

3.1 Data Sources

The 12 years from 2000 to 2011 were chosen as the study period. Best-track data provided by the Joint Typhoon Warning Center (JTWC) were used to determine the positions and intensities of TCs in the BoB. For analysis of large-scale seasonal environmental conditions related to cyclone formation over the BoB, the National Centers for Environmental Prediction (NCEP) Climate Forecast System Reanalysis (CFSR) data product was used. The 6-hourly NCEP–CFSR data were obtained with a coupled atmosphere–ocean–sea ice–land model system. The data product has a horizontal resolution of $0.5^\circ \times 0.5^\circ$ and it uses a hybrid sigma–pressure vertical coordinate system with 64 levels, with a top pressure of ~ 0.266 hPa. For the seasonal-scale analysis, monthly averaged NCEP–CFSR reanalysis data were used and 6-hourly NCEP–CFSR data of specific parameters were used. RTG SST data with a $0.5^\circ \times 0.5^\circ$ resolution were used to calculate SST during the study period. The Grid Analysis and Display System (GrADS) was used to display data. GrADS used a 4 dimensional data environment: longitude, latitude, vertical level, and time. GrADS interprets station data as well as gridded data.

The details of used data sources i.e. JTWC, NCEP-CFSR and RTG_SSTs are described below:

3.1.1 Joint Typhoon Warning Center (JTWC) Best track Data

For determining the positions, intensities and duration of TCs used the best-track data provided by the Joint Typhoon Warning Center (JTWC). The JTWC is a joint United States Navy – United States Air Force task force located in Pearl Harbor, Hawaii. The JTWC is responsible for the issuing of tropical cyclone warnings in the North West Pacific Ocean, South Pacific Ocean and Indian Ocean for United States Department of Defense interests.

The JTWC maintains an archive of tropical cyclone track data, commonly referred to as "best-tracks". Each best-track file contains tropical cyclone center locations and intensities (i.e., the maximum 1-minute mean sustained 10-meter wind speed) at six-hour intervals. The geographical domain of the archive is the western North Pacific (WP), North Indian Ocean (IO) and Southern Hemisphere (SH). Its area of responsibility covers 89% of the world's tropical cyclone activity. JTWC monitors, analyzes, and forecasts tropical cyclone formation, development, and movement year round. JTWC provides two areas of information for historical purposes. Historical tropical cyclone tracks are available from the Tropical Cyclone Best Track page. Tropical cyclone narratives are available from the Annual Tropical Cyclone Report (ATCR). JTWC uses several tools and techniques to estimate tropical cyclone intensity, including subjective Dvorak estimates, objective fix data, and observations. The Dvorak technique is based on the analysis of cloud patterns in visible and infrared imagery from geostationary and polar-orbiting satellites. The Dvorak technique results in a decimal number, called a T-number, which in turn corresponds to an intensity estimate. The current numerical model consensus track forecast used at JTWC, called CONW, is composed of six baroclinic dynamical models and one barotropic model. The baroclinic models providing track forecasts included in the consensus are: NOGAPS, GFDN, GFS, JGSM, UKMET, and ECMWF. The sole barotropic track model is the Weber Barotropic Model (WBAR). In the Indian Ocean and South Pacific, JTWC labels ALL tropical cyclones as "Tropical Cyclone," regardless of estimated intensity. For tropical cyclones occurring in the western Pacific and Indian Oceans, JTWC products are transmitted no later than 3 hours past the synoptic hour. Because the synoptic hours are 00Z, 06Z, 12Z, and 18Z, warnings will be available by 03Z, 09Z, 15Z, or 21Z [66].

3.1.2 National Centers for Environmental prediction (NCEP) Climate Forecast System Reanalysis (CFSR) Data

The NCEP/NCAR Reanalysis project was a joint product from the National Centers for Environmental Prediction (NCEP) and the National Center for Atmospheric Research (NCAR). The NCEP/NCAR Reanalysis data set (1948–2014) was a continually updating gridded data set that represented the state of the Earth's atmosphere, incorporating observations and numerical weather prediction (NWP) model output from 1948 to present. For analysis of large-scale seasonal environmental conditions related to cyclone intensity over the BoB, the National Centers for Environmental Prediction (NCEP) Climate Forecast System Reanalysis (CFSR) 6-hourly data has been used. The NCEP–CFSR used a coupled atmosphere ocean sea-ice land model system to present high resolution data for period from 1948 to present. This data has a horizontal resolution of $0.5^\circ \times 0.5^\circ$ and it uses a hybrid sigma-pressure vertical coordinate system with 64 levels, with a top pressure of 0.266 hPa. There are 80 different variables (including geopotential height, temperature, relative humidity, U and V component, etc) in several different coordinate systems, such as 17-pressure level on $2.5^\circ \times 2.5^\circ$ degree grids. The NCEP/NCAR Reanalysis data is a set suitable short and long-term climate research. observation from land surface, ship, rawinsonde, pibal, aircraft, satellite and other data are quality controlled and assimilated into the model, the model/data assimilation procedure has remain essentially unchanged during the project; data assimilation includes SSM/I surface winds and tropospheric and stratospheric temperature retrieved from TOVS [67].

3.1.3 Real-Time Global, Sea Surface Temperature (RTG_SST) Data

A daily, high-resolution, real-time, global, sea surface temperature (RTG_SST) analysis has been developed at the National Centers for Environmental prediction/Marine Modeling and Analysis Branch. The analysis was implemented in the NCEP production suite 30 January 2001. The daily sea surface temperature product is produced on a half-degree (latitude, longitude) grid, with a two-dimensional variational interpolation analysis of the most recent 24-hours buoy and ship data, satellite-retrieved SST data, and SST's derived from satellite-observed sea-ice coverage.

The NCEP high-resolution Real-Time Global Sea Surface Temperatures (RTG_SSTs) for the daily sea surface temperatures with a $0.5^\circ \times 0.5^\circ$ resolution data will be used to calculate SST during the study period [68].

3.2 Study Area

Cyclones formed over the (5° N to 22° N and 80° E to 95° E) are considered in this study. BoB is a part of NIO with geographical area $5 - 25^\circ \text{ N}$ and $75^\circ - 105^\circ \text{ E}$ is the study area which is indicated in Fig 3.1. JTWC records show that in the 12 years from 2000 to 2011, 44 cyclones formed over the BoB, 36.36 % during the pre-monsoon and 63.64 % during the post-monsoon season. The cyclones were widely distributed across the BoB, but they were concentrated in the central region. In this study, a maximum wind speed of 18 m s^{-1} around the TC center is considered to indicate the initial stage of cyclone development. This criterion is similar to that for a „cyclonic storm“ on the cyclone-intensity scale of the Indian Meteorology Department.

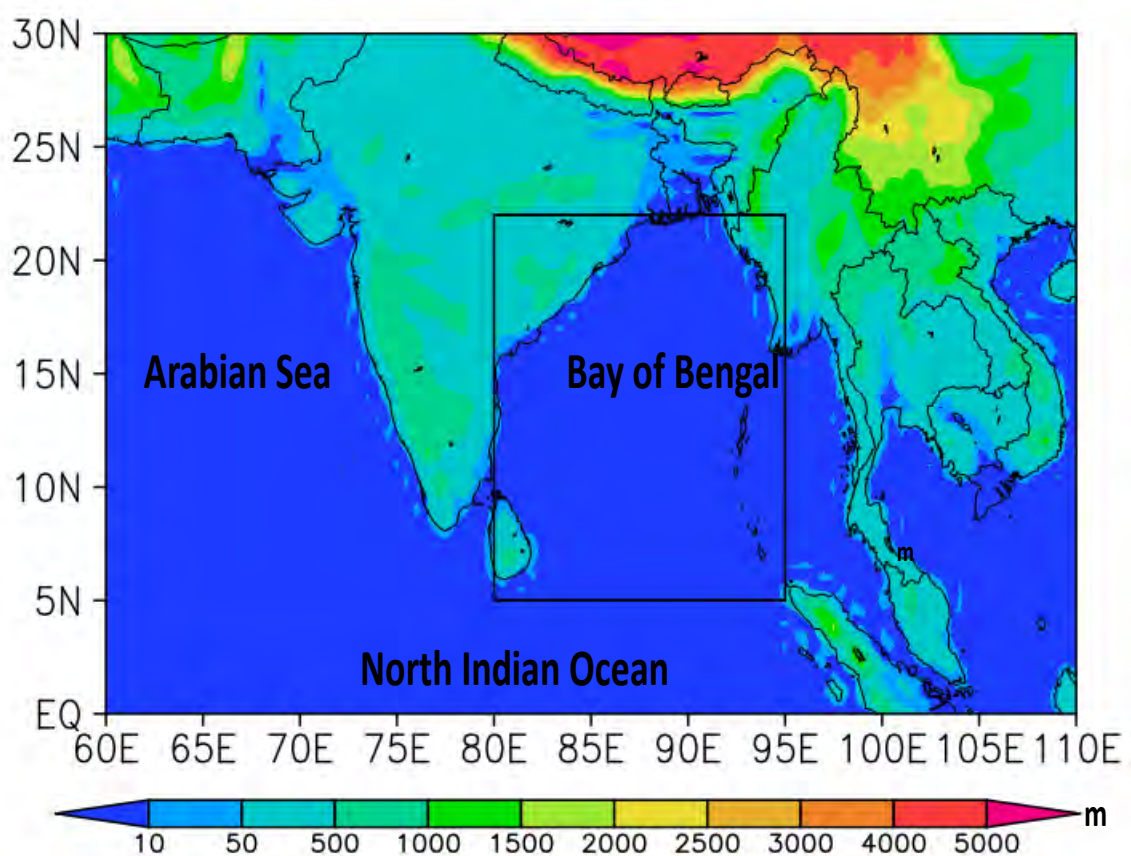


Fig 3.1: Location map of study area (BoB)

3.3 Scale Used for Cyclone Intensity

Tropical systems are officially ranked by several tropical cyclone scales according to their maximum sustained winds and in what oceanic basin they are located. Any tropical cyclone that develops within the North Indian Ocean between 100° E and 45° E is monitored by the India Meteorological Department (IMD). IMD has used five different categories to measure the wind speed of a tropical cyclone based on the maximum sustained winds over a 3-minute averaging period (Table.2). The lowest official classification used in the North Indian Ocean is a Depression, which has 3-minute sustained wind speeds of between 17–27 knot (20–31 mph; 31–49 km/h). The Depression (Dep) intensify further then it will become a Deep Depression (DDep.), which has winds between 28–33 knot (32–38 mph; 50–61 km/h). The system classified as a Cyclonic Storm (CS) and assigned a name by the IMD, when gale force wind speeds develop of between 34–47 knot (39–54 mph; 62–88 km/h). Severe Cyclonic Storms (SCS) have storm force wind speeds of between 48–63 knot (55–72 mph; 89–117 km/h), while Very Severe Cyclonic Storms (VSCS) have maximum winds of 64–89 knot (73–102 mph; 118–166 km/h). The highest classification used in the North Indian Ocean is a Super Cyclonic Storm (SuperCS) have maximum winds of above 90 knot (166 km/h, 104 mph).

Table 2: Tropical Cyclone Intensity Scale according to IMD

Category	Sustained winds (3-min average)
Super Cyclonic Storm	≥120 kt ≥222 km/h
Very Severe Cyclonic Storm	64–89 kt 118–166 km/h
Severe Cyclonic Storm	48–63 kt 89–117 km/h
Cyclonic Storm	34–47 kt 62–88 km/h
Deep Depression	28–33 kt 50–61 km/h
Depression	17–27 kt 31–49 km/h

In this study TC Intensity Scale of IMD (Table 2) has been used for analyzing the cyclone intensities.

3.4 Cyclones in the study periods

Fig. 3.2 shows total number of tropical cyclones over the BOB during study period (2000-2011). Cyclones are bimodal in nature i.e. they formed only in pre-monsoon (Mar-May) and post-monsoon (Oct-Dec). In monsoon season no cyclones are formed because of strong vertical wind shear. In the study period 44 cyclones are formed among them 16 cyclones are developed in pre-monsoon and 28 cyclones are developed in post-monsoon seasons. Among them, the 10 cyclones which have higher intensity (≥ 64 kt) are considered for the study purpose. Details of the cyclones are mentioned below:

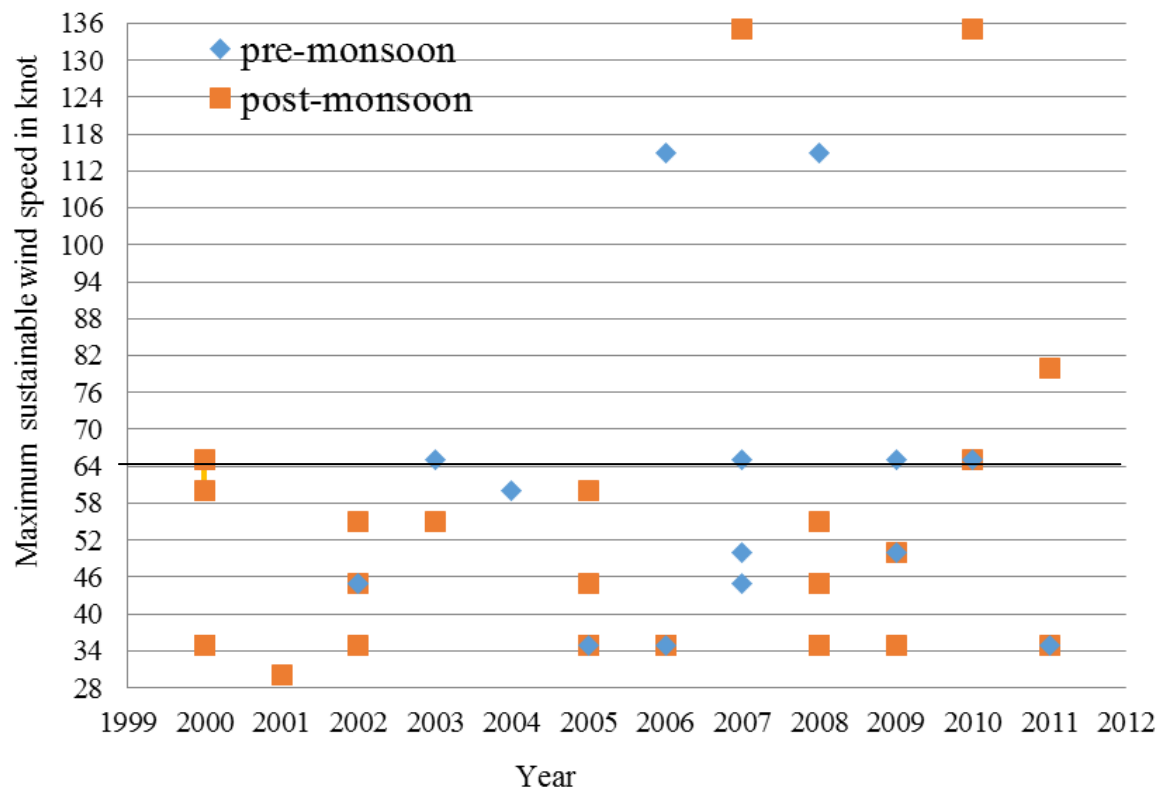


Fig 3.2: Total number of TCs over BoB during 2000-2011.

3.4.1 Pre-monsoon cyclones

Within 10 higher intensity cyclones, the 6 pre-monsoon cyclones named Cylone-2004, Mala-2006, Akash-2007, Nargis-2008, Aila-2009 and Laila-2010, have the intensity ≥ 64 knot. The detail of the cyclones are given below:

3.4.1.1 Cyclone-2004

This storm formed as a depression on May 16 in the central Bay of Bengal (latitude 14.8° N and longitude 89.7° E). The storm intensified while meandering over open waters and began eventually steady northeastward motion due to a ridge to the north over India. An eye developed in the center of the storm while approaching land. On May 19, the cyclone made landfall along northwestern Myanmar near Sittwe, with maximum sustained winds estimated at 165 km/h (105 mph) by the IMD [69]. The storm rapidly weakened over land, although its remnants spread rainfall into northern Thailand. Fig 25 shows the cyclone-2004 track.

The cyclone caused heavy damage throughout Rakhine State, destroying or heavily damaging 4,035 homes and leaving 25,000 people homeless and damage in Myanmar estimated over K621 million kyat (\$99.2 million USD).

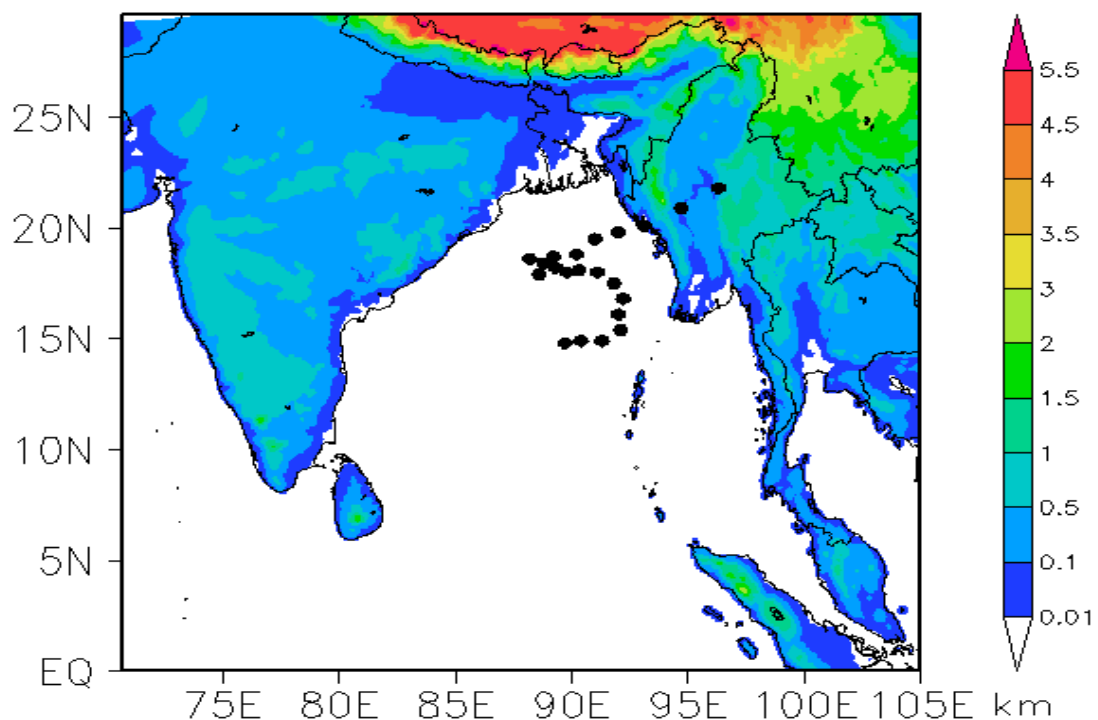


Fig 3.3: Track of Cyclone-2004

3.4.1.2 Mala-2006

Cyclone Mala was the strongest tropical cyclone of the 2006 Over North Indian. In mid-April, an area of disturbed weather formed over the southern Bay of Bengal and nearby Andaman Sea. The system became increasingly organized and was classified as a depression on April 24. The storm slowly intensified as it drifted in a general northward direction. It attained gale-force winds and was named Mala the next day. On April 27 Conditions for strengthening improved markedly and Early on April 28, the cyclone had estimated winds of 185 km/h (115 mph). Steady weakening ensued thereafter and the storm made landfall in Myanmar's Rakhine State on April 29. Fig 3.4 shows the cyclone Mala track. The storm claimed 37 lives in the country and left US\$6.7 million in damage [70].

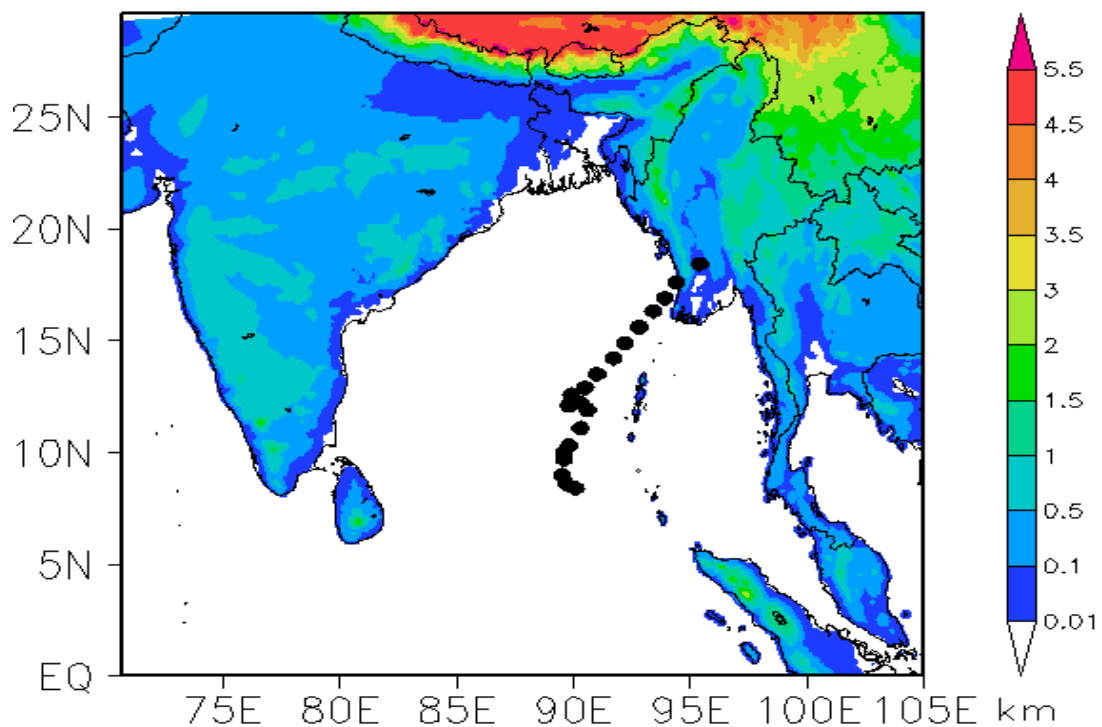


Fig 3.4: Track of Cyclone Mala-2006

3.4.1.3 Akash-2007

Akash (2007) formed from an area of disturbed weather on the Bay of Bengal on May 12, and gradually organized as it drifted northward. An eye began to develop as it approached land, and after reaching peak 3-min sustained winds of 85 km/h (50 mph) it struck about 115 km (70 mi) south of Chittagong in Bangladesh.

Akash rapidly weakened over land, and advisories were discontinued on May 15. Fig 3.5 shows the cyclone Akash track. Akash killed at least one fisherman, and left about 100 others missing. Crops were destroyed and power was cut as Akash neared the coast, and almost 80,000 people had to be evacuated to cyclone shelters [71].

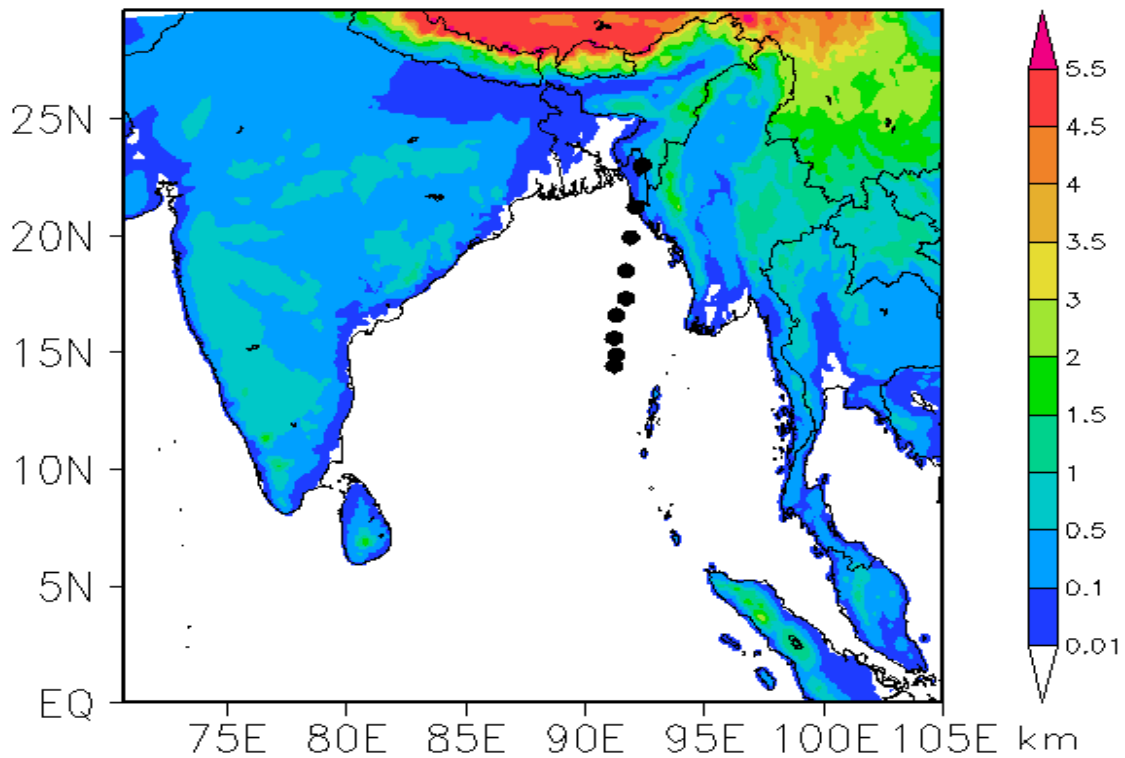


Fig 3.5: Track of Cyclone Akash-2007

3.4.1.4 Nargis-2008

In late April, the Intertropical Convergence Zone became very active over the Bay of Bengal and later spawned a low-pressure area on April 26. Tracking slowly westward, the depression intensified, becoming Cyclonic Storm Nargis on April 28. That day, steering currents weakened, causing the system to become nearly stationary before a trough influenced more northeasterly, and later easterly, movement. On April 29, the system attained hurricane-force winds. Hours before striking southern Myanmar on May 2, Nargis attained its peak intensity with winds of 165 km/h (105 mph) and an estimated central pressure of 962 mbar (hPa; 28.41 in Hg). The JTWC estimated the system to have been somewhat stronger, attaining one-

minute sustained winds of 215 km/h (135 mph). Once onshore, the system gradually weakened and dissipated early on May 4. Fig 3.6 shows the cyclone Nargis track. Nargis is regarded as the worst disaster in the country's history and ranks as the fourth-deadliest tropical cyclone on record. Approximately 23,500 km² of land was inundated by the storm, affecting roughly 11 million people, 2.4 million severely and destroyed 75 percent of healthcare facilities and damaged US\$12.9 billion [72].

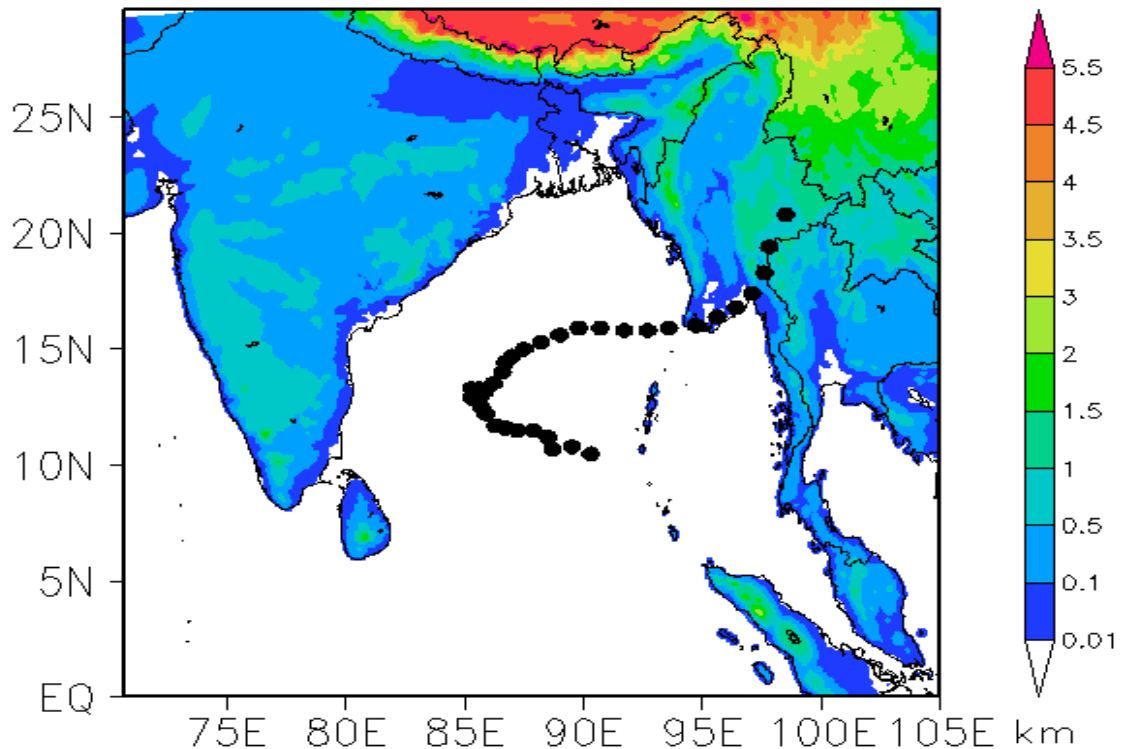


Fig 3.6: Track of Cyclone Nargis-2008

3.3.1.5 Aila-2009

Severe Cyclonic Storm Aila was the worst natural disaster to affect Bangladesh since Cyclone Sidr in November 2007. Aila formed over the Bay of Bengal on May 23. The Cyclone crossed the West Bengal coast with maximum wind of 112 km/hr. Aila became a severe cyclonic storm at 06 UTC on May 25 and made landfall at its peak intensity (60kt, 967hPa) between 08 and 09 UTC. Fig 3.7 shows the Aila track. Approximately 600,000 thatched homes, 8,800 km (5,500 mi) of roads, 1,000 km (620 mi) of embankments, and 123,000 hectares (300,000 acres) of land were damaged or destroyed and 9.3 million people were affected by the cyclone. One Total damage amounted to 18.85 billion taka (US\$269.28 million) [73].

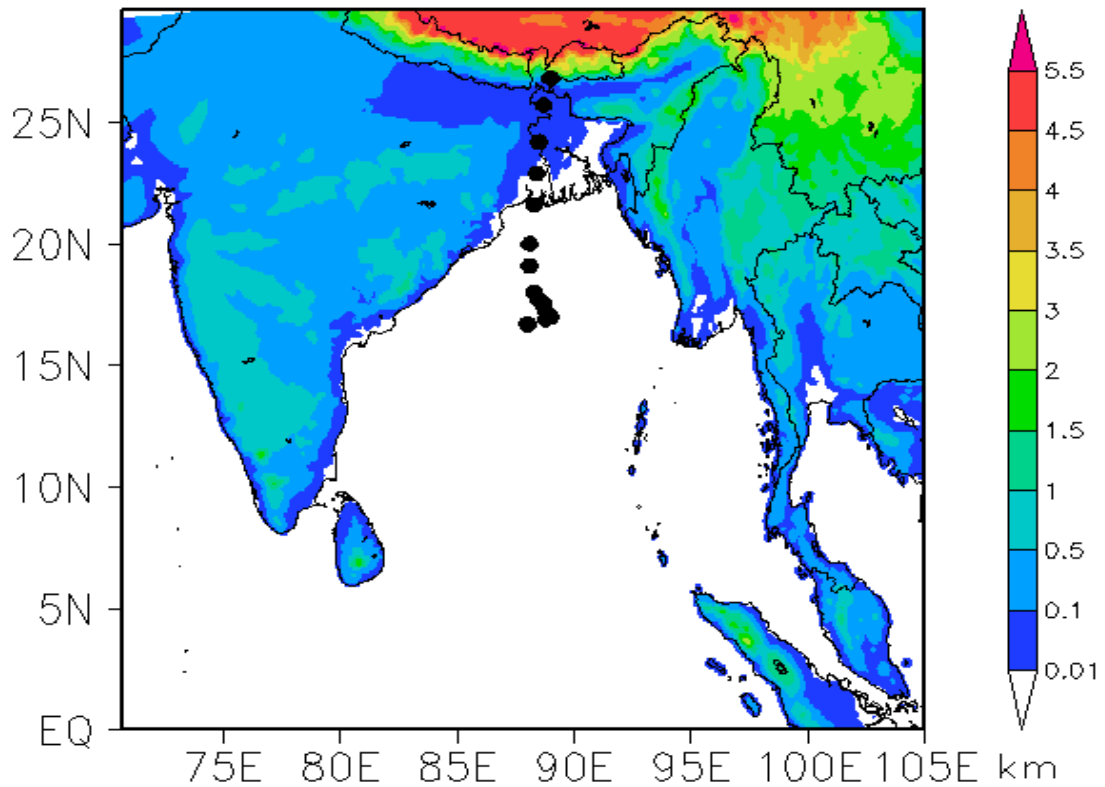


Fig 3.7: Track of Cyclone Aila-2009

3.3.1.6 Laila-2010

Laila developed on May 17 in the Bay of Bengal from a persistent area of convection. Strengthening as it tracked northwestward, it became a severe cyclonic storm on May 19. The next day, Laila made landfall in Andhra Pradesh, and it later dissipated over land. Cyclone Laila track was shown in fig 3.8. The cyclone caused heavy destruction in Prakasam, Krishna and Guntur districts and preliminary reports prepared by the State government put the loss at over Rs 500 core. According to a BBC report, Cyclone Laila is the worst storm to hit Andhra Pradesh in 14 years [74].

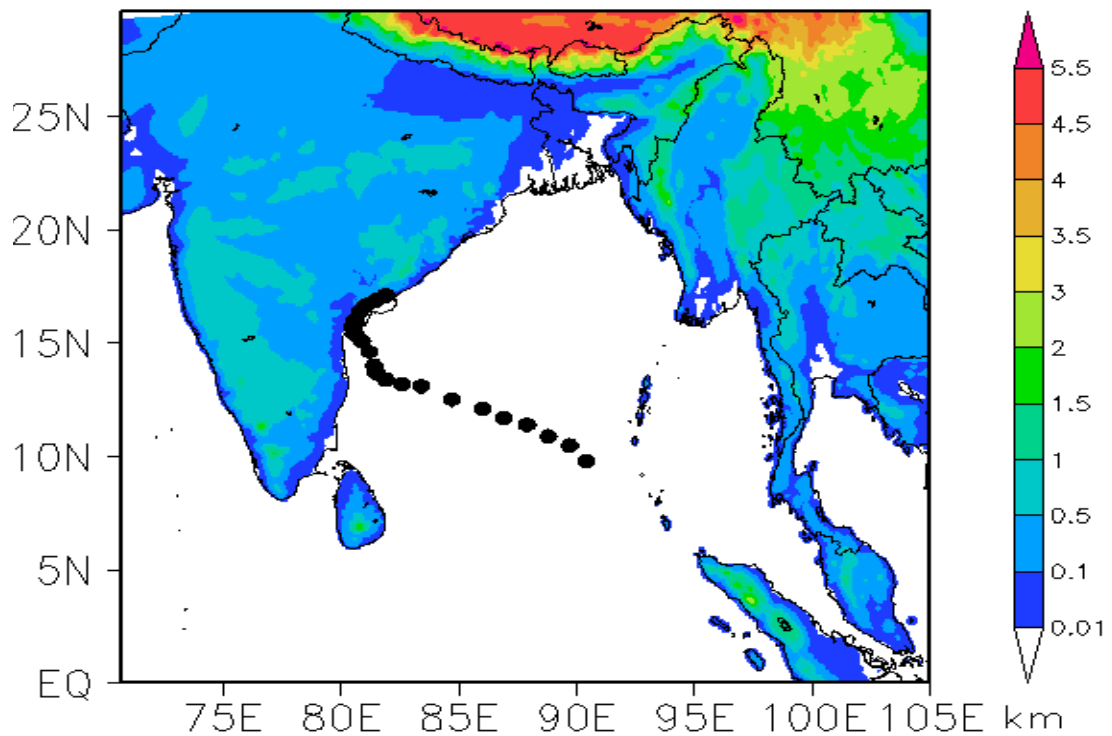


Fig 3.8: Track of Cyclone Laila-2010

3.4.2 Post-Monsoon Cyclones

The 4 cyclones are found more intense (≥ 64 kt) during the study period of 2000-2011. The details of the cyclones are given below:

3.4.2.1 Cyclone-2000

On November 24 an upper-level low persisted over the Andaman Sea. The IMD classified the system as a depression on early 26 November. Outflow and convective organization gradually increased, and late on November 26 the JTWC classified it as Tropical Cyclone 03B. As the rainbands organized around the center, the winds increased; the IMD upgraded the system to a cyclonic storm on November 27, and to a severe and later a very severe cyclonic storm on November 28. The storm weakened slightly before making landfall on November 29 in eastern India near Cuddalore and weakened rapidly over land, and degenerated into a remnant low

on November 30. Fig 3.9 shows the cyclone track. Overall damaged by the storm were estimated at \$15 million USD, and there were 12 deaths [75].

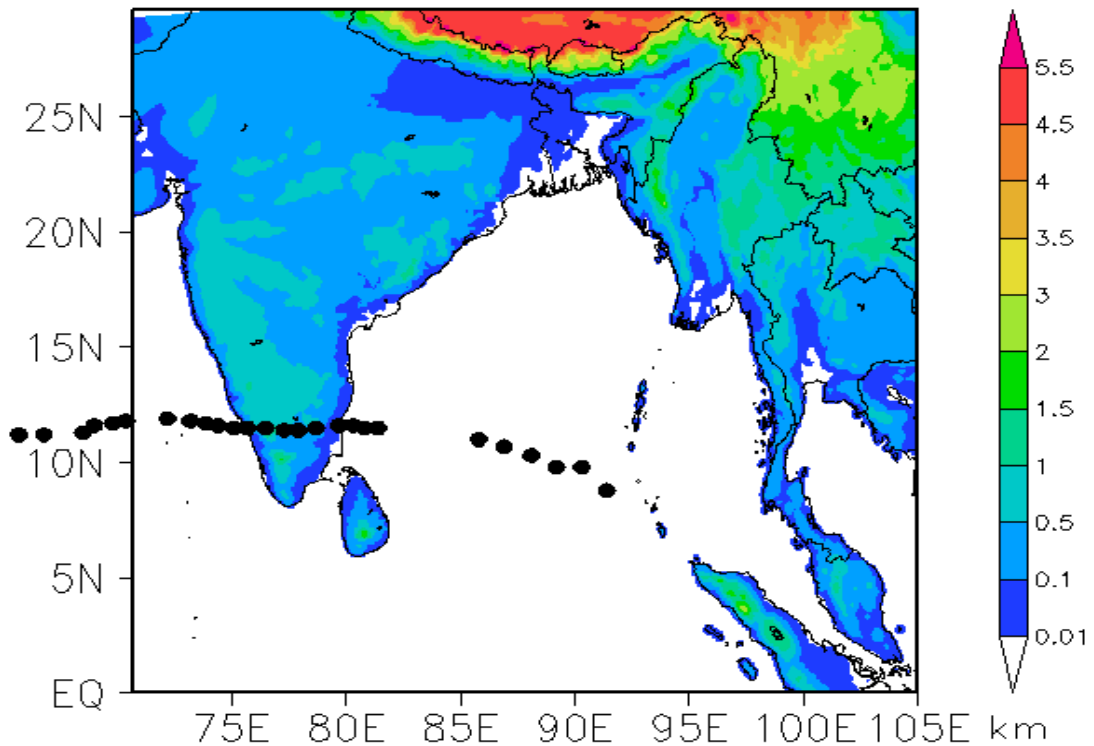


Fig 3.9: Track of Cyclone-2000

3.4.2.2 Sidr-2007

Cyclone Sidr was a tropical cyclone that resulted in one of the worst natural disasters in Bangladesh. An area of disturbed weather developed near the Andaman Islands on November 9. It gradually became better organised as it passed to the south of the islands, and the system was designated Depression BOB 09 by the India Meteorological Department early on November 11. The IMD upgraded the system to Cyclonic Storm Sidr early on November 12. The system then began to intensify quickly as it moved slowly northwestward, and the IMD upgraded it to a severe cyclonic storm later that day and a very severe cyclonic storm early the next day. On the morning of November 15, the cyclone intensified to reach peak winds of 215 km/h (135 mph) according to the IMD, and a peak of 260 km/h (160 mph) according to the JTWC. Sidr officially made landfall around 1700 UTC later that day, with sustained winds of 215 km/h (135 mph). Fig 3.10 shows the cyclone Sidr track. The storm eventually made landfall in Bangladesh on November 15, 2007, causing large-scale

evacuations. The number of deaths associated with the cyclone about ~ 15,000 and damaged was estimated at \$1.7 billion USD [76].

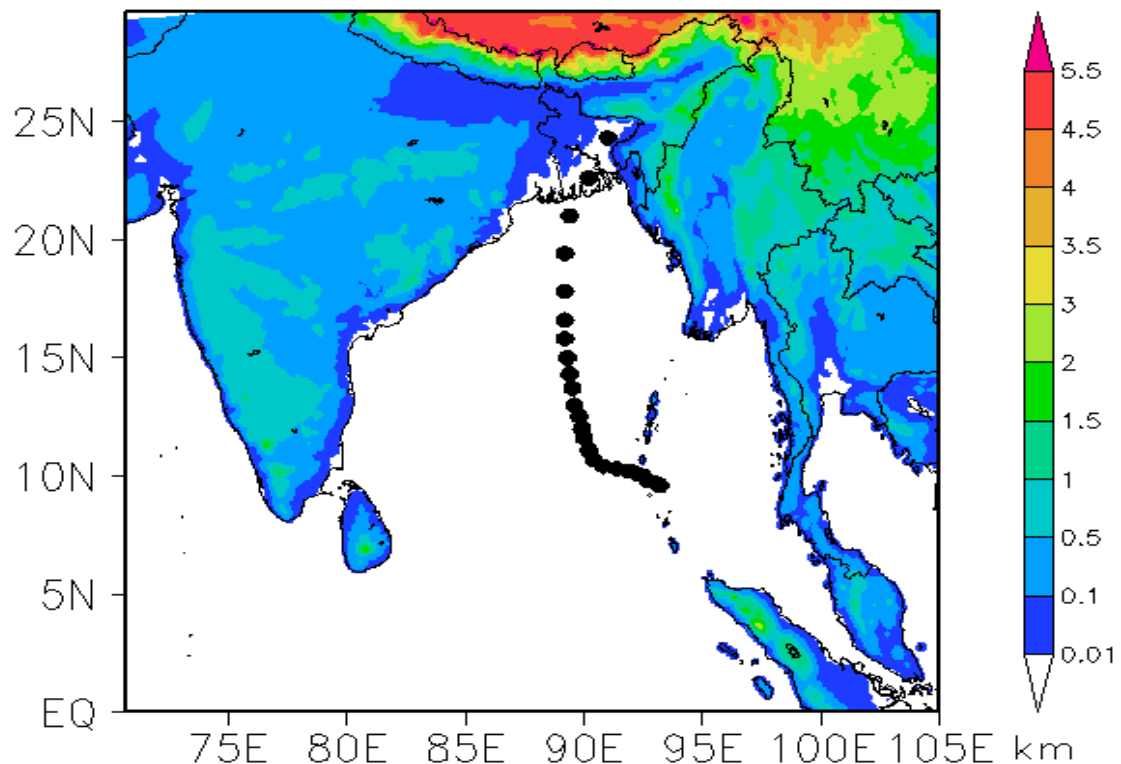


Fig 3.10: Track of Cyclone Sidr-2007

3.4.2.3 Giri-2010

Very Severe Cyclonic Storm Giri also known as Cyclone Giri was a powerful tropical cyclone which caused catastrophic damage in parts of Myanmar in late October 2010. Originating from an area of low pressure over the Bay of Bengal on October 19, the system began as a weak depression 250 km (155 mi) south of Myanmar. Over the following few days, the depression underwent explosive intensification, reaching its peak intensity with winds of 165 km/h (105 mph 3-minute sustained) on October 22. Cyclone Giri made landfall roughly 50 km (31 mi) northwest of Kyaukpyu, shortly after peaking. Within hours of moving onshore, the system had substantially weakened. By the following day, Giri had degenerated into a tropical depression and the final advisory was issued on the storm. The track of cyclone Giri was shown in fig 33. The storm claimed 157 lives in the country and left US\$359 million in damage [77].

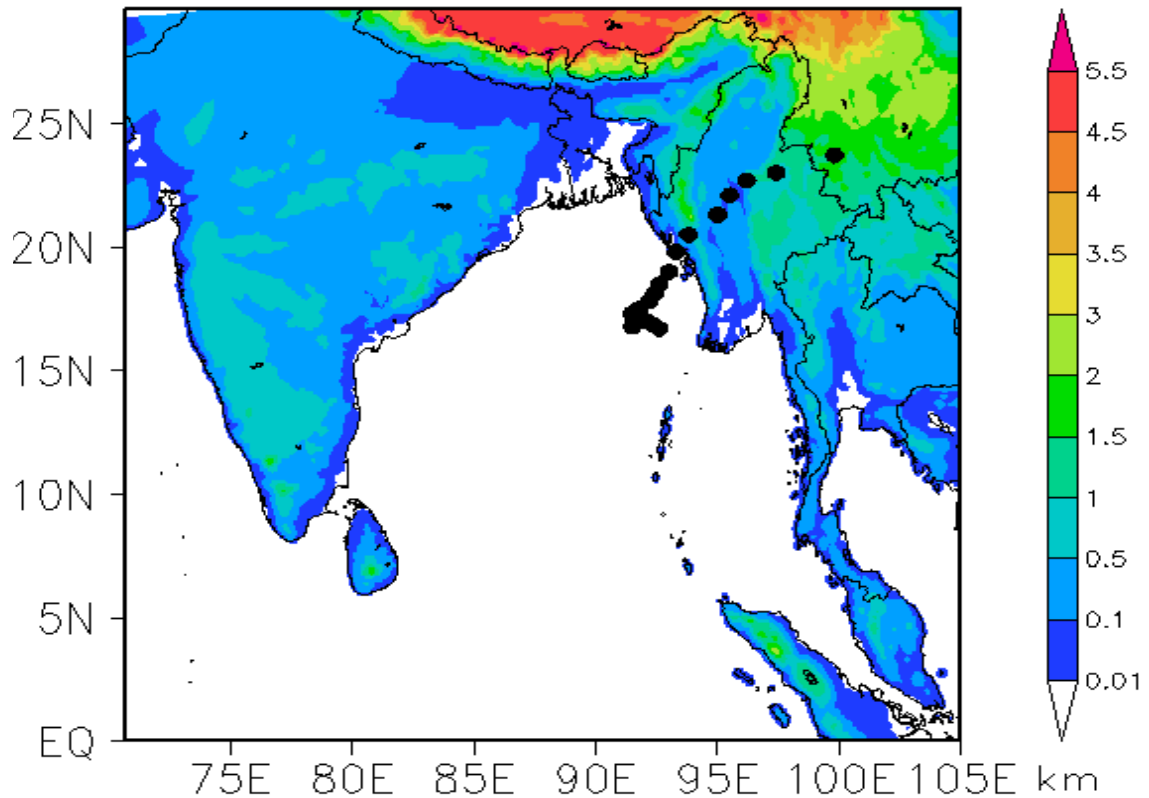


Fig 3.11: Track of Cyclone Giri-2010

3.4.2.4 Thane-2011

Very Severe Cyclonic Storm Thane also known as Cyclone Thane was the strongest tropical cyclone of 2011 within the North Indian Ocean. Thane initially developed as a tropical disturbance within the monsoon trough to the west of Indonesia. On December 25 depression was declared as Cyclonic Storm Thane. As it was named, Thane started to turn towards the west under the influence of a subtropical ridge of high pressure before its development slowed down during December 27 and became a Very Severe Cyclonic Storm during December 28. Thane then made landfall early on December 30, on the north Tamil Nadu coast between Cuddalore and Puducherry and rapidly weakened into a depression. Fig 3.12 shows the cyclone Thane track. Thane was responsible for the deaths of 46 people with total damage to India, estimated at between 235 – 275 million USD [78].

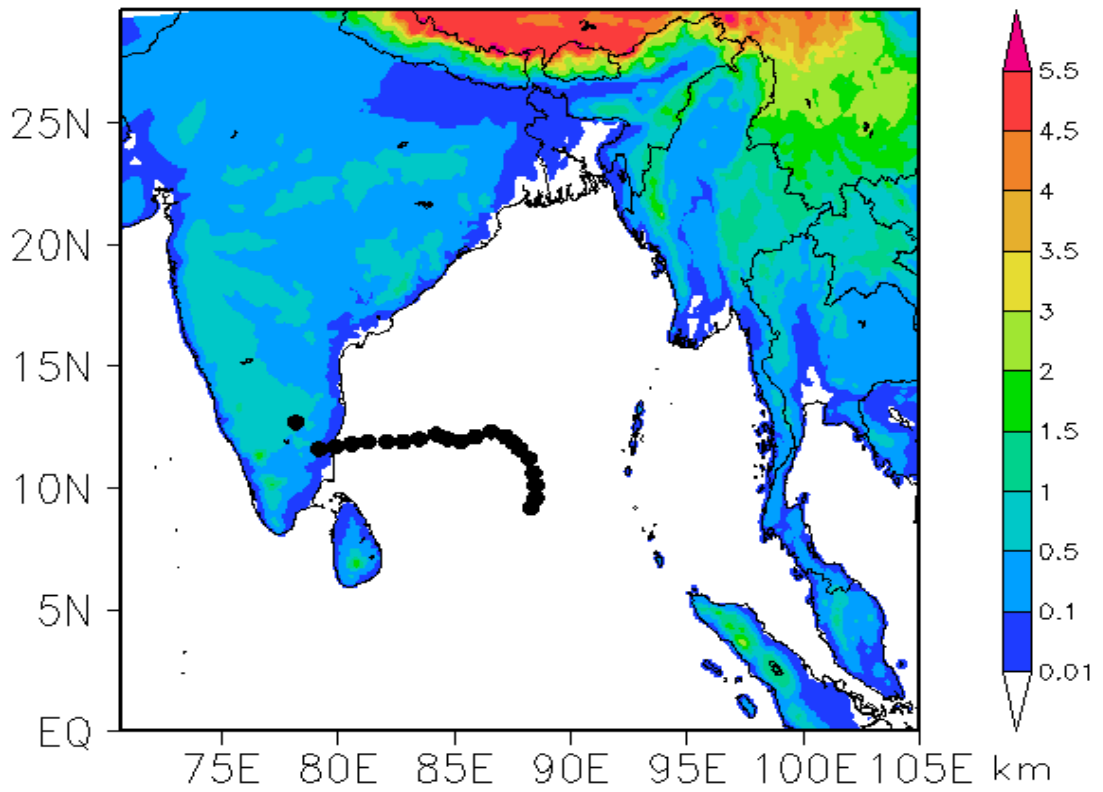


Fig 3.12: Track of Cyclone Thane-2011

Comprehensive information i.e. Cyclone formation time, landing time, intensity and damage or deaths about studied Cyclones are shown at Table 3.

Table 3: Summary of studied Cyclones information

	Cyclone Name	Formation Time	Landing Time	Cyclone Intensity (3-min sustained)	Damage or Death
Pre-monsoon	Cyclone 2004	0900 <u>UTC</u> May 16 2004	0300 UTC May 19, 2004	165 km/h (105 mph)	\$99.2 Million <u>USD</u>
	Mala 2006	0600 <u>UTC</u> April 24 2006	0600 <u>UTC</u> April 30, 2006	185 km/h (115 mph)	\$6.7 million <u>USD</u> , 37 died
	Akash 2007	1200 UTC April 12 2007	1500 UTC April 15, 2007	85 km/h (50 mph)	\$982 million USD, 14 died
	Nargis 2008	0300 <u>UTC</u> April 27 2008	0600 <u>UTC</u> May 03, 2008	165 km/h (105 mph)	\$12.9 billion USD, 146,000 died
	Aila 2009	1800 UTC May 23 2009	0900 UTC May 25, 2009	110 km/h (70 mph)	\$295.6 million <u>USD</u> , 339 died
	Laila 2010	0000 UTC May 18 2010	1200 UTC, May 21, 2010	100 km/h (65 mph)	\$117.49 million USD, 65 died
Post-monsoon	Cyclone 2000	0600 UTC November 26, 2000	0600 UTC November 30, 2000	190 km/h (115 mph)	\$15 million USD, 12 died
	Sidr 2007	1200 UTC November 11, 2007	0000 UTC, November 16, 2007	215 km/h (130 mph)	\$1.7 billion USD, 15,000 died
	Giri 2010	1800 UTC October 20 2010	0000 UTC, October 2 3, 2010	195 km/h (120 mph)	\$359 million USD, 157 died
	Thane 2011	1200 UTC December 25, 2011	0600 UTC, December 31, 2011	140 km/h (85 mph)	\$235 million USD, 48 died

3.5 Used Environmental Data

The following 12 environmental dynamic and thermodynamics parameters are considered for the study and their values are extracted from NCEP-CFSR data according to all JTWC (3-6 hourly) cyclone points and average all data in between two intensity level to relate with the change in intensity of cyclone.

1. Relative vorticity between 1000 to 850 hPa
2. Relative vorticity between 850 to 500 hPa
3. Moisture flux between 1000 to 850 hpa
4. Low level vertical wind shear between 1000 to 850 hPa
5. Sea Surface Temperature (SST)
6. Relative humidity at 500 hPa
7. Convective Available Potential Energy (CAPE) at surface
8. Convective Inhibition (CIN) at surface
9. Precipitable water (total depth of water upto the troposphere)
10. Geopotential thicknesss between 1000 to 200 hPa
11. Mean Sea Level Pressure (MSLP)

The above mentioned parameters are analyzed and compared for all pre-monsoon and post-monsoon cyclones.

3.6 Study Method

3.6.1 Environmental Data Collection Method

Cyclones has six intensity levels according to IMD scale. During each intensity level, the environmental conditions are checked which can affect the change of intensity. The various data are extracted and averaged from each intensity level. Area is selected for 5° X 5° horizontal scale centering the eye of the cyclone. From the center of eye it covers 2.5° area all around. Example is given in Fig. 3.13 where Sidr (2007) cyclone is used. Depression (≤ 27 Kt), Deep Depression (28-33 Kt), Cyclonic Storm (34-47 Kt), Severe Cyclonic Storm (48-63 Kt), Very Severe Cyclonic Storm (64-119), Super Cyclonic Storm (>120 Kt) are pointed out in the figure. For every (3-6) hourly position the different environment data are extracted for the area (5° X 5°) centered the location of eye. After that, the extracted values are averaged for each intensity levels i.e. environment between Depressions to Deep Depression is the environment for Deep Depression intensity level and so on. By this process environmental data values are collected and compared for all cyclones during each

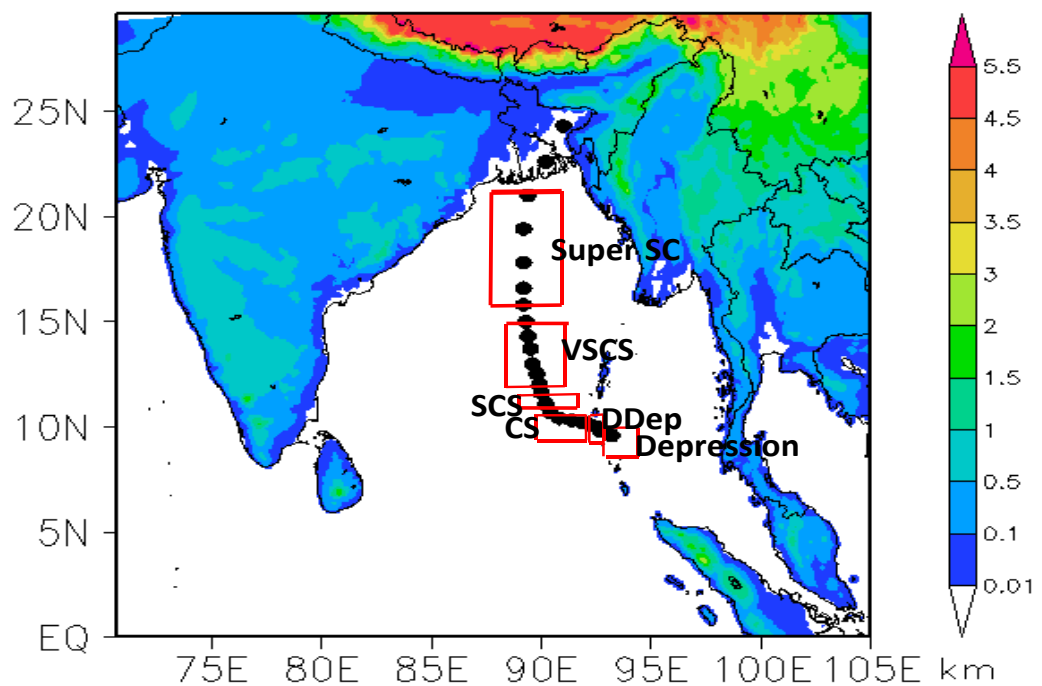


Fig 3.13: Example for extracting method for environmental data

3.6.2 Grid Analysis and Display System (GrADS)

The Grid Analysis and Display System Analysis (GrADS) are used for data extraction and display. The details of the application tool GrADS is given below:

The Grid Analysis and Display System Analysis (GrADS) is an interactive desktop tool that is used for easy access, manipulation, and visualization of earth science data. The format of the data may be either binary, GRIB, NetCDF, or HDF-SDS (Scientific Data Sets). GrADS has been implemented worldwide on a variety of commonly used operating systems and is freely distributed over the Internet. GrADS has a programmable interface (scripting language) that allows for sophisticated analysis and display applications. GrADS uses a 4-Dimensional data environment: longitude, latitude, vertical level, and time. Data sets are placed within the 4-D space by use of a data descriptor file. GrADS interprets station data as well as gridded data, and the grids may be regular, non-linearly spaced, Gaussian, or of variable resolution. Data may be displayed using a variety of graphical techniques: line and bar graphs, scatter plots, smoothed contours, shaded contours, streamlines, wind vectors, grid boxes, shaded grid boxes, and station model plots. Graphics may be output in PostScript or image formats. GrADS was used to draw the cyclone tracks, calculate the areal average of environmental parameters at different area and to display those parameters [79].

Chapter Four

Results

The environmental dynamic and thermodynamic parameters are analyzed structurally and numerically for 10 cyclones (6 pre-monsoon, 4 post-monsoon) formed during 2000 to 2011 using NCEP-CFSR data. It is to be mentioned that all pre-monsoon cyclones i.e. Cyclone (20004), Akash (2007), Nargis (20008), Aila (2009) and Laila (2010) has the maximum intensity up to VSCS except Mala (2006) which has more intense (Super SC) than other, whereas in post-monsoon, two cyclones i.e. cyclone (2000), Thane (2011) have the intensity of VSCS and other two cyclones have higher intensity of Super SC.

4.1 Dynamic parameters

4.1.1 Low level relative vorticity (1000-850 hPa)

Pre-monsoon Cyclones

Low level relative vorticity is the vorticity between 1000 hPa and 850 hPa. The spatial distribution of low-level relative are plotted during cyclone periods for each pre-monsoon cyclones in Fig 4.1. Average distribution of relative vorticity shows the positive vorticity over the BoB in all cases. Among them Akash (2007) and Aila (2009) have intense vorticity ($>16 \times 10^{-5} \text{ s}^{-1}$) than the others. Relative vorticity are averaged for total cyclone period in each case. The relative vorticity are varied among the cyclones. Maximum value found in cyclone Aila ($14 \times 10^{-5} \text{ s}^{-1}$) and cyclone Laila ($3 \times 10^{-5} \text{ s}^{-1}$) shows the minimum value. The average values of low level relative vorticities collected from each cyclone intensity for each pre-monsoon cyclone are shown in Fig 4.2. Data extract and average procedure are explained in section 3. The values for each cyclone are plotted individually in Fig 4.2 with increasing or decreasing trend line and co-efficient of determinant (R^2) value. However, for comparing all pre-monsoon cyclone together, the relative vorticity are plotted combinely in Fig 4.3. Initial vorticity values during depression are found different in each case i.e. formation of cyclone does not depends on the

particular value of relative vorticity however, values are increasing with the change of intensity. Almost all cyclone shown positively increasing trends from the lowest (Depression) to the highest intensity (VSCS/Super CS). In case of Cyclone (2004), Akash (2007) and Mala (2006) the trend are increasing, however, at the highest level the values for pre-monsoon cyclones are relatively lower ($\sim 2 \times 10^{-5} \text{ s}^{-1}$) from the previous intensity.

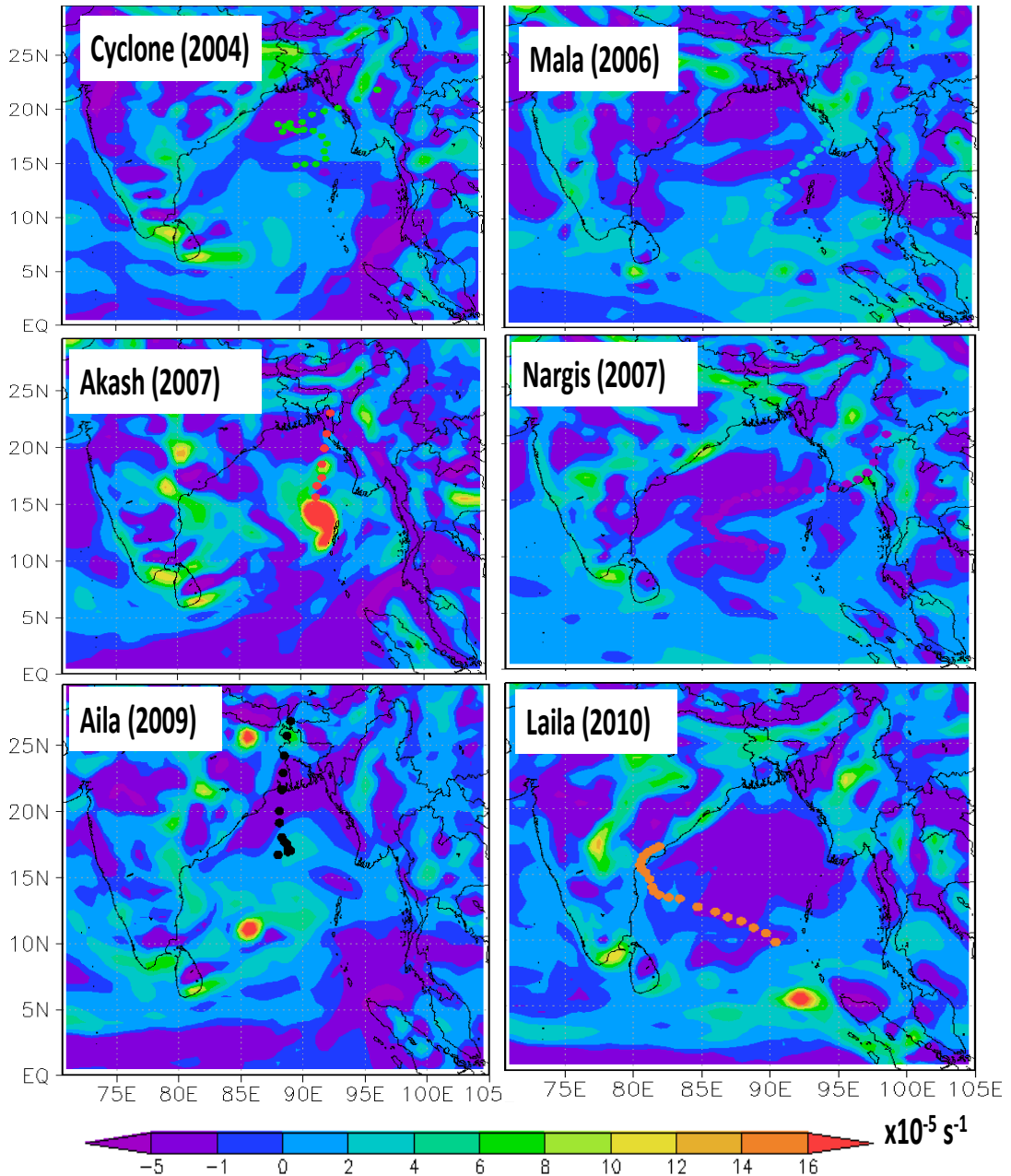


Fig 4.1: Spatial distribution of average low level relative vorticity ($\times 10^{-5} \text{ s}^{-1}$) during cyclone period of each pre-monsoon cyclones.

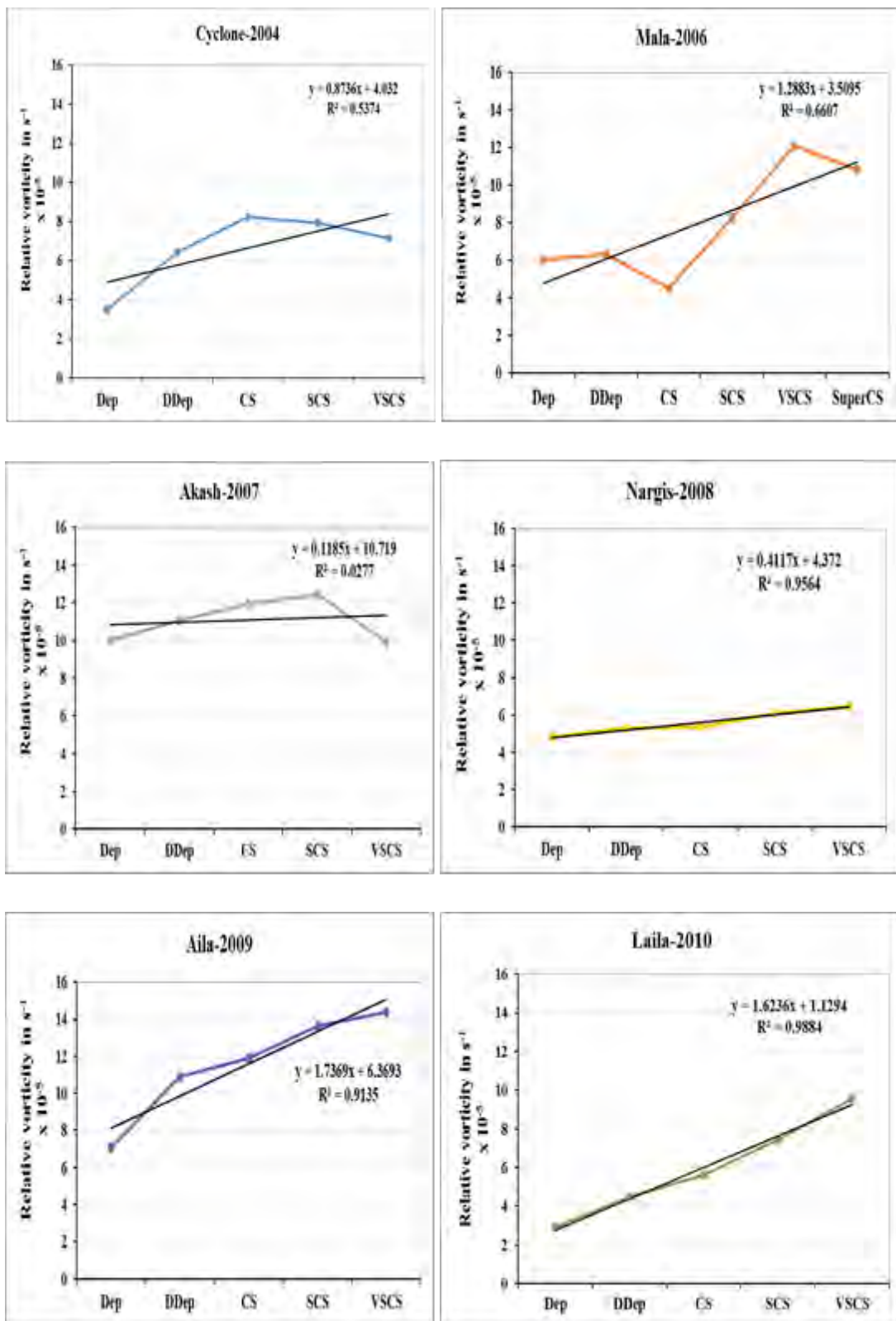


Fig 4.2: Relative vorticity (1000-850 hpa) for individual pre-monsoon cyclone.

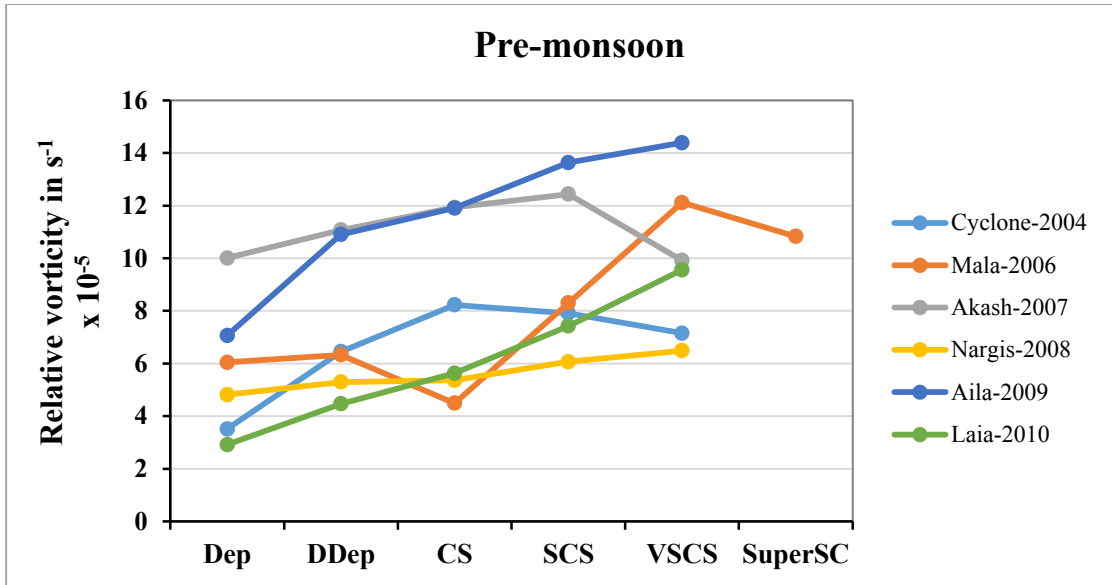


Fig 4.3: Low level relative vorticity for pre-monsoon cyclones.

For all graphs, coefficient of determination (R^2 value) is calculated and found significance i.e. for pre-monsoon cyclones it has the value ≥ 0.53 except for Akash which has the value 0.02. The value of relative vorticity at VSCS is very less in Akash which lowers the R^2 value.

Characteristics of low level relative vorticity is summarized in Table 4. Highest, lowest and average value of relative vorticity for all pre-monsoon cyclones are calculated along with average percentage increment from initial intensity level to highest intensity level.

From the Table 4, we found that the average low level relative vorticity varied from 5.4×10^{-5} to $10.53 \times 10^{-5} \text{ s}^{-1}$ for pre-monsoon cyclones. The average value of all the pre-monsoon cyclone is found $8.16 \times 10^{-5} \text{ s}^{-1}$. The average increment per intensity level is found $0.9 \times 10^{-5} \text{ s}^{-1}$ i.e. the average relative vorticity increases 17.9% from each level in case of pre-monsoon cyclones.

Table 4: Characteristics of low level relative vorticity for pre-monsoon cyclones

Pre-monsoon Cyclones	Lowest value (s ⁻¹) X 10 ⁻⁵	Highest value (s ⁻¹) X 10 ⁻⁵	Average value (s ⁻¹) X 10 ⁻⁵	Average increment/ decrement per intensity level	
				s ⁻¹ X 10 ⁻⁵	%
Cyclone 2004	3.515	8.226	6.653	0.909	24.417
Mala 2006	4.491	12.116	8.019	0.957	19.167
Akash 2007	9.920	12.437	11.074	-0.023	0.592
Nargis 2008	4.817	6.491	5.607	0.418	7.830
Aila 2009	7.067	14.387	11.580	1.830	20.877
Laila 2010	2.990	9.559	6.0	1.660	34.927
Average for all pre-monsoon cyclones	5.455	10.536	8.155	0.959	17.969

Post-monsoon Cyclones

The spatial distribution of low level relative vorticity for all post-monsoon cyclone are plotted in Fig 4.4. Relative vorticity are average for total cyclone period in each case. The relative vorticity are varied among the cyclones. Average relative vorticity is found intense for Cyclone (2000). In other cases positive vorticity is prominent. The average value of low level relative vorticity with cyclones intensity for individual post-monsoon cyclone shown in Fig 4.5. Except few points all post-monsoon cyclones shown positively increasing trends for low level relative vorticity. Sidr (2007), Giri (2010) and Thane (2011) shows some fluctuations, however, in

Thane (2011) the highest intensity level value is relatively lower ($\sim 1 \times 10^{-5} \text{ s}^{-1}$) from the previous intensity level. For Cyclone (2000), little fluctuation has been observed in graph. The reason of the highest value in Deep Depression level will be explained in the discussion chapter.

The combined figure of relative vorticity for post-monsoon cyclones is shown in the Fig. 4.6. Relative vorticity increases with intensity change from the lowest intensity level (Dep) to the highest intensity level (VSCS/SuperCS) but each cyclone has different relative vorticity at each intensity level

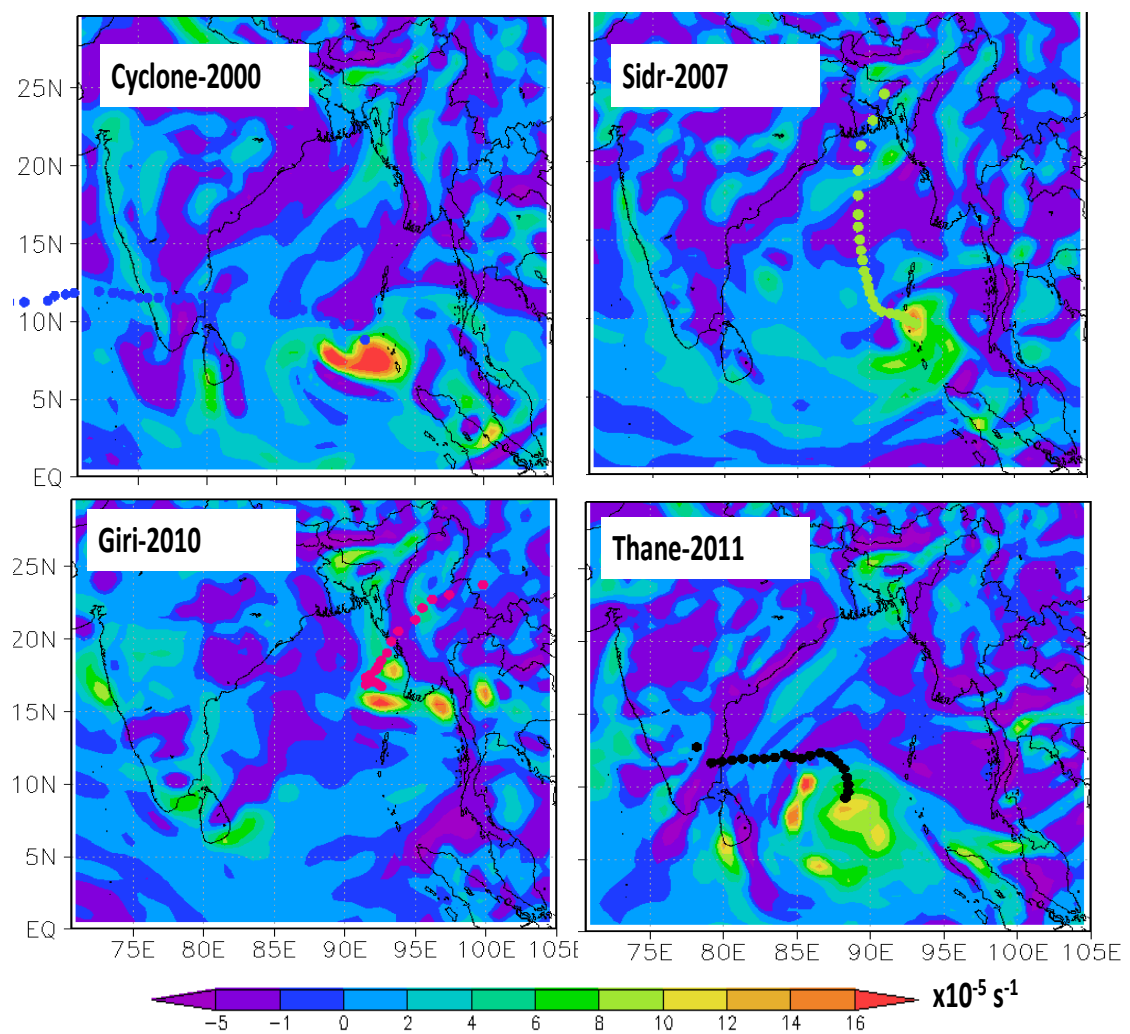


Fig 4.4: Spatial distribution of average low level relative vorticity ($\times 10^{-5} \text{ s}^{-1}$) during cyclone period of each post-monsoon cyclone.

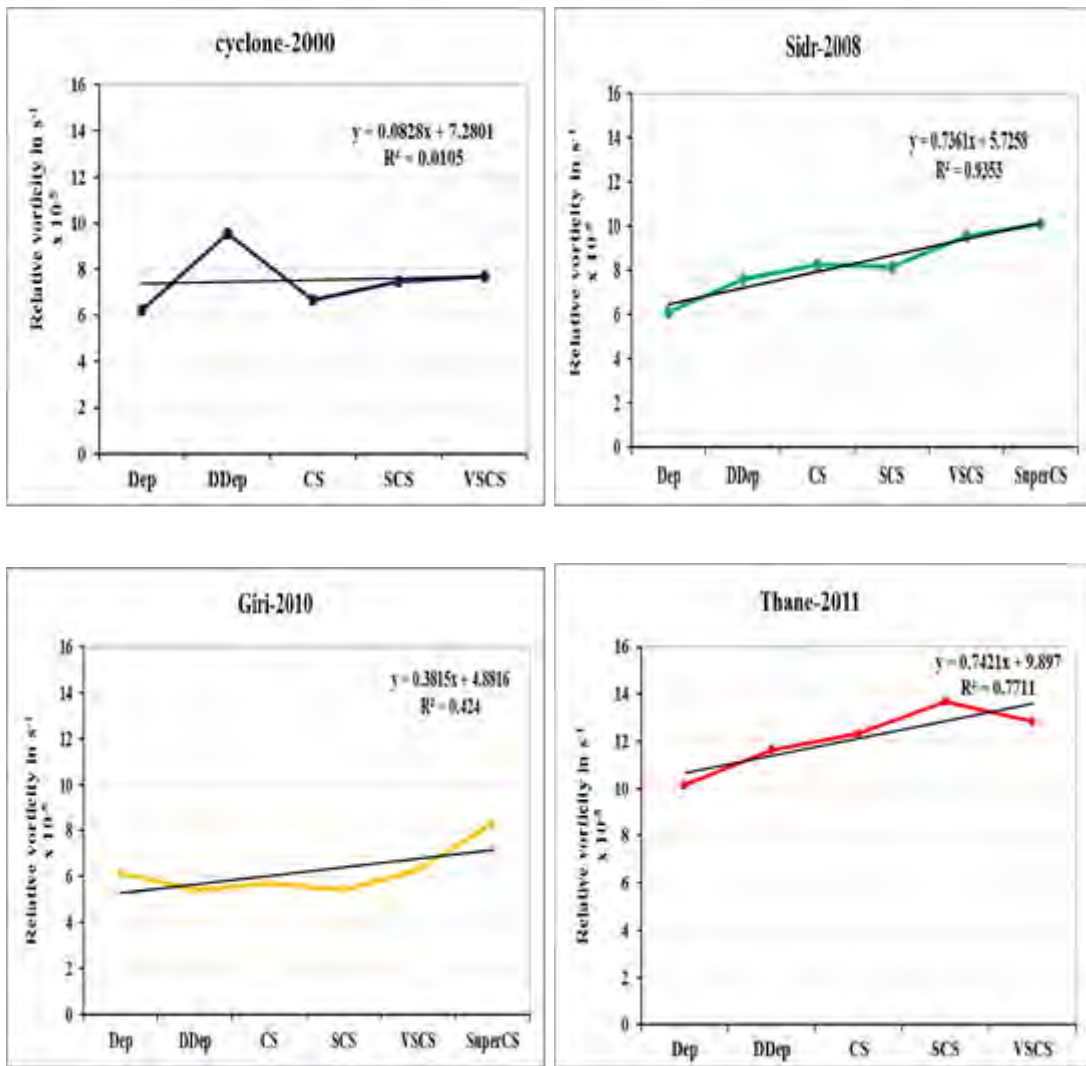


Fig 4.5: Relative vorticity (1000-850hPa) for individual post-monsoon cyclone

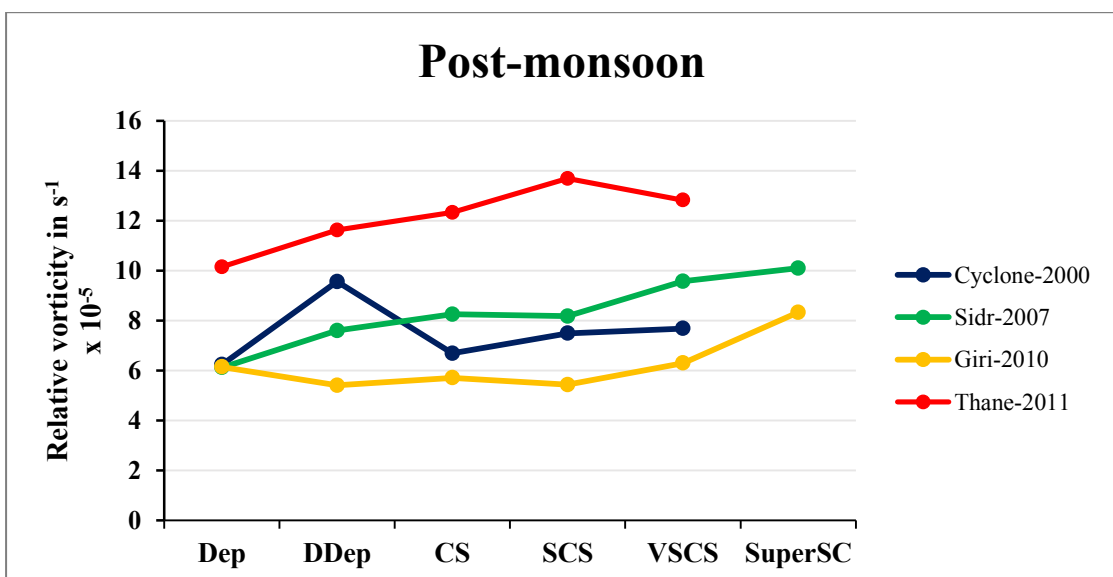


Fig 4.6: Low level relative vorticity for post-monsoon cyclones

The coefficient of determination (R^2 value) is found significant for Sidr (2007) and Thane (2011) with the value ≥ 0.7 . Giri (2010) has the R^2 of almost 0.4. However R^2 value for Cyclone (2000) is 0.01 because of fluctuation of relative vorticity of DDep.

From the following Table 5, compact scenario of relative vorticity change is found. Highest, lowest and average value of relative vorticity for all post-monsoon cyclones are calculated along with the average percentage increment from initial intensity level to highest intensity level.

Average low level relative vorticity for each post-monsoon cyclone varied from 6.97×10^{-5} to $10.42 \times 10^{-5} \text{ s}^{-1}$ with an overall average value of $8.54 \times 10^{-5} \text{ s}^{-1}$ shown in Table 5. In case of post-monsoon cyclones average increment of relative vorticity per intensity level is calculated $0.57 \times 10^{-5} \text{ s}^{-1}$ which means the average relative vorticity increases 8.53% from each intensity level.

Low level relative vorticity for both pre- and post-monsoon cyclone shows positively increasing trends. Average values of relative vorticity for both period were almost same (8.15×10^{-5} and $8.5 \times 10^{-5} \text{ s}^{-1}$). Value of relative vorticity varies from approximately 6 to $12 \times 10^{-5} \text{ s}^{-1}$ for both season. However average percentage increment per intensity level for pre-monsoon cyclones was 17.9% which was almost double from post-monsoon average value (8.53%). Except pre-monsoon cyclone Akash (2007), the average increment per intensity level for pre-monsoon TCs always shows higher value than for post-monsoon TCs.

Table 5: Characteristics of low level relative vorticity for post-monsoon cyclones

Post-monsoon Cyclones	Lowest value (s^{-1}) $\times 10^{-5}$	Highest value (s^{-1}) $\times 10^{-5}$	Average value (s^{-1}) $\times 10^{-5}$	Average increment/decrement per intensity level	
				s^{-1} $\times 10^{-5}$	%
Cyclone 2000	6.232	9.558	7.528	0.362	9.478
Sidr 2007	6.116	10.10	8.302	0.0797	10.902
Giri 2010	5.401	8.326	6.217	0.437	7.394
Thane 2011	10.148	13.69	12.123	0.669	6.333
Average for all post-monsoon cyclones	6.974	10.418	8.542	0.566	8.527

Fig 4.7 shows the average value of low level relative vorticity (1000-850 hPa) with cyclones. Values of low level relative vorticity are positive and increasing nature in case of pre- and post-monsoon cyclones. Average value of relative vorticity are fluctuate minimum $5 \times 10^{-5} s^{-1}$ to maximum $12 \times 10^{-5} s^{-1}$, with an average value about $8 \times 10^{-5} s^{-1}$ where post-monsoon cyclone Thane (2011) shows maximum value and pre-monsoon cyclone Nargis (2009) shows minimum value.

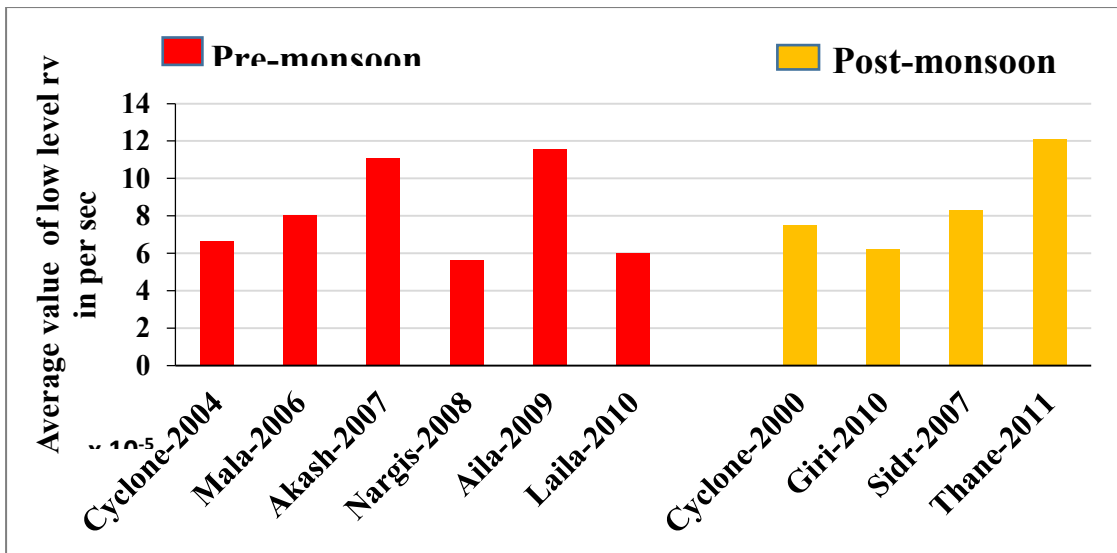


Fig 4.7 : Average value of low level relative vorticity (1000-850 hPa) during studied cyclones period.

The average increment of low level relative vorticity (%) per intensity level with studied cyclones shows in Fig 4.8. Low level relative vorticity shows positive increment per intensity level for all cyclones.

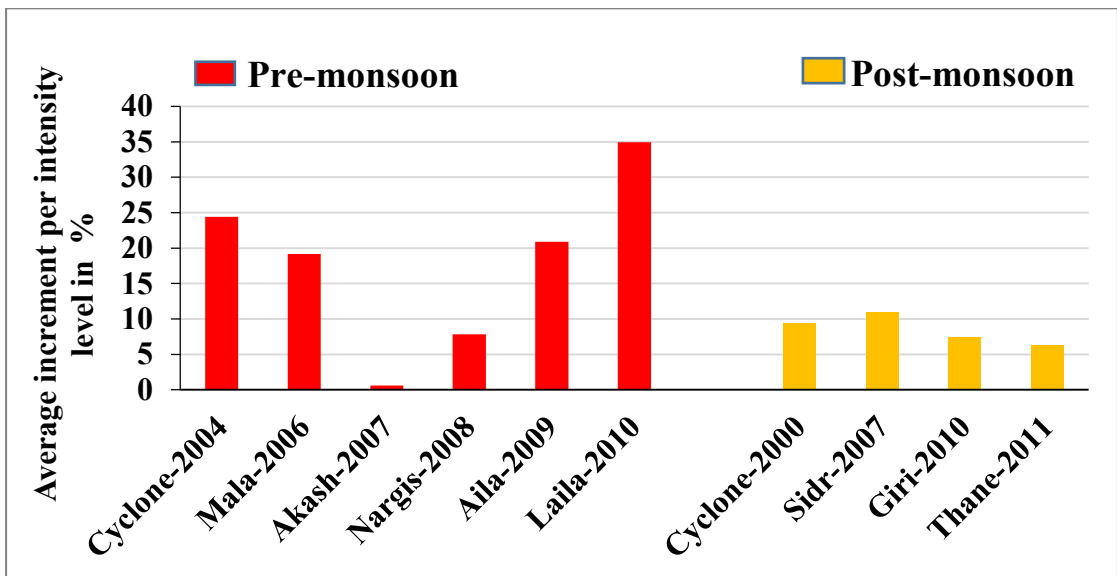


Fig 4.8: Average increment per intensity level of relative vorticity (%) at low level (1000-850 hPa) for all studied cyclones.

Average increment per intensity level is 18% in case of pre-monsoon cyclones and 9% in case of post-monsoon cyclones, which is almost half than pre-monsoon.

4.1.2 Mid-tropospheric relative vorticity (850-500 hPa)

Pre-monsoon cyclones

Mid-tropospheric relative vorticity is considered as the average vorticity between 850 hPa to 500 hPa. Fig 4.9 shows the spatial distribution of mid-tropospheric relative vorticity for all pre-monsoon cyclones. Mala (2006) and Aila (2009) shows higher relative vorticity than other cyclones. In other cases positive relative vorticity is dominated for all cyclones. Fig 4.10 and 4.11 shows the average values of relative vorticity with intensity change for individual pre-monsoon cyclones and all pre-monsoon cyclone together respectively. Here relative vorticity varies from the minimum value of $2 \times 10^{-5} \text{ s}^{-1}$ to maximum value of $12 \times 10^{-5} \text{ s}^{-1}$, this range of variation is favorable for cyclone intensification. Relative vorticity at 850-500 hPa shows positively increasing trend with cyclone intensity for all pre-monsoon cyclone except some points. Cyclone (2004), Mala (2006) and Akash (2007) shows increasing trend, however, at the highest intensity level vorticities are relatively lower ($\sim 1 \times 10^{-5} \text{ s}^{-1}$) than previous intensity level.

Coefficient of determination (R^2 value) has been calculated and found significant i.e. ≥ 0.7 for all pre-monsoon cyclones except Akash which has value 0.4.

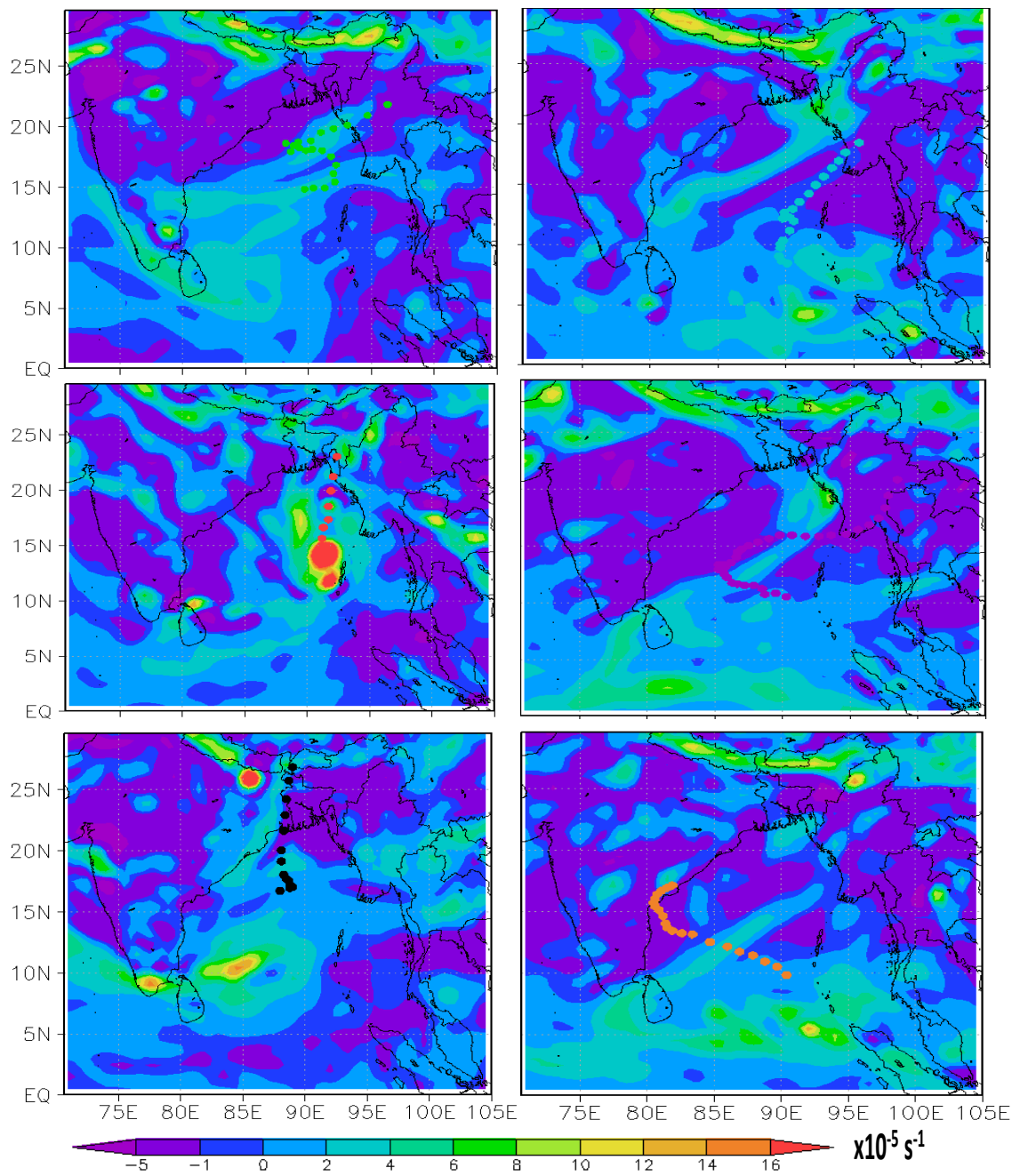


Fig 4.9: Spatial distribution of mid level (850-500 hPa) relative vorticity ($\times 10^{-5} \text{ s}^{-1}$) during cyclone periods of each pre-monsoon cyclones.

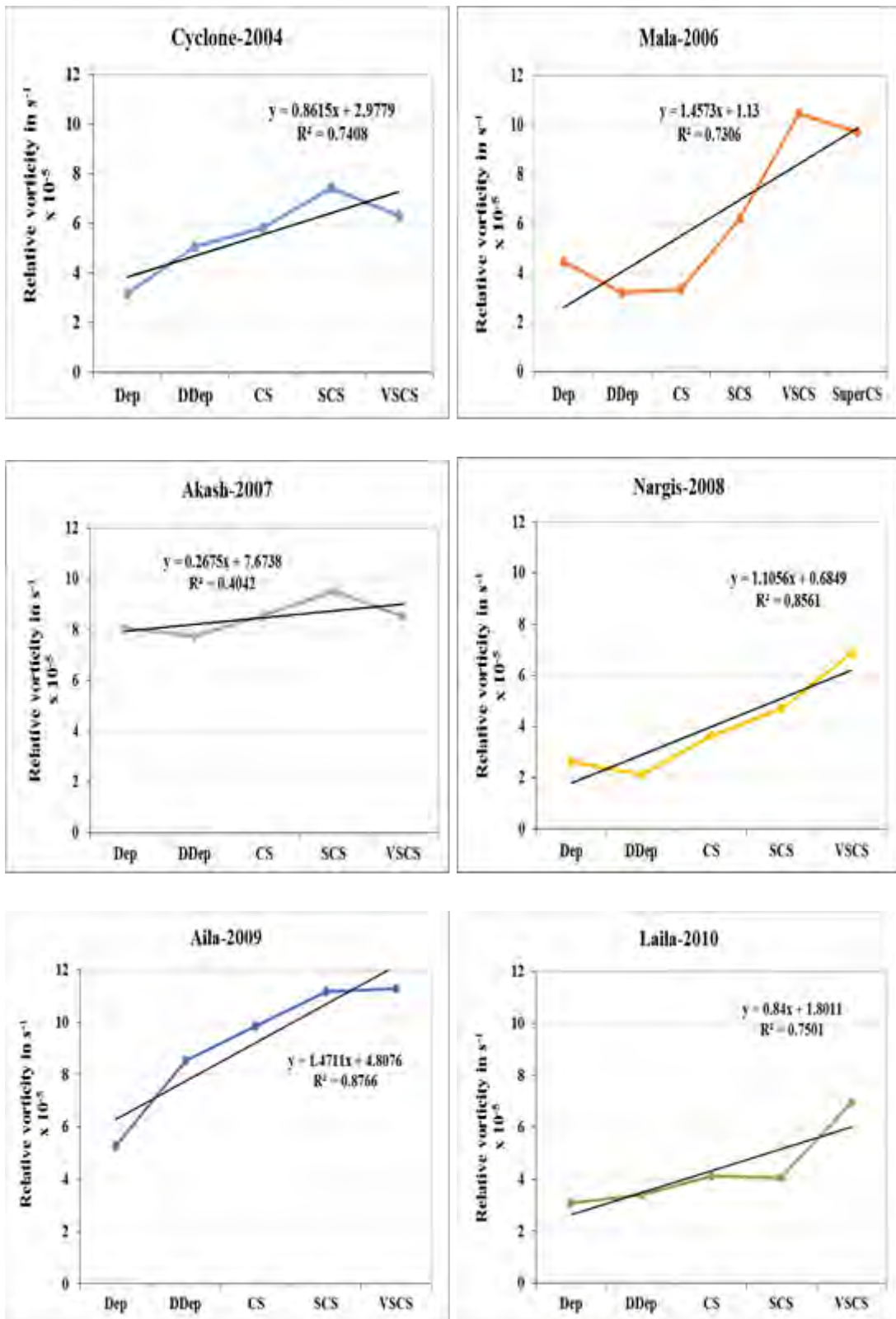


Fig 4.10: Relative vorticity (850-500 hpa) for individual pre-monsoon cyclone.

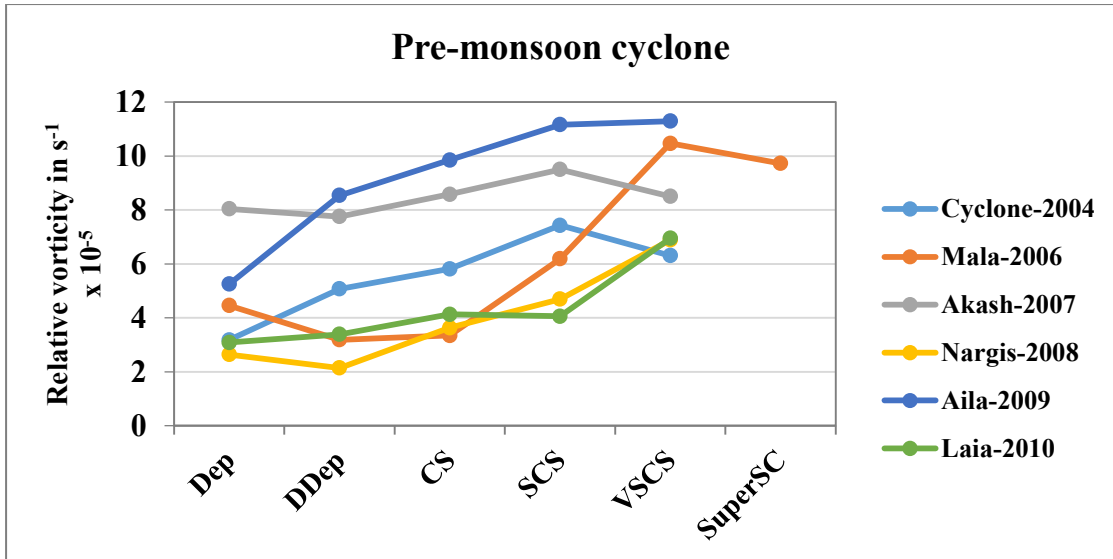


Fig 4.11: Mid-tropospheric relative vorticity for pre-monsoon cyclones.

Characteristic of relative vorticity for pre-monsoon cyclone shown in Table 6. From the Table 6, we found that the average mid-tropospheric relative vorticity varied from 4.13×10^{-5} to $8.8 \times 10^{-5} s^{-1}$ with an average value $6.32 \times 10^{-5} s^{-1}$ for all cyclones. Averages of the highest and lowest value of relative vorticity for all cyclones are indicated increasing trend from initial intensity level to final intensity level. The average increment per intensity level is found $0.915 \times 10^{-5} s^{-1}$ means average relative vorticity increases 21.4% from each intensity level in case of pre-monsoon cyclones.

Table 6: Characteristic of mid-tropospheric relative vorticity for pre-monsoon cyclones

Pre-monsoon Cyclones	Lowest value (s ⁻¹) X 10 ⁻⁵	Highest value (s ⁻¹) X 10 ⁻⁵	Average value (s ⁻¹) X 10 ⁻⁵	Average increment/decrement per intensity level	
				(s ⁻¹) X 10 ⁻⁵	%
Cyclone 2004	3.181	7.429	5.562	0.782	21.703
Mala 2006	3.349	10.47	6.231	1.053	24.674
Akash 2007	7.753	9.499	8.476	0.116	1.836
Nargis 2008	2.144	6.893	4.002	1.063	31.667
Aila 2009	5.254	11.295	9.221	1.51	23.097
Laila 2010	3.084	6.947	4.321	0.966	25.299
Average for all pre-monsoon cyclones	4.127	8.755	6.302	0.915	21.379

Post-monsoon cyclones

The spatial distribution of mid-tropospheric relative vorticity are plotted for pre-monsoon cyclones in Fig 4.12. In all cases, positive vorticity is prominent over BoB. Maximum value of relative vorticity found in cyclone Thane (2011) and minimum in cyclone Giri (20100). Again Fig 4.13 shows how mid-tropospheric relative vorticity are varied with individual post-monsoon cyclones intensity change. Fig 4.14 shows all post-monsoon cyclones trend together.

In case of Sidr (2008) and Giri (2010) the trends are increasing. For cyclone (2000) and Thane (2011), little fluctuation has been observed in graph, however, for Thane the value in highest intensity level is relatively lower ($0.5 \times 10^{-5} \text{ s}^{-1}$) than previous intensity level.

For all cases, coefficient of determination (R^2 value) are found significance i.e. for all post-monsoon cyclones the value is ≥ 0.5 .

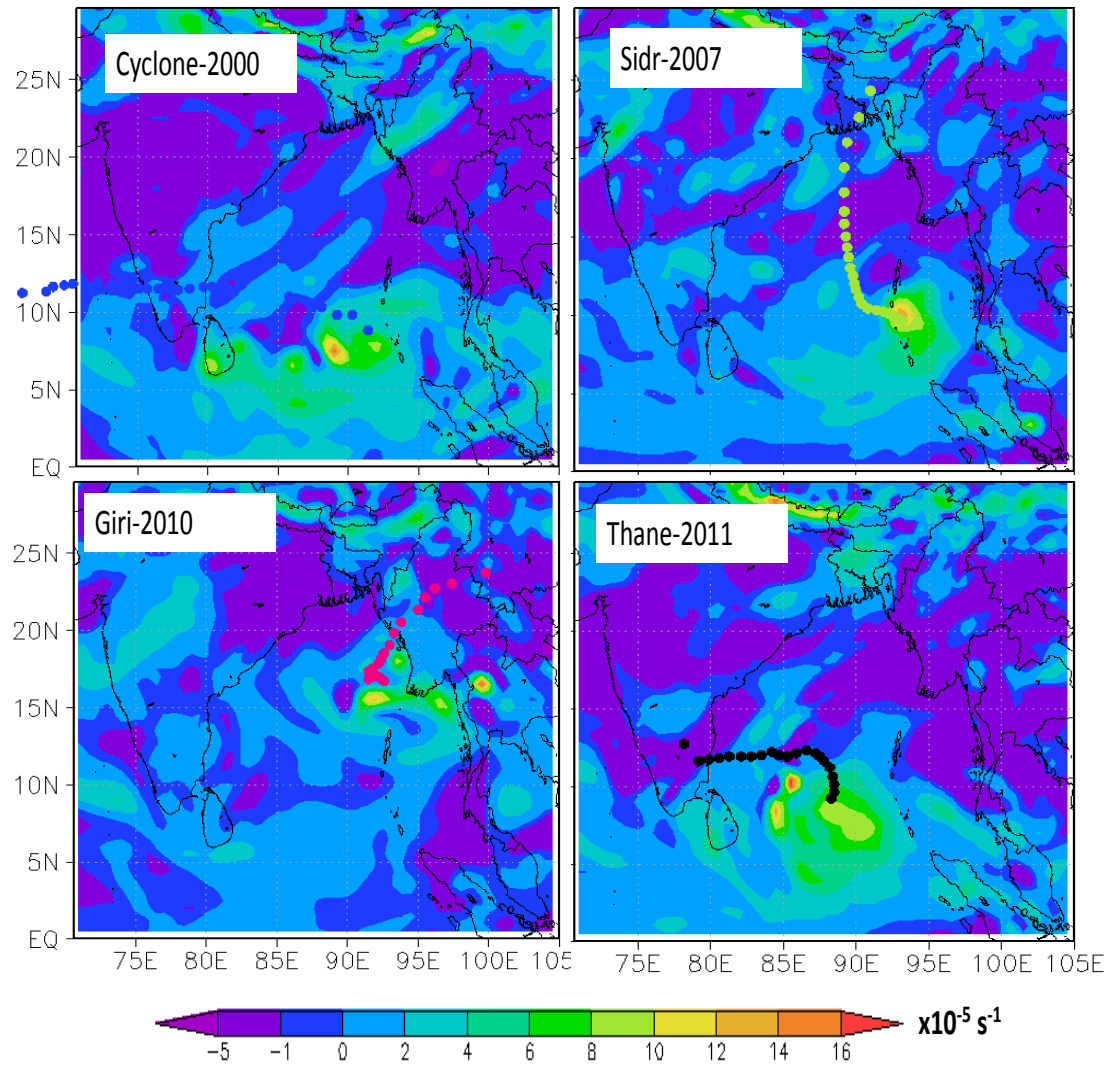


Fig 4.12: Spatial distribution of mid level (850-500 hPa) relative vorticity ($\times 10^{-5} \text{ s}^{-1}$) during cyclone periods of each post-monsoon cyclones.

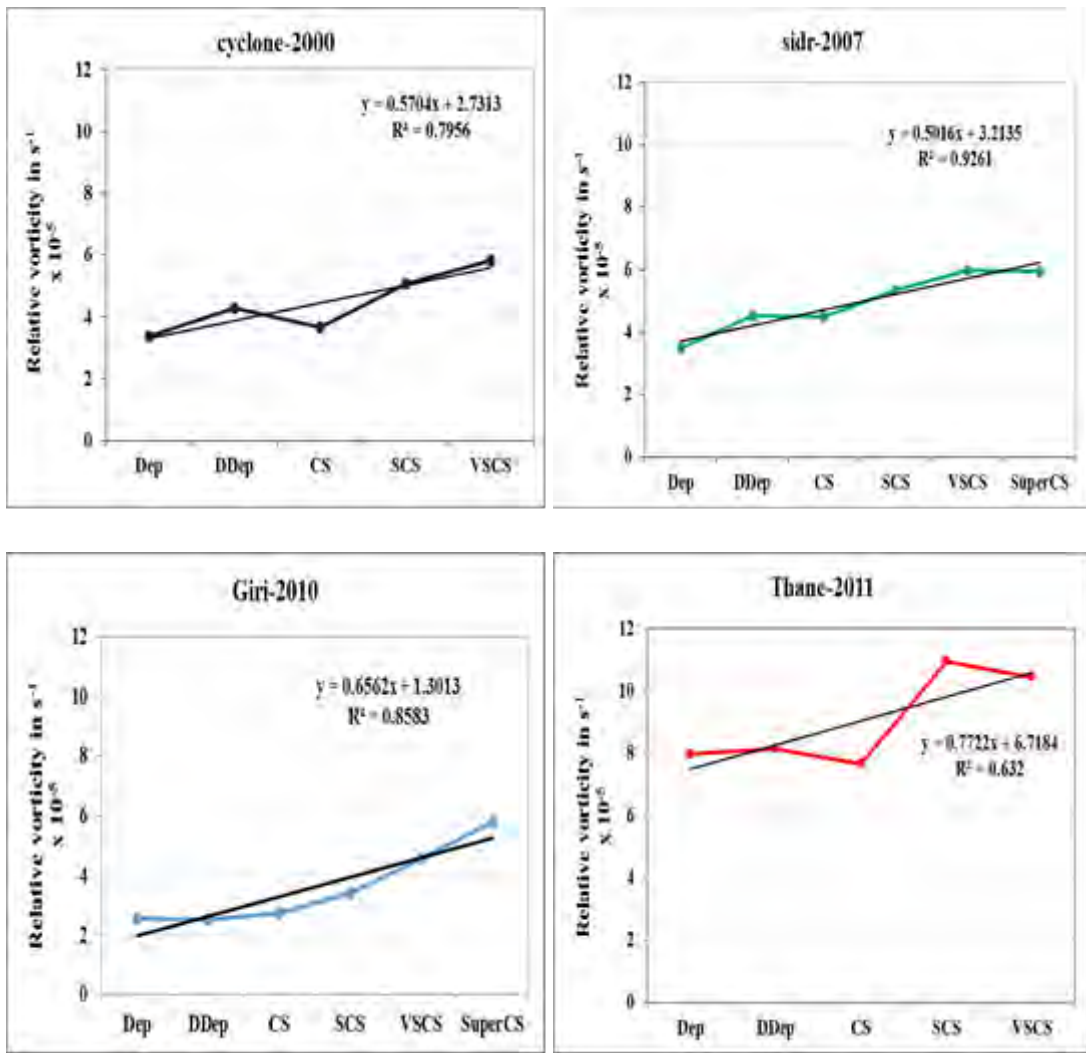


Fig 4.13: Relative vorticity (850-500 hPa) for individual post-monsoon cyclone

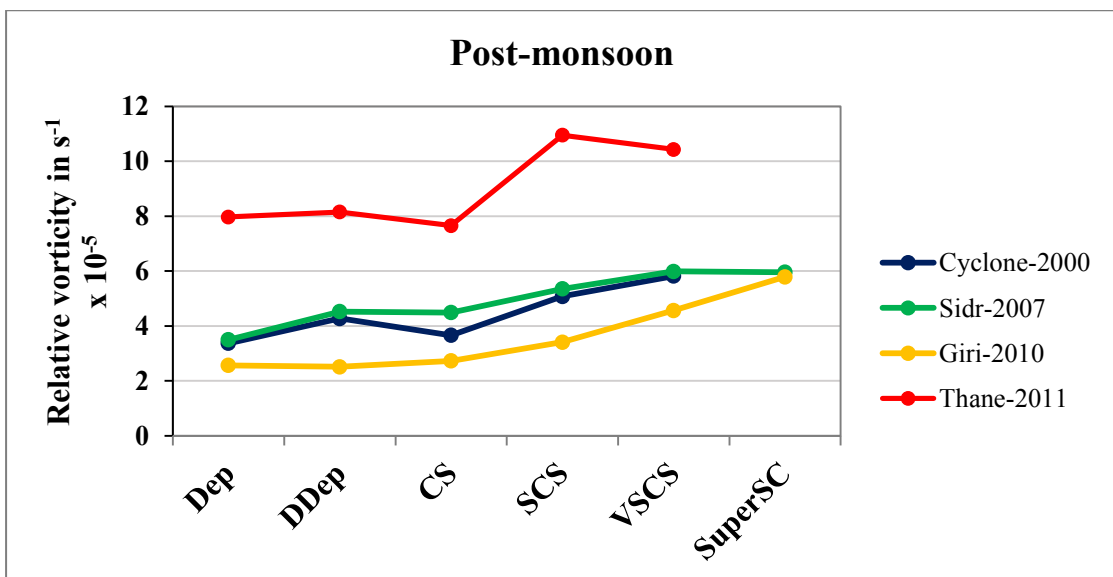


Fig 4.14: Mid-tropospheric relative vorticity for post-monsoon cyclones.

Overall summary of mid-level relative vorticity for post-monsoon cyclones is shown in Table 7. From the Table 7, found that average mid-tropospheric relative vorticity varied from 4.3×10^{-5} to $7.14 \times 10^{-5} \text{ s}^{-1}$ in each cyclones, with an average value of $5.51 \times 10^{-5} \text{ s}^{-1}$ for post-monsoon cyclones. The average increment per intensity level is found $0.6 \times 10^{-5} \text{ s}^{-1}$ which means that it increases 13.82 % for each level in case of post-monsoon cyclones.

Table 7: Characteristics of mid-tropospheric relative vorticity for post-monsoon cyclones

Post-monsoon Cyclones	Lowest value (s^{-1}) $\times 10^{-5}$	Highest value (s^{-1}) $\times 10^{-5}$	Average value (s^{-1}) $\times 10^{-5}$	Average increment/decrement per intensity level	
				s^{-1} $\times 10^{-5}$	%
Cyclone 2000	3.372	5.821	4.443	0.612	16.427
Sidr 2007	3.499	5.987	4.969	0.492	11.835
Giri 2010	2.515	5.791	3.598	0.644	18.43
Thane 2011	7.659	10.953	9.035	0.615	8.621
Average for all post-monsoon cyclones	4.261	7.138	5.511	0.591	13.828

Mid-tropospheric (850-500 hPa) relative vorticity for both pre- and post-monsoon cyclones shows positively increasing trends. Average values of relative vorticity for pre-monsoon cyclones is greater than post-monsoon cyclones. Relative vorticity averagely varies from $4-8 \times 10^{-5} \text{ s}^{-1}$ for both season. Average increment with per intensity level for pre-monsoon cyclones (0.9 s^{-1} or 21.38 %) is higher than post-monsoon cyclones (0.59 s^{-1} or 13.83 %).

Changes of average mid level relative vorticity (850-500 hPa) with cyclones shows in Fig 4.15. Mid level relative vorticity also shows positive increasing nature for all cyclones. In this case average relative vorticity fluctuate minimum $3.5 \times 10^{-5} \text{ s}^{-1}$ to maximum $9.5 \times 10^{-5} \text{ s}^{-1}$ with an average $6 \times 10^{-5} \text{ s}^{-1}$. Pre-monsoon cyclone Aila (2009) has maximum relative vorticity and post-monsoon cyclone Giri (2010) has minimum relative vorticity value.

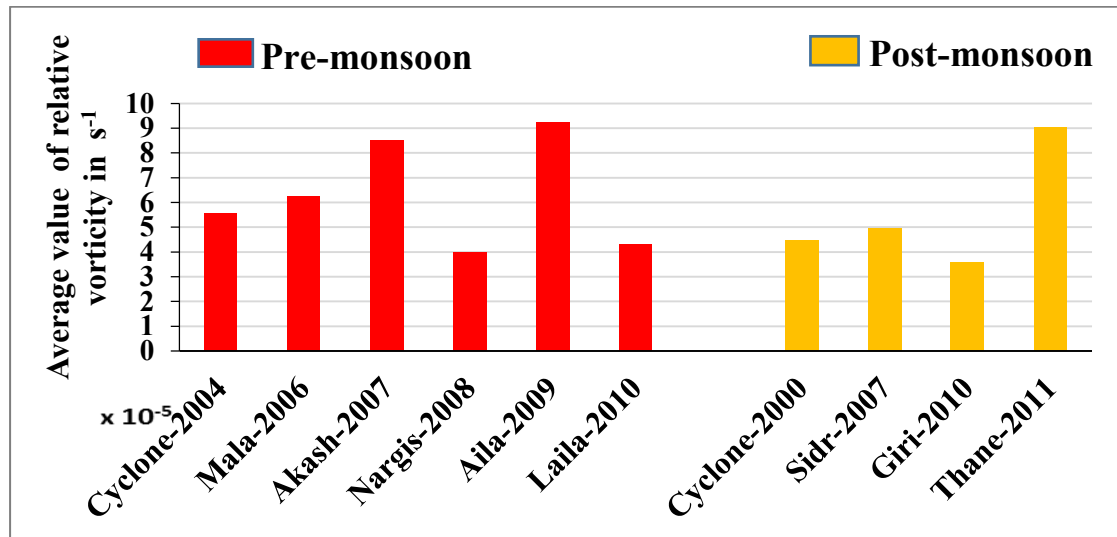


Fig 4.15: Average value of mid level relative vorticity (850-500 hPa) during cyclones period.

Again Fig 4.16 shows the average increment per intensity level of mid level relative vorticity (%) with cyclones.

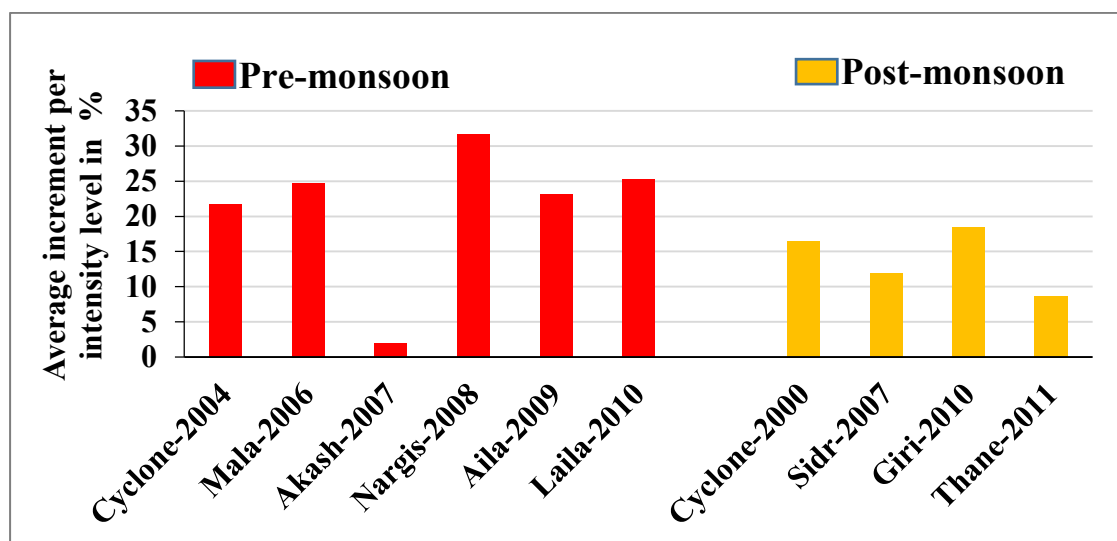


Fig 4.16: Average increment per intensity level of relative vorticity (%) at mid level (850-500 hPa) for all cyclones.

Average increment of mid level relative vorticity per intensity level in case of pre-monsoon cyclone is 22 % and post-monsoon cyclone is 14 %.

The average value of relative vorticity at low and mid level are found positive for all cyclones. Increment of relative vorticity per intensity level in case of pre-monsoon is higher than that of post-monsoon in both levels. However, mid level increment value is higher than low level value. This is the reason for bottom-up process, which incorporates cycles of deep, moist convective activity called vertical hot towers (VHTs), where the lower-tropospheric vortices are formed within the embryonic environment of MCVs. The combined effect of the upscale growth of cyclonic vortices and their integration contributes to the development of the TC vortex [66].

4.1.3 Low level vertical wind shear (1000-850 hPa)

Pre-monsoon cyclones

Vertical wind shear (VWS) is the most important factor for the cyclone formation and intensification. The spatial distribution of low level VWS are plotted for all pre-monsoon cyclones in Fig 4.17. VWS are averaged for total cyclone period in each case. Intensity of VWS of all cyclones are randomly distributed because it is the average of the cyclone period of each case. However, Mala (2006) and Nargis (2008) have higher intensity of VWS in the middle of BoB and Cyclone (2004) has intense VWS in the south west of the BoB, Other cyclones have less VWS. The variation of low level VWS along with pre-monsoon cyclone intensity change shows in Fig 4.18 and Fig 4.19. Low level VWS are the average of the 1000-850 hPa level.

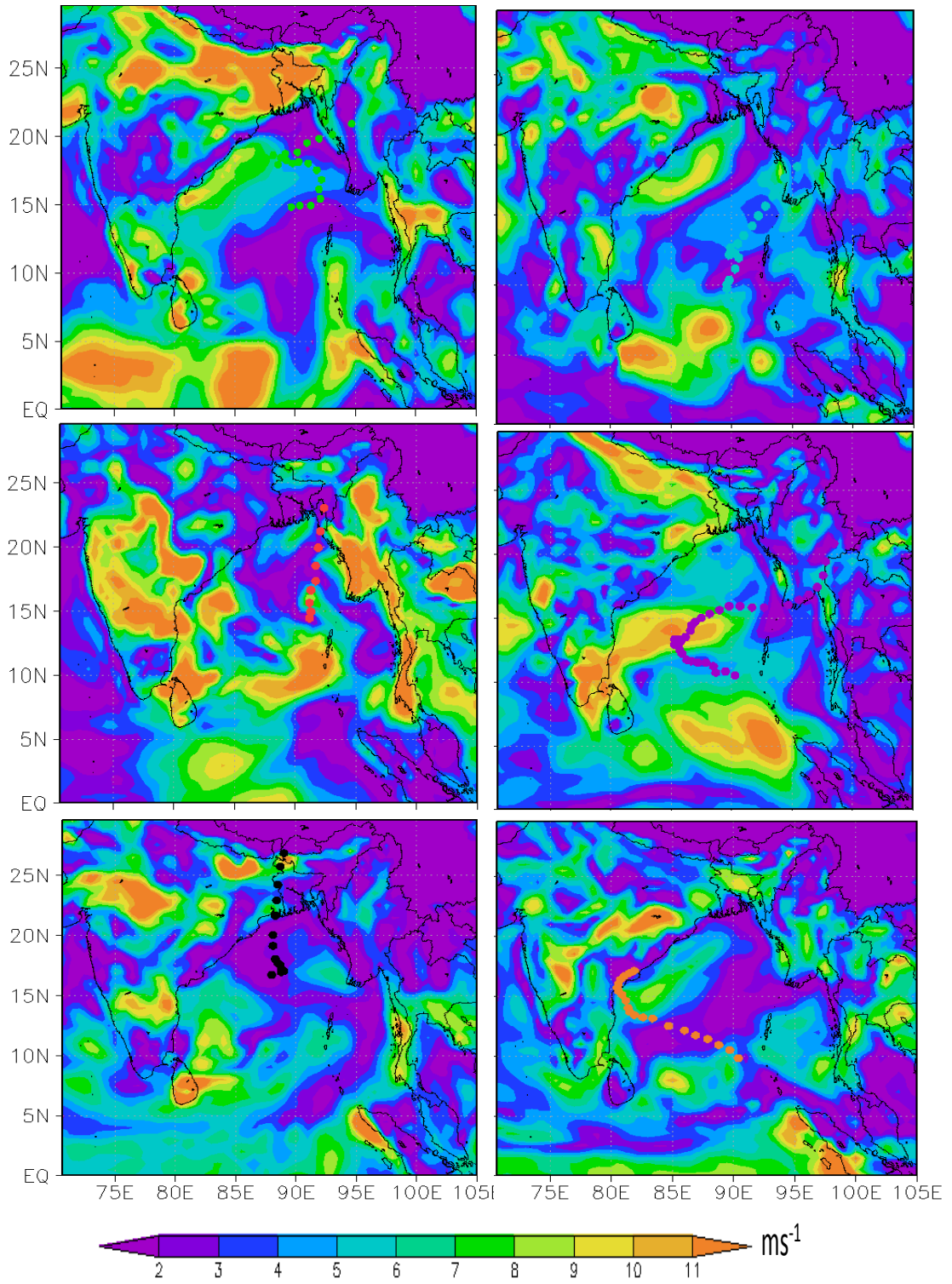


Fig 4.17: Spatial distribution of average low level VWS during cyclone period of each pre-monsoon cyclone.

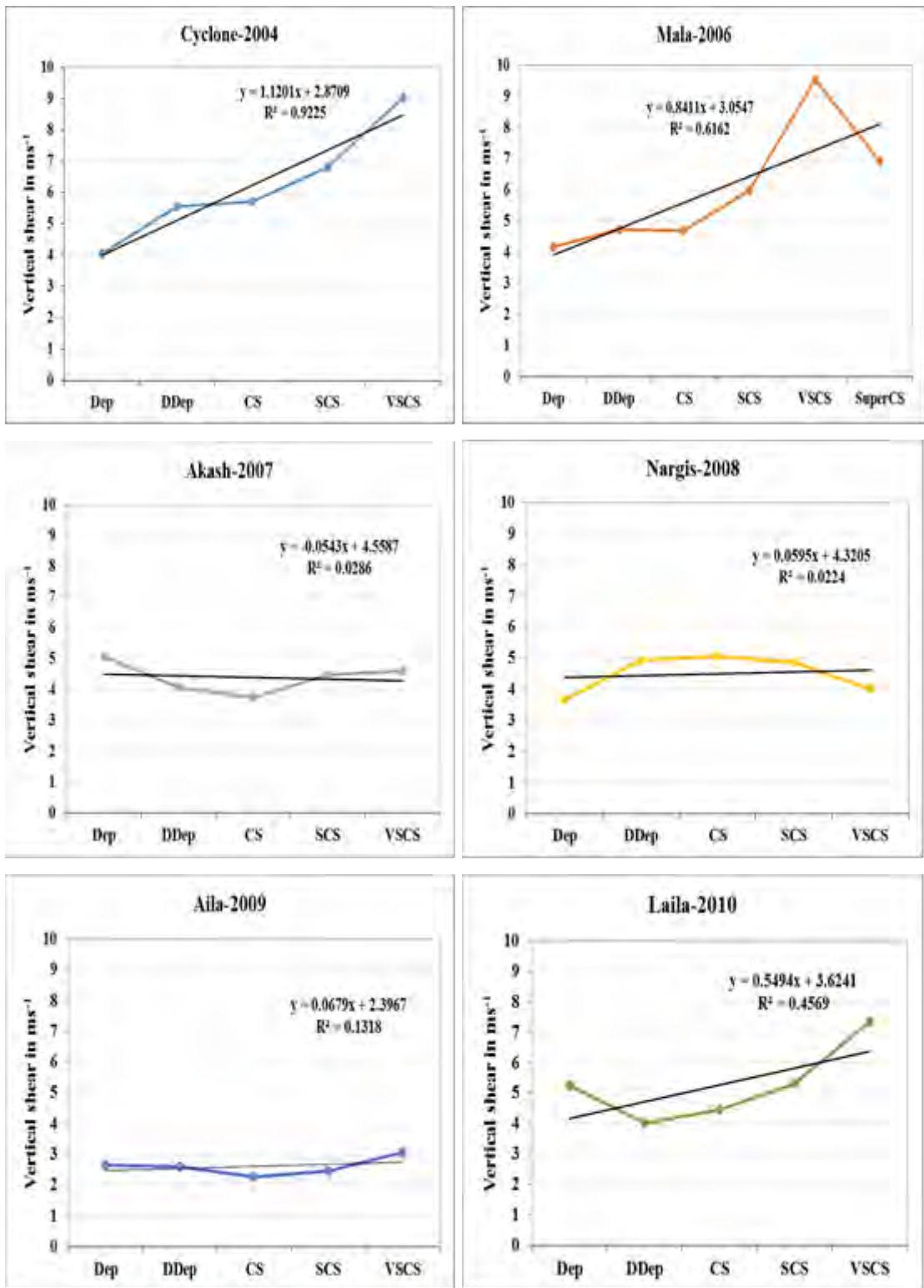


Fig 4.18: Low level(1000-850 hpa) VWS for individual pre-monsoon cyclone.

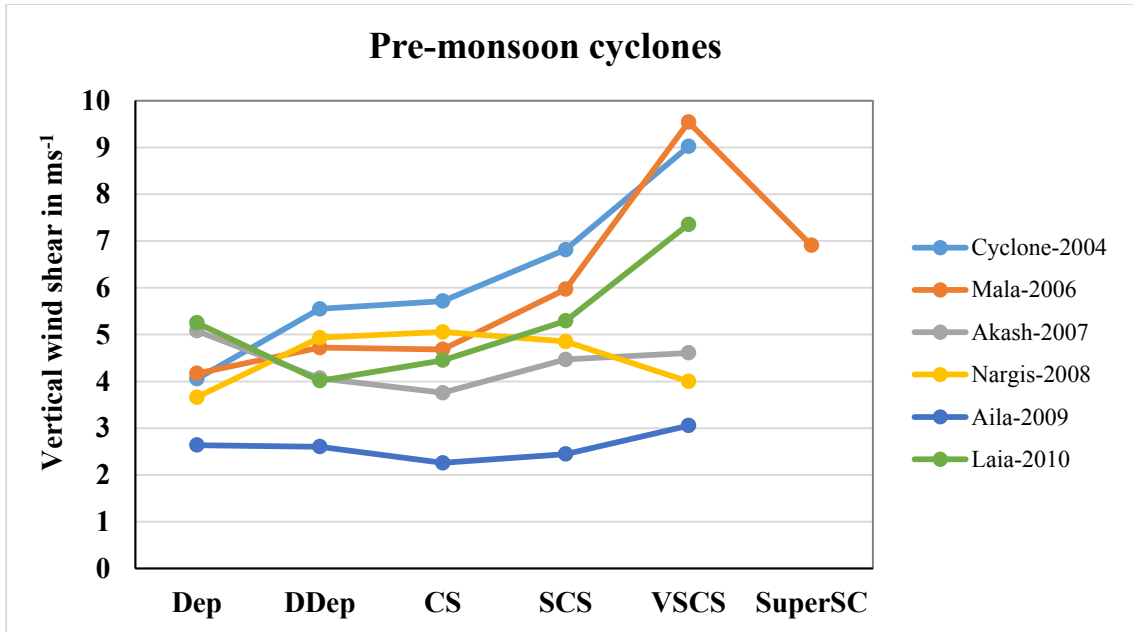


Fig 4.19: Low level (1000-850) VWS for pre-monsoon cyclones

The figures shows that in all cases has the value lower than 10 m s^{-1} which is essential for cyclone activity. Maintaining the lower range, VWS shows almost increasing trend with intensity change. Fluctuations of the value are found but these fluctuation is very small i.e. less than 2 ms^{-1} . In case of Akash (2007) and Nargis (2008) the trend remains almost constant.

For cyclone (2004) and Mala (2006), the coefficient of determination (R^2 value) values are greater than 0.6, but for other pre-monsoon cyclones it has values <0.5 .

From Table 8 found that the average low-level VWS varies from 3.7 ms^{-1} to 6.5 m s^{-1} , with an mean value of 4.83 ms^{-1} for pre-monsoon cyclones which is very low ($<5 \text{ ms}^{-1}$) and favorable for cyclone intensification. Average decrement per intensity level for Akash is 0.12 ms^{-1} or 1.37%. However for all pre-monsoon cyclones average increment per intensity level is found 0.4 ms^{-1} i.e. 9.3%.

Table 8: Characteristics of low level VWS for pre-monsoon cyclones

Pre-monsoon Cyclones	Lowest value (ms ⁻¹)	Highest value (ms ⁻¹)	Average Value (ms ⁻¹)	Average increment/decrement per intensity level	
				(ms ⁻¹)	%
Cyclone 2004	4.054	9.022	6.231	1.242	22.874
Mala 2006	4.17	9.542	5.998	0.547	14.422
Akash 2007	3.757	5.078	4.395	-0.118	-1.374
Nargis 2008	3.657	5.056	4.499	0.085	3.918
Aila 2009	2.259	3.055	2.601	0.104	4.658
Laila 2010	4.012	7.355	5.272	0.527	11.314
Average for all pre-monsoon cyclones	3.652	6.518	4.832	0.398	9.302

Post-monsoon cyclones

Fig 4.20 shows the spatial distribution of Post-monsoon cyclones. VWS are averaged for total cyclone period in each case. Here Cyclone (2000) and Thane have higher intensity of VWS, which prominent over BoB. Other two cyclone have lower VWS value. Low level VWS trend with post-monsoon cyclone intensity was shown in the Fig 4.21 and Fig 4.22.

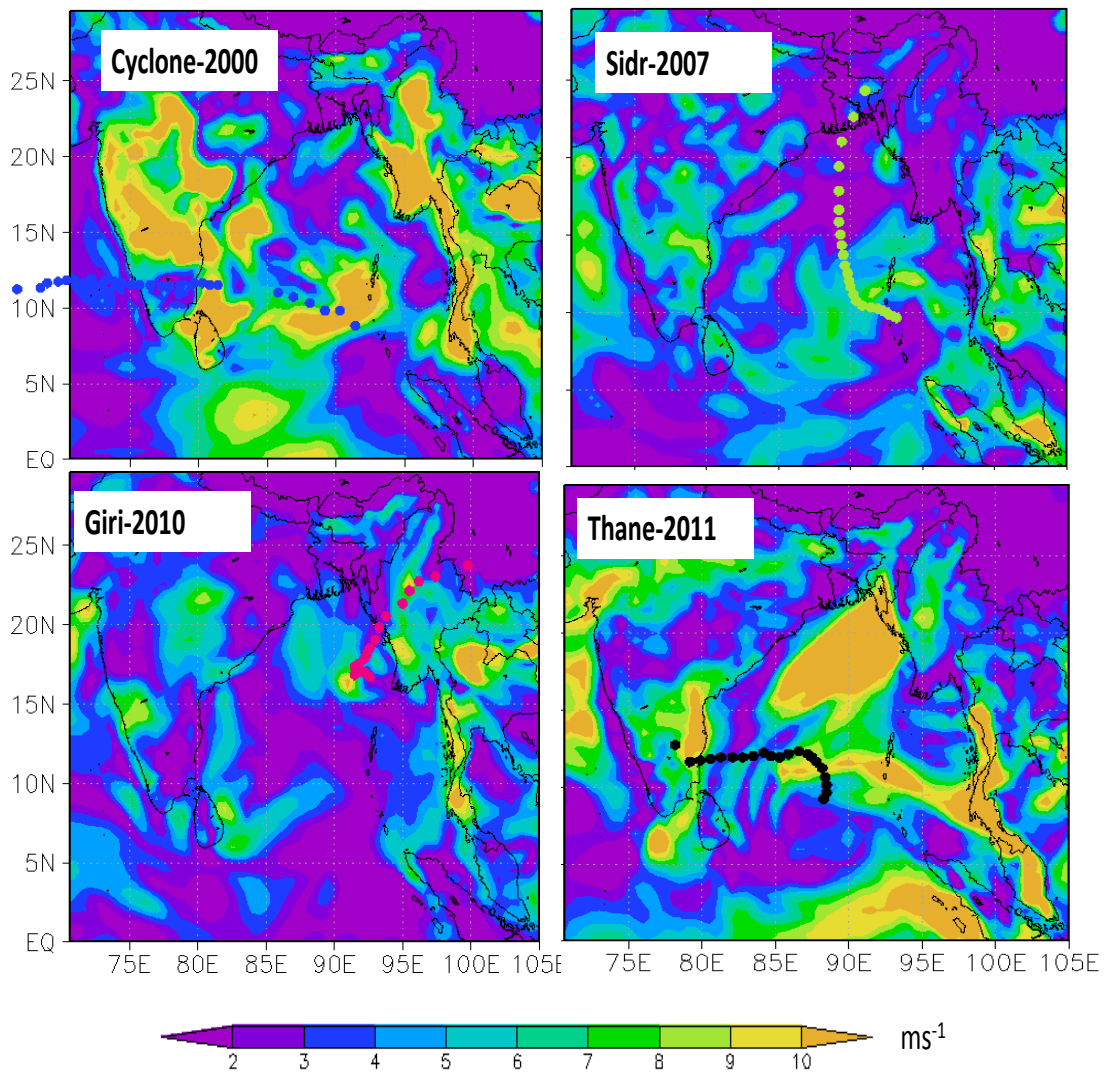


Fig 4.20: Spatial distribution of average low level VWS during cyclone period of each post-monsoon cyclone.

For Cyclone (2000), Sidr (2007), Giri (2010) and Thane (2011) the low level VWS are also found lower than 10 ms^{-1} . Within these low value, VWS shows almost increasing trend with post-monsoon cyclone intensity. Fluctuation of VWS value is very small i.e. less than 2 ms^{-1} .

For all graphs R^2 value is calculated and found significance for Giri (2010) and Thane (2011) i.e. for those cyclone it has the value ≥ 0.5 , but for Cyclone (2000) and Sidr (2007) it has the value < 0.5 .

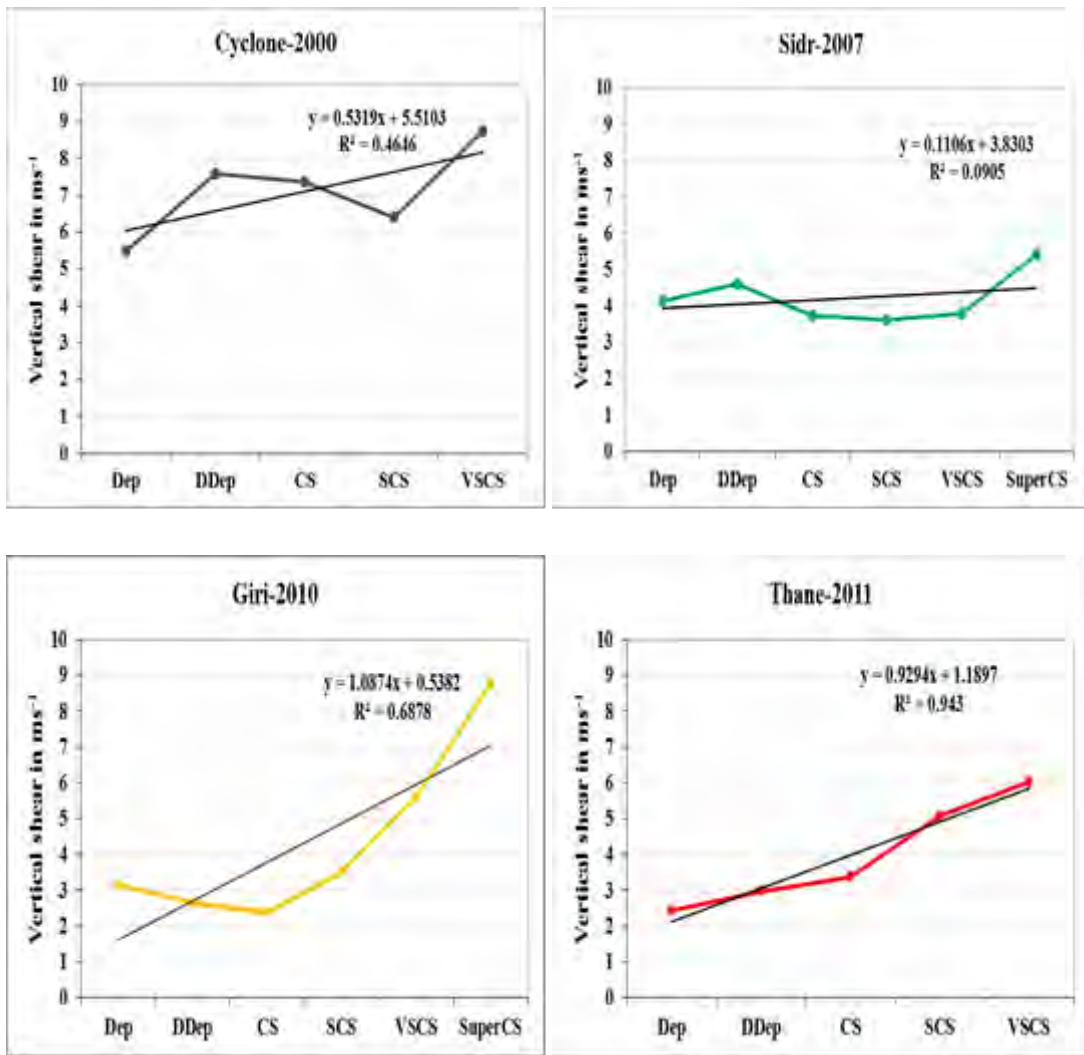


Fig 4.21: Low-level VWS for individual post-monsoon cyclone

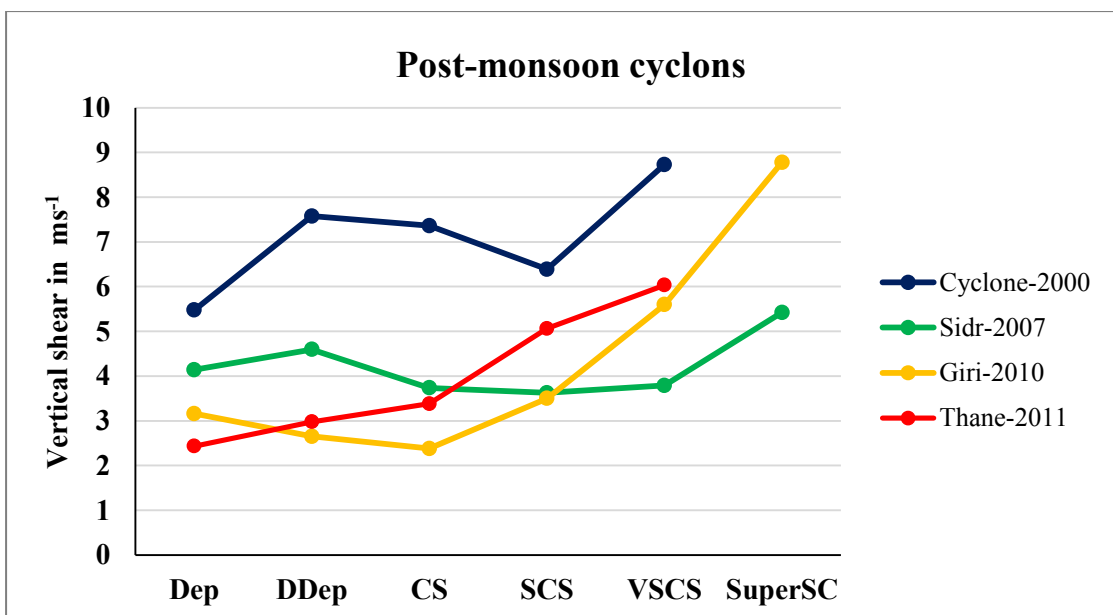


Fig 4.22: Low level VWS for post-monsoon cyclones

According to Table 9, low level VWS varied from 3.5 ms^{-1} to 7.2 ms^{-1} with an average value of 4.9 ms^{-1} for all post-monsoon cyclones. The average VWS increases 18.9 % or 0.8 s^{-1} from each level in case of post-monsoon cyclones.

Table 9: Characteristic of low level VWS for post-monsoon cyclones

Post-monsoon Cyclones	Lowest value (m s^{-1})	Highest value (m s^{-1})	Average value (m s^{-1})	Average increment/decrement per intensity level	
				m s^{-1}	%
Cyclone 2000	5.477	8.729	7.106	0.813	14.729
Sidr 2007	3.624	5.421	4.217	0.256	7.388
Giri 2010	2.377	8.779	4.344	1.124	27.517
Thane 2011	2.432	6.034	3.977	0.901	26.227
Average for all post-monsoon cyclones	3.477	7.241	4.911	0.773	18.965

Average value of low level VWS in different cyclones shows in Fig 4.23. Average values of VWS are positive and decreases with cyclone onward. Low level VWS values are found fluctuate from maximum 7.2 ms^{-1} to minimum 3 ms^{-1} with an average 5 ms^{-1} during study period. Post-monsoon Cyclone (2000) has maximum VWS value and pre-monsoon cyclone Aila (2009) has minimum VWS value.

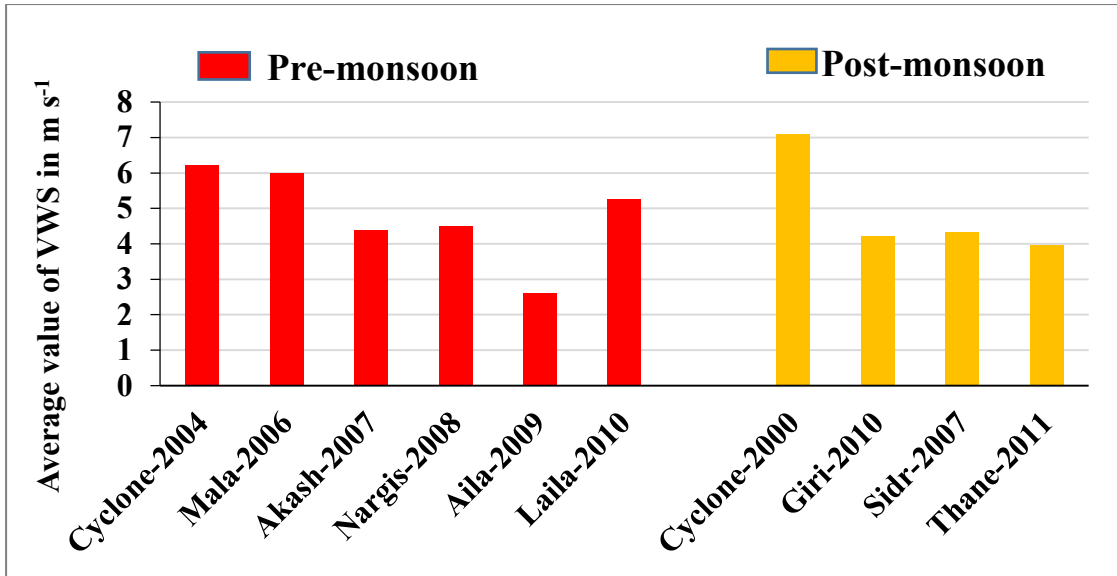


Fig 4.23: Average value of low level VWS (1000-850 hPa) during cyclones period.

The average increment of VWS (%) per intensity level with pre- and post-monsoon cyclone at low level shows in Fig 4.24

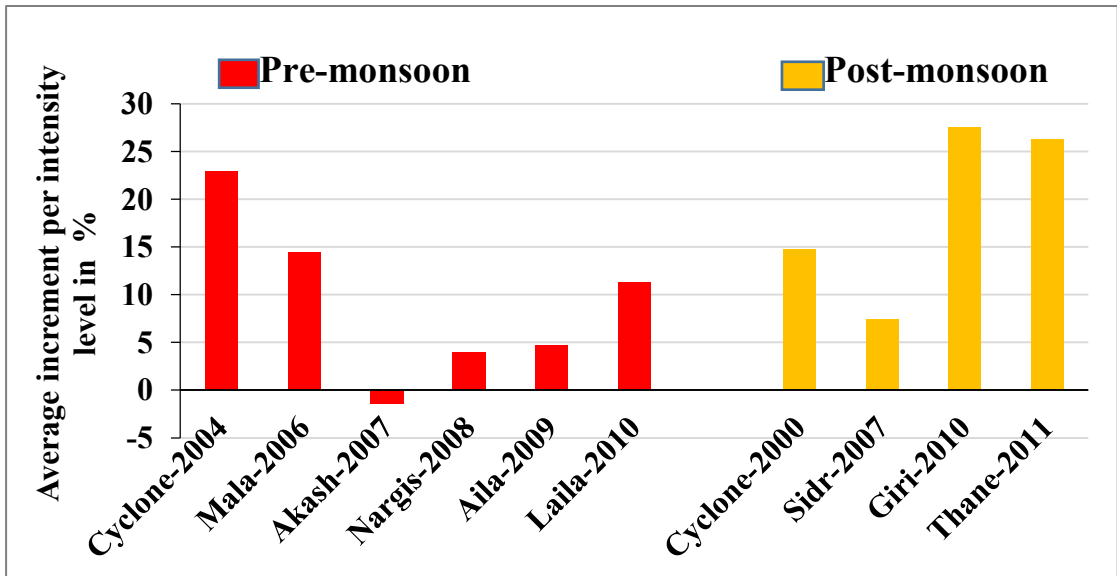


Fig 4.24: Average increment per intensity level of VWS (%) at low level.

VWS shows positive increment per intensity level for all cyclones except Akash (2007) which has negative value per intensity level. Average increment per intensity level is 9.3 % in case of pre-monsoon and 19% for post-monsoon which is greater than pre-monsoon cyclone. However, increment depends on case by case. Cyclone intensity change may not significantly related with the low level VWS change, as fluctuation is very less in both cases.

4.1.4 Low level moisture flux (1000-850 hPa)

Pre-monsoon cyclones

Moisture flux convergence is direct related to the intensity of TC. The spatial distribution of low level moisture flux are plotted for all pre-monsoon cyclones in Fig 4.25. Cyclone Laila (2010) shows minimum value and Akash (2007) shows maximum value of moisture flux. Intense moisture flux in the North West region of Akash (2007) and in the Southern part of BoB in case of Cyclone (2004) and Aila (2009).

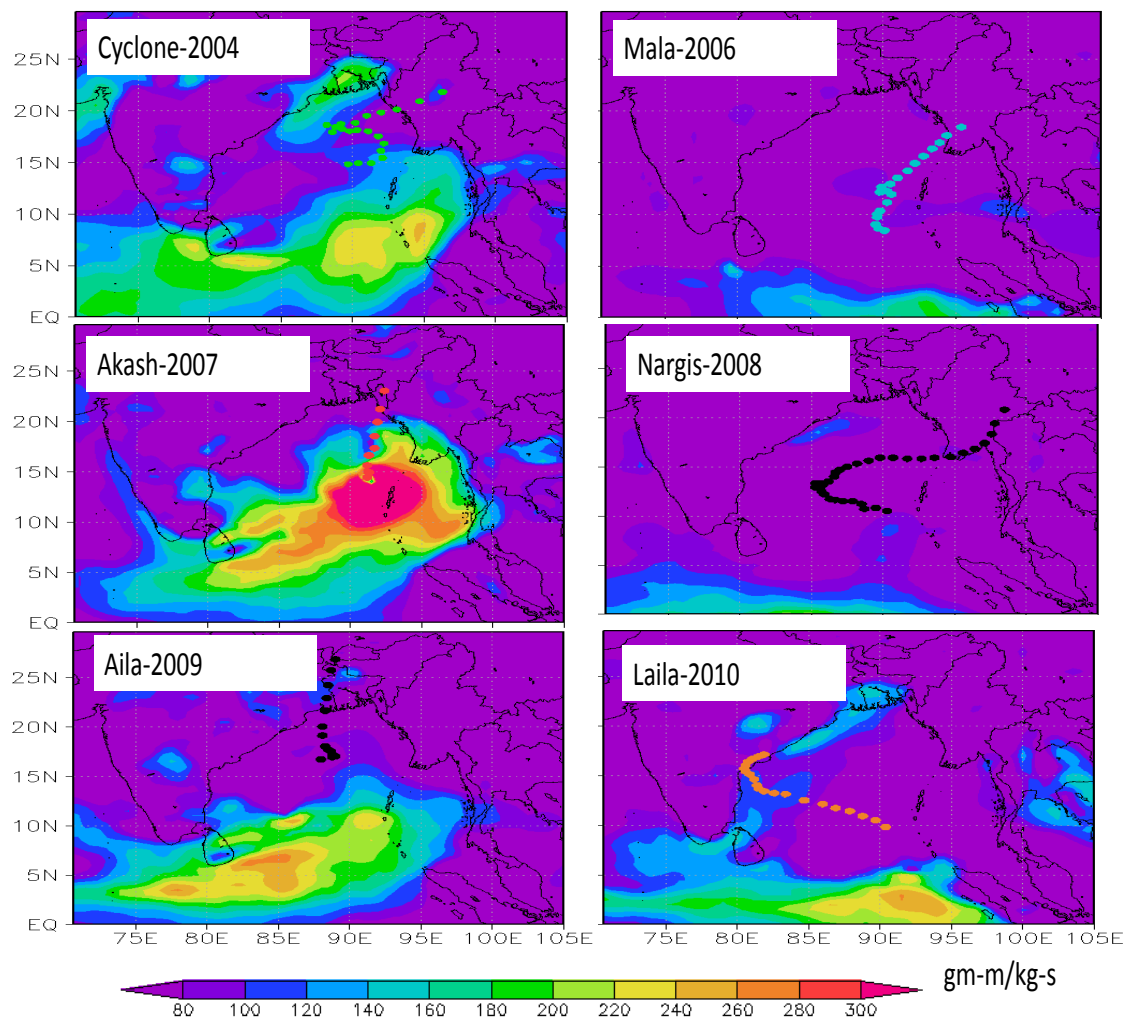


Fig 4.25: Spatial distribution of average low level moisture flux from 1000-850 hPa during cyclone period of each cyclone.

Variation of low level moisture flux with intensity for each pre-monsoon cyclones shown in Fig 4.26 and all pre-monsoon cyclones in Fig 4.27.

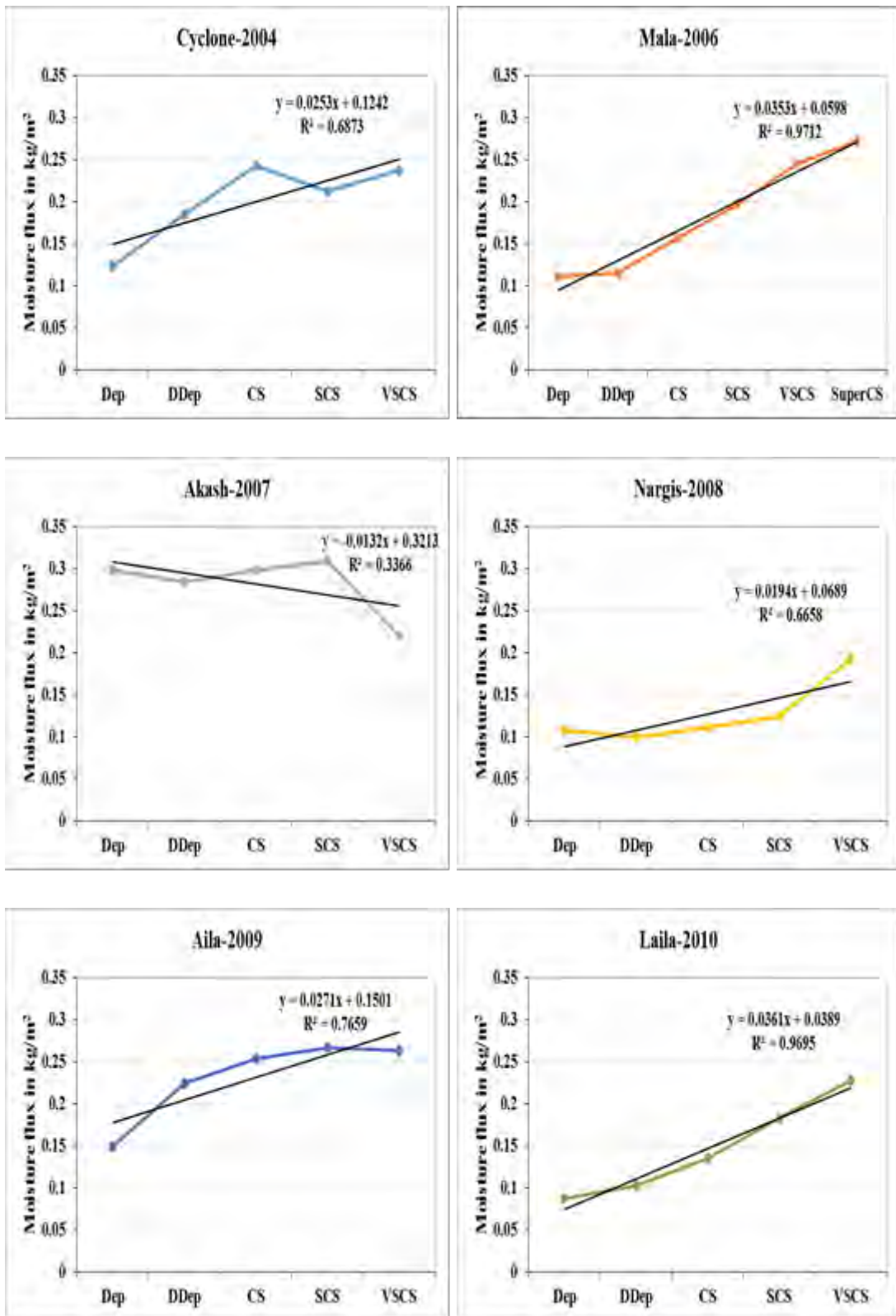


Fig 4.26: Low level moisture flux for individual pre-monsoon cyclone

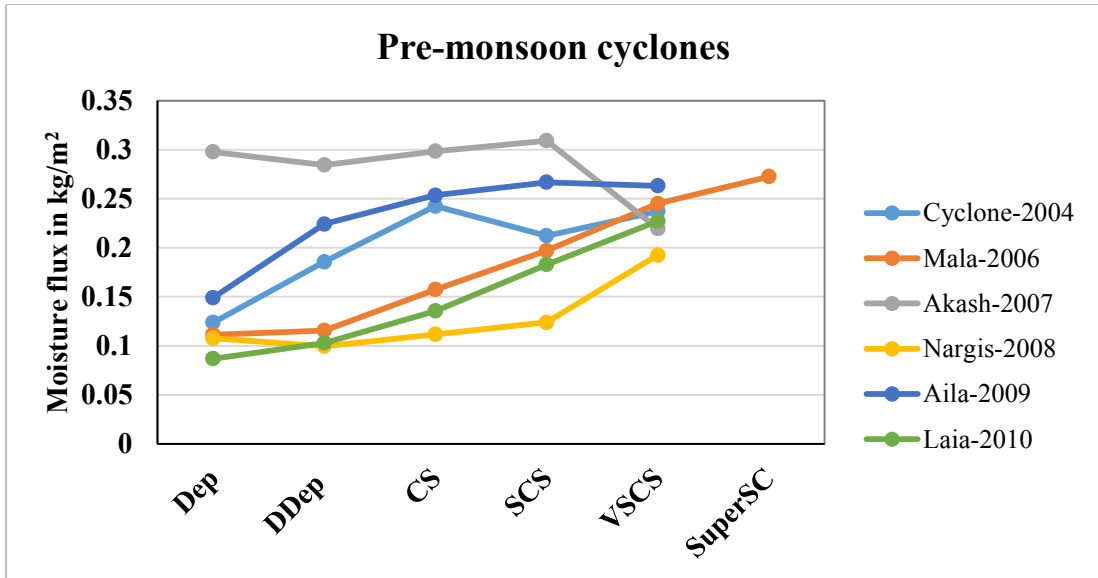


Fig 4.27: Low level moisture flux for pre-monsoon cyclones

Moisture flux are the average of the 1000-850 hPa level. Low level moisture flux shows increasing trend with all pre-monsoon cyclones intensity change except Akash (2007). Moisture flux values were found from minimum 87 gm-m/kg-s to maximum 309 gm-m/kg-s and fluctuate <0.03 for pre-monsoon cyclones.

For all graphs, R^2 value is calculated and found significance i.e. for all pre-monsoon cyclones the value is ≥ 0.66 except Akash which has the value of 0.34.

From table 10, the average low level moisture flux are found minimum 132gm-m/kg-s to maximum 251 gm-m/kg-s with an average value 195 gm-m/kg-s in case of pre-monsoon. Akash (2007) showed decreasing trend and average decrement per intensity level in case of Akash (2007) is 19 gm-m/kg-s or 6.242% . However average increment per intensity level is found 21 gm-m/kg-s i.e. the average moisture flux increases 15.955% from each intensity level in case of pre-monsoon cyclones.

Table 10: Characteristic of low level moisture flux for pre-monsoon cyclones

Pre-monsoon Cyclones	Lowest value (gm-m/kg-s)	Highest value (gm-m/kg-s)	Average value (gm-m/kg-s)	Average increment/decrement per intensity level	
				gm-m/kg-s	%
Cyclone 2004	123	242	201	0.028	19.949
Mala 2006	111	273	183	0.032	20.151
Akash 2007	219	309	282	-0.019	-6.242
Nargis 2008	99	192	127	0.021	17.735
Aila 2009	149	266	231	0.028	16.820
Laila 2010	87	227	147	0.035	27.319
Average for all pre-monsoon cyclones	132	251	195	0.021	15.955

Post-monsoon cyclones

The spatial distribution of moisture flux for all post-monsoon cyclone are plotted in Fig 4.28. Intense moisture flux in the Southern region of Cyclone (2000) and Thane (2011). Maximum value found in cyclone Giri (2010) and cyclone Thane (2011) shows the minimum value. Again Fig 4.29 and Fig 4.30 shows the variation of low level moisture flux with cyclones intensity change for all post-monsoon cyclones.

For all post-monsoon cyclones coefficient of determination (R^2 value) is found significant i.e. it has the value ≥ 0.5 .

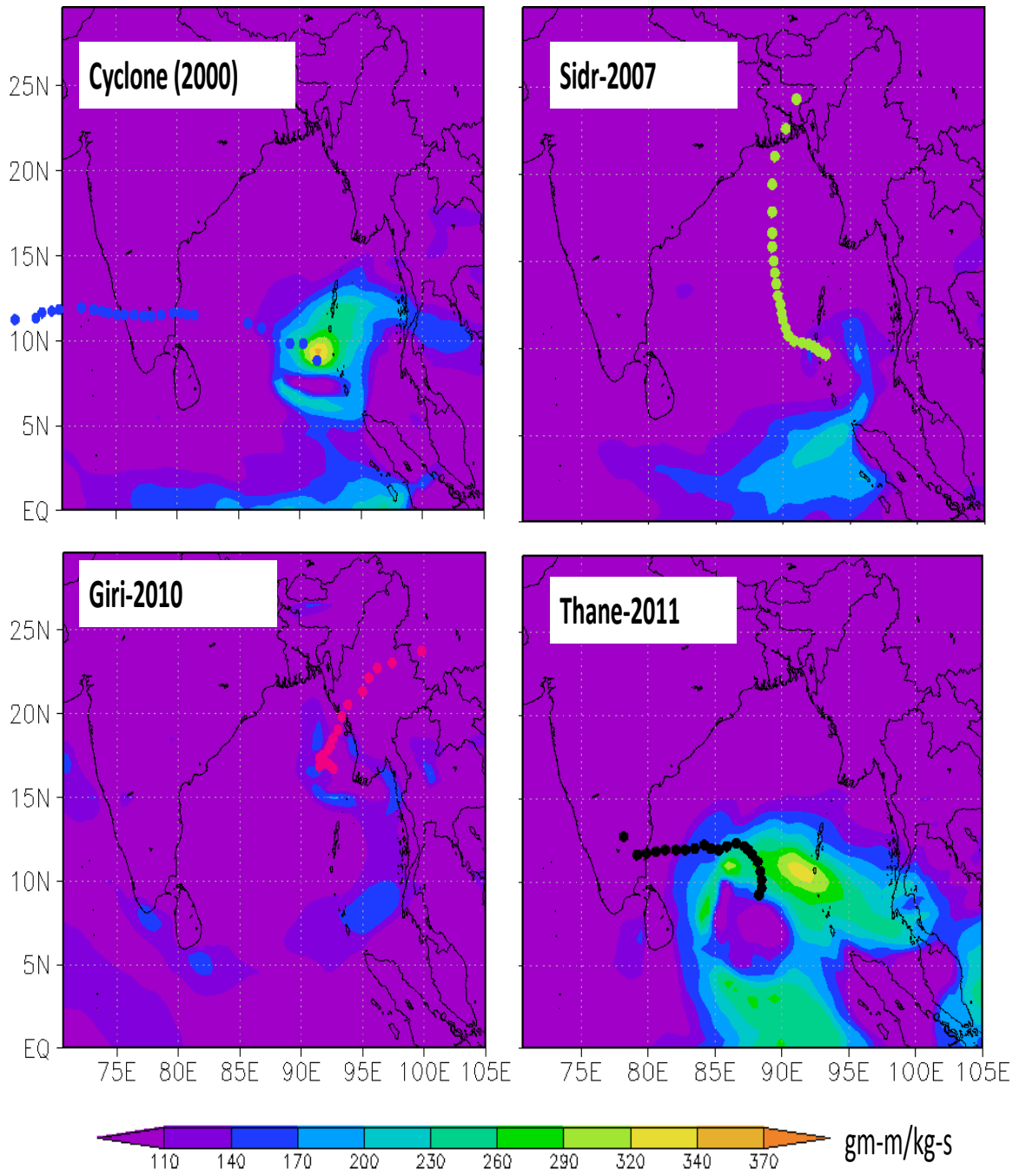


Fig 4.28: Spatial distribution of average low level moisture flux from 1000-850 hPa during cyclone period of each post-monsoon cyclone.

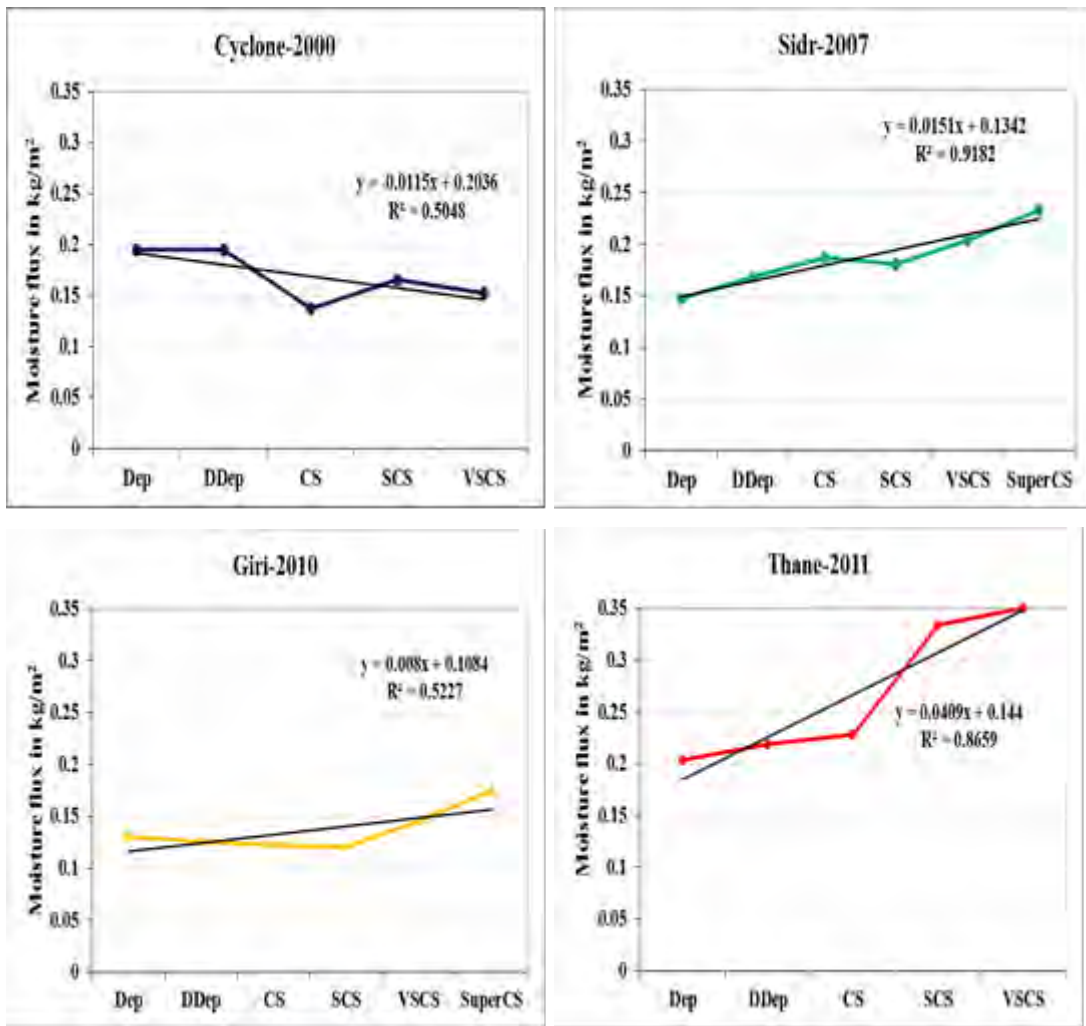


Fig 4.29: Low level moisture flux for individual post-monsoon cyclones

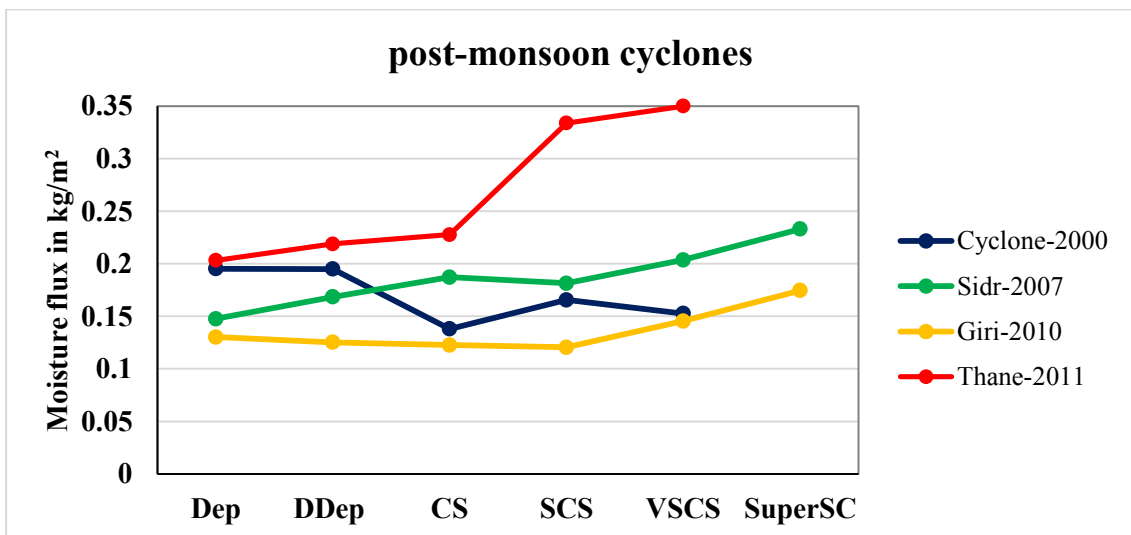


Fig 4.30: Low level moisture flux for post-monsoon cyclones

Low level moisture flux found positive value for post-monsoon cyclone which is important for cyclone intensification. Moisture flux shows positively increasing trend with all post-monsoon cyclone intensity change except cyclone (2004). In case of cyclone (2004) moisture flux is positive but shows decreasing trend. Moisture flux values were found from minimum 0.14×10^3 to maximum 0.35×10^3 gm-m/kg-s and fluctuation <0.06 for post-monsoon cyclones.

Overall summary for the parameter of moisture flux is shown in table 11. Highest, lowest, average value of moisture flux for all post-monsoon cyclones are indicated along with average percentage increment from initial level to highest intensity level.

From the table, found that the average moisture flux varied from 152 gm-m/kg-s to 238 gm-m/kg-s for post-monsoon cyclones, with an average value of 189 gm-m/kg-s. The average decrement per intensity level in case of cyclone (2004) is 11 gm-m/kg-s or 6.968%. In case of post-monsoon cyclone the average moisture flux increases per intensity level is found 13 gm-m/kg-s or 6.968% from each level.

For all pre- and post- monsoon cyclone low level moisture flux value varied from minimum 130 gm-m/kg-s to maximum 240 gm-m/kg-s. Average value of moisture flux for pre-monsoon is higher than post-monsoon cyclones. Except Akash (2007) and Cyclone (2000) almost all pre- and post-monsoon cyclones shown positively increasing trends from the lowest intensity level (Dep) to the highest intensity level (VSCS/SuperCS). Again average increment per intensity level of moisture flux in pre-monsoon is greater than post-monsoon.

Table 11: Characteristic of low level moisture flux for post-monsoon cyclones.

Post-monsoon Cyclones	Lowest value (gm-m/kg-s)	Highest value (gm-m/kg-s)	Average value (gm-m/kg-s)	Average increment/decrement per intensity level	
				(gm-m/kg-s)	%
Cyclone 2000	138	195	169	-11	-4.299
Sidr 2007	147	233	187	17	9.765
Giri 2010	120	174	136	9	6.603
Thane 2011	203	350	267	37	15.805
Average for all post-monsoon cyclones	152	238	189	13	6.968

Fig 4.31 shows the average values of moisture flux in different cyclones. Moisture flux values fluctuate from maximum 282 gm-m/kg-s to minimum 127 gm-m/kg-s with average 192 gm-m/kg-s. Pre-monsoon cyclone Akash (2007) has maximum value and Nargis (2008) has minimum value of moisture flux. Average value of moisture flux in case of pre-monsoon is higher than post-monsoon.

Again average increment of moisture flux per intensity level at low level for pre- and post-monsoon shows in Fig 4.32. For all cyclones average increment of moisture flux per intensity level are positive except Akash (2007) and Cyclone (2000).

Moisture flux average increment in pre-monsoon cyclon (16%) is higher than post-monsoon (7%). This is because Southwesterly wind started to enter into the BoB during pre-monsoon and carry moisture from the Ocean.

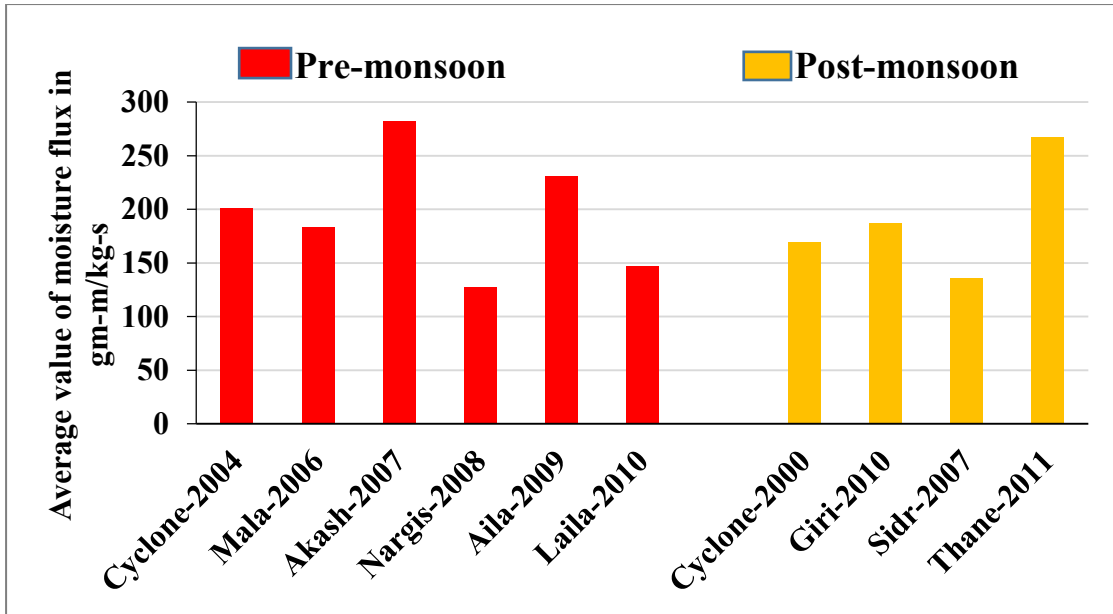


Fig 4.31: Average value of low level moisture flux (1000-850 hPa) during cyclones period.

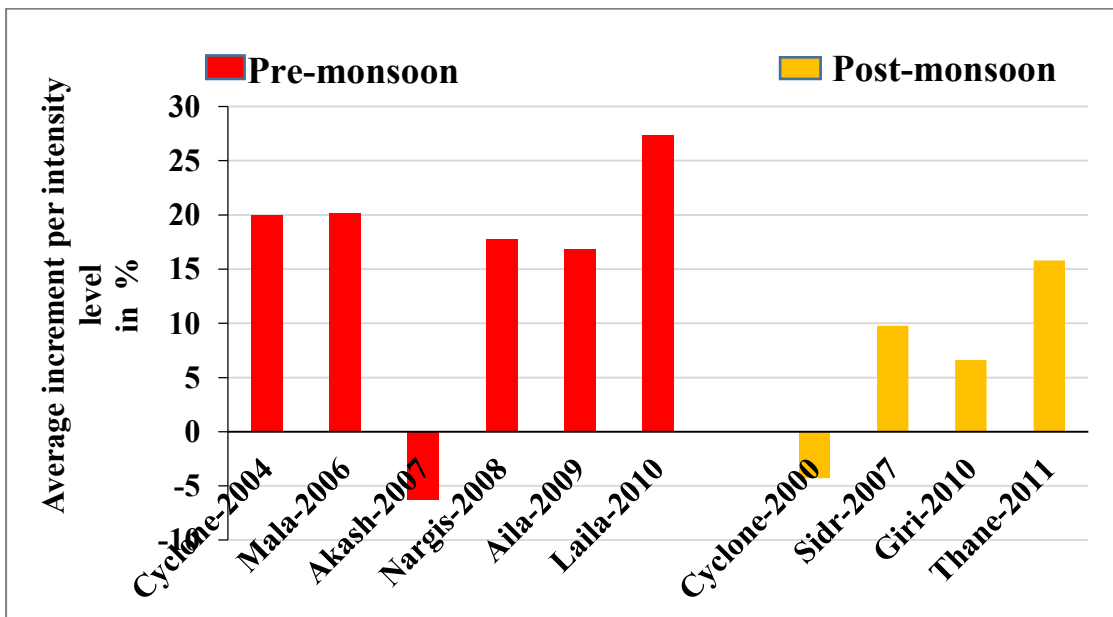


Fig 4.32: Average increment per intensity level of moisture flux (%) at low level.

4.2 Thermodynamic parameters

4.2.1 Mid-tropospheric relative humidity (500 hPa)

Pre-monsoon cyclones

Relative humidity is an important environmental thermodynamic parameter for cyclogenesis and cyclone intensification. Environmental relative humidity (ERH) increases with increasing TC intensity and intensification rate. The Fig 4.33 shows the spatial distribution of relative humidity at 500 hPa for all pre-monsoon cyclones. Most of the cases relative humidity is more in the Eastern side of BoB. Intense relative humidity found all pre-monsoon cyclone, however, cyclone Mala (2006) shows lower intense than others. The movement of mid-level relative humidity with pre-monsoon cyclones intensity change shown in Fig 4.34 and Fig 4.35.

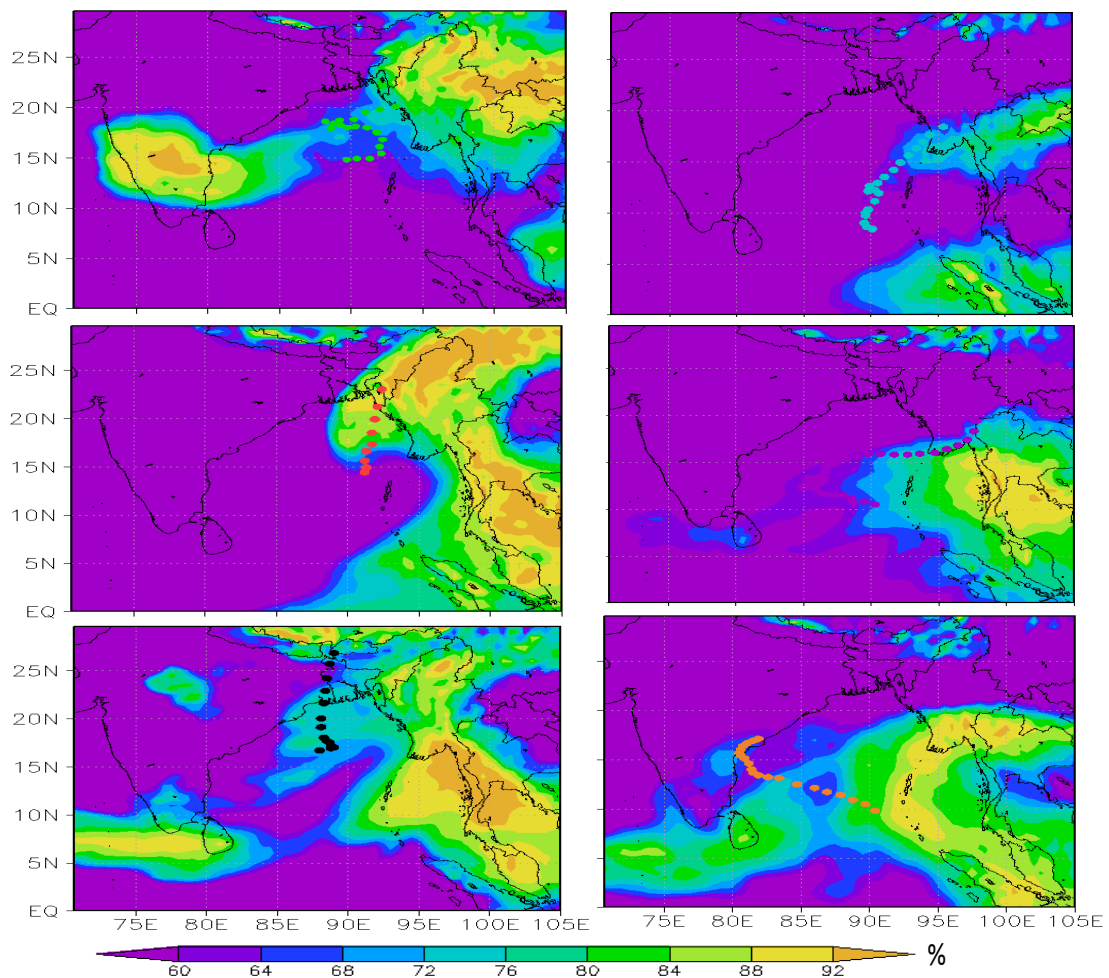


Fig 4.33: Spatial distribution of average mid-tropospheric relative humidity during cyclone period of each cyclone.

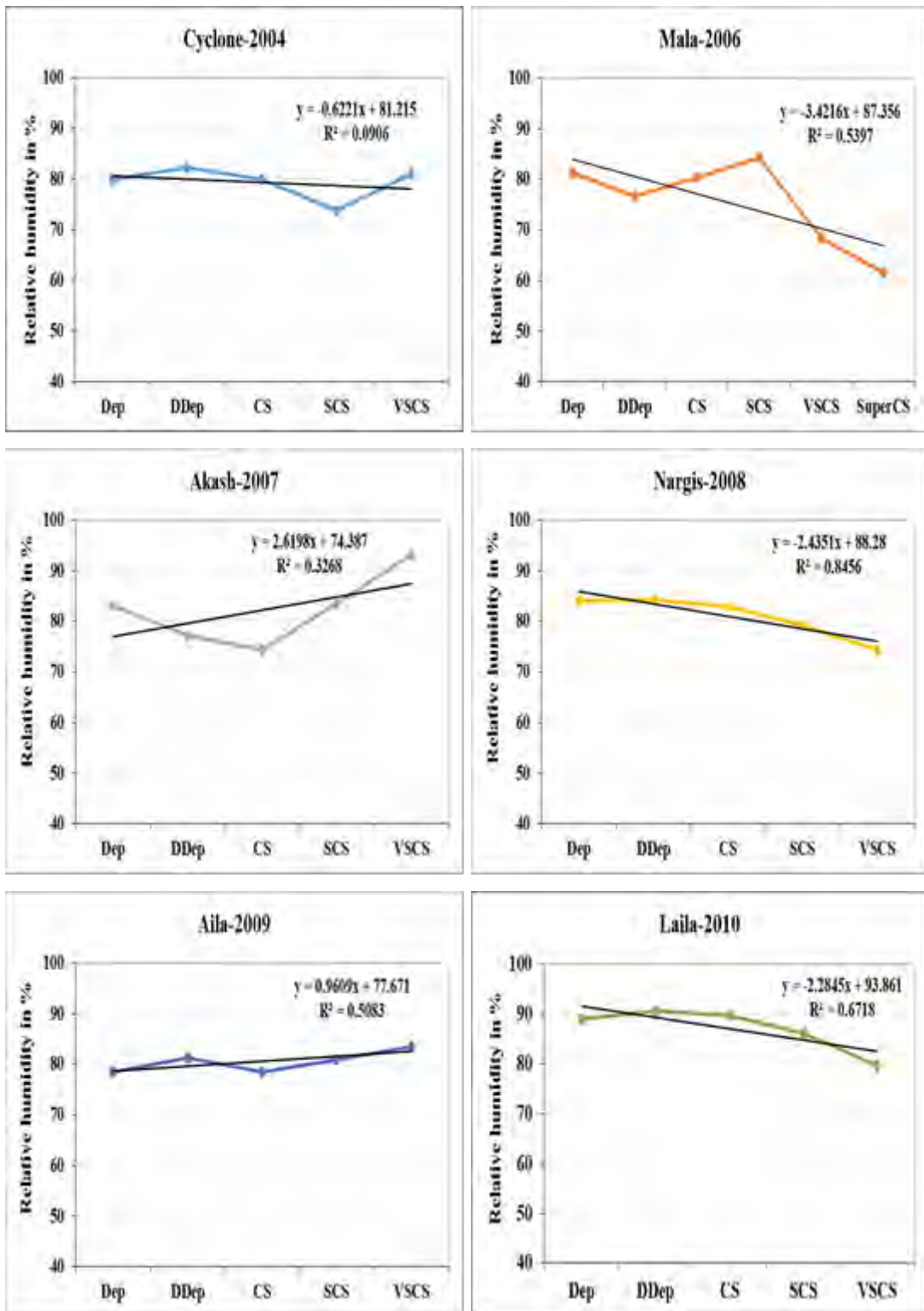


Fig 4.34 : Mid-tropospheric relative humidity for individual pre-monsoon cyclone.

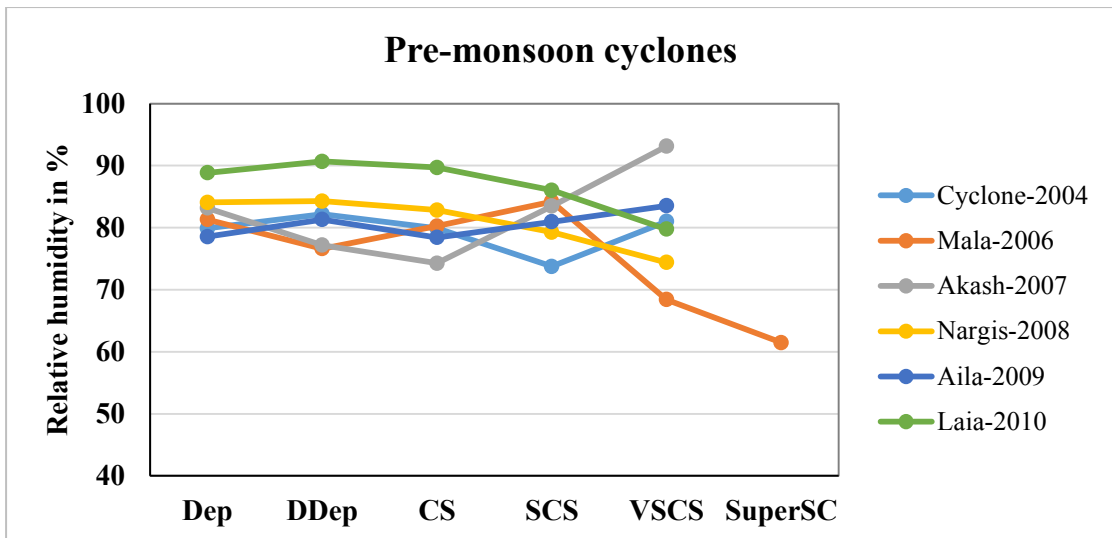


Fig 4.35: Mid-level relative humidity for pre-monsoon cyclones.

Mid-level relative humidity is found from minimum 60 % to maximum 95 % in case of all pre-monsoon cyclones which is essential for cyclone formation and intensification. Within these values, relative humidity shows almost decreasing trend except Akash (2007) and Aila (2009) with all pre-monsoon cyclone intensity change.

Relative humidity shows increasing trend in case of Akash (2007) but for Aila (2009) the trend is constant. Except Cyclone (2004) and Akash (2007), R^2 value for all graphs is found significant i.e. it has value ≥ 0.5 .

Overall summary for the parameter of relative humidity is shown in table 12. From table 12 found that values of average mid-level relative humidity varied from minimum 75.2 % to maximum 86.3 % with an average 80.9 % in case of pre-monsoon cyclones which is almost constant. However for all pre-monsoon cyclones average decrement per intensity level is less than 1 %. So relative humidity remain almost constant with cyclone intensity change.

Table 12: Characteristic of mid-tropospheric relative humidity for pre-monsoon cyclones

Pre-monsoon Cyclones	Lowest value (%)	Highest value (%)	Average value (%)	Average increment/decrement per intensity level (%)
Cyclone 2004	73.75	82.185	79.348	0.277
Mala 2006	61.488	84.193	75.380	-3.279
Akash 2007	83.17	93.126	82.247	2.487
Nargis 2008	74.401	84.281	80.974	-2.418
Aila 2009	78.422	83.535	80.553	1.245
Laila 2010	79.759	90.68	87.007	-2.274
Average for all pre-monsoon cyclones	75.166	86.333	80.918	-0.660

Post-monsoon cyclones

The spatial distribution of mid-level relative humidity for all post-monsoon cyclones are plotted in Fig 4.36. Intense relative humidity in the Eastern part of BoB for all cyclones. Again Fig 4.37 and Fig 4.38 shows variation of mid-tropospheric relative humidity with the post-monsoon cyclones intensity change. For post-monsoon cyclones relative humidity is found to vary from minimum 40 % to maximum 91 % which is favorable for cyclone intensification. Here relative humidity also shows decreasing trend with intensity change except Cyclone (2000) which shows increasing trend. Though Cyclone (2000) shows increasing trend, however in Cyclone (2000) the highest level value is relatively lower (~ 6 %) from the previous level. In case of Sidr (2007) relative humidity sharply decrease from 91 % to 46 % which will be later.

For Sidr (2007) and Giri (2010) R^2 value is found significant i.e. it has value ≥ 0.5 , but for Cyclone (2000) and Thane (2011) R^2 value is < 0.5 .

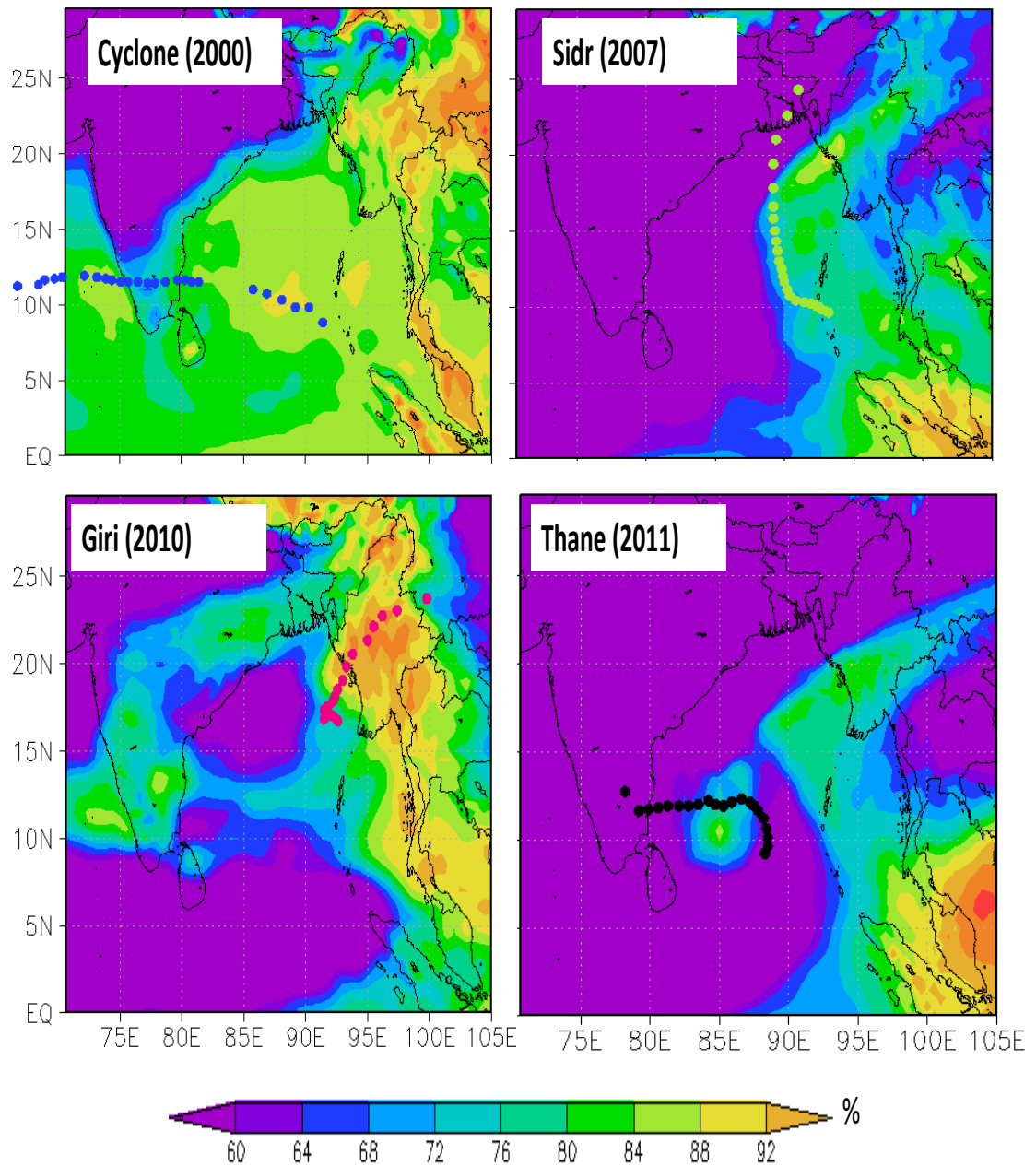


Fig 4.36: Spatial distribution of average mid-tropospheric relative humidity during cyclone period of each post-monsoon cyclone.

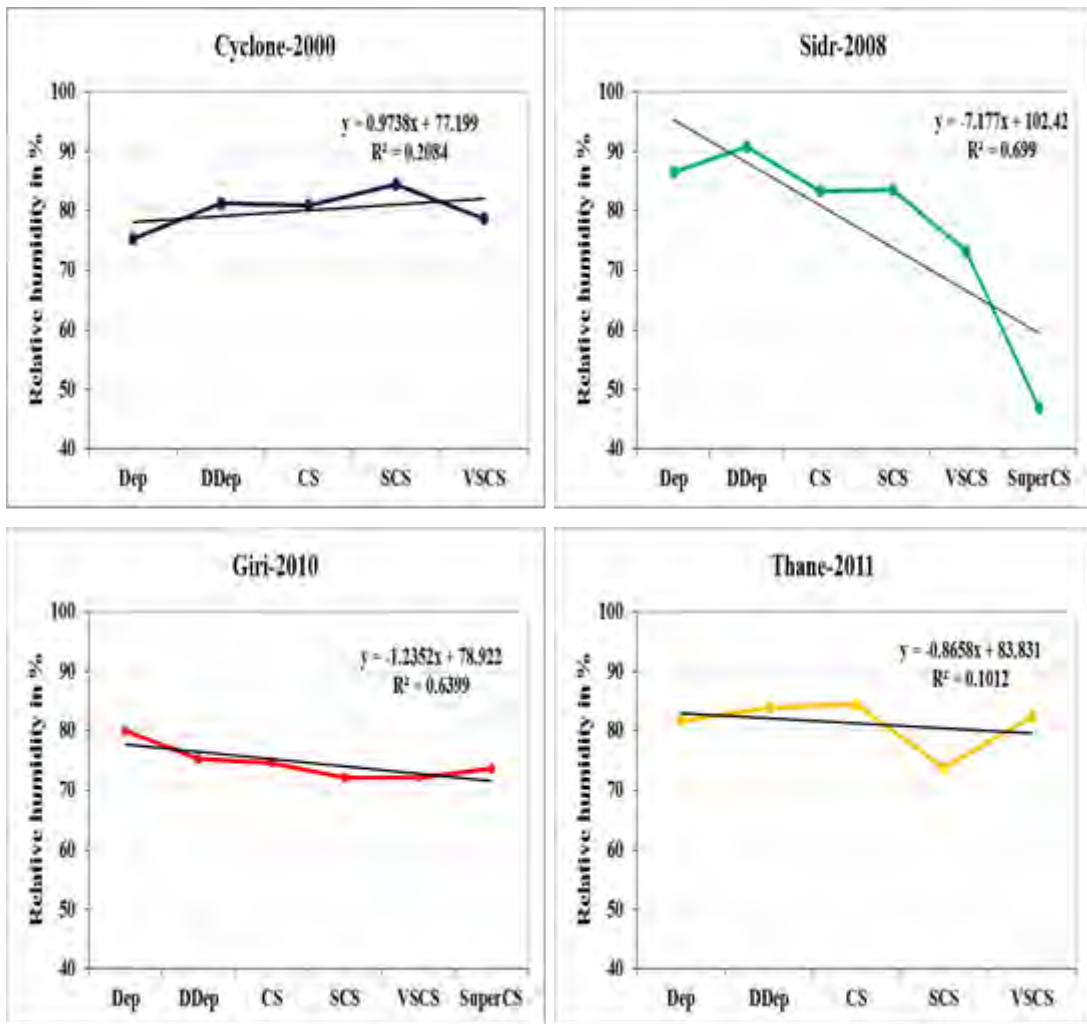


Fig 4.37: Mid-tropospheric relative humidity for individual post-monsoon cyclones.

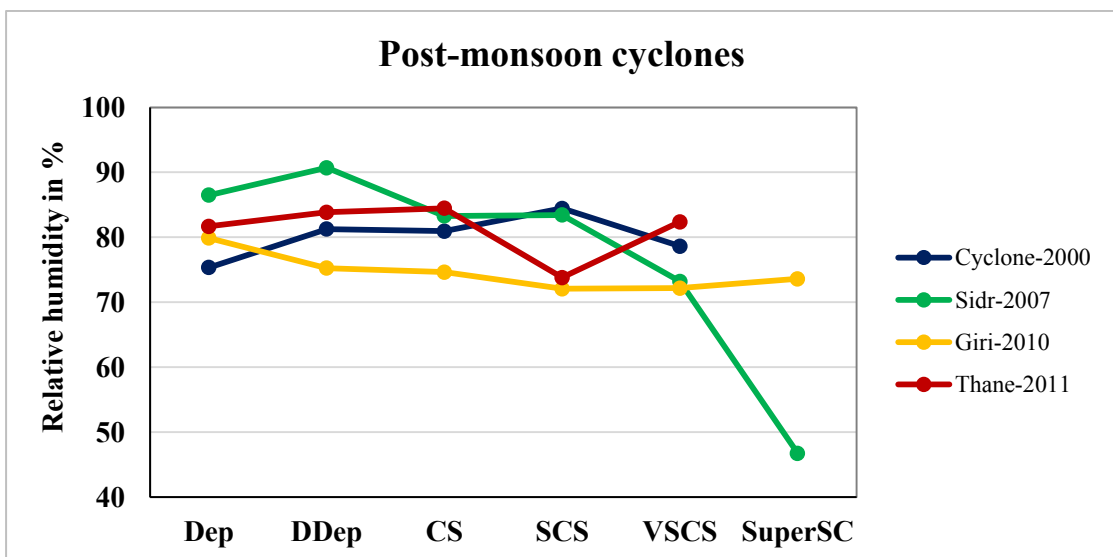


Fig 4.38: Mid-tropospheric relative humidity for post-monsoon cyclones.

From the table 13, found that the average relative humidity varied from 67% to 85% for post-monsoon cyclones, with an average value of 78.3%. Here Sidr (2008) and Giri (2010) shows average decrement per intensity level on other hand cyclone (2000) and Thane (2011) shows average increment per intensity level. However the average decrement is found 2.1% from each level in case of post-monsoon cyclones which is also low.

Table 13: Characteristic of mid-tropospheric relative humidity for post-monsoon cyclones.

Post-monsoon Cyclones	Lowest value (%)	Highest value (%)	Average value (%)	Average increment/decrement per intensity level (%)
Cyclone 2000	75.347	84.426	80.120	0.821
Sidr 2007	46.713	90.709	77.302	-7.953
Giri 2010	72.064	79.887	74.598	-1.257
Thane 2011	73.799	84.472	81.233	0.174
Average for all post-monsoon cyclones	66.981	84.874	78.313	-2.0541

For both monsoon cyclones relative humidity at 500 hPa level is varied from minimum 40% to maximum 95% which is essential for cyclogenesis and intensification. Average relative humidity for both season cyclones is greater than 50%, is the primary condition for cyclone formation. Average relative humidity in case of pre-monsoon is higher than post-monsoon cyclone. But for both season cyclones average relative humidity remain almost constant with cyclone intensity.

Fig 4.39 shows the average value of relative humidity in different cyclones. Relative humidity averagely fluctuate from maximum 87 % to minimum 75 % with an average 79.5 % during cyclone period. Relative humidity is maximum in case of Laila (2010)

and minimum in case of Giri (2010). Average value of relative humidity for pre-monsoon (81 %) is higher than post-monsoon (78 %) cyclones.

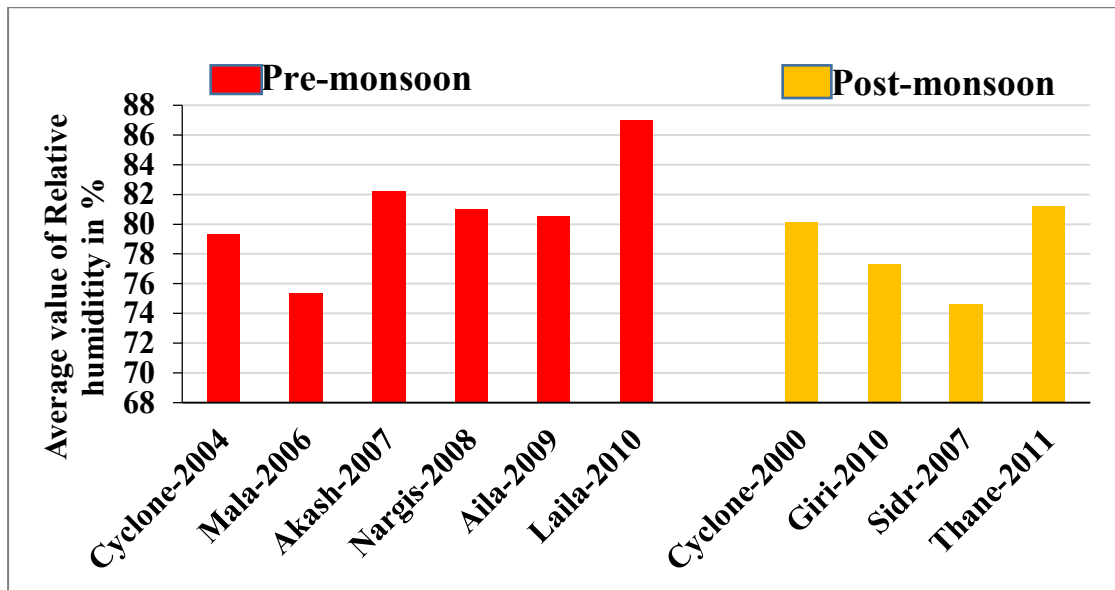


Fig 4.39: Average value of relative humidity at 500 hPa during cyclones period.

Average increment per intensity level of relative humidity (%) for pre- and post-monsoon at mid-tropospheric is shown in Fig 4.41. In case of Cyclone (2004) 0.27 %, Akash (2007) 2.5 %, Aila (2009) 1.25 %, Cyclone (2000) 0.82% and Thane (2011) 0.17 % relative humidity are increased per intensity level. On the other hand, in case of Mala (2006) 3.3 %, Nargis (2008) 2.42 %, Laila (2010) 2.27 %, Sidr (2007) 7.9 % and Giri (2010) 1.3 % relative humidity are decreased per intensity level. So no particular value of mid- tropospheric relative humidity is significant for the intensity of cyclones. However, value of relative humidity more than 75% is significant for cyclone to be active. Low value of relative humidity may die down the cyclone.

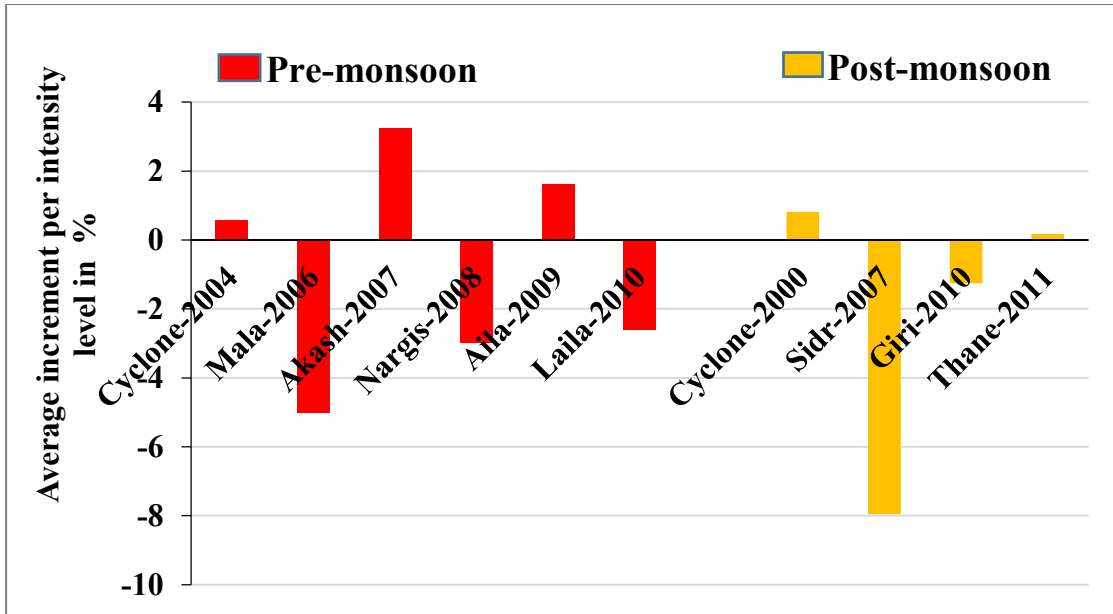


Fig 4.40: Average increment per intensity level of relative humidity (%) at 500 hPa.

4.2.2 Convective available potential energy (CAPE) at surface

Pre-monsoon cyclones

Convective available potential energy (CAPE) is an indicator of the environmental potential for cyclone formation and intensification. It is found that CAPE was high in the initial stages of development but as the cyclone intensified CAPE decreased. Intensification rate in the tropical cyclone is highly influenced by CAPE. Fig 4.41 shows the spatial distribution of CAPE for all pre-monsoon cyclone. High CAPE is prominent for all cyclones. CAPE is more than 2000 j/kg in the North Western part of BoB in all case. Again the variation of CAPE with cyclone intensity change in case of pre-monsoon cyclones shown in Fig 4.42 and Fig 4.43. For pre-monsoon cyclones CAPE is found to vary from minimum 300 j/kg to maximum 2500 j/kg, this wide range variation is favorable for cyclone intensification. CAPE decreases or constant for all cyclones except Nargis (2008).

Characteristic of CAPE for pre-monsoon cyclones is shown in Table 14. Here average CAPE varies from minimum 909.23 j/kg to maximum 1819.74 j/kg with an average value 1325.10 j/kg in case of pre-monsoon cyclone. Without Nargis (2007)

all pre-monsoon cyclones shows decrement per intensity level and average decrement is 108.1 j/kg or 9.71%.

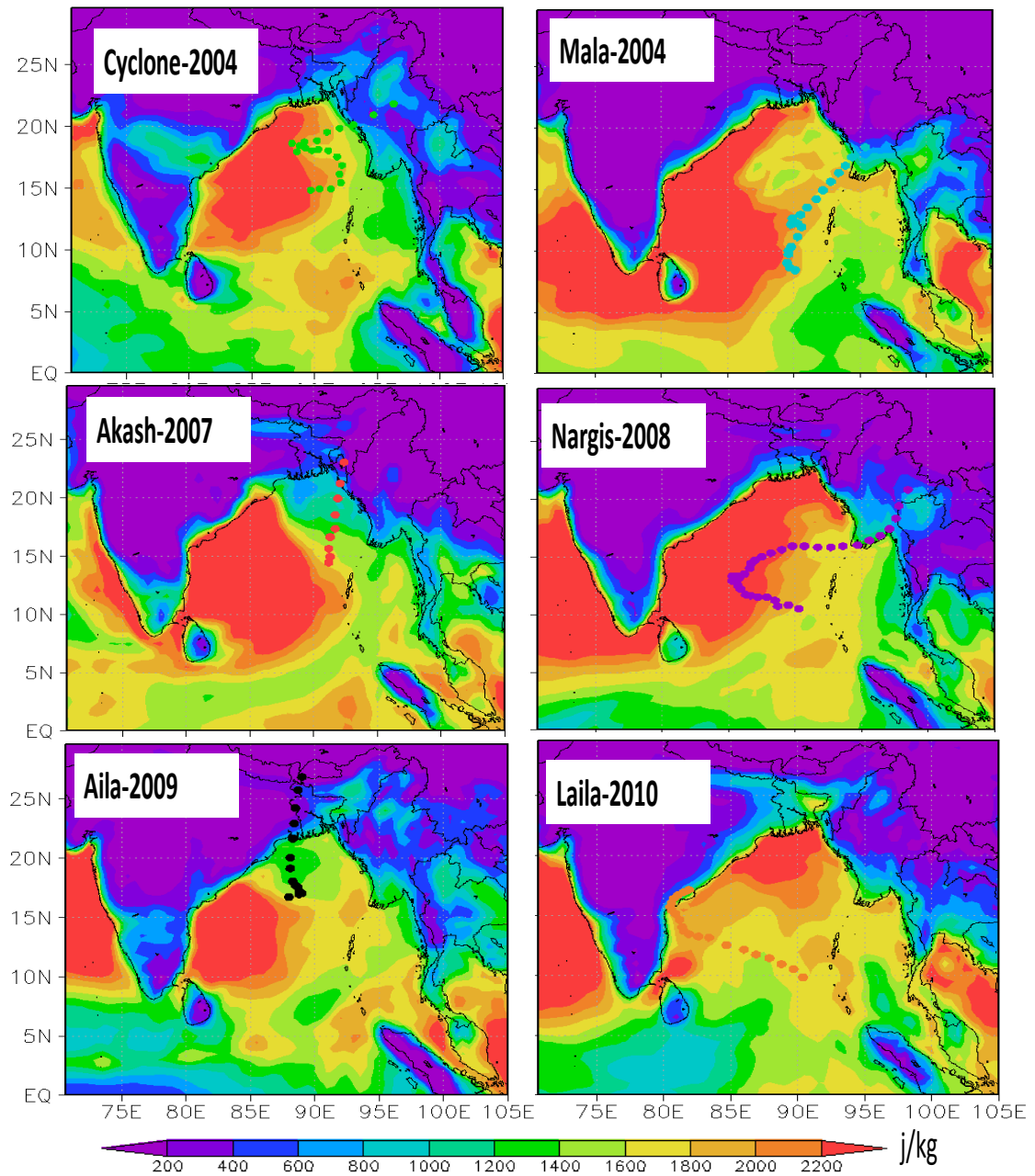


Fig 4.41: Spatial distribution of average CAPE during cyclone period of each pre-monsoon cyclone.

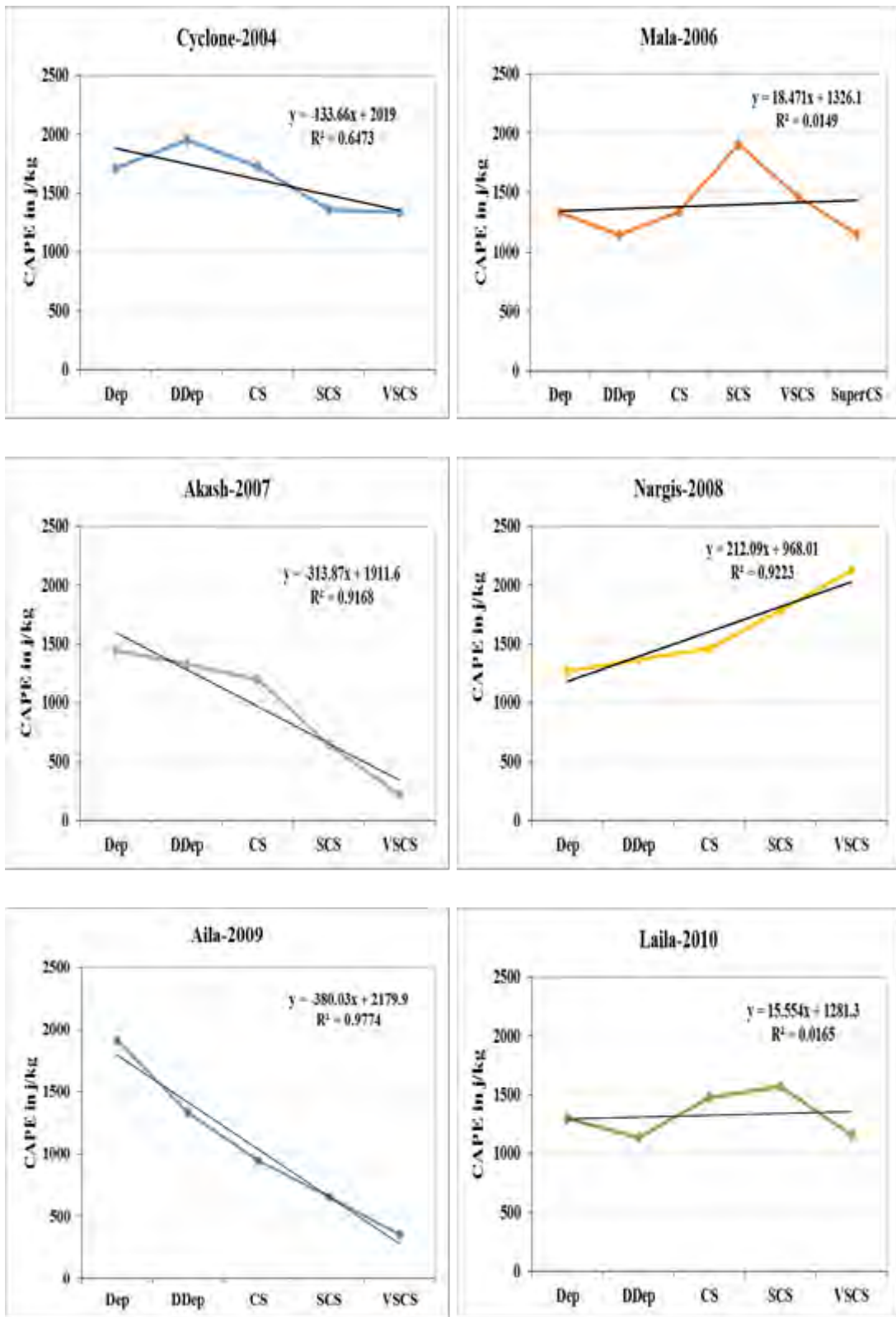


Fig 4.42: CAPE for individual pre-monsoon cyclones

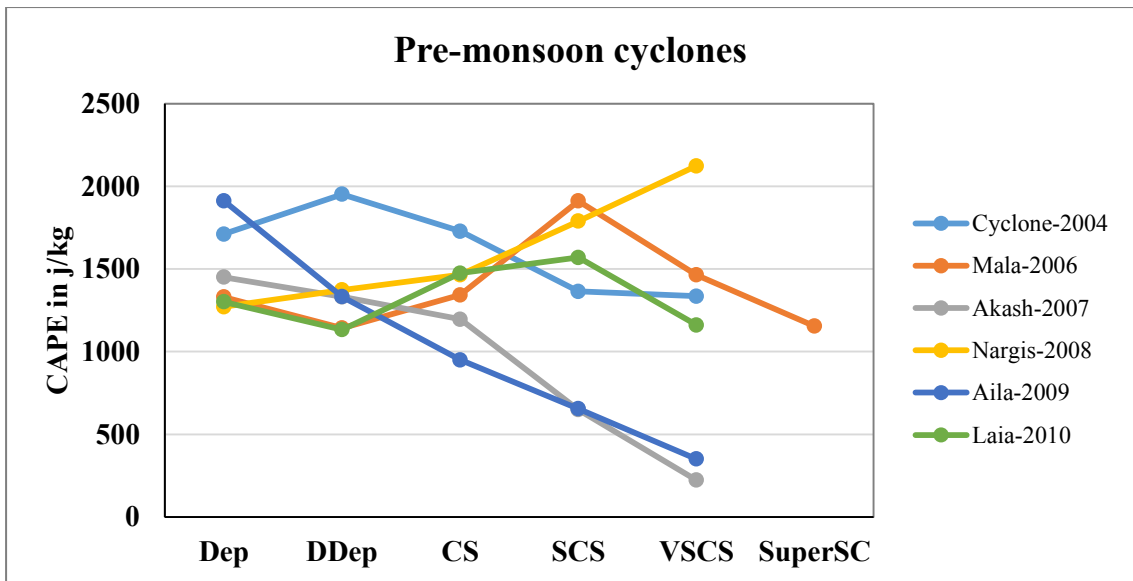


Fig 4.43: CAPE for all pre-monsoon cyclones.

Table 14: Characteristic of CAPE for pre-monsoon cyclones

Pre-monsoon Cyclones	Lowest value (j/kg)	Highest value (j/kg)	Average value (j/kg)	Average increment/decrement per intensity level	
				j/kg	%
Cyclone 2004	1335.525	1951.51	1617.965	-93.682	-5.125
Mala 2006	1142.62	1911.09	1390.708	-35.372	0.226
Akash 2007	222.49	1450.605	969.938	-307.028	32.459
Nargis 2008	1271.298	2123.52	1604.281	213.055	13.878
Aila 2009	350.253	1911.91	1039.767	-390.414	-34.148
Laila 2010	1133.19	1569.79	1327.964	-35.133	-0.597
Average for all pre-monsoon cyclones	909.229	1819.738	1325.104	-108.096	-9.704

Post-monsoon cyclones

The spatial distribution of CAPE for all post-monsoon cyclone shows in Fig 4.44 CAPE are varied among the cyclones. Intense CAPE in the Western region of Giri (2010) and in the Southern part of Cyclone (2000) and Sidr (2007). Maximum value found in cyclone Giri (2010) and cyclone Thane (2011) shows the minimum value.

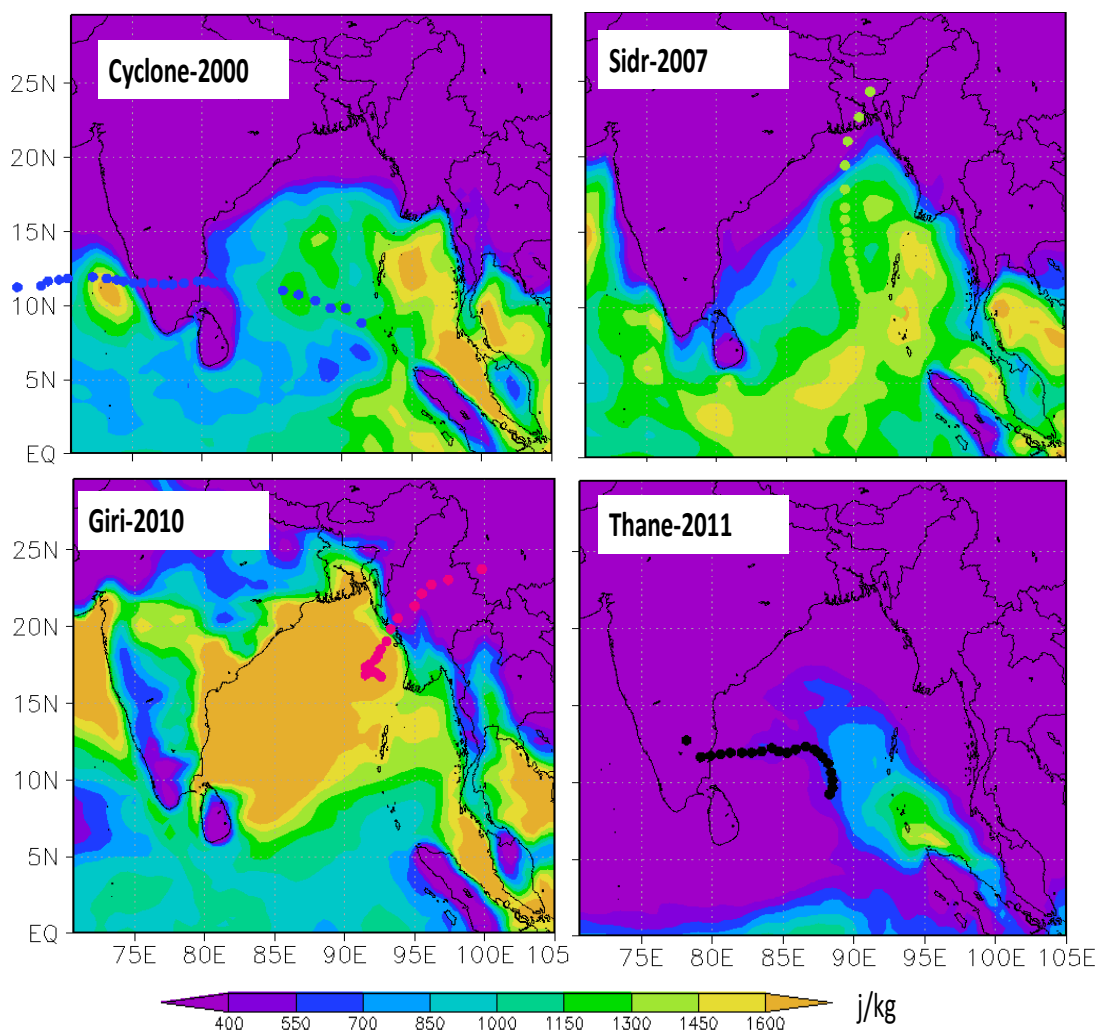


Fig 4.44: Spatial distribution of average CAPE during cyclone period of each post-monsoon cyclone.

Fig 4.45 and Fig 4.46 shows the trend of CAPE with individual and combine post-monsoon cyclone intensity change. CAPE at surface shows decreasing trend with all post-monsoon cyclones intensity except Sidr (2007) which shows increasing trend.

In case of post-monsoon cyclones CAPE value decreases from maximum 1600 j/kg to minimum 400 j/kg which meet the primary condition of cyclone intensification. In case of Sidr (2007) at the highest intensity level CAPE value is relatively lower (~ 150 j/kg) from the previous intensity level.

For all graphs R-squared value is calculated and found significance for Cyclone(200), and Sidr (2007) where it has the value ≥ 0.5 , for other post-monsoon cyclones i.e. for Giri(2010), and Thane (2011) it has the value < 0.5 .

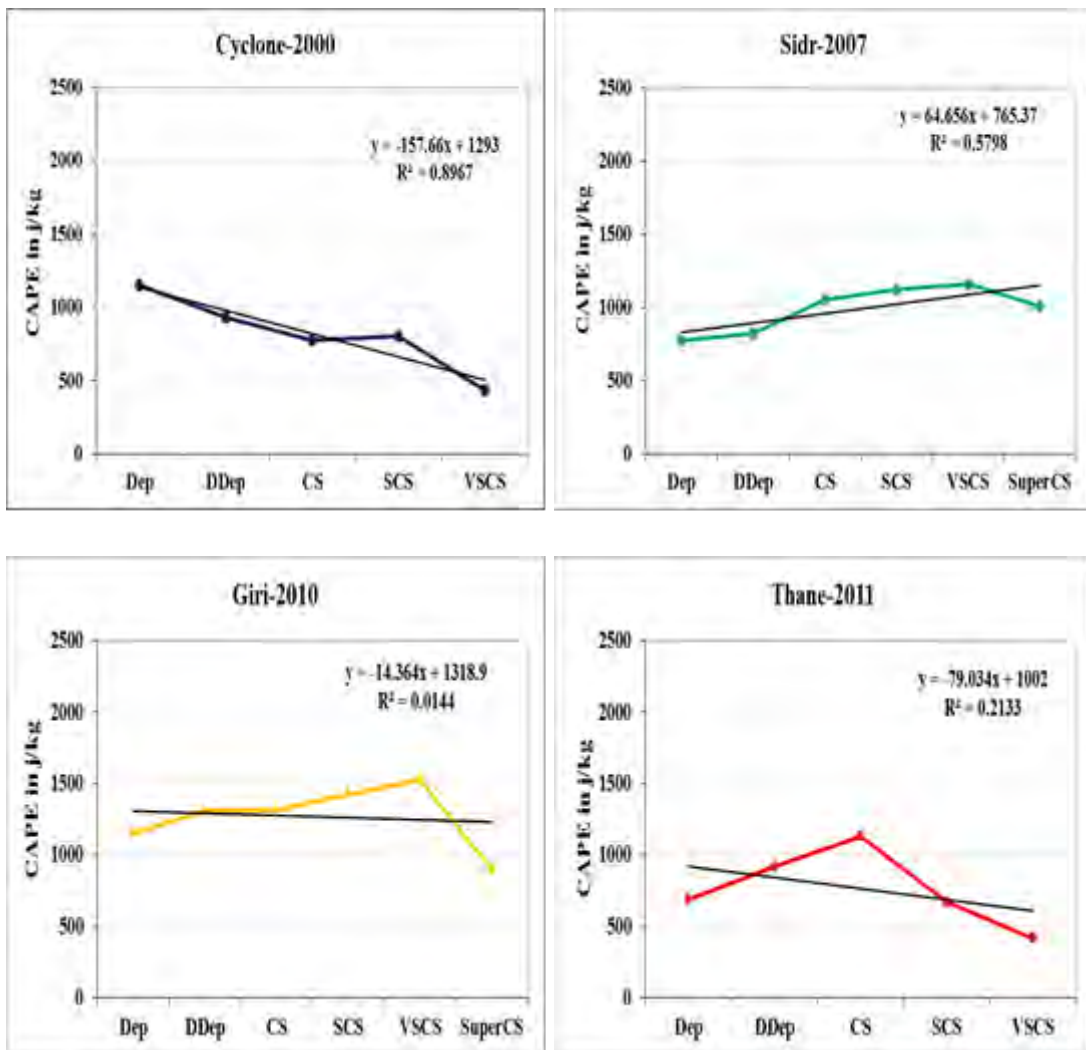


Fig 4.45: CAPE for individual post-monsoon cyclones.

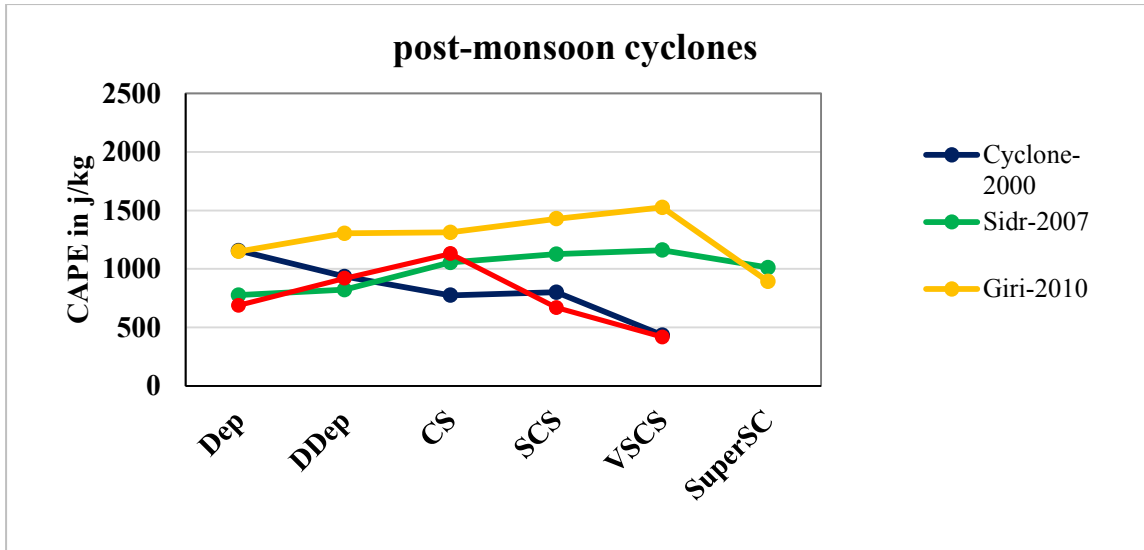


Fig 4.46: CAPE for all post-monsoon cyclones.

Overall summary for the parameter of CAPE is shown in Table 15. From the table, it is found that the average CAPE varied from 630.06 j/kg to 1243 j/kg for post-monsoon cyclones, with an average value of 961.30 j/kg. For all cyclone the average decrement per intensity level is found 63.02 j/kg i.e. the average CAPE decreases 5.30% from each level in case of post-monsoon cyclones.

CAPE value varied from 630-1820 j/kg for both season cyclones which is essential for cyclone intensification. Average CAPE value in case of pre-monsoon is higher than post-monsoon cyclone. Overall CAPE shows decreasing trend with cyclone intensity change for both season cyclone.

Table 15: Characteristic of CAPE for post-monsoon cyclones

Post-monsoon Cyclones	Lowest value(j/kg)	Highest value(j/kg)	Average value(j/kg)	Average increment/decrement per intensity level	
				j/kg	%
Cyclone 2000	434.126	1155.82	820.016	-180.423	-19.658
Sidr 2007	775.385	1160.709	991.667	47.112	6.247
Giri 2010	892.894	1525.193	1268.638	-51.21	-2.339
Thane 2011	417.831	1130.31	764.895	-67.559	-5.450
Average for all post-monsoon cyclones	630.059	1243.008	961.304	-63.019	-5.30

Average CAPE value are fluctuate from maximum 1650 j/kg to minimum 770 j/kg shows in Fig 4.47. Average CAPE for pre-monsoon cyclones (1325 j/kg) is greater than in case of post-monsoon cyclones (962 j/kg). This is because during pre-monsoon, BoB maintains higher SSTs, which in turn influences the vertical gradient of potential temperature and result increased CAPE compared with post-monsoon season. Cyclone (2004) has maximum CAPE value and Thane (2011) has minimum value.

Again Fig 4.48 shows the average increment per intensity level of CAPE for pre- and post-monsoon cyclones. In case of Nargis (2008) and Sidr (2007) CAPE values are positively increase with intensity change. In case of rest of cyclones i.e. Cyclone (2004), Mala (2006), Akash (2007), Aila (2009), Laila (2010), Cyclone (2000), Giri (2010) and Thana (2011) CAPE values are negative with per intensity level. CAPE value averagely decreased 5 to 10 % due to change of intensity level for all cases.

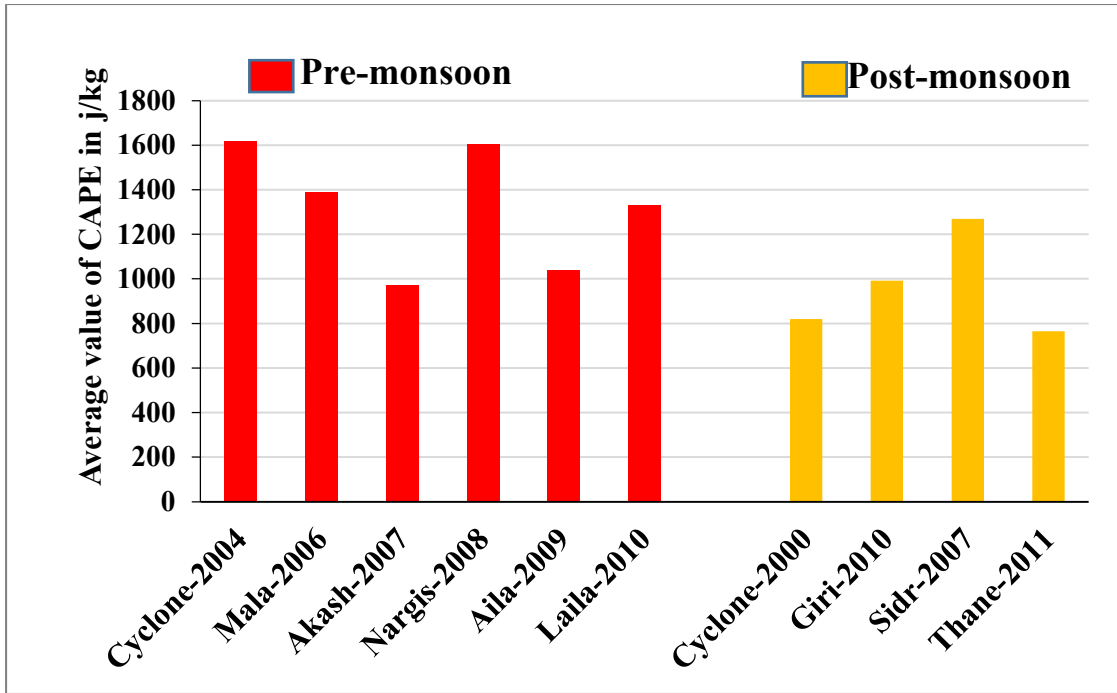


Fig 4.47: Average value of CAPE during cyclones period.

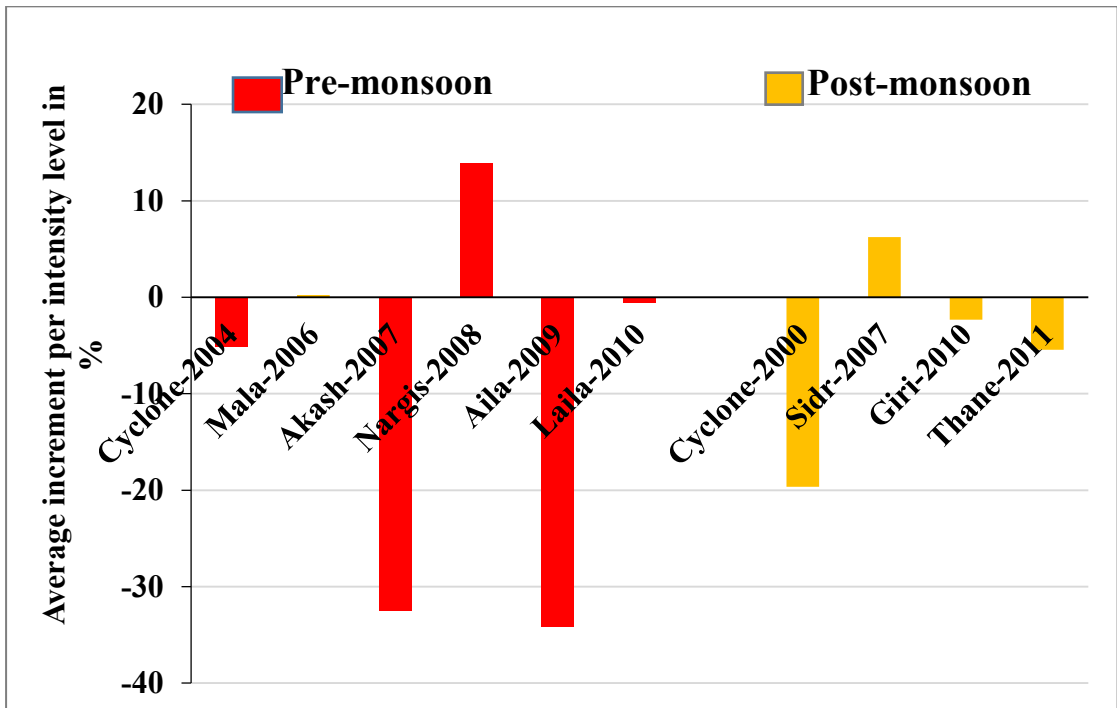


Fig 4.48: Average increment per intensity level of CAPE (%) at surface.

4.2.3 Convective inhibition (CIN) at surface

Pre-monsoon cyclones

Convective inhibition (CIN) is a measure of the strength of the stable layer. CIN is defined as the negative buoyant energy which can limit convection. Environmental CIN value is important for cyclone formation and intensification. The spatial distribution of CIN for all pre-monsoon cyclones shows in Fig 4.49. CIN is the highest in the North Western part of the BoB. Maximum CIN value found in Cyclone (2004) and minimum in cyclone Mala (2006). Again Fig 4.50 and Fig 4.51 shows the trend of CIN with cyclone intensity change in case of pre-monsoon cyclone.

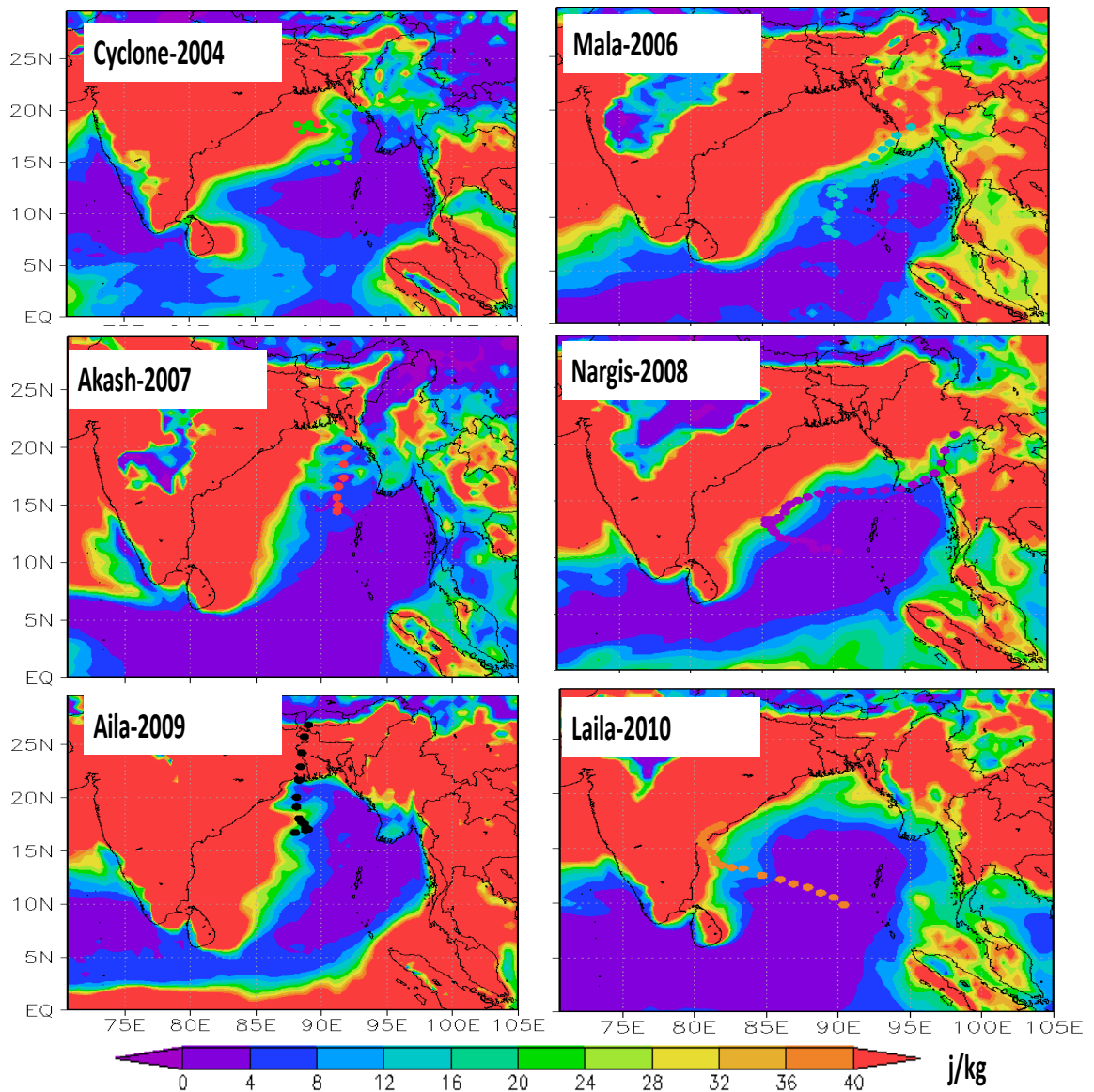


Fig 4.49: Spatial distribution of average CIN during cyclone period of each pre-monsoon cyclone

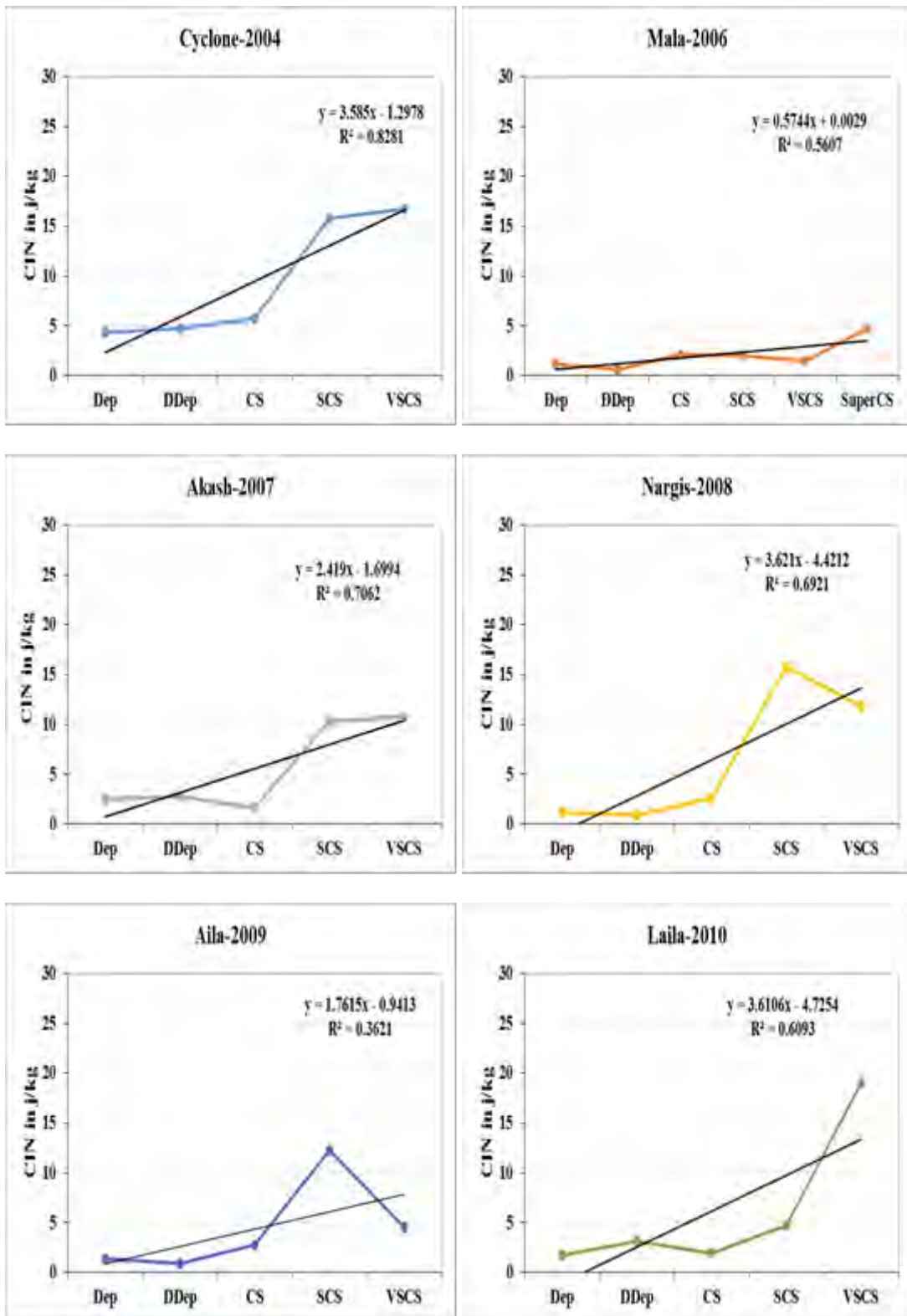


Fig 4.50: CIN for individual each pre-monsoon cyclone.

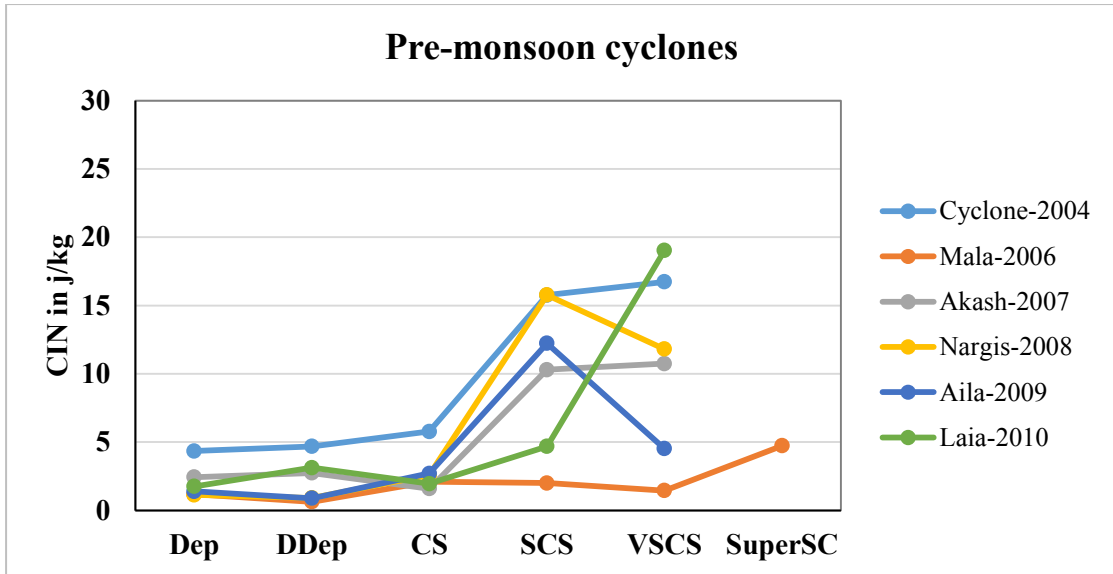


Fig 4.51: CIN for all post-monsoon cyclone.

Magnitude of CIN value is negative and variation are less than 50 j/kg in case of pre-monsoon cyclones, which is favorable condition for cyclogenesis and intensification. CIN increases especially, after cyclone storm level for intensity change. Though in case of cyclone Nargis and Aila the trend are increasing however, at the highest intensity level values are relatively lower (~ 5 j/kg) from the previous intensity level. For all graphs co-efficient of determination is found significant i.e. it has value > 0.5 except Aila.

From the Table 16, it is found that the average CIN varied from 1.68 j/kg to 13.2 j/kg for pre-monsoon cyclones, with an average value of 5.65 j/kg. The average increment per intensity level is found 2.3 j/kg or 44.39 % from each level in case of pre-monsoon cyclones.

Table 16: Characteristic of CIN for pre-monsoon cyclones

Pre-monsoon Cyclones	Lowest value (j/kg)	Highest value (j/kg)	Average value (j/kg)	Average increment/decrement per intensity level	
				j/kg	%
Cyclone 2004	4.345	16.731	9.457	3.096	23.79553
Mala 2006	0.63	4.725	2.013	0.71	43.63478
Akash 2007	1.588	10.742	5.557	2.078	35.434
Nargis 2008	0.907	15.766	6.442	2.669	48.46918
Aila 2009	0.881	12.232	4.343	0.783	61.18983
Laila 2010	1.751	19.022	6.106	4.318	53.80319
Average for all pre-monsoon cyclones	1.684	13.203	5.653	2.276	44.38775

Post-monsoon cyclones

Fig 4.52 shows the spatial distribution of CIN for all post-monsoon cyclones. Most of the cases CIN is more in the Western part of BoB. The movement of CIN with the post-monsoon cyclones intensity change shows in Fig 4.53 and Fig 4.54 CIN values are found to vary from minimum 2 j/kg to maximum 30 j/kg, high value of CIN try to suppress convection. For all post-monsoon cyclone CIN shows increasing trend with intensity change except few points. For all graphs coefficient of determination (R-squared value) is calculated and found significant i.e. for all post-monsoon cyclones it has the value ≥ 0.5 except for Sidr (2007) the value is 0.14.

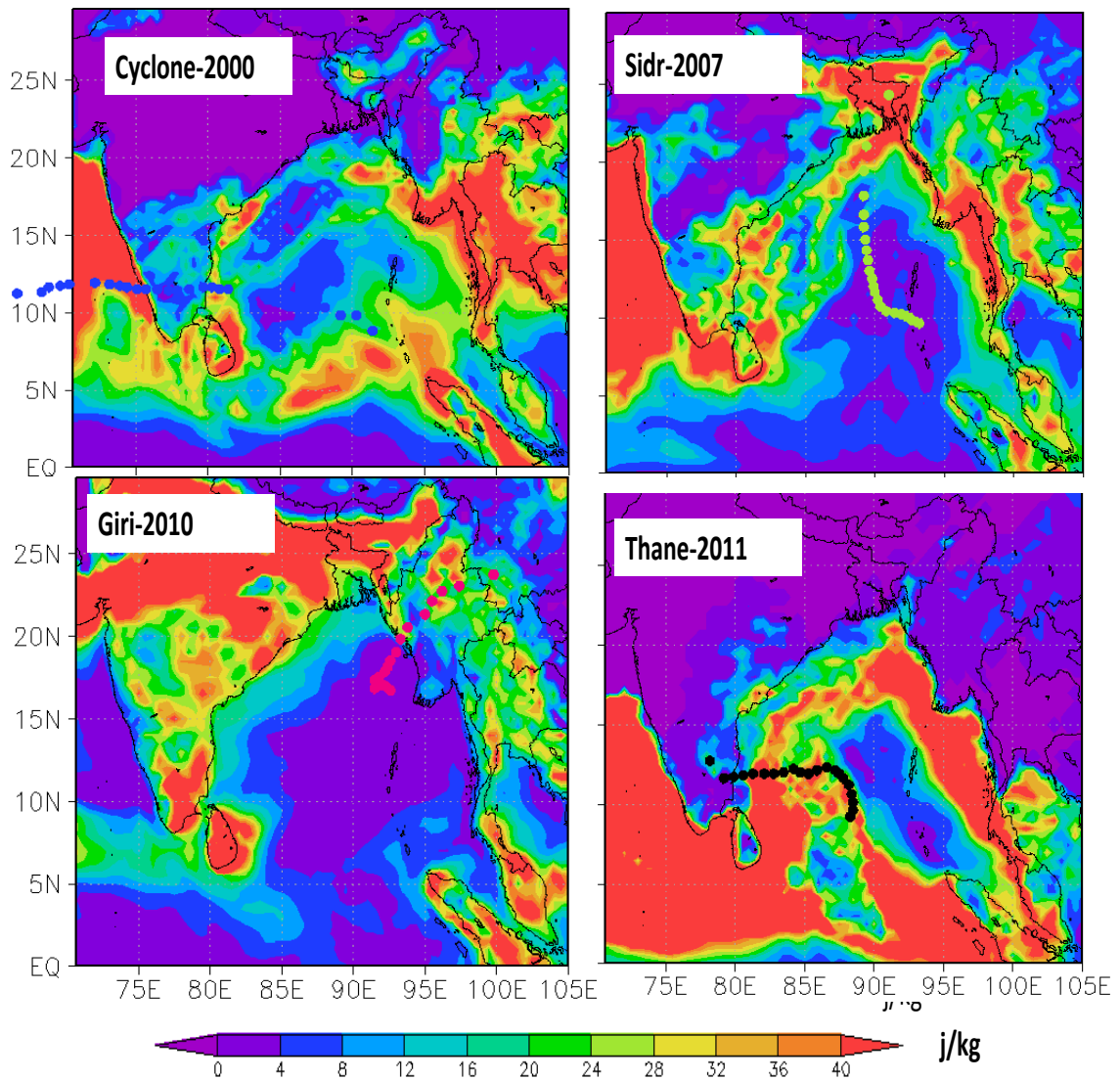


Fig 4.52: Spatial distribution of average CIN during cyclone period of each post-monsoon cyclone.

Overall summary for the parameter of CIN is shown in Table 17. Highest, lowest, average value of CIN for all pre-monsoon cyclones are indicated along with average percentage increment from initial level to highest intensity level. From the table, we found that the average CIN varied from minimum 1.5 j/kg to maximum 14.55 j/kg for post-monsoon cyclones, with an average value of 6.2 j/kg. The average increment per intensity level is found 2.8 j/kg i.e. the average CIN increases 42.42% from each level in case of post-monsoon cyclones.

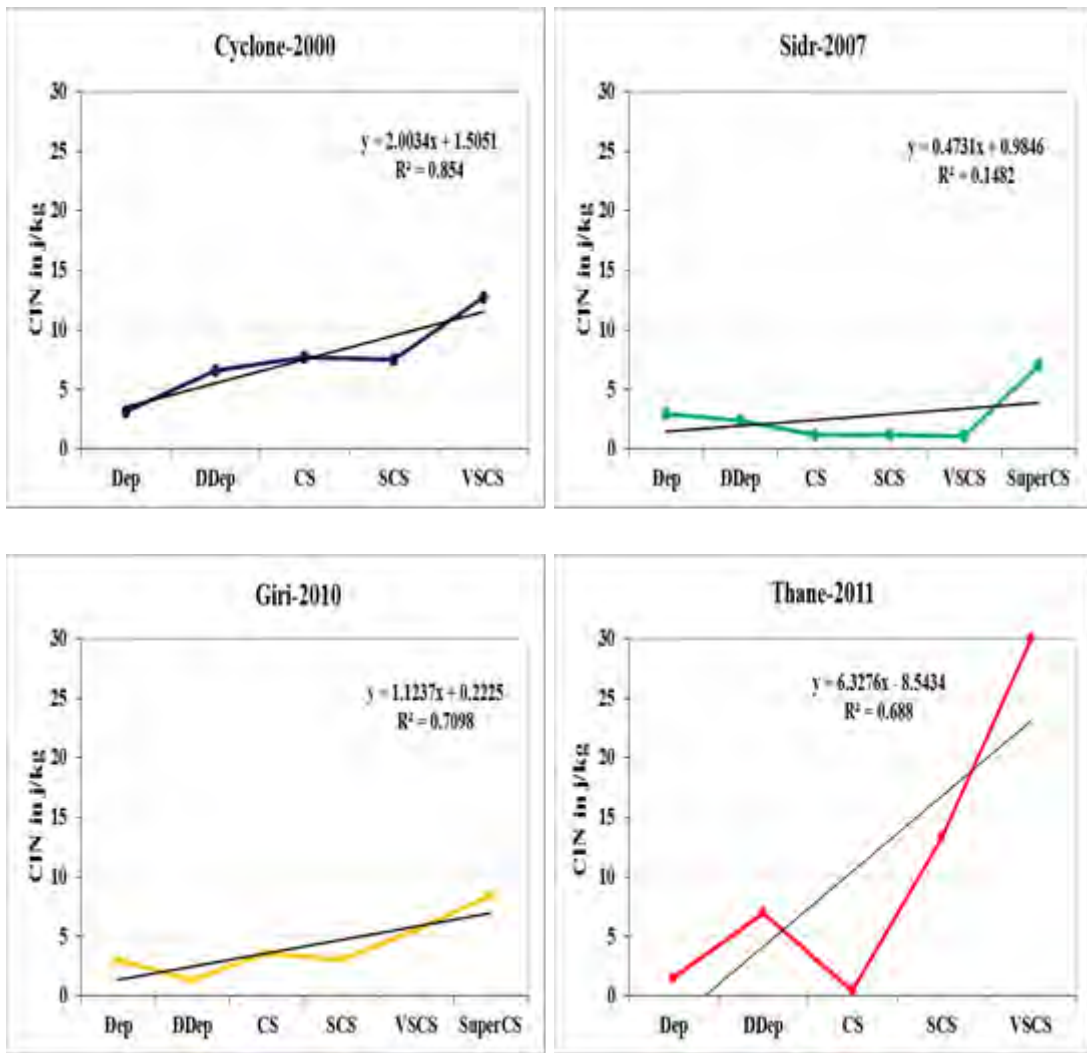


Fig 4.53: CIN for individual post-monsoon cyclone.

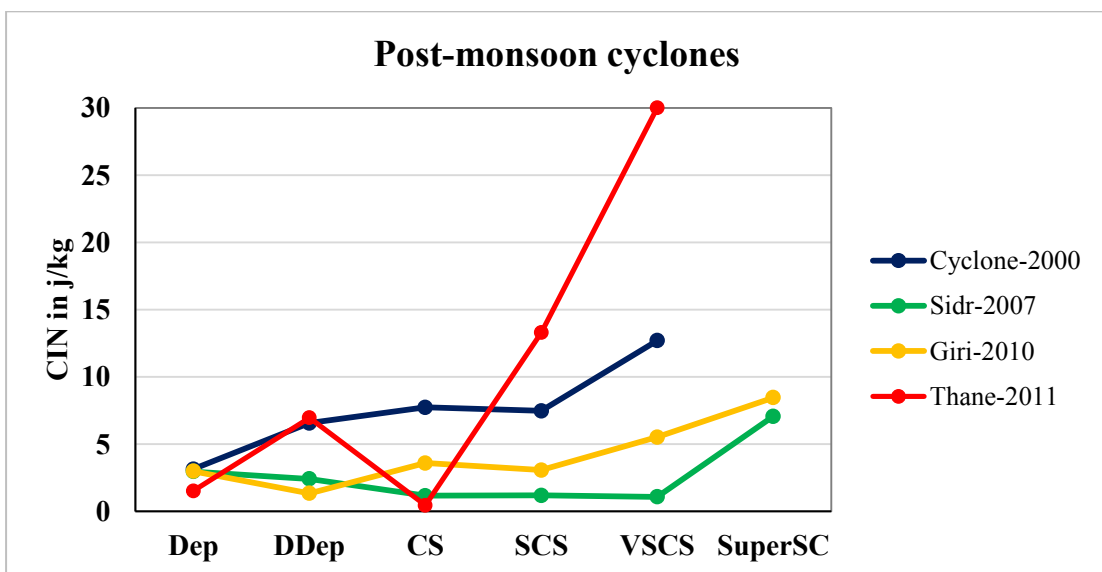


Fig 4.54: CIN for all post-monsoon cyclones.

Table 17: Characteristic of CIN for post-monsoon cyclones.

Post-monsoon Cyclones	Lowest value (j/kg)	Highest value (j/kg)	Average value (j/kg)	Average increment/decrement per intensity level	
				j/kg	%
Cyclone-2000	3.131	12.694	7.515	2.391	13.21589
Sidr-2007	1.082	7.059	2.640	0.820	33.11535
Giri-2010	1.338	8.452	4.155	1.093	42.34686
Thane-2011	0.448	29.992	10.439	7.118	81.00592
Average for all post-monsoon cyclones	1.499	14.548	6.187	2.855	42.421

CIN values (at surface) are found minimum 2 j/kg to maximum 30 j/kg and average CIN values are < 50 j/kg for both season cyclones which is favourable condition for cyclogenesis and intensification. Average CIN value for post-monsoon (6.2 j/kg) is higher than pre-monsoon (5.6 j/kg). Average increment of CIN with intensity for post-monsoon is greater than pre-monsoon.

Fig 4.55 shows the average value of CIN in different cyclones during study period. CIN values are averagely fluctuate from minimum 2 j/kg to maximum 11 j/kg with average 6 j/kg where Cyclone (2004) shows maximum value and Mala (2006) shows minimum value. Average CIN value for pre-monsoon is 5.65 j/kg and for post-monsoon is 6.18 j/kg, which is greater than pre-monsoon.

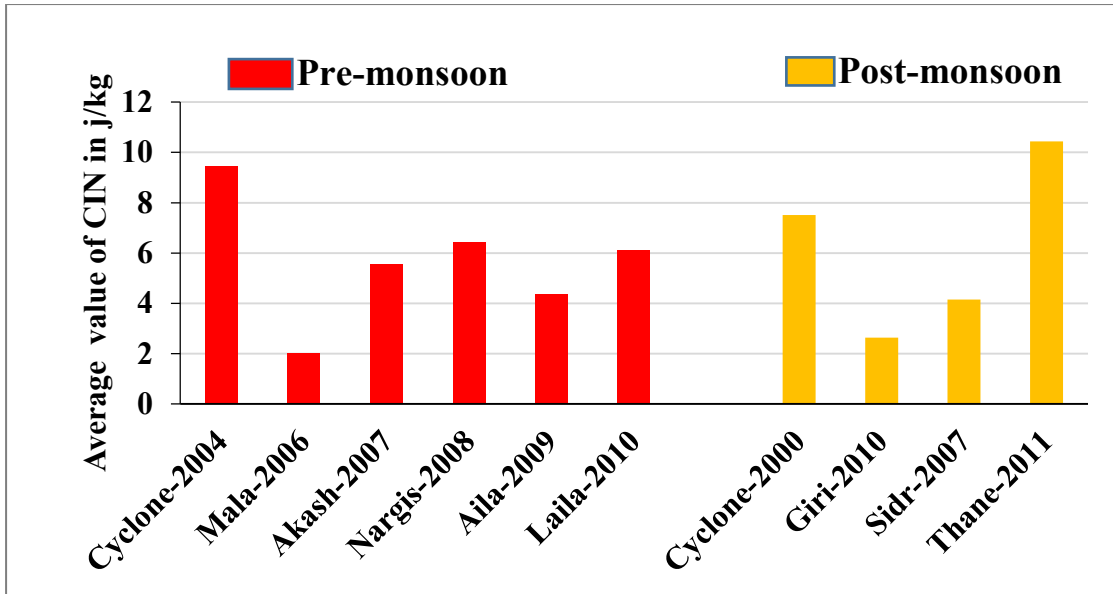


Fig 4.55: Average value of CIN during cyclones period.

Average increment per intensity level of CIN for pre- and post-monsoon is plotted in Fig 4.56. Average increment of CIN with intensity change for pre-monsoon (44.4 %) is greater than for post-monsoon (42.42 %), though average CIN value is higher than pre-monsoon. During pre-monsoon, average CIN increased gradually from northwestern India toward the BoB and almost half of the BoB capped by the CIN of greater than 50 j kg^{-1} . In contrast, during the post-monsoon, the entire BoB maintained the constant geopotential thickness and CIN is less than 30 j kg^{-1} .

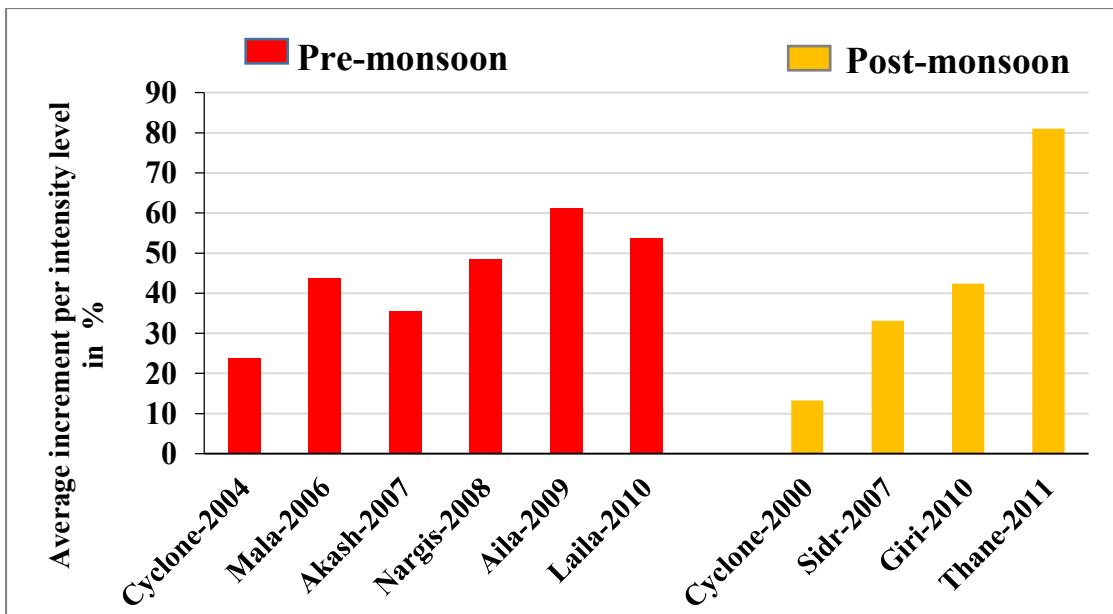


Fig 4.56: Average increment per intensity level of CIN (%) at surface.

4.2.4 Precipitable water (total depth of water upto the troposphere)

Pre-monsoon cyclones

Precipitable water (PW) parameter which gives the amount of moisture in the troposphere. PW is determined by taking all the mass of water vapor in the troposphere and depositing it on the earth's surface. The depth of moisture that would be on the earth's surface is the PW value. PW is the important environmental parameter for cyclone intensification.

The spatial distribution of PW for all pre-monsoon cyclone are plotted in Fig 4.57. PW value found little variation among cyclones. Maximum found in cyclone Laila (2010) and minimum in cyclone Mala (2006). Again Fig 4.58 and Fig 4.59 shows the variation of PW with pre-monsoon cyclones intensity change. Here PW value varied from minimum 50 kg/m^2 to maximum 80 kg/m^2 , which is almost constant, but this range contain sufficient amount of moisture for cyclone intensification. Overall PW shows decreasing trend with intensity change for pre-monsoon cyclone.

For all graphs coefficient of determination is calculated and found < 0.5 for all pre-monsoon cyclone except Akash and Nargis.

Overall summery for the parameter of PW is shown in Table 18. Highest, lowest, average value of PW for all pre-monsoon cyclones are indicated along with average percentage increment from initial level to highest intensity level.

From the Table, it is found that PW value remain almost constant with cyclone intensity change for all pre-monsoon cyclone and its average value is 66.1 j/kg . Again the average decrement per intensity level is found very low (0.3 j/kg or 0.45%) which means PW values are remain same in case of pre-monsoon cyclones.

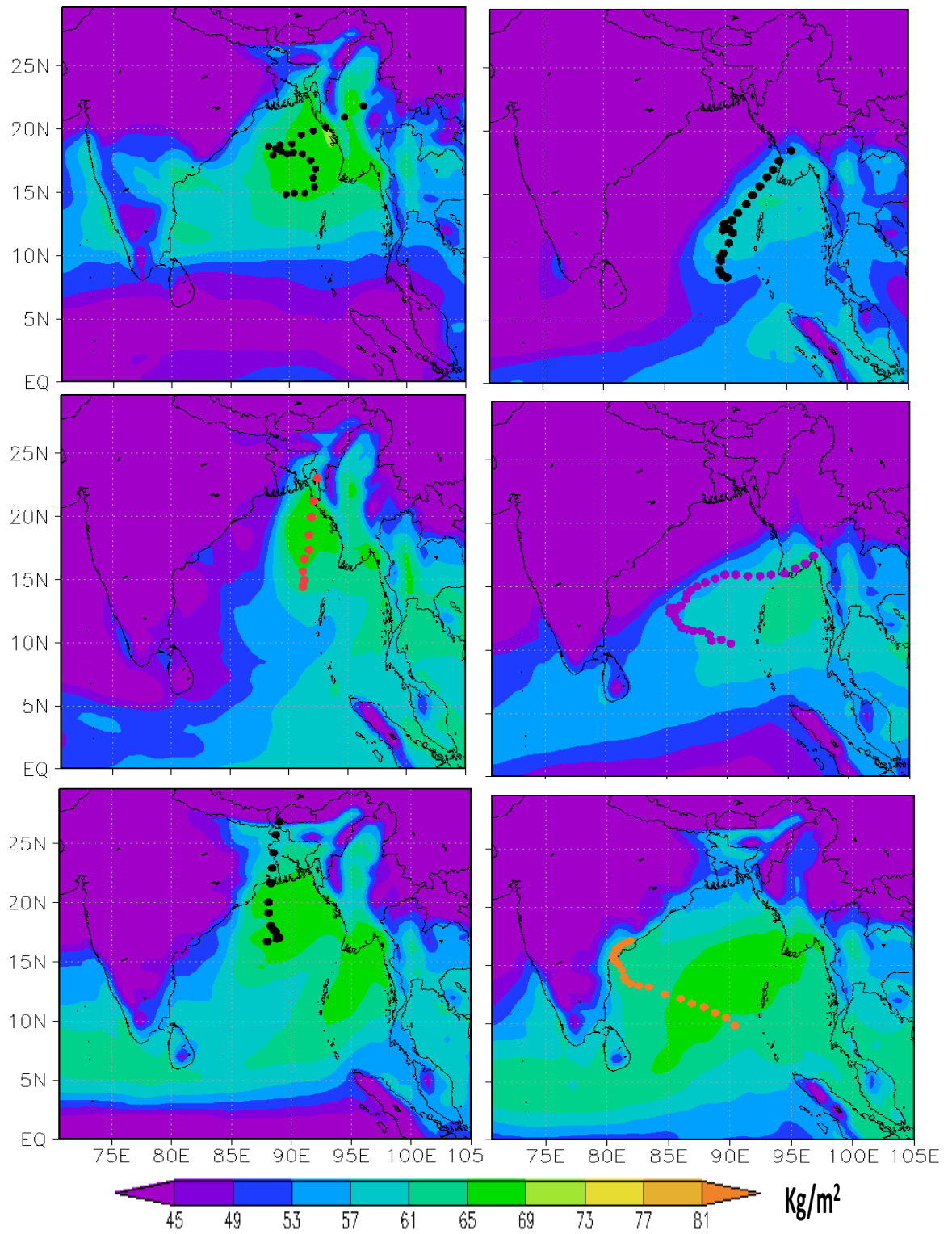


Fig 4.57: Spatial distribution of average PW during cyclone period of each pre-monsoon cyclone.

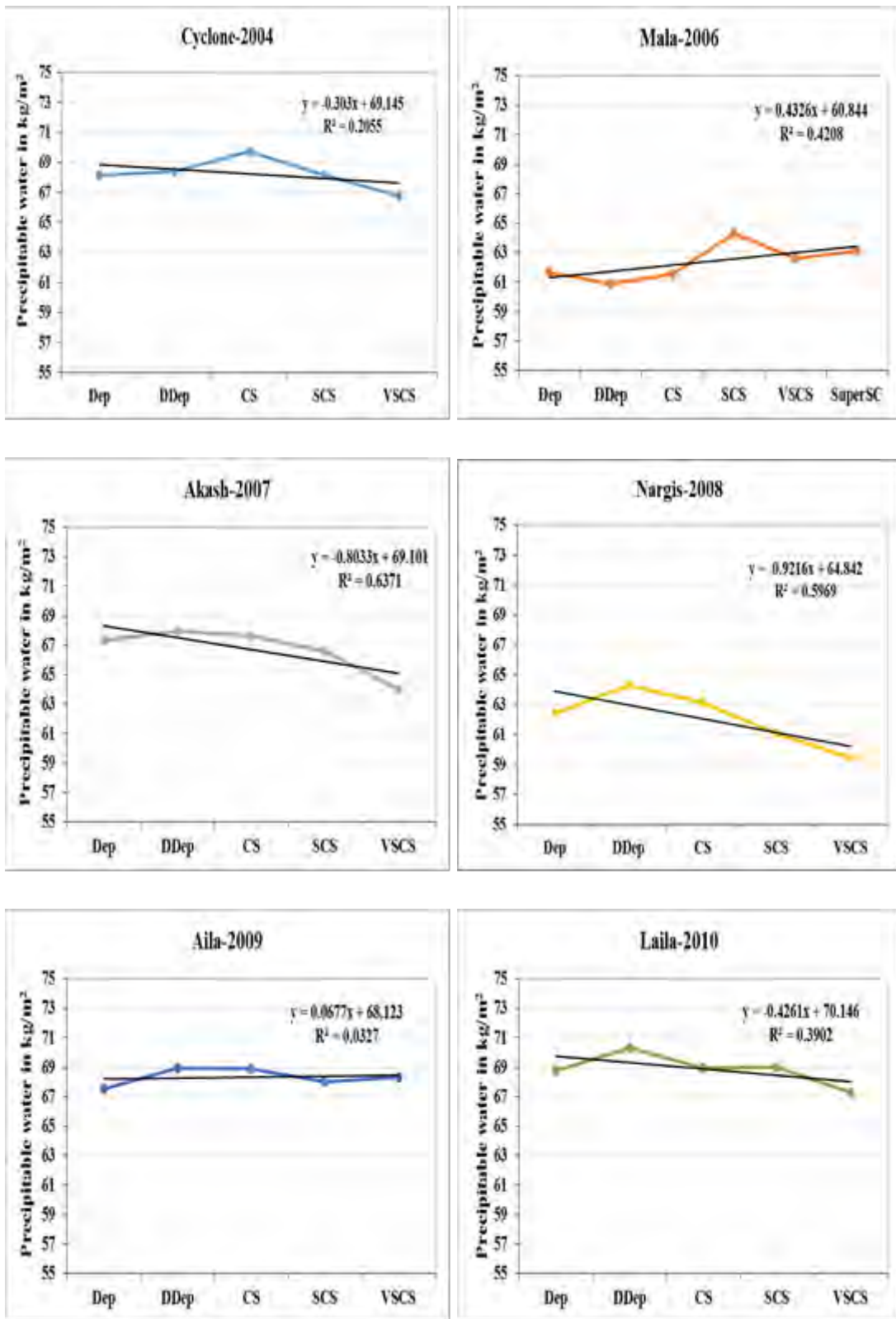


Fig 4.58 : PW for individual pre-monsoon cyclone.

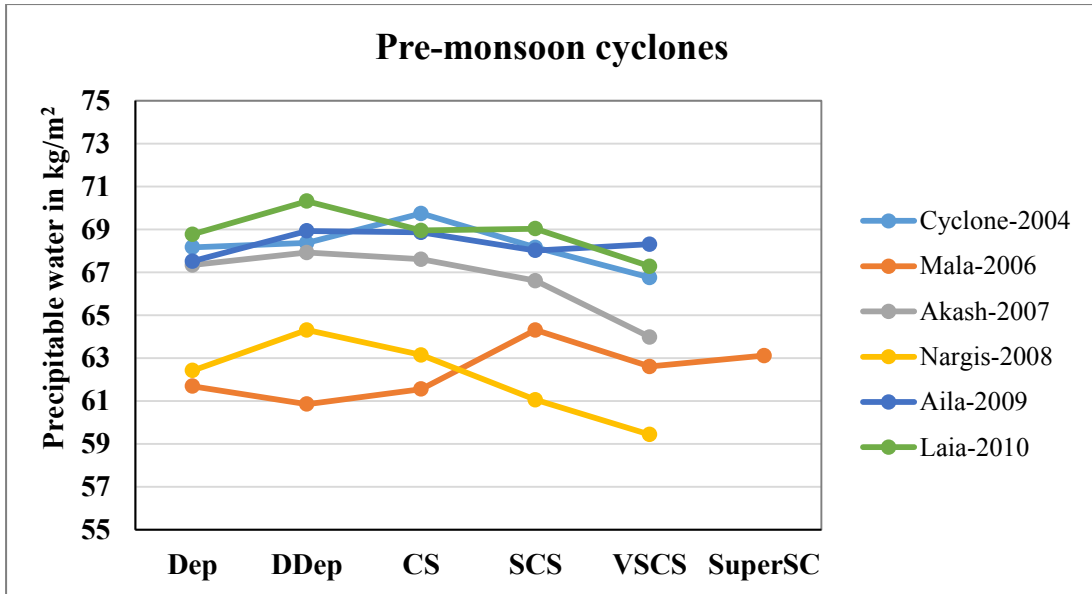


Fig 4.59: PW for all pre-monsoon cyclones.

Table 18: Characteristic of PW for pre-monsoon cyclones.

Pre-monsoon Cyclones	Lowest value (kg/m ²)	Highest value (kg/m ²)	Average value (kg/m ²)	Average increment/decrement per intensity level	
				kg/m ²	%
Cyclone 2004	66.757	69.736	68.236	-0.352	-0.505
Mala 2006	60.86	64.31	62.357	0.286	0.48
Akash 2007	63.979	67.918	66.69	-0.840	-1.256
Nargis 2008	59.442	64.308	62.076	-0.746	-1.186
Aila 2009	67.514	68.928	68.326	0.198	0.3
Laila 2010	67.279	70.312	68.867	-0.372	-0.528
Average for all pre-monsoon cyclones	64.305	67.585	66.092	-0.304	-0.448

Post-monsoon cyclones

Fig 4.60 shows the spatial distribution of PW for all post-monsoon cyclones. Here PW value remain almost same for all post-monsoon cyclones. The variation of PW with cyclones intensity change in case of post-monsoon cyclone shows in Fig 4.61 and 4.62. Among four post-monsoon cyclones, Cyclone (2000) and Thane (2011) has the maximum intensity up to VSCS and other two cyclones i.e. Sidr (2007) and Giri (2010) has more intense level (SuperSC). In this case PW value remain almost constant with cyclone intensity change. Overall PW shows decreasing trend with all post-monsoon cyclone intensity change.

For all graphs coefficient of determination (R-squared value) is calculated and found it has the value <0.5 for cyclone except Cyclone (2000) in which it has the value 0.62.

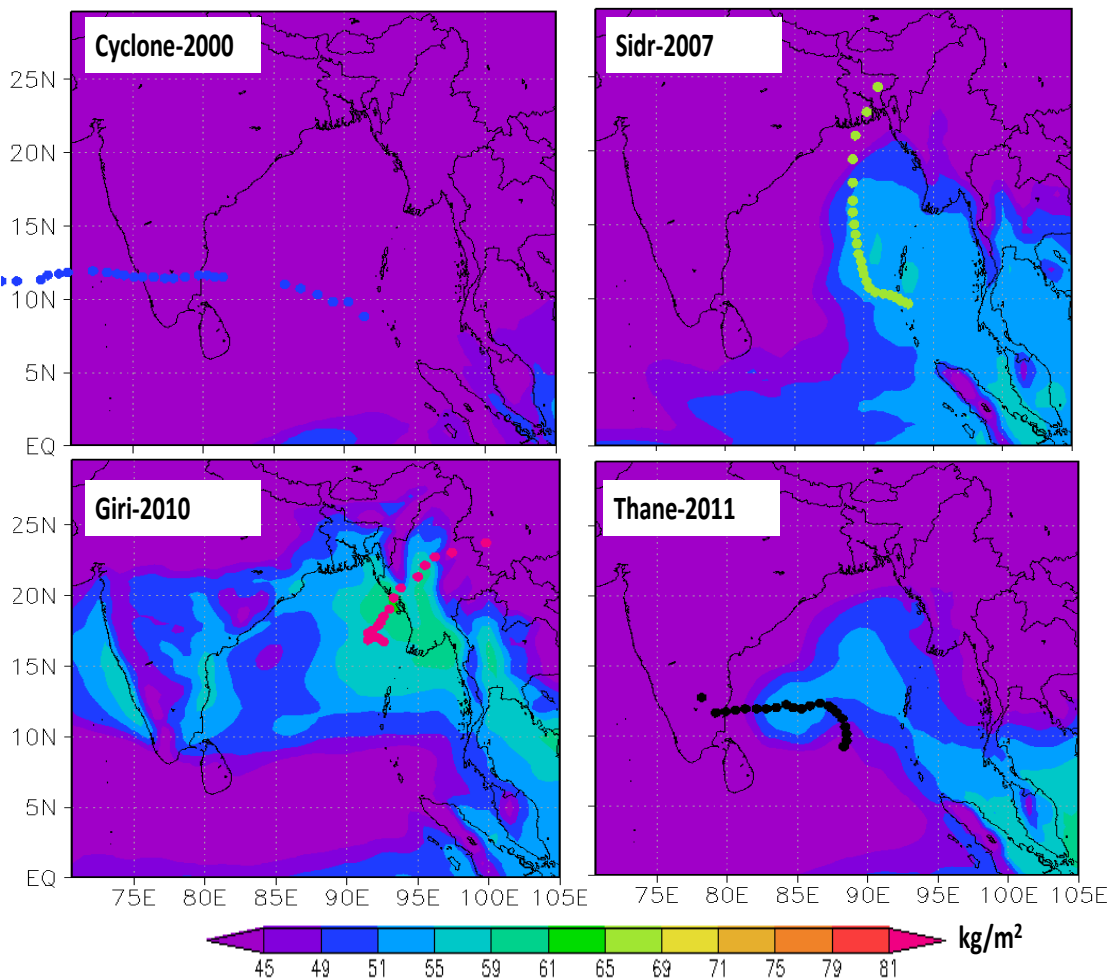


Fig 4.60: Spatial distribution of average PW during cyclone period of each post-monsoon cyclone.

Characteristic of PW for post-monsoon cyclones is shown in Table 19. Highest, lowest, average value of PW for all pre-monsoon cyclones are indicated along with average percentage increment from initial level to highest intensity level. From the table, it is found that the PW varied from minimum 59.55j/kg to maximum 64.9 j/kg with an average value of 62.06 j/kg. The average decrement per intensity level is found 0.49 j/kg or 0.76% in case of post-monsoon cyclones.

PW remain almost constant with cyclone intensity change for both season cyclones. Average value of PW for pre-monsoon cyclone is higher than post-monsoon. Again average value of PW is higher than 60 kg/m², means environment contain more than 60 % moisture which is favorable for cyclone intensification.

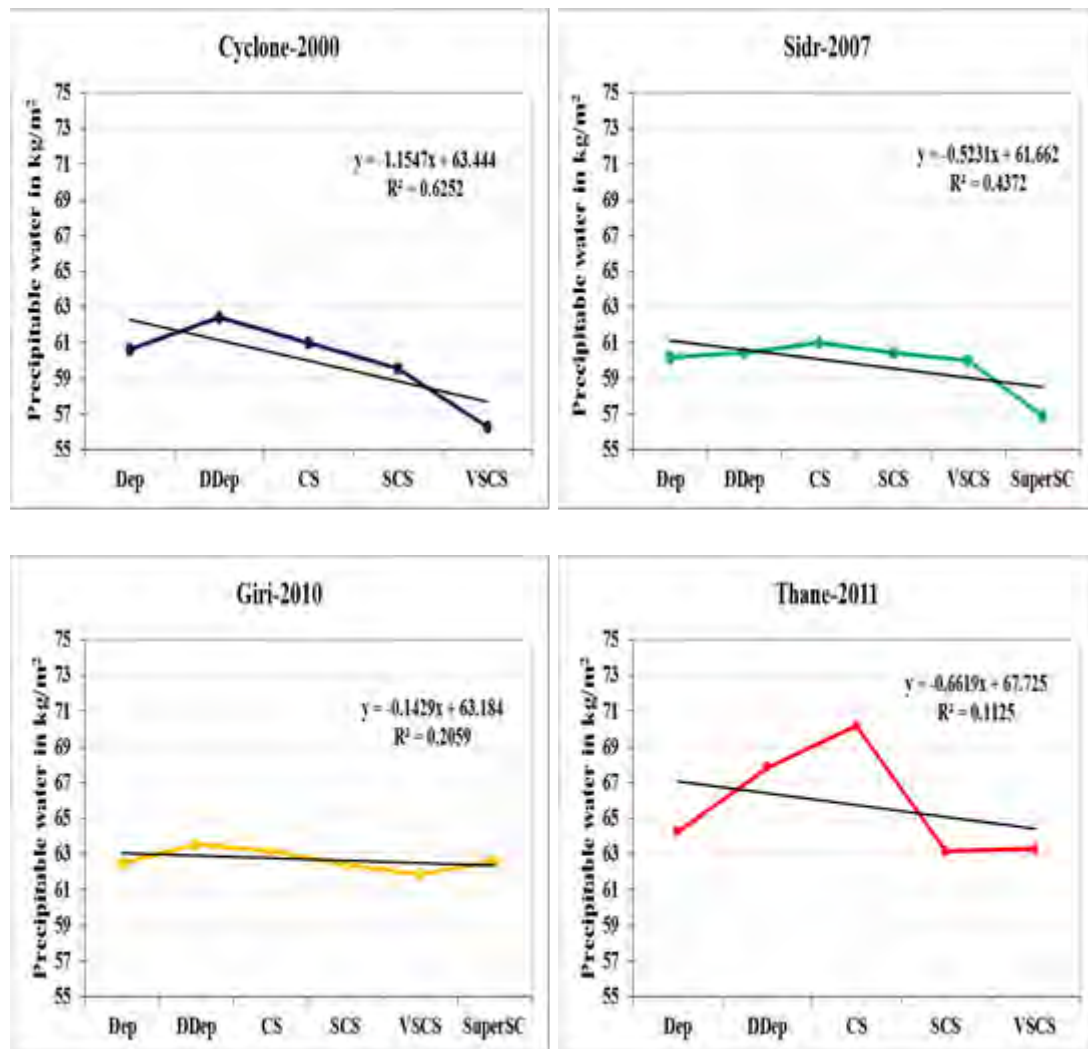


Fig 4.61: PW for individual post-monsoon cyclone.

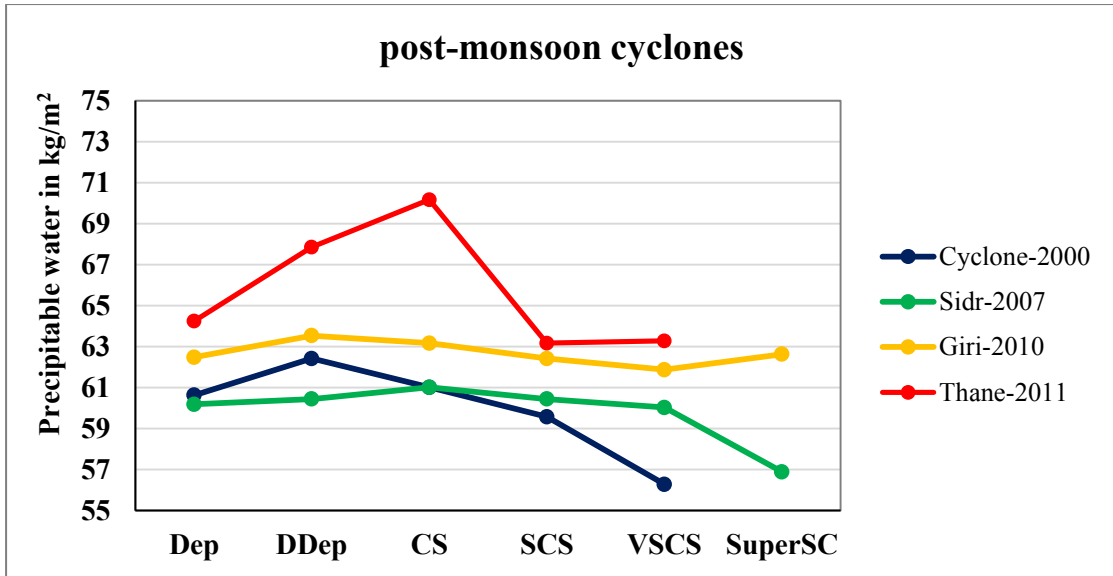


Fig 4.62: PW for all post-monsoon cyclone.

Table 19: Characteristic of PW for post-monsoon cyclones

Post-monsoon Cyclones	Lowest value (kg/m ²)	Highest value (kg/m ²)	Average value (kg/m ²)	Average increment/decrement per intensity level	
				kg/m ²	%
Cyclone 2000	56.274	62.417	59.980	-1.087	-1.79
Sidr 2007	56.889	61.013	59.831	-0.66	-1.095
Giri 2010	61.87	63.536	62.683	0.029	0.055
Thane 2011	63.163	70.164	65.739	-0.242	-0.193
Average for all post-monsoon cyclones	59.549	64.283	62.058	-0.489	-0.758

Average values of PW are found fluctuate from minimum 60 kg/m² to maximum 69 kg/m² with an average 64 kg/m² during cyclone period shows in Fig 4.63. Laila (2010) has maximum PW value and Giri (2010) has minimum value. Average values

of PW for all cyclones are $\geq 60 \text{ kg/m}^2$, means environment contain more than 60% moisture which is favorable for cyclone intensification.

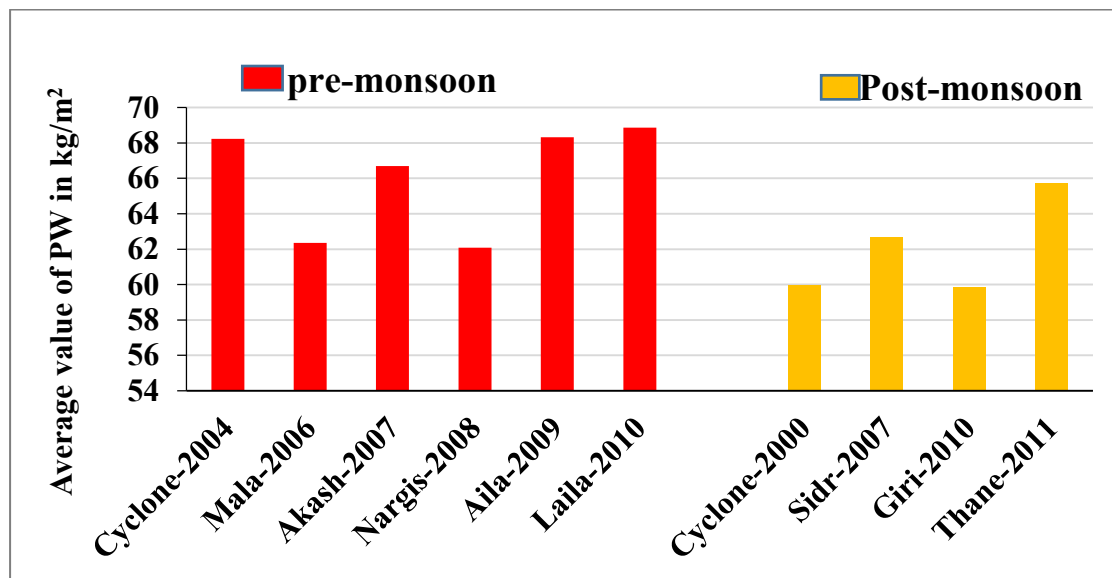


Fig 4.63: Average value of PW during cyclones period.

Average increment per intensity level of PW (%) for pre- and post-monsoon cyclones shows in Fig 4.64. Average decrement of PW in post-monsoon (0.75 %) is higher than pre-monsoon (0.45%). Almost all cyclones shows 0.5 to 1.8 % decreasing value due to the change of intensity level. But this % is small, almost they maintain the constant value.

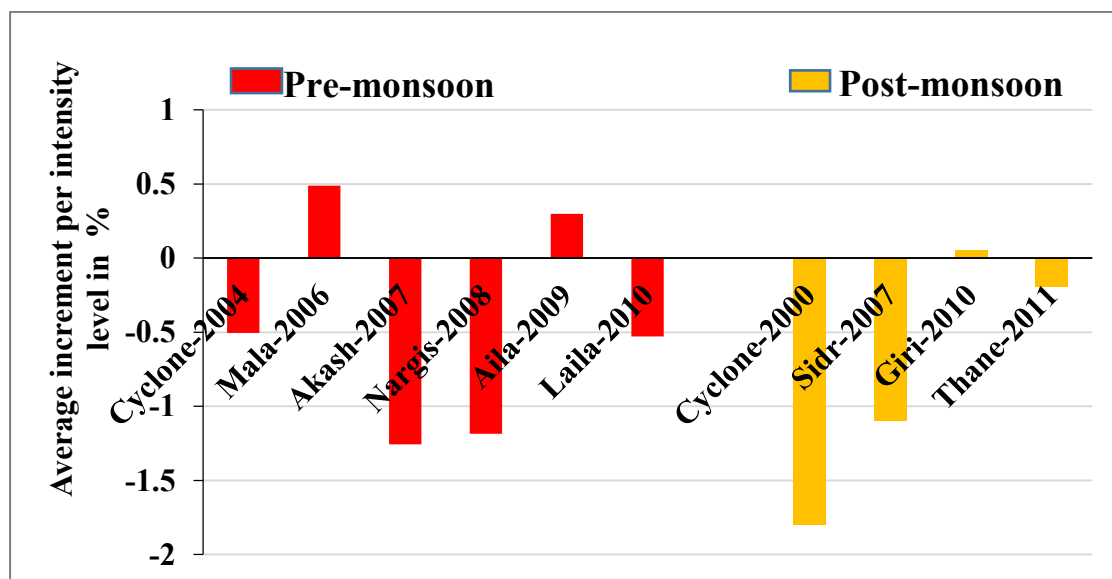


Fig 4.64: Average increment per intensity level of PW (%)

4.2.5 Sea surface temperature (SST)

Pre-monsoon cyclones

Sea surface temperature (SST) is an adequate predictor of tropical cyclone intensity. The distribution of SST exceeding 26 °C is one of the precursors needed to maintain a tropical cyclone.

The spatial distribution of SST for all pre-monsoon cyclones are plotted in Fig 4.65. High SST prominent over BoB. SST is more than 30 °C in the Eastern part of BoB in the most of cyclones. Fig 4.66 and 4.67 shows how SST moved with pre-monsoon cyclones intensity change. Here SST moves from minimum 28 °C to maximum 32 °C in case of pre-monsoon cyclone. However, individual cyclone variation are less than 2 °C. From the graphs, it is found that at the lowest intensity level (Dep) SST value is almost same (>29 °C) which favorable for cyclone intensification.

Overall summery for the parameter of SST is shown in Table 20. Highest, lowest, average value of SST for all pre-monsoon cyclones are indicated along with average percentage increment from initial level to highest intensity level.

From the table, it is found that the variation of SST are very small from minimum 29 °C to maximum 32 °C, with an average value 30.32 °C in case of pre-monsoon cyclones. Overall SST shows constant trend with cyclone intensity change in case of pre-monsoon cyclones.

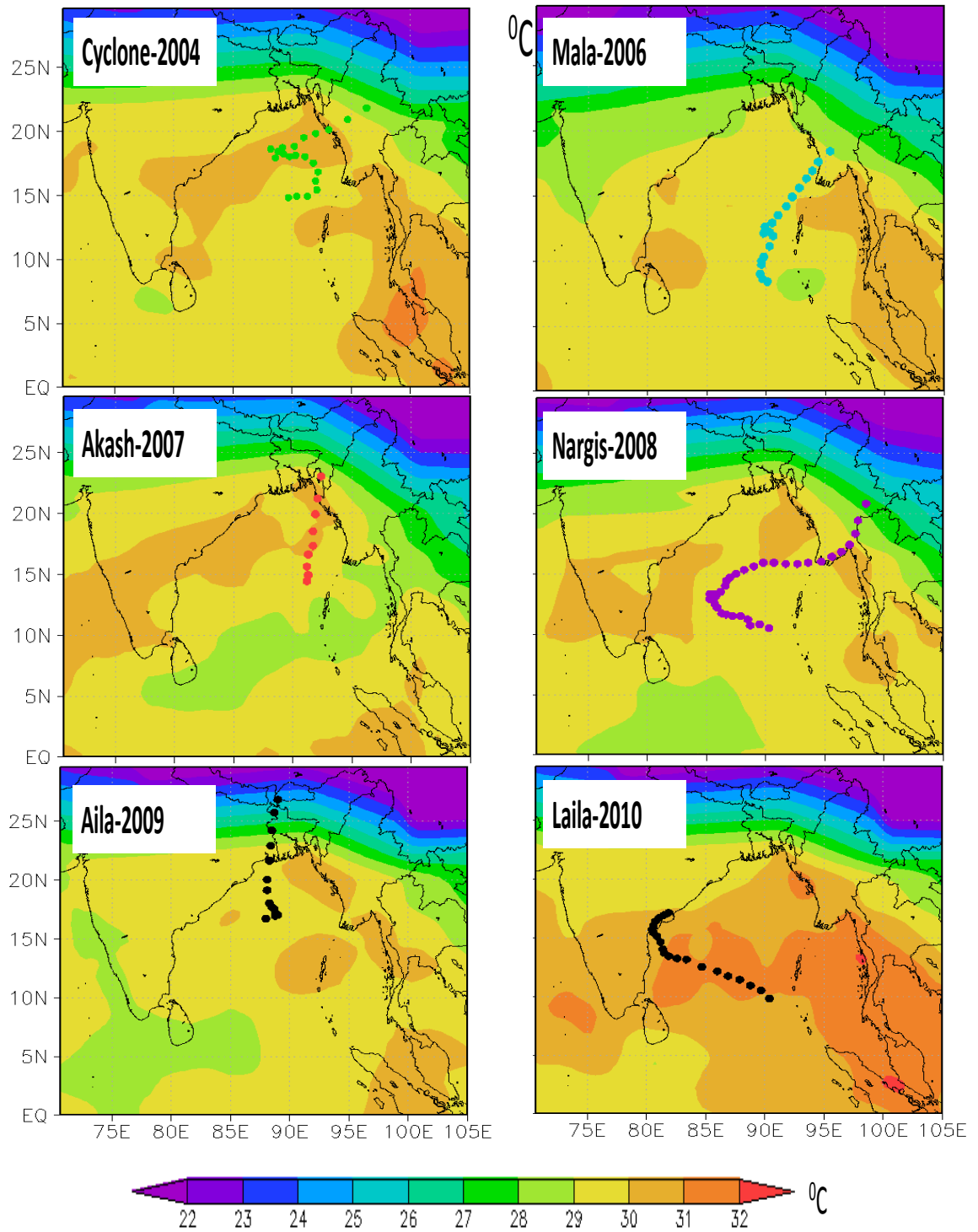


Fig 4.65: Spatial distribution of average SST during cyclone period of each pre-monsoon cyclone.

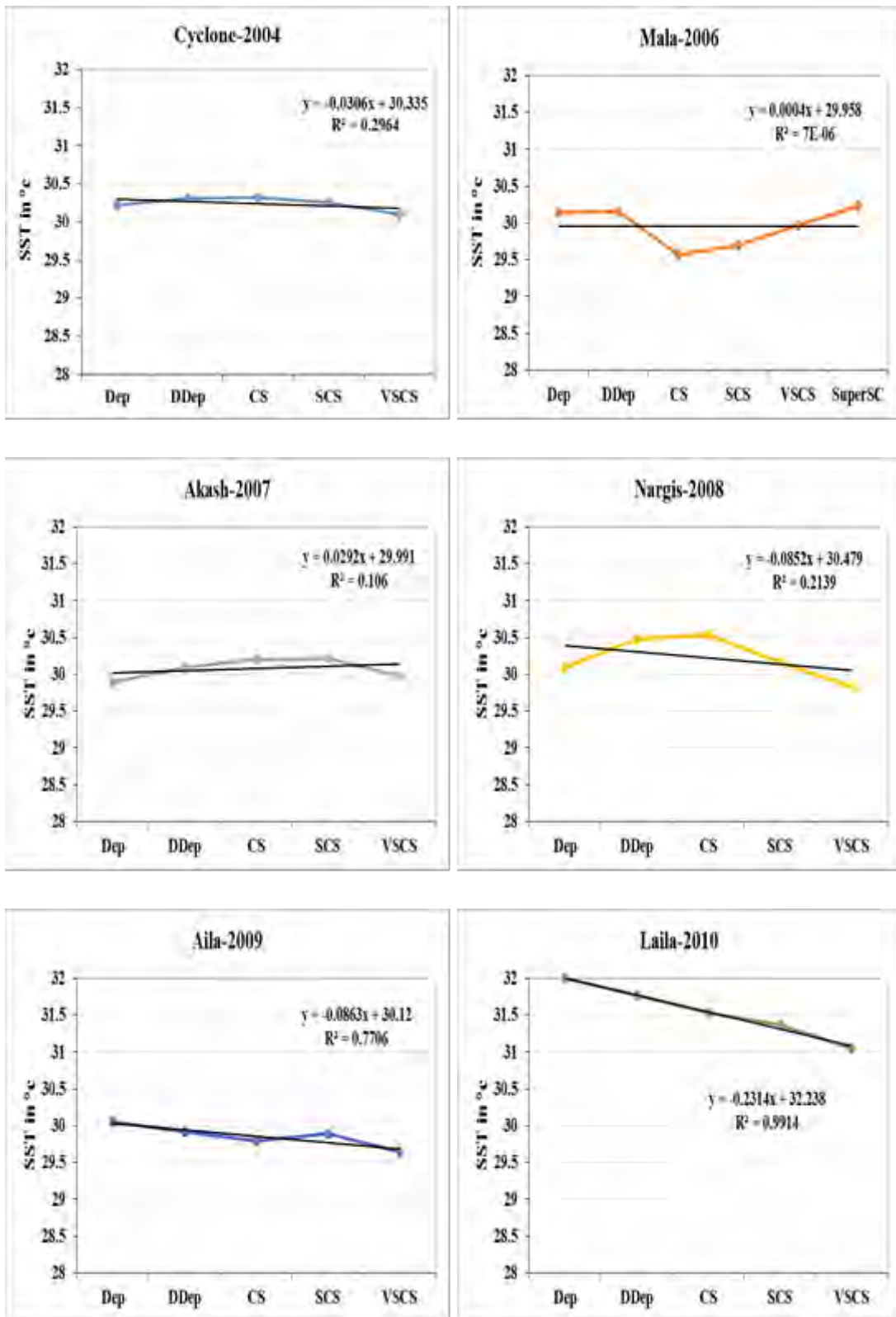


Fig 4.66: SST for all individual pre-monsoon cyclones

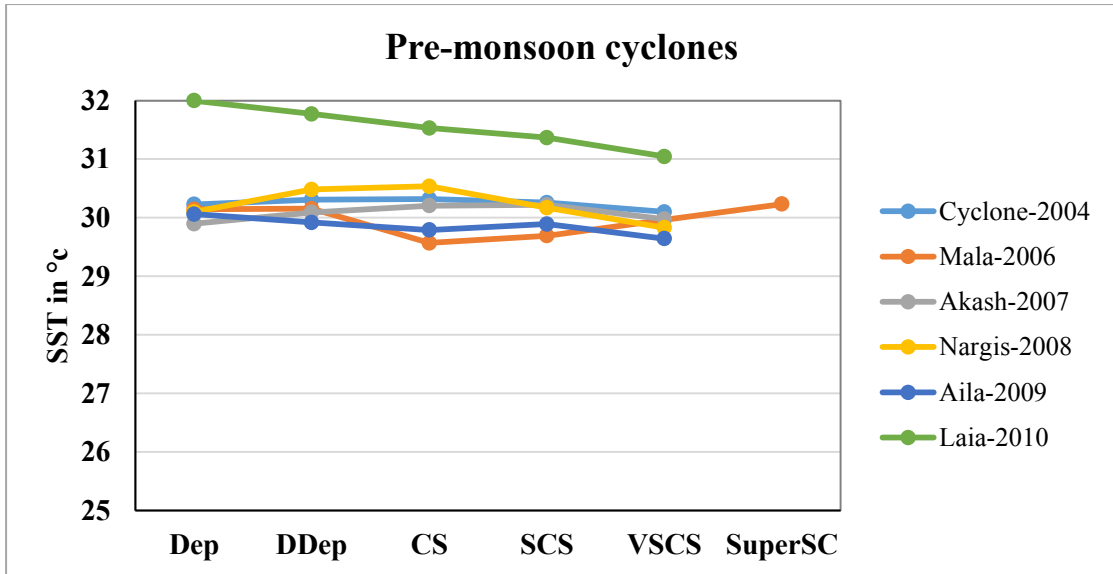


Fig 4.67: SST for all pre-monsoon cyclones.

Table 20: Characteristic of SST for pre-monsoon cyclones.

Pre-monsoon Cyclones	Lowest value (°C)	Highest value (°C)	Average value (°C)	Average increment/decrement per intensity level	
				°C	%
Cyclone 2004	30.099	30.322	30.243	-0.032	-0.105
Mala 2006	29.568	30.233	29.959	0.018	0.065
Akash 2007	29.896	30.221	30.078	0.020	0.069
Nargis 2008	29.828	30.536	30.223	-0.067	-0.220
Aila 2009	29.643	30.06	29.861	-0.104	-0.348
Laila 2010	31.045	32	31.543	-0.239	-0.754
Average for all pre-monsoon cyclones	30.013	30.562	30.318	-0.067	-0.216

Post-monsoon cyclones

Fig 4.68 shows the spatial distribution of SST for all post-monsoon cyclones. SST is highest in the Southern region of BoB. The movement of SST with the post-monsoon cyclones intensity change shows in Fig 4.69 and Fig 4.70. In case of post-monsoon cyclones SST varies from minimum 25 °C to maximum 29 °C which is less than pre-monsoon cyclones. Individual cyclone variation is less than 1 °C. For all post-monsoon cyclones SST shows constant trend with cyclone intensity change.

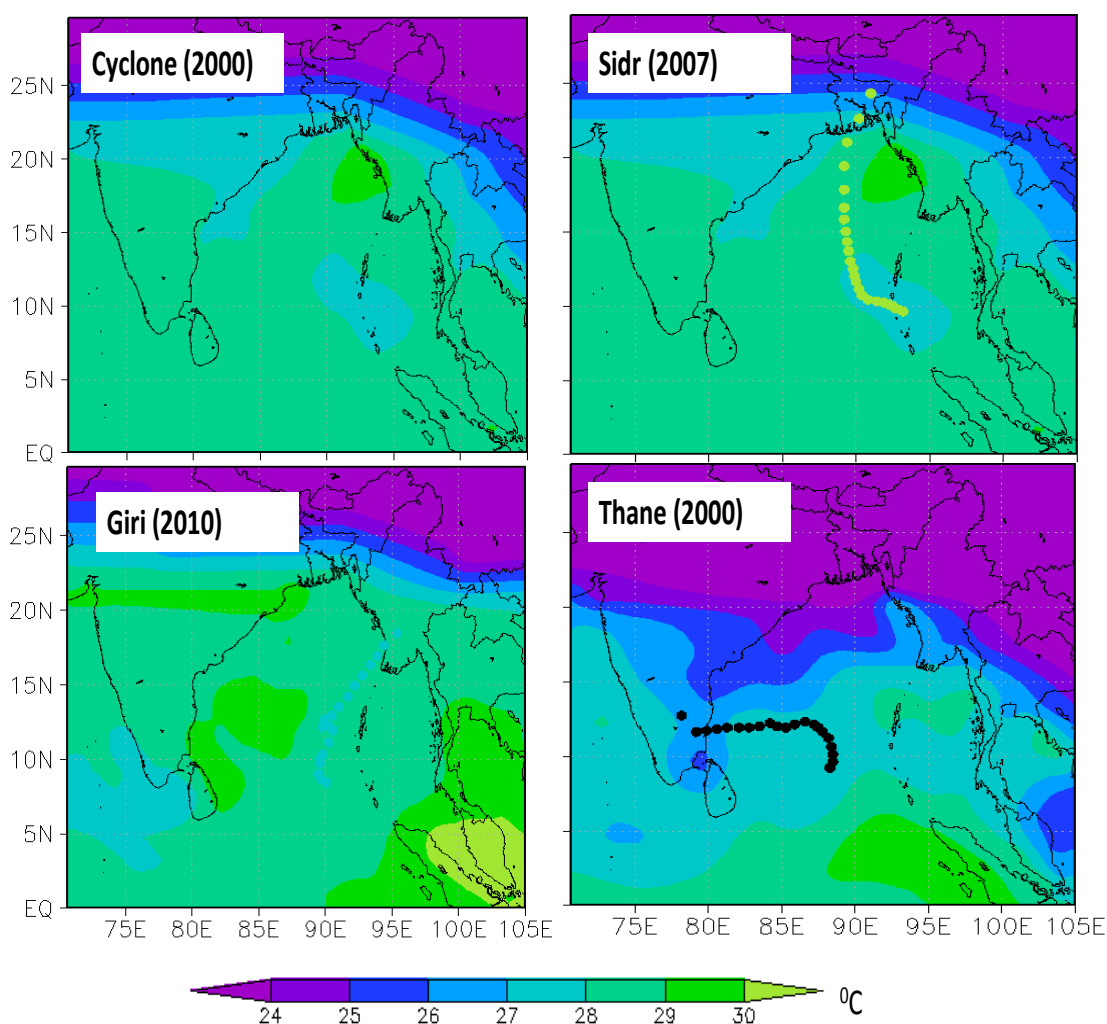


Fig 4.68: Spatial distribution of average SST during cyclone period of each post-monsoon cyclone.

For all graphs R-squared value is calculated and found significant i.e. for all post-monsoon cyclone value is ≥ 0.5 except Sidr (2007) in which the value is 0.1.

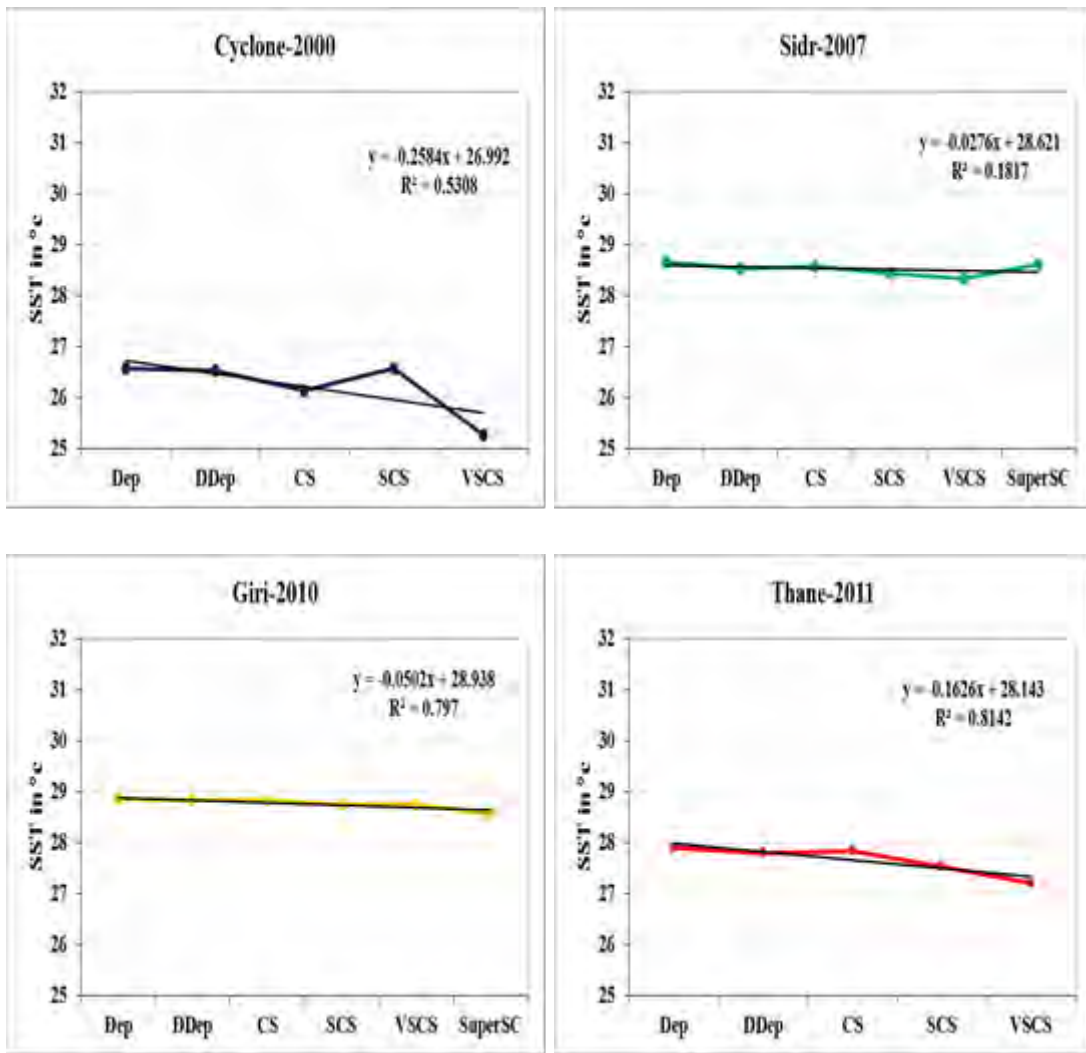


Fig 4.69: SST for individual post-monsoon cyclones.

Overall summary for the parameter of SST is shown in Table 21. From the Table 21, found that the variation of average SST is $<1\text{ }^{\circ}\text{C}$ i.e. from $27.34\text{ }^{\circ}\text{C}$ to $27.99\text{ }^{\circ}\text{C}$, with an average value $27.78\text{ }^{\circ}\text{C}$ for post-monsoon cyclones.

Here SST value ranging from minimum $27\text{ }^{\circ}\text{C}$ to maximum $31\text{ }^{\circ}\text{C}$ for both seasonal cyclone. Average value of SST for both seasonal cyclone is greater than $27\text{ }^{\circ}\text{C}$ which meet the require condition ($> 26\text{ }^{\circ}\text{C}$) for cyclone formation and intensification. Again average value of SST for pre-monsoon cyclone is higher than post-monsoon cyclone. SST remain constant with cyclone intensity change for both case.

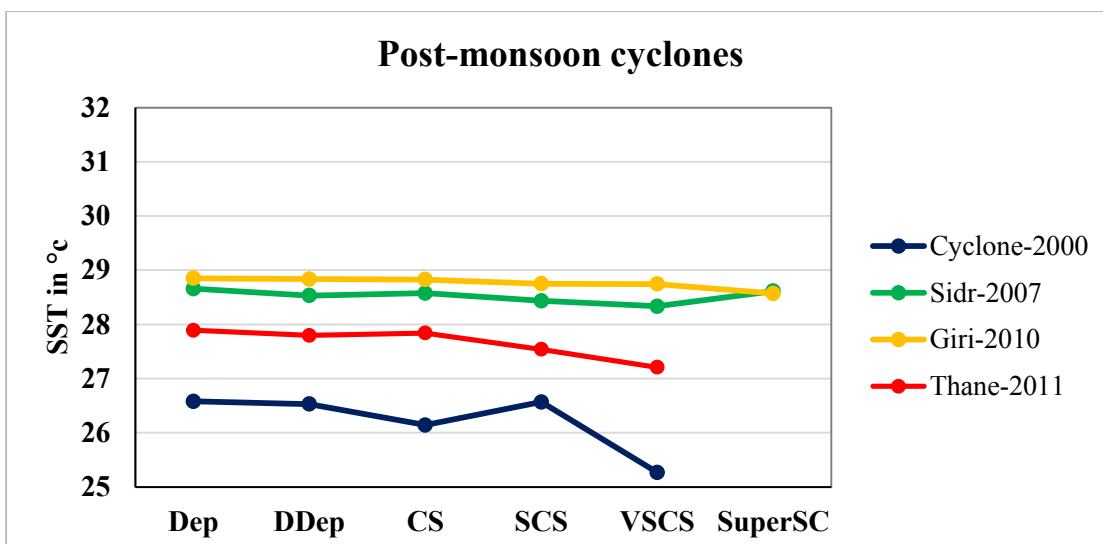


Fig 4.70: SST for all post-monsoon cyclones

Table 21: Characteristic of SST for post-monsoon cyclones.

Post-monsoon Cyclones	Lowest value (°C)	Highest value (°C)	Average value (°C)	Average increment/decrement per intensity level	
				°C	%
Cyclone 2000	25.26	26.58	26.22	-0.328	-1.22
Sidr 2007	28.33	28.66	28.52	-0.009	-0.03
Giri 2010	28.56	28.85	28.76	-0.056	-0.195
Thane 2011	27.2	27.891	27.65	-0.171	-0.617
Average for all post-monsoon cyclones	27.34	27.99	27.78	-0.141	-0.5155

Fig 4.71 shows the average value of SST in different cyclones during cyclone period. SST varies from minimum 25 °C to maximum 32 °C. Average value of SST in case of pre-monsoon (30.32 °C) is greater than post-monsoon (27.78 °C), this is because during pre-monsoon, direct heating of the Ocean by the sun increases SST. However SST exceeded the threshold of 26 °C for both season cyclone.

The average increment per intensity level of SST for pre- and post-monsoon cyclones shows in Fig 4.72. In case of Mala (2006) and Akash (2007) SST shows 0.07 % increment which is very small. Almost all cyclones shows 0.1 to 1.2 % decreasing value of SST due to the change of intensity level. But this % is small, almost they maintain the constant value.

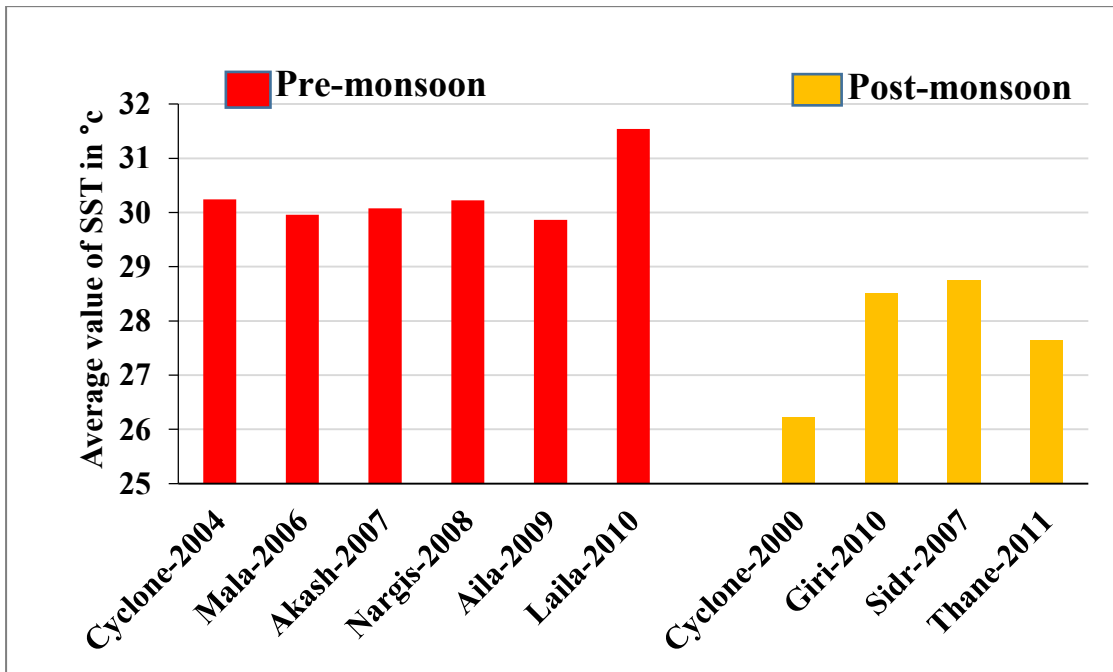


Fig 4.71: Average value of SST during cyclones period.

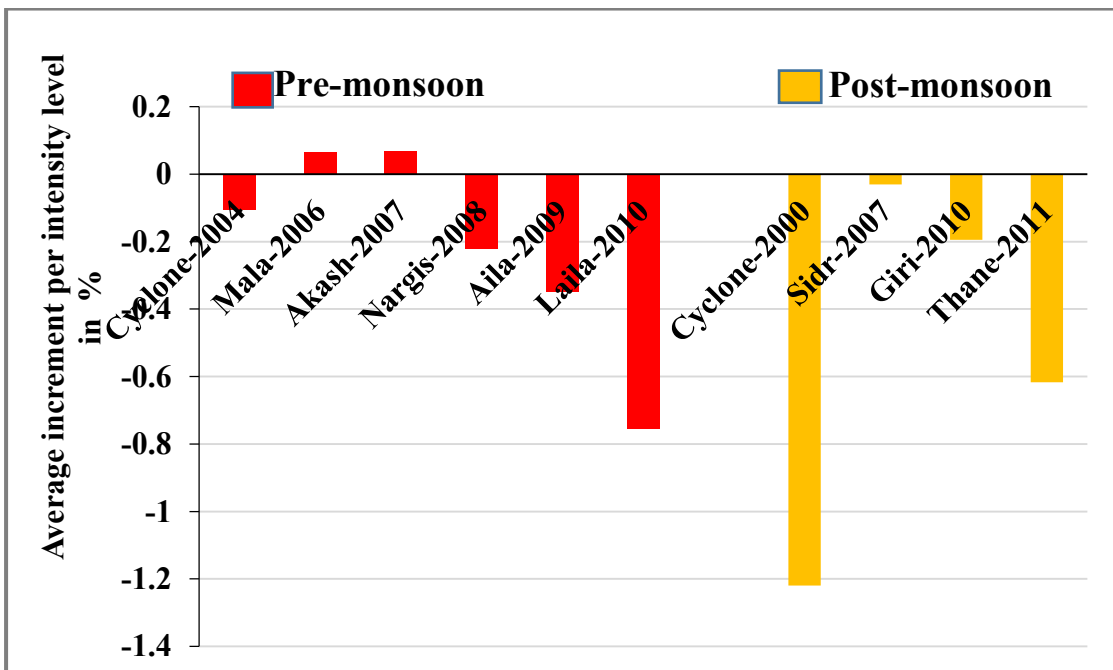


Fig 4.72: Average increment per intensity level of SST (%).

4.2.6 Geopotential Thickness (1000-200 hPa)

Pre-monsoon cyclones

Geopotential thickness is the difference in the geopotential height of two constant pressure surfaces in the atmosphere. Geopotential thickness is used as a good predictor of tropical cyclone motion and intensity change. Geopotential thickness data is used in the statistical prediction of tropical cyclone intensity change.

The spatial distribution of geopotential thickness for all pre-monsoon cyclones are plotted in Fig 4.73. Intense geopotential thickness is prominent in the middle of BoB.

Again Fig 4.74 and Fig 4.75 show the variation of geopotential thickness with cyclones intensity change in case of pre-monsoon cyclones. Geopotential thickness are the average of the 1000-200 hPa level. Here geopotential thickness are found from minimum 12300 m to maximum 12600 m. Geopotential thickness shows a positive value i.e. increasing trend with all pre-monsoon cyclone intensity change except Akash.

For all graphs R-squared value is calculated and found significant i.e. for all pre-monsoon cyclones the value is ≥ 0.5 except Akash (2007) and Nargis (2008) in which the value is < 0.5 .

Overall summary for the parameter of geopotential thickness is shown in table 22. From the table, it is found that the average geopotential thickness varied from 12467.88 m to 12512.50 m for pre-monsoon cyclones, with an average value of 12493.37 m. The average increment per intensity level is found 8.92 or 0.07 % in case of pre-monsoon cyclones which is very small.

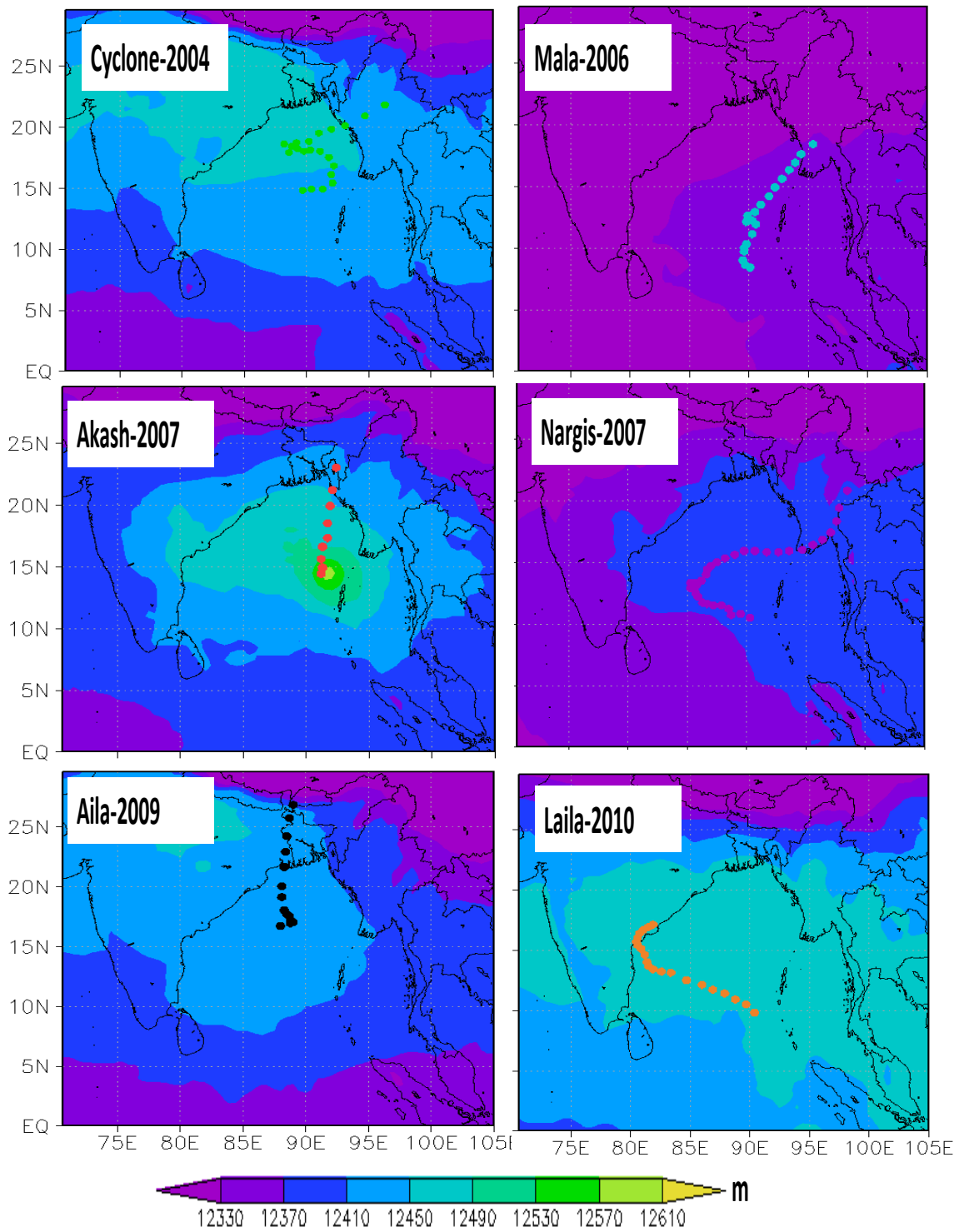


Fig 4.73: Spatial distribution of average geopotential thickness during cyclone period of each pre-monsoon cyclone.

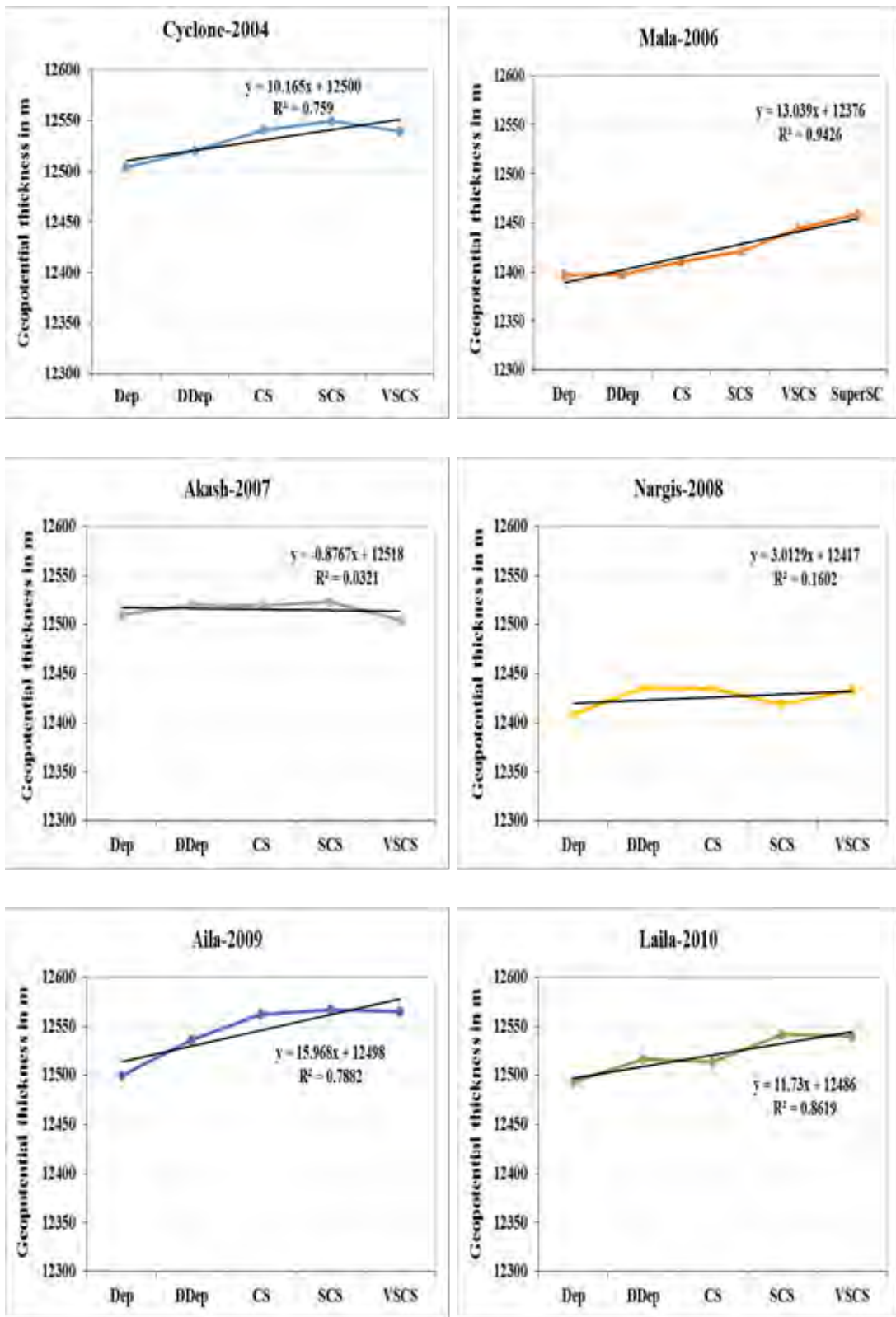


Fig 4.74: Geopotential thickness (1000-200 hPa) for individual pre-monsoon cyclones.

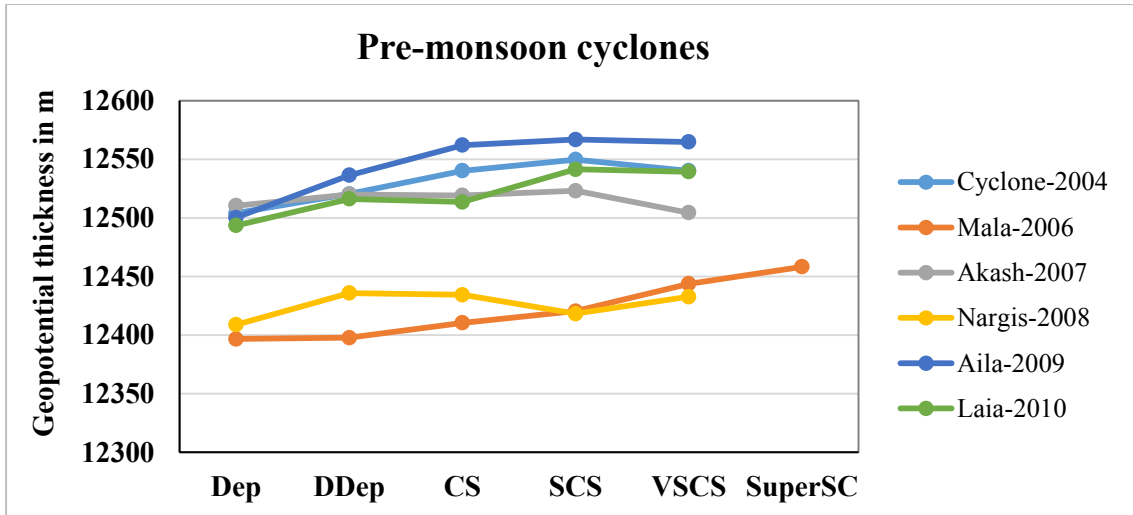


Fig 4.75: Geopotential thickness for all pre-monsoon cyclones.

Table 22: Characteristic of geopotential thickness for pre-monsoon cyclones

Pre-monsoon Cyclones	Lowest value (m)	Highest value (m)	Average value (m)	Average increment/decrement per intensity level	
				m	%
Cyclone 2004	12503.92	12549.7	12530.85	9.04	0.072
Mala 2006	12396.65	12458.25	12421.21	12.32	0.099
Akash 2007	12504.4	12523.03	12515.38	-1.48	-0.012
Nargis 2008	12408.78	12435.9	12425.99	5.96	0.048
Aila 2009	12500.15	12566.75	12546.01	16.16	0.13
Laila 2010	12493.4	12541.4	12520.76	11.5	0.092
Average for all pre-monsoon cyclones	12467.88	12512.50	12493.37	8.92	0.07

Post-monsoon cyclones

Fig 4.76 shows the spatial distribution of geopotential thickness for all post-monsoon cyclones. Intense geopotential thickness in the Northern part of BoB in case of Giri (2010) and in the southern part of BoB in case of Thane (2011). The variation of geopotential thickness with cyclones intensity change in case of post-monsoon shows in Fig 4.77 and Fig 4.78. In case of post-monsoon cyclones geopotential thickness value are found minimum 12300 m to maximum 12500 m with variation less than 20 m per intensity level. Geopotential thickness shows almost constant trend for post-monsoon cyclones.

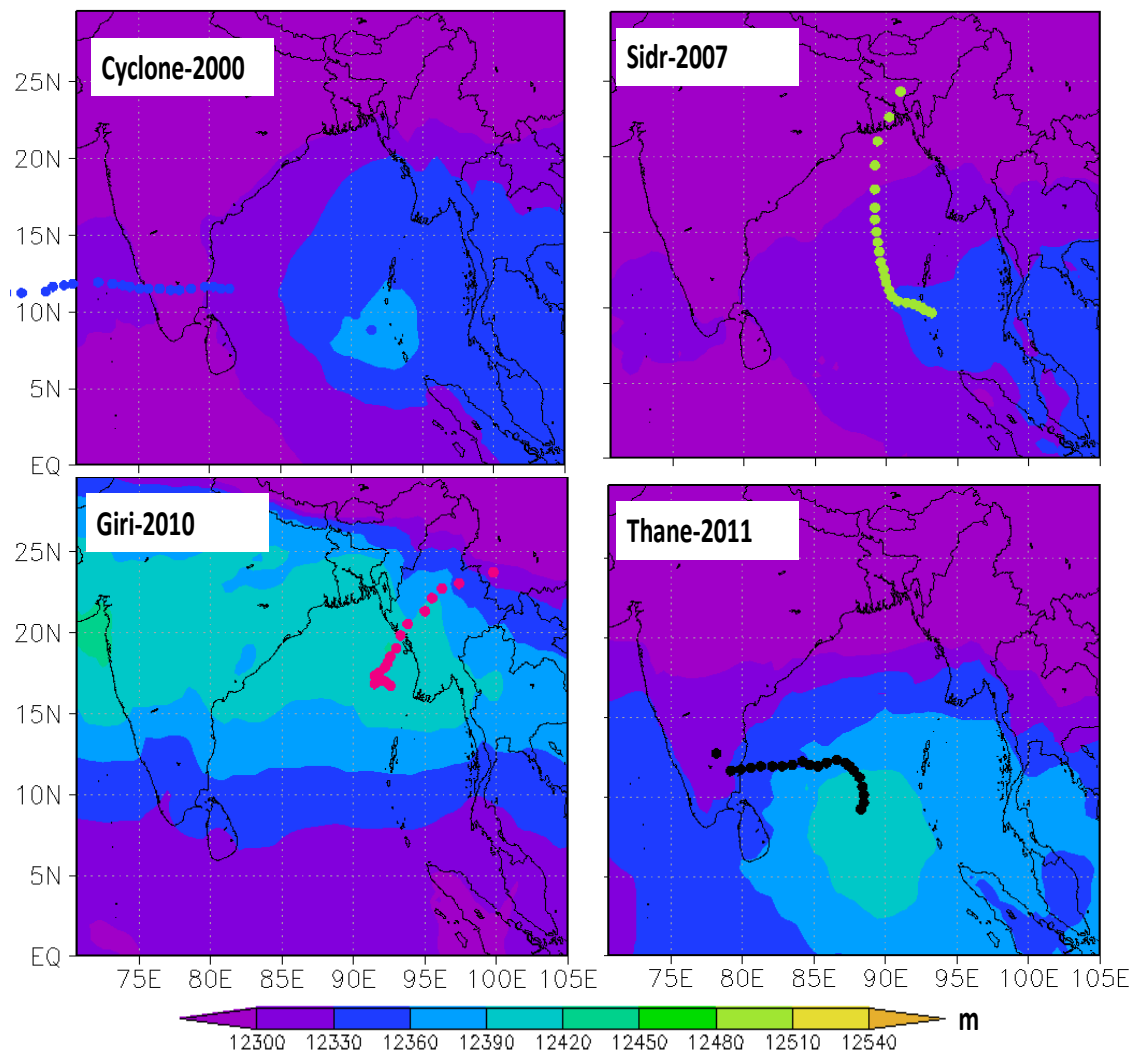


Fig 4.76: Spatial distribution of average geopotential thickness during cyclone period of each post-monsoon cyclone.

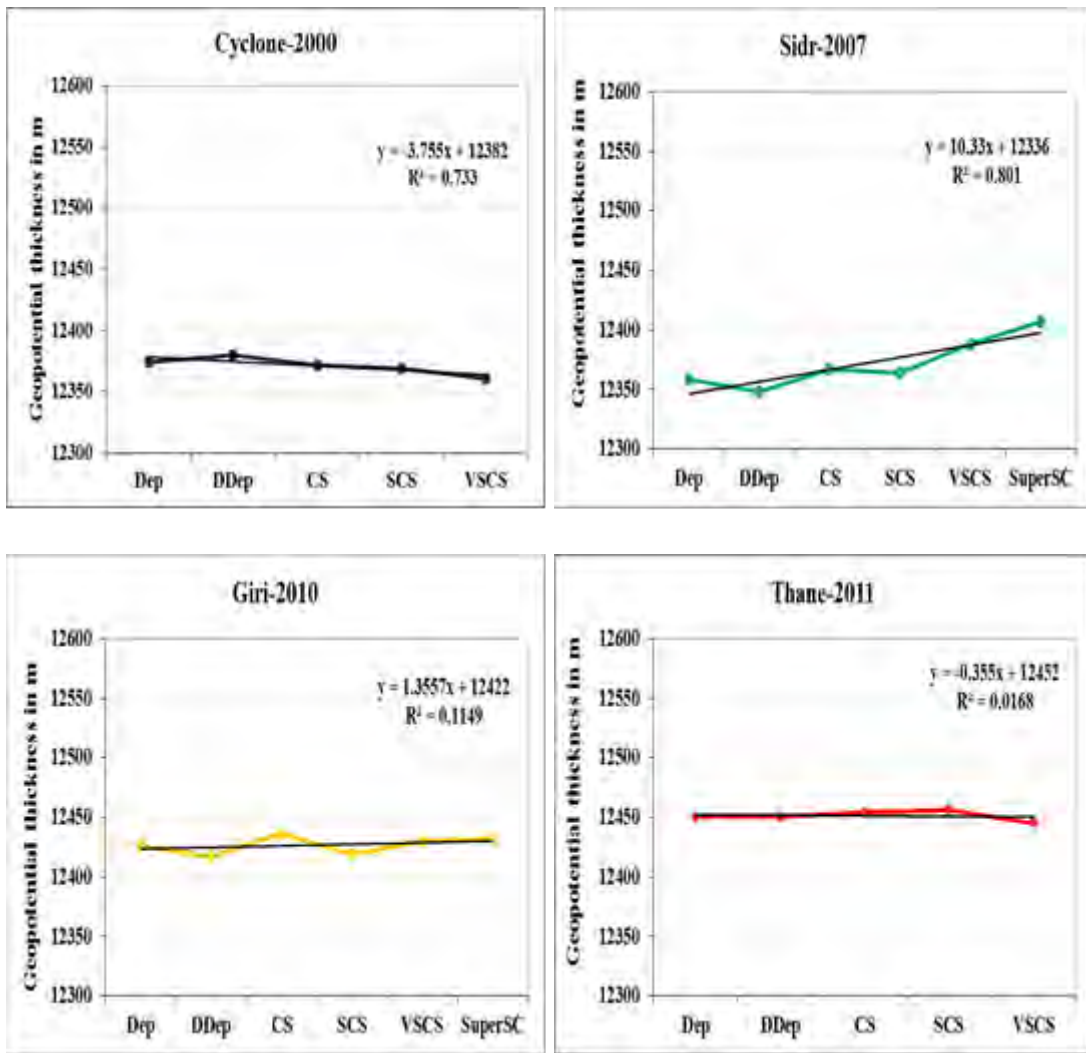


Fig 4.77: Geopotential thickness for individual post-monsoon cyclone.

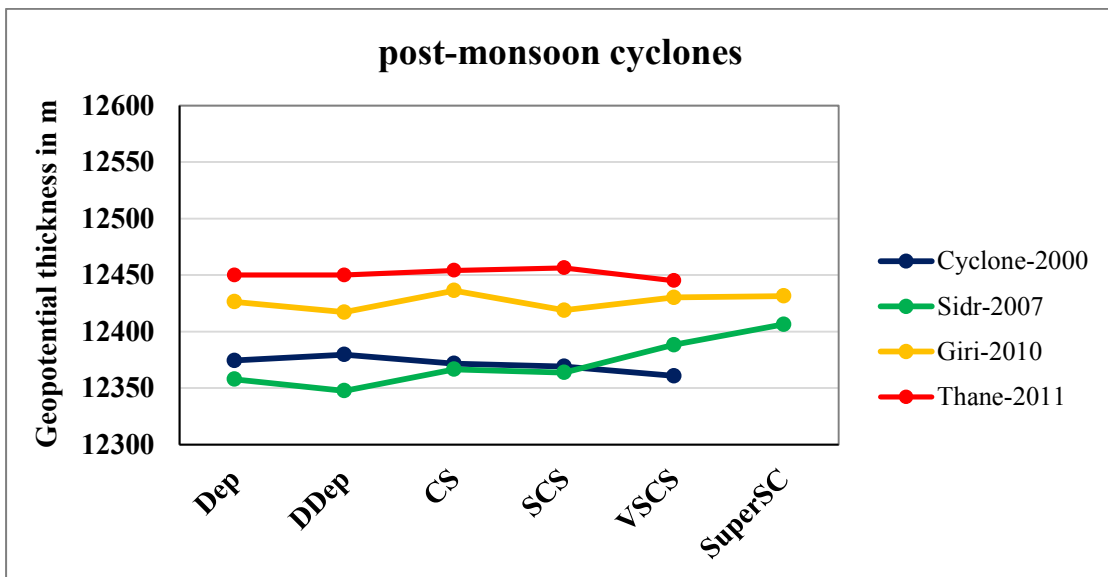


Fig 4.78: Geopotential thickness for all post-monsoon cyclones.

For all graphs R-squared value is calculated and found significance for Cyclone (2000) and Sidr (2007) in which it has value ≥ 0.5 but for Giri (2010) and Thane (2011) it has the value ≤ 0.1 .

Characteristic of geopotential thickness is shown in Table 23. Highest, lowest, average value of geopotential thickness for all pre-monsoon cyclones are indicated along with average percentage increment from initial level to highest intensity level.

From the table, it is found that the average geopotential thickness remain almost constant with cyclone intensity change, with an average value of 12405.19 m.

Table 23: Characteristic of geopotential thickness for post-monsoon cyclones

Post-monsoon Cyclones	Lowest value (m)	Highest value (m)	Average value (m)	Average increment/decrement per intensity level	
				m	%
Cyclone 2000	12360.85	12379.6	12371.14	-3.39	-0.03
Sidr 2007	12347.7	12406.36	12371.76	9.71	0.08
Giri 2010	12417.15	12436.3	12426.75	1.02	0.01
Thane 2011	12445.08	12456.33	12451.11	-1.23	-0.01
Average for all post-monsoon cyclones	12392.69	12419.65	12405.19	1.53	0.01

Geopotential thickness is a good tool for predicting tropical cyclone motion and intensity change. For maximum use in motion predication, thickness data must be convert into deep-layer-mean or mid-tropospheric height. Sometime geopotential thickness data used to analysis the condition of different pressure level. Here geopotential thickness varies from minimum 12300 m to maximum 12600 m for both cyclones, this range of value indicate that environment is favorable for cyclone movement and become severe. Average geopotential thickness for pre-monsoon

(12493.37 m) is higher than post-monsoon (12405.20 m) cyclone. Overall geopotential thickness shows constant trend with cyclone intensity change.

Geopotential thickness averagely fluctuate from minimum 12372 m to maximum 12547 m with an average 12449 m shows in Fig 4.79. All pre-monsoon cyclones averagely have 12494 m geopotential thickness and post-monsoon cyclones have 12406 m, which is less than pre-monsoon. It indicates warmer layer in pre-monsoon than post-monsoon. As CAPE is high in pre-monsoon, more convection, more latent heat release in the mid and upper level which could cause the warm vertical column than post-monsoon.

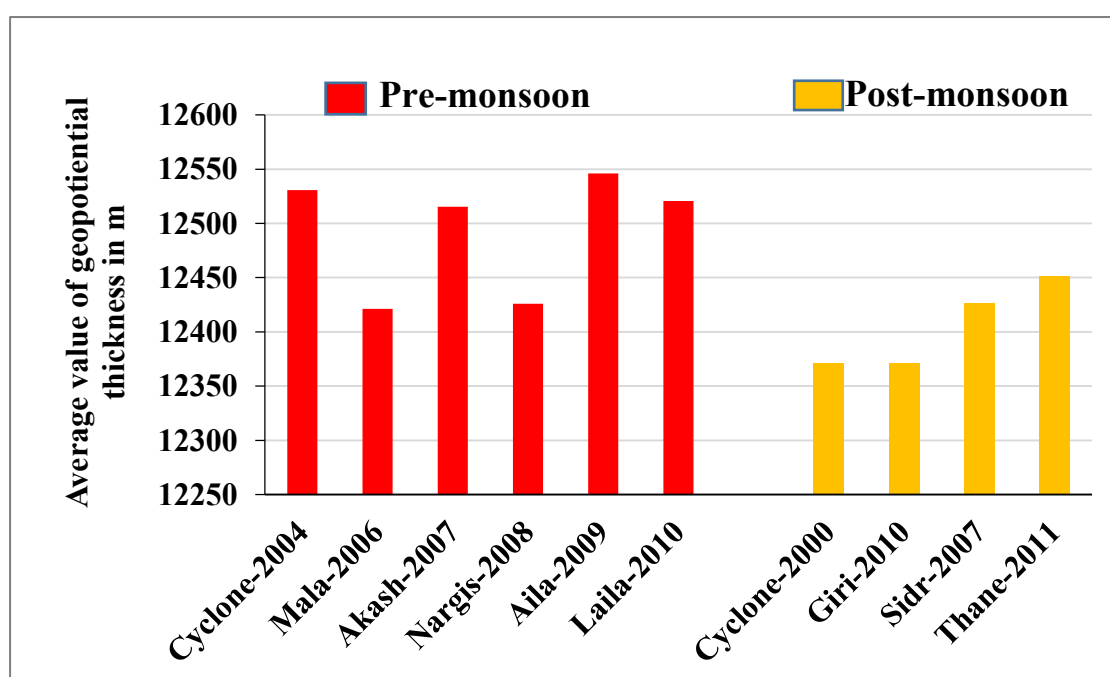


Fig 4.79: Average value of geopotential thickness during cyclones period.

Again Fig 4.80 shows average increment per intensity level of geopotential thickness during cyclone period. Almost all cyclones shows less than 0.5 % increasing value due to the change of intensity level. However increment of geopotential thickness with intensity change is positive and variation is very small ($< 0.1\%$).

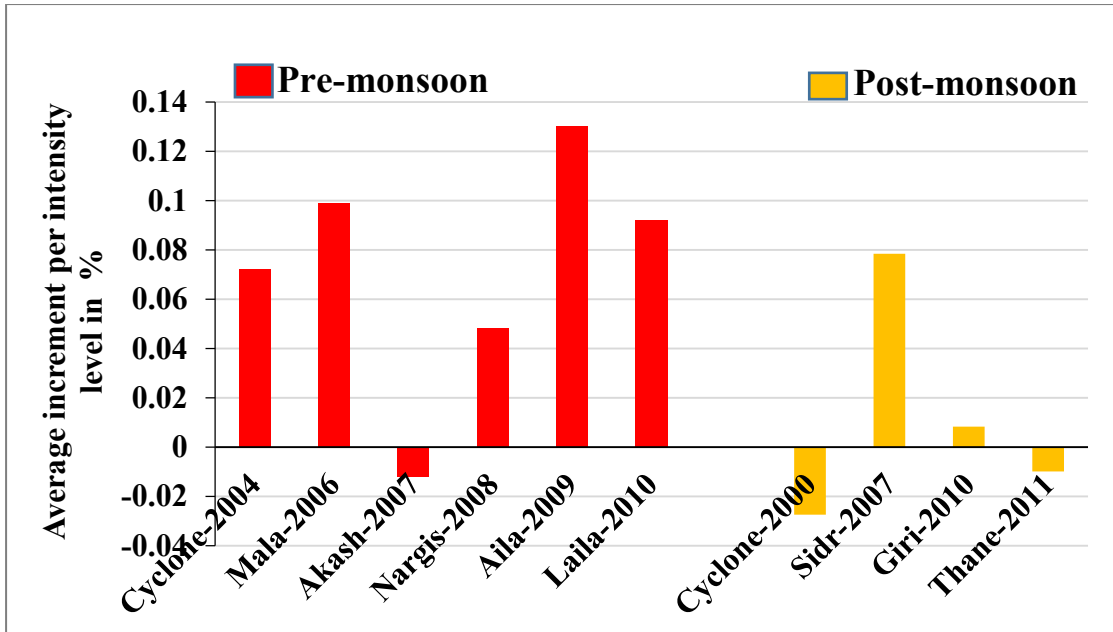


Fig 4.80: Average increment per intensity level of geopotential thickness (%).

4.2.7 Mean sea level pressure (MSLP)

As pressure within the cyclone center is defined the cyclone intensity. So we specify the $1^\circ \times 1^\circ$ area focusing the eye of cyclone.

Pre-monsoon cyclones

The maximum sustained surface wind in tropical cyclone is a function of the local maximum pressure gradient. Tropical cyclone intensity is controlled by MSLP. The spatial distribution of MSLP for all pre-monsoon cyclone are plotted in Fig 4.81. MSLP value varies among cyclones. Most of the cases low MSLP in the North Western part of BoB. The Fig 4.82 and Fig 4.83 shows how MSLP are varied with pre-monsoon cyclones intensity change within considered area. Here MSLP decreasing from maximum 1010 hPa to minimum 985 hPa, which favorable for forming and intensifying cyclone. Individual cyclone variation are less (< 1 hPa). MSLP shows decreasing trends with all pre-monsoon cyclone intensity change i.e. with increases of cyclone intensity MSLP decreases, meets the environmental

condition of cyclone intensification. In case of Akash (2007) little fluctuation has been observed which will be explained discussion chapter. Most significant thing of the graph is that for all cyclones the highest intensity level has lowest pressure which coincide with condition.

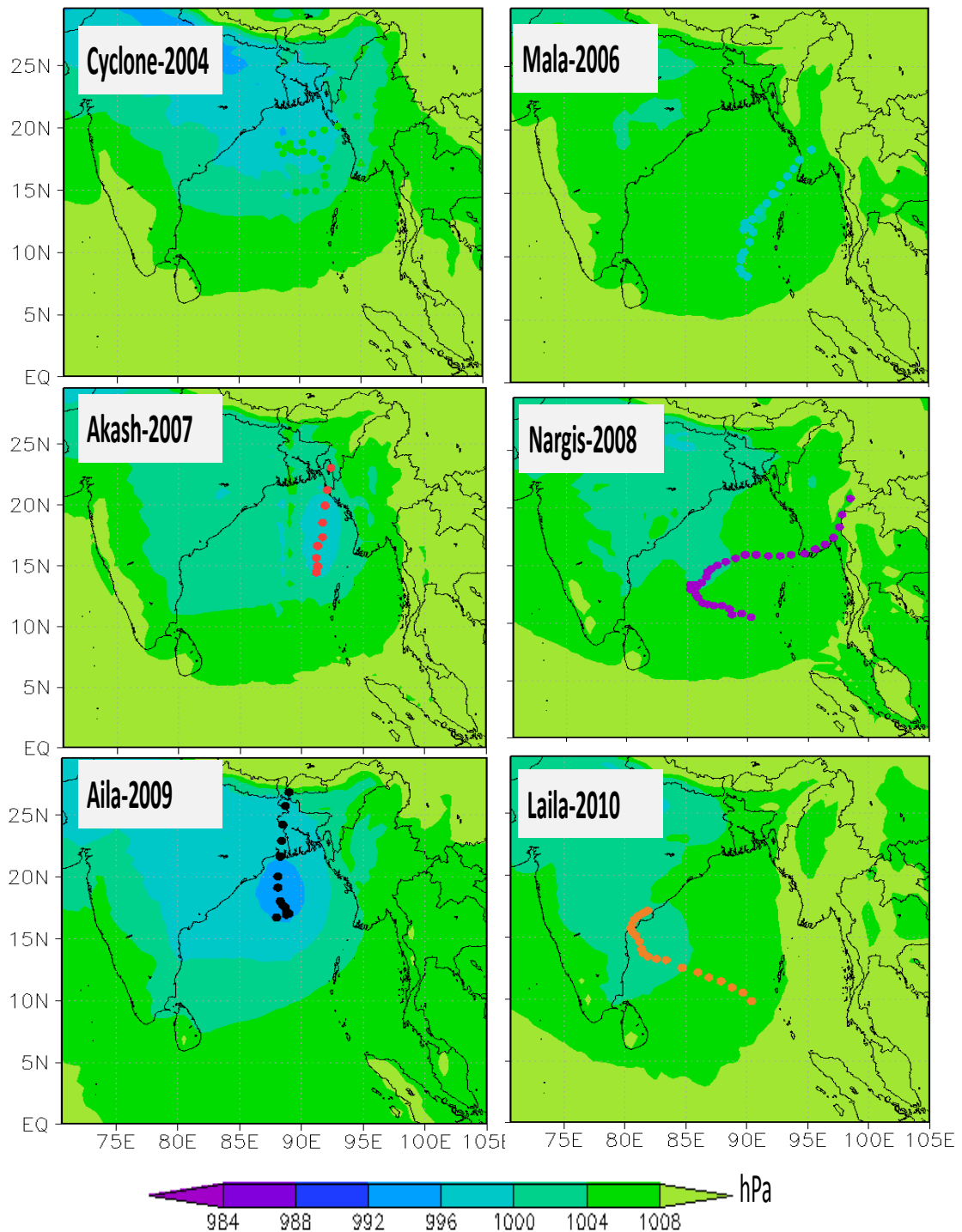


Fig 4.81: Spatial distribution of average MSLP during cyclone period of each pre-monsoon cyclone.

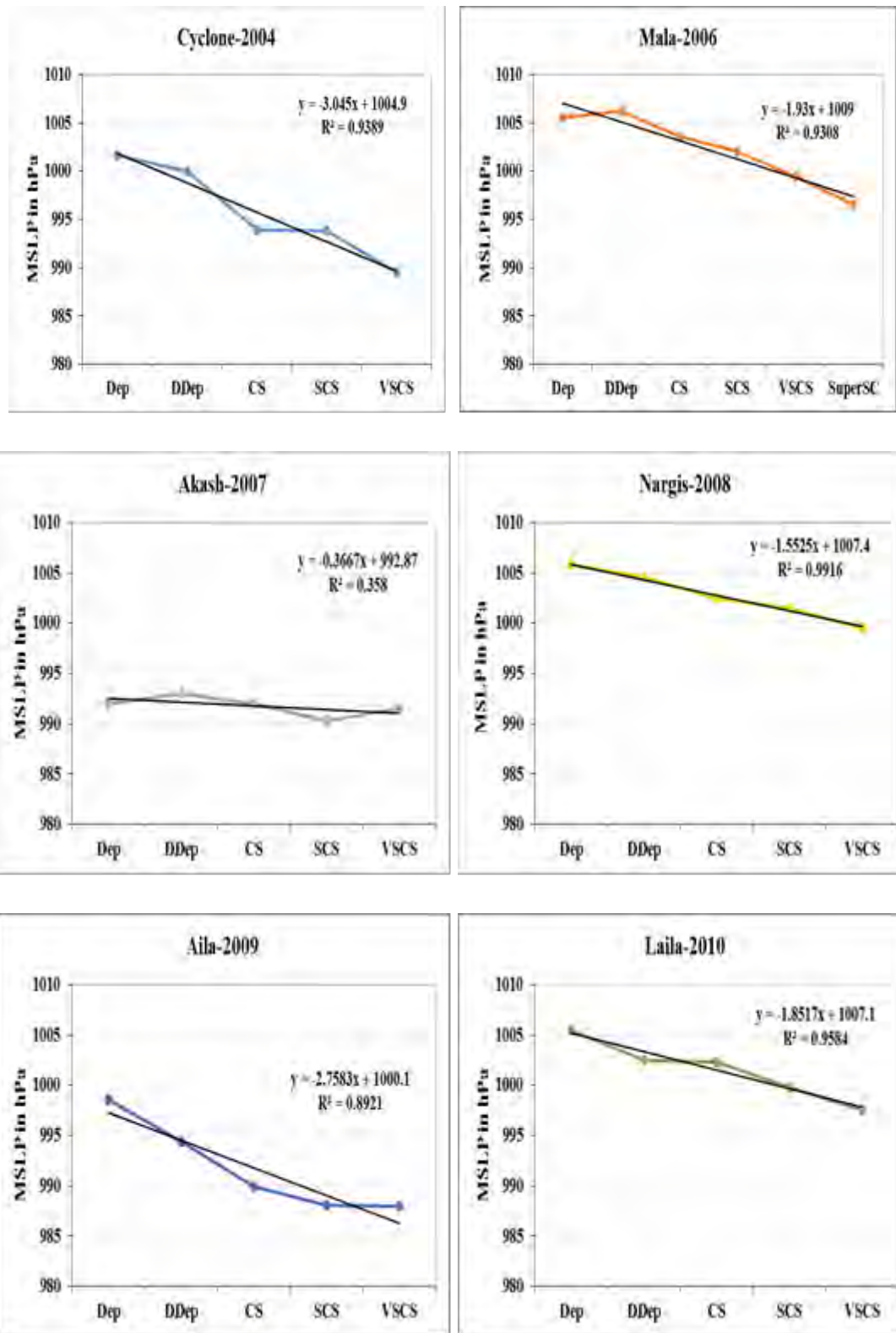


Fig 4.82: MSLP for individual pre-monsoon cyclone.

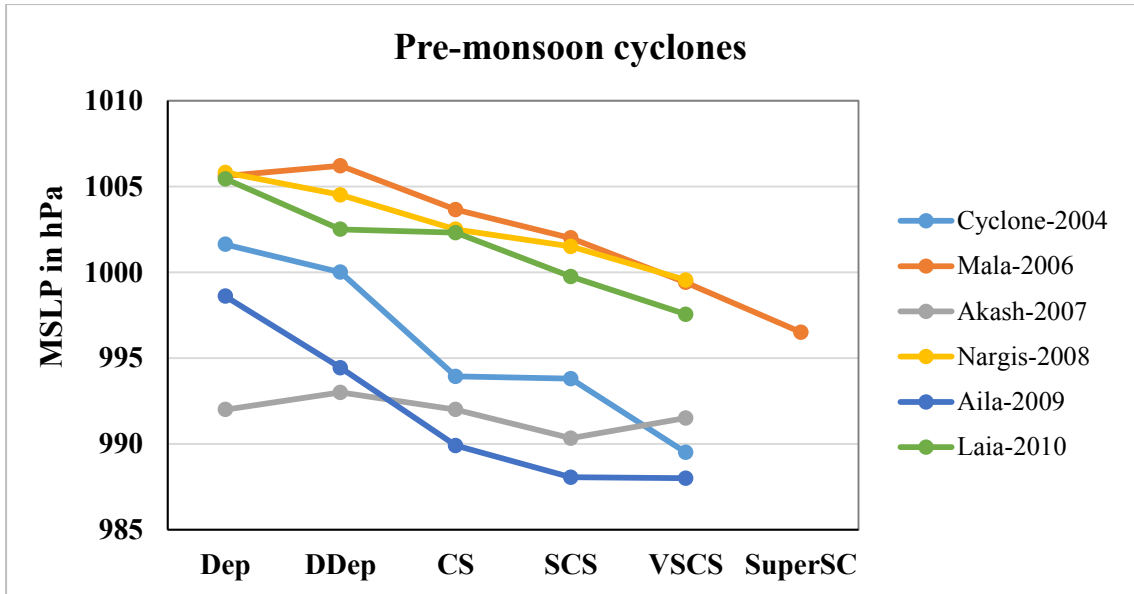


Fig 4.83: MSLP for all pre-monsoon cyclones.

For all graphs R-squared value is calculated and found significance i.e. for all pre-monsoon cyclones it has the value ≥ 0.5 except Akash (2007) in which it has the value 0.38.

Overall summary for the parameter of MSLP is shown in Table 24. From the table, average MSLP found varied from minimum 993.57 hPa to maximum 1001.77 hPa for pre-monsoon cyclones, with an average value of 997.64 hPa, this variation is favorable for cyclone intensification. The average decrement per intensity level is found 1.86 hPa or 0.19 % in case of pre-monsoon cyclones.

Table 24: Characteristic of MSLP for pre-monsoon cyclones.

Pre-monsoon Cyclones	Lowest value (hPa)	Highest value (hPa)	Average value (hPa)	Average increment/decrement per intensity level	
				hPa	%
Cyclone 2004	989.5	1001.63	995.77	-3.03	-0.303
Mala 2006	996.5	1006.2	1002.22	-1.82	-0.18
Akash 2007	990.33	993	991.76	-0.12	-0.012
Nargis 2008	999.54	1005.81	1002.77	-1.56	-0.16
Aila 2009	988	998.6	991.79	-2.65	-0.26
Laila 2010	997.55	1005.43	1001.51	-1.97	-0.19
Average for all pre-monsoon cyclones	993.57	1001.77	997.64	-1.86	-0.19

Post-monsoon cyclones

The spatial distribution of MSLP for all post-monsoon cyclones in Fig 4.84. MSLP value varies little among cyclone. Low MSLP in the North Western part of BoB in case of Giri (2010). In other cases high MSLP prevailed over BoB.

Again Fig 4.85 and Fig 4.86 shows the variation of MSLP with the post-monsoon cyclone intensity change. In case of post-monsoon cyclones MSLP varies from minimum 990 hPa to maximum 1006 hPa which is greater than pre-monsoon cyclone value. MSLP shows decreasing trend with all post-monsoon cyclones intensity change, it means the highest intensity level has minimum pressure. Individual cyclone variation is < 0.5 hPa in case of post-monsoon cyclone.

For all graphs R-squared value is calculated and found significant i.e. for all post-monsoon cyclones the value is ≥ 0.5 .

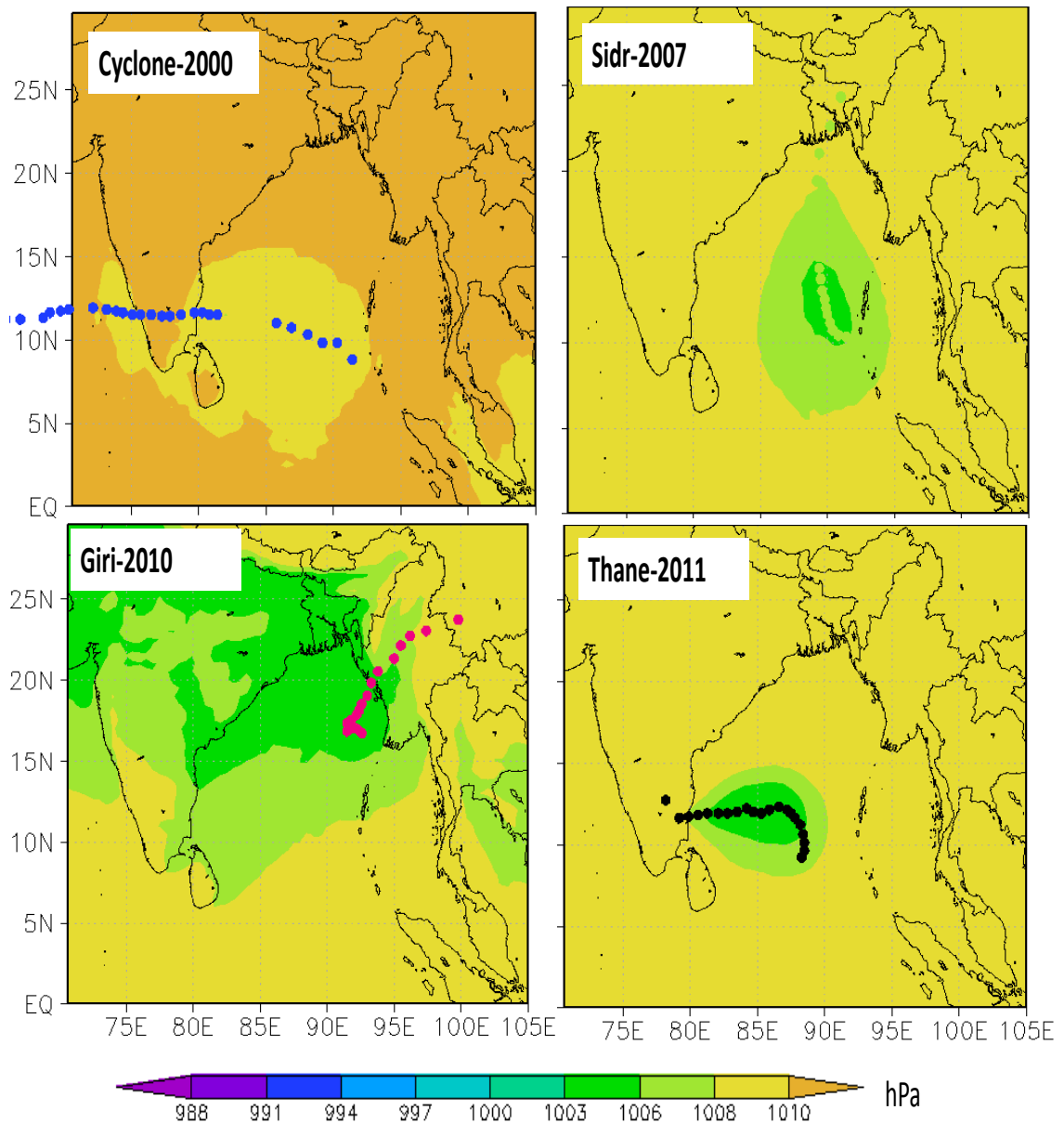


Fig 4.84: Spatial distribution of average MSLP during cyclone period of each post-monsoon cyclone.

Overall summary for the parameter of MSLP is shown in Table 25. From the table, it is found that the average MSLP varied from minimum 998.66 hPa to maximum 1004.07 hPa, with an average value of 1001.86 hPa for post-monsoon cyclone. The average decrement per intensity level is found 1.13 hPa or 0.11 % in case of post-monsoon cyclones.

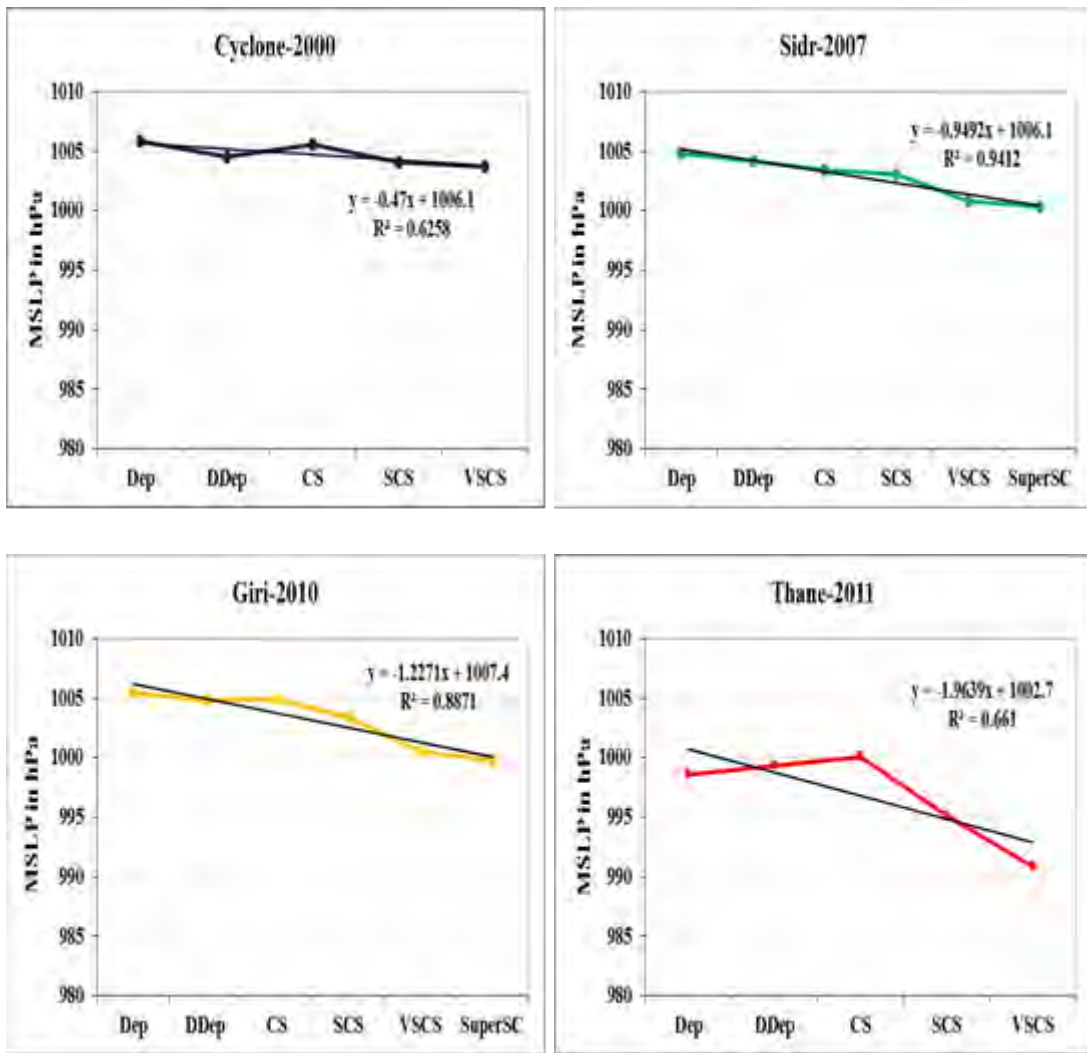


Fig 4.85: MSLP for individual post-monsoon cyclone.

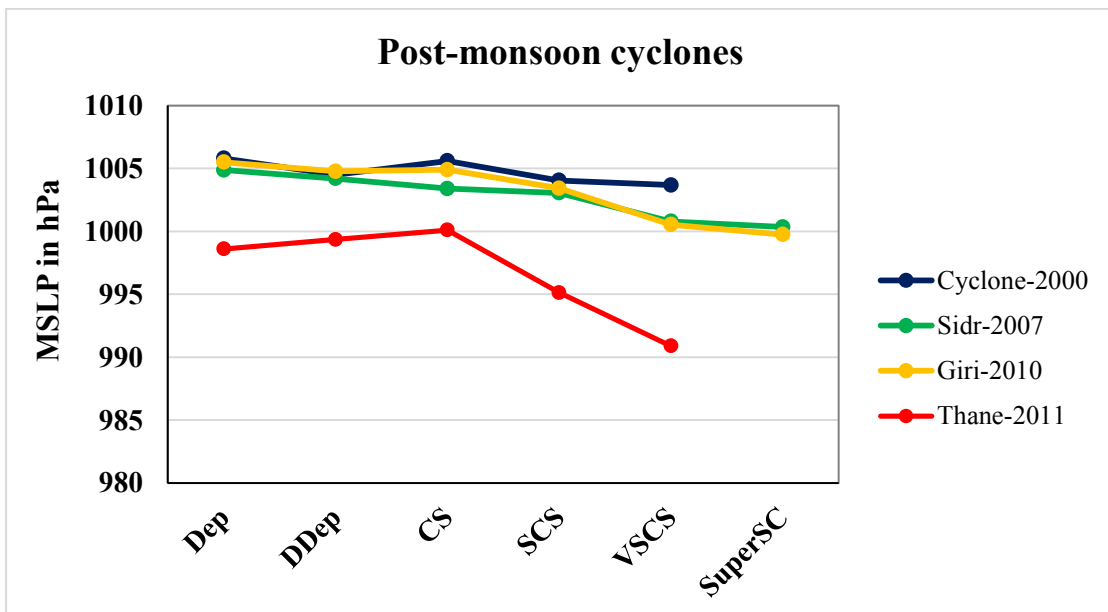


Fig 4.86: MSLP for all post-monsoon cyclones.

Table 25: Characteristic of MSLP for post-monsoon cyclones.

Post-monsoon Cyclones	Lowest value (hPa)	Highest value (hPa)	Average value (hPa)	Average increment/decrement per intensity level	
				hPa	%
Cyclone 2000	1003.67	1005.8	1004.72	-0.53	-0.05
Sidr 2007	1000.34	1004.87	1002.77	-0.91	-0.09
Giri 2010	999.75	1005.5	1003.15	-1.15	-0.11
Thane 2011	990.89	1000.1	996.82	-1.93	-0.19
Average for all post-monsoon cyclones	998.66	1004.07	1001.86	-1.13	-0.11

MSLP values decreases from maximum 1010 hPa to minimum 990hPa for both season cyclones. Average value of MSLP for pre-monsoon cyclones (997.64 hPa) is lower than post-monsoon cyclones (1001.86 hPa) which indicate that pre-monsoon season is more favorable for severe cyclone formation than post-monsoon. MSLP shows decreasing trend with cyclone intensity change. Average decrement of MSLP per intensity level for pre-monsoon is higher than post-monsoon cyclones.

MSLP values are averagely fluctuate from minimum 992 hPa to maximum 1005 hPa shows in Fig 5.87. Cyclone (2000) has maximum MSLP value and Akash (2007) has minimum MSLP value. For all pre-monsoon cyclones average value of MSLP is 997.64 hPa and 1001.86 hPa for all post-monsoon cyclone which is lower than pre-monsoon value.

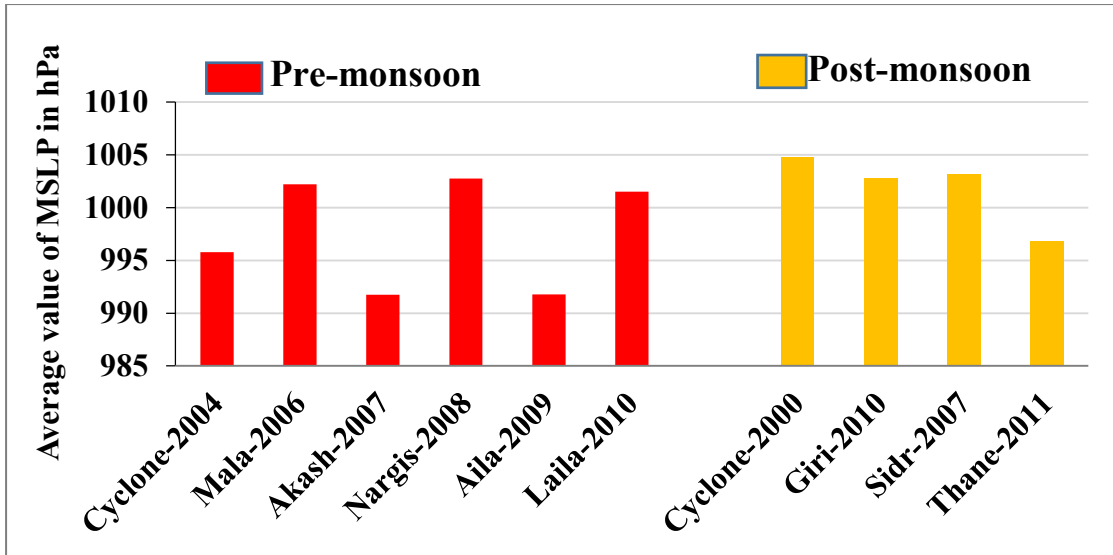


Fig 4.87: Average value of MSLP during cyclones period.

Fig 4.88 shows the average increment of MSLP per intensity level for pre- and post-monsoon cyclones. Almost all cyclones show 0.01 to 0.5 % decreasing value due to the change of intensity level. Average decrement of MSLP per intensity level for pre-monsoon (0.19 %) is higher than post-monsoon (0.11 %), though average value of MSLP is lower than post-monsoon. Due to increase of geopotential thickness during pre-monsoon rises warm vertical column than post-monsoon. Warm column reduce the pressure level which is directly related with the intensity of the cyclone. As the cyclone become more intense, MSLP value become lower.

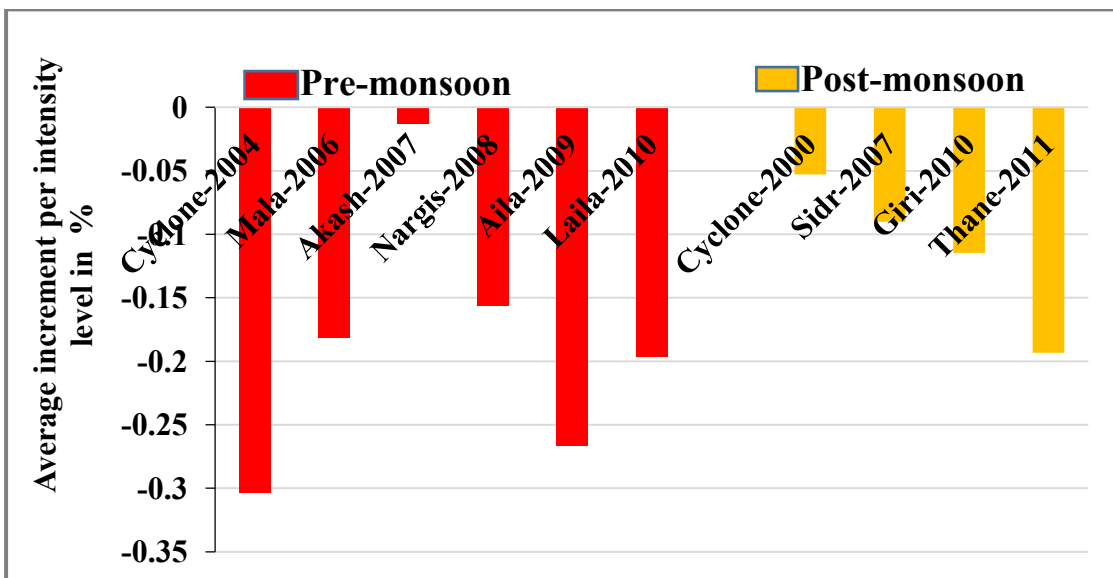


Fig 4.88: Average increment per intensity level of MSLP (%).

From above discussion found that, almost all cases, Akash (2007) shows exception from other cyclone. Akash (2007) is different because it is formed along the dry line in the northwest BoB during pre-monsoon shows in Fig 4.89. Mesoscale Convective System (MCS) formed during genesis of cyclone Akash (2007) was a severe BOW echo which causes severe downward damage surface wind 20 m/s. These wind may affect the environment around the cyclone [80]. Here found few fluctuation in other cyclones also which can be described by the individual cyclone analysis i.e. their recurvative nature, during progression long time stay in a particular position etc.

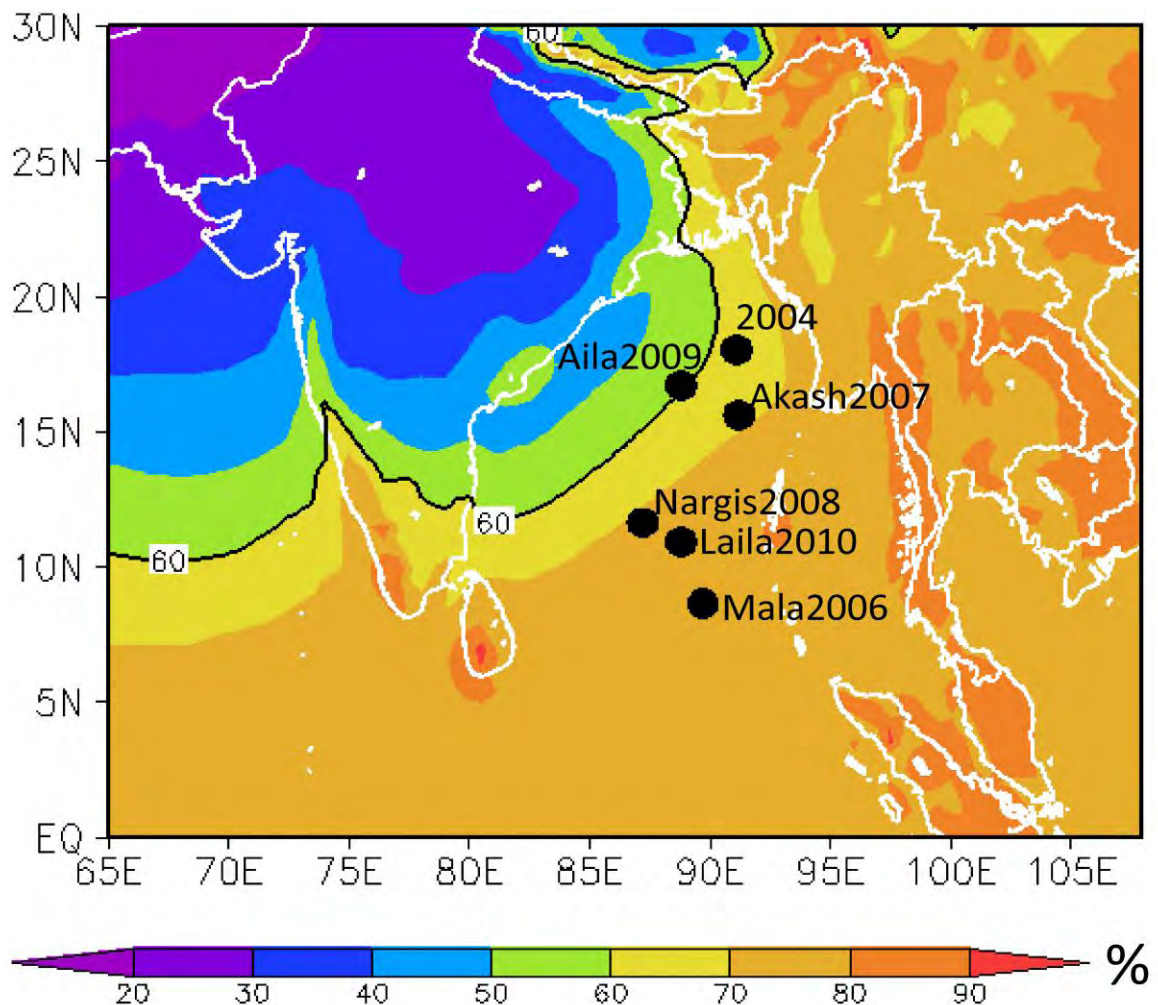


Fig 4.89: Dry line (yellow contour, %) for 2000-2011 during the pre-monsoon.

Chapter Six

Conclusion

The strongest and deadliest tropical cyclones (TCs) in the world are favorable to form in the environment of the funnel shaped Bay of Bengal (BoB), which is the important branch of the North Indian Ocean. Cyclones formed over the 5° N to 22° N and 80° E to 95° E are considered in this study. The best-track data from the Joint Typhoon Warning Center (JTWC) are used to determine the positions, intensities and duration of the TCs developed in the BoB for 12 years from 2000 to 2011. During this period, a total of 44 active TCs were formed in the BoB, which were bimodal in distribution for the pre- and post-monsoon seasons. Among them, only 6 TCs named as Cyclone(2004), Mala (2006), Akash (2007), Nargis (2008), Aila (2009) and Laila (2010) in the pre-monsoon and 4 TCs named as Cyclone(2000), Sidr (2007), Giri (2010) and Thane (2011) in the post-monsoon were found to have sustainable maximum wind speed of ≥ 64 kt (≥ 33 m/s). These ten high intensity TCs (≥ 64 kt) have been chosen to establish the relationship between the change of their intensities and the environment over the BoB. For this purpose, the National Centers for Environmental Prediction (NCEP) Climate Forecast System Reanalysis (CFSR) 6-hourly data with horizontal resolution of 0.5° X 0.5° and Real-Time, Global, Sea Surface Temperature (RTG_SST) with a 0.5° X 0.5° resolution data have been used to analysis dynamic and thermodynamic environmental parameters. In this study, vertical wind shear (VWS), relative vorticity and moisture flux are considered as dynamic parameters and relative humidity, convective available potential energy (CAPE), convective inhibition (CIN), sea surface temperature (SST), geopotential thickness and mean sea level pressure are the thermodynamic parameters.

Relative vorticity is an important parameter in determining regions of high possibility of tropical cyclone genesis. In this study, low level relative vorticities from 1000 to 850 hPa for both pre- and post-monsoon cyclones show positively increasing trends with the change of cyclone intensity. The average value of low level relative vorticities for all intensity levels is found about $8 \times 10^{-5} \text{ s}^{-1}$ for all cyclones with minimum value in Laila ($5.6 \times 10^{-5} \text{ s}^{-1}$) and maximum value in Thane ($12 \times 10^{-5} \text{ s}^{-1}$).

Again mid level relative vorticities at 850 to 500 hPa are also found positive for all cyclones in both seasons. In this case, the average value of mid level relative vorticities is about $6 \times 10^{-5} \text{ s}^{-1}$ for all cyclones. Minimum value is found in cyclone Giri ($4 \times 10^{-5} \text{ s}^{-1}$) and maximum value found in Aila ($9.2 \times 10^{-5} \text{ s}^{-1}$). Average increment of relative vorticity per intensity at mid-level is 4.3% higher than low level value. Also study reveals that increment rate of relative vorticities per intensity level is 8.3% higher in the pre-monsoon cyclones than that in post-monsoon cyclones. Therefore the positive increase in low level and mid level relative vorticities increases the cyclone intensity during cyclone period.

Vertical wind shear that describes the change of mean large-scale horizontal wind with height is analyzed in this study for low level from 1000 to 850 hPa. The average value of VWS for cyclones in both seasons are very low ($< 10 \text{ m s}^{-1}$) which is favorable for cyclone intensification. Variation of low level VWS with cyclone intensity is very little ($< 2 \text{ m s}^{-1}$) for all pre- and post-monsoon cyclones. The average increment of low level VWS per intensity level in all pre-monsoon cyclones are about 10% less than post-monsoon cyclones. However, cyclone intensity change may not significantly related with the low level VWS change, as fluctuation is very less in both cases.

The relation between moisture flux and the intensity of TC are calculated in this study as moisture flux is important to intensification of MCSs within cyclone eye and its rainband. In addition, TC size depends on the moisture content in the environment. Here, for both pre- and post-monsoon cyclones the average value of low level moisture flux are found greater than 170 gm-m/kg-s . For all cyclones average increment of moisture flux per intensity level are positive except Akash (2007) and Cyclone (2000). Moisture flux increment per intensity level in the pre-monsoon is 9% higher than that in the post-monsoon cyclones. As southwesterly wind starts to enter into the BoB during pre-monsoon and carry moisture from the Indian Ocean in the equatorial region. Except Akash (2007) all pre- and post-monsoon cyclones show positively increasing trends with cyclone intensity change.

The formation of tropical cyclone is directly related to the mid-tropospheric (500 hPa) relative humidity. No particular value of relative humidity is significant for the intensity of cyclones. However, the average value of mid-tropospheric relative humidity for all pre- and post-monsoon cyclones are found more than 75% which is

significant for cyclone to be alive, because low value of relative humidity may die down the cyclone.

Mesoscale convective system (MCS) as well as tropical cyclones are highly influenced by the environmental CAPE. It is found that CAPE is high in the initial stages of development but as the cyclone intensified CAPE decreases. CAPE shows decreasing trend with the change of cyclone intensity for both season cyclones. Average CAPE value for the pre-monsoon cyclones (1325 jkg^{-1}) is higher than the post-monsoon cyclones (962 jkg^{-1}). This is because, during pre-monsoon, the BoB maintains higher SSTs, which in turn influences the vertical gradient of potential temperature and results an increased CAPE compared with that in the post-monsoon season. However, CAPE is not steady for the progression of the cyclone as MCSs vary from cyclone to cyclone.

CIN is a measure of the strength of the stable layer. CIN is the negative energy which could limit the convection if the value is more than 50 j/kg . In all cases CIN values are found less than 30 j/kg which coincide with the cyclone formation and intensification condition. For all pre- and post-monsoon cyclones, CIN shows increasing trend with the change of cyclone intensity except few points. Average CIN value for the post-monsoon cyclones is higher than the pre-monsoon cyclones but average increment per intensity level for the pre-monsoon is 2 % higher than that in the post-monsoon. During pre-monsoon, the average CIN value increased gradually from northwestern India toward the BoB and almost half of the BoB capped by the CIN. In contrast, during the post-monsoon, the entire BoB maintained the constant temperature aloft and CIN is less.

In this study, precipitable water and cyclone intensity are tried to correlate as precipitable water gives the amount of moisture in the troposphere. For both cyclone seasons, average values of precipitable water are higher than 60 kg/m^2 , means environment contain more than 60 % moisture. No particular value of precipitable water is significant for intensity change, however, precipitable water maintains an almost constant value with cyclone intensity.

Sea surface temperature is the dominant factor in tropical cyclone formation and intensification. In all case SSTs are found $2\text{-}5 \text{ }^\circ\text{C}$ higher than cyclone formation temperature ($26 \text{ }^\circ\text{C}$). However, the average value of SST for pre-monsoon is about 3

°C higher than post-monsoon, since during pre-monsoon, direct heating of the Ocean by the sun increases SST. SST remains almost constant with the change of cyclone intensity levels. Therefore, BoB is characterized by a higher SST during cyclone genesis and this value is maintained during the cyclone period without changing the cyclone intensity.

Geopotential Thickness is used as a good predictor of tropical cyclone motion and intensity change. Average value of geopotential thickness for the pre-monsoon (12494 m) is found higher than the post-monsoon (12405 m) which indicates a warmer layer in the pre-monsoon than post-monsoon. In this study, except Akash (2007) and Cyclone (2000) geopotential thickness is increased with increasing intensity. However, increment of geopotential thickness with intensity change is very small (< 0.1%).

Tropical cyclone intensity is generally measured by MSLP at center of the cyclone. For all cases MSLP show decreasing trend with the change of cyclone intensity. MSLP values decrease from the maximum value of 1010 hPa to the minimum value 990 hPa for cyclones in both seasons. Average value of MSLP for the pre-monsoon cyclones (998 hPa) is lower than that in the post-monsoon cyclones (1002 hPa), which indicate that pre-monsoon season is more favorable for severe cyclone formation than post-monsoon. Due to increase of geopotential thickness during pre-monsoon raises warm vertical column than post-monsoon. Warm column reduce the pressure level which is directly related with the intensity of the cyclone. As the MSLP value become lower, cyclone become more intense.

Overall study reveals that not only mean sea level pressure at centre and low level relative vorticity of the cyclone vorticity can measure the cyclone intensity also mid-tropospheric relative vorticity, low level moisture flux, and geopotential thickness can closely related with the change of the cyclone intensity. Again mid-tropospheric relative humidity more than 75%, precipitable water more than 60 kg/m², Sea surface temperature more than 26 °c, Convective inhibition value less than 30 j/kg, low level vertical wind shear less than 10 m/s are the favorable environment for maintaining the existing cyclone.

REFERENCES

- 1) <http://www.nhc.noaa.gov/climo>, access time and date: 11.00 P.M., 05 October 2014.
- 2) https://en.wikipedia.org/wiki/Bay_of_Bengal, access time and date: 11.00 P.M., 05 October 2014.
- 3) Neumann CJ, Global guide to tropical cyclone forecasting, WMO, Geneva, Switzerland, 1.1–1.56, 1993.
- 4) Gray W. M., “Tropical cyclone genesis” Dept. of Atmos. Sci., paper no. 234, Colo State University, Ft Collins, CO, 121, 1975.
- 5) Gray W. M., “Hurricanes: their formation, structure and likely role in the tropical circulation.” In Shaw DB (ed). Meteorology over the tropical oceans, RMS, James Glaisher House, Grenville Place, Bracknell, Berkshire, RG 12 1BX, pp. 155–218, 1979.
- 6) Ginis I., “Tropical Cyclone-Ocean Interactions”, Atmosphere-Ocean Interactions, Advances in Fluid Mechanics Series, No. 33, WIT Press, 83-114.
- 7) Palmén, E., “On the formation and structure of the tropical hurricane”, Geophysica, vol. 3, pp. 26-38, 1948.
- 8) Emanuel, K.A., “The maximum intensity of hurricanes”, J. Atmos. Sci., vol. 45, pp. 1143-1155, 2003.
- 9) Wang, Y., “How do outer spiral rainbands affect tropical cyclone structure and intensity?”, J. Atmos. Sci., vol. 66, pp. 1250–1273, DOI:10.1175/2008JAS2737.1, 1988.
- 10) Gray M. W., “Global view of the origin of tropical disturbances and storms”, Mon. Wea. Rev., vol. 96, pp. 669-700, DOI: 10.1175/1520-0493(1968)096<0669:GVOTOO.2.0.CO;2, 1968.
- 11) DeMaria M., “The effect of vertical shear on tropical cyclone intensity change”, J. Atmos. Sci, vol. 53, pp. 2076-2086, 1996.
- 12) Shoujuan S., Yuan w., and Lina B., “Insight into the role of lower-layer vertical wind shear in tropical cyclone intensification over the Western North Pacific”, Acta meteorologica sinica, vol. 27, No-3, pp. 356-363, 2013.

- 13) Zeng Z., Wang Y., and Chen L., “A statistical analysis of vertical shear effect on tropical cyclone intensity change in the North Atlantic”, *Geophys. Res. Lett.*, vol.37, L02802, DOI: 10.1029/2009 GL041788, 2010.
- 14) Akter N. and Tsuboki K., “Role of synoptic-scale forcing in cyclogenesis over the Bay of Bengal”, *Clim. Dyn.*, DOI: 10.1007/ s00382-014-2077-9, 2014.
- 15) Brand D. "Colossal cyclone swirling near Martian North Pole is observed by Cornell-led team on Hubble telescope", Cornell University, 15 June 2008.
- 16) **Oceanservice.noaa.gov/facts/cyclone.html**, access time and date: 11.00 P.M., 10 October 2014.
- 17) Wang Y., Rao Y, Tan Z., and Schönemann D. : A Statistical Analysis of Vertical Wind Shear on Tropical Cyclone Intensity Change over the Western North Pacific. *Mon. Wea. Rev.*, Vol. 143, pp 3434–3453. DOI: <http://dx.doi.org/10.1175/MWR-D-15-0049.1>, 2015.
- 18) Paterson L.A., Hanstun B.N., Davidson N.E. and Neber H.C., "Influence of Environmental Vertical Wind Shear on the Intensity of Hurricane-Strength Tropical Cyclones in the Australian Region", *Mon. Wea. Rev.*, vol. 133, pp. 3644-3659, DOI: <http://dx.doi.org/10.1175/MWR3041.1> 2005.
- 19) Emanuel K., Desautels C., Holloway C., and Korty R., "Environmental Control of Tropical Cyclone Intensity", Program in Atmospheres, Oceans and Climate, Massachusetts Institute of Technology, Cambridge, Massachusetts, 2003.
- 20) DeMaria M. and Kaplan J. “A Statistical Hurricane Intensity Prediction Scheme (SHIPS) for the Atlantic Basin” *wea, Forecasting*, vol. 9, pp 209-220, DOI: [http://dx.doi.org/10.1175/1520-0434\(1994\)009<0209:ASHIPS>2.0.CO;2](http://dx.doi.org/10.1175/1520-0434(1994)009<0209:ASHIPS>2.0.CO;2), 1994.
- 21) **www.bom.gov.au/australia/charts/Interpreting_MSLP.shtml**, access time and date: 10.00 P.M., 12 October 2014.
- 22) Andreas E. L. and Emanuel K. A. “Effects of Sea Spray on Tropical Cyclone Intensity” *J. Atmos. Sci*, vol. 58, pp. 3741-3750, DOI: [http://dx.doi.org/10.1175/15200469\(2001\)058<3741:EOSSOT>2.0.CO;2](http://dx.doi.org/10.1175/15200469(2001)058<3741:EOSSOT>2.0.CO;2), 2001

- 23) Frank W.M., "The Structure and Energetics of the Tropical Cyclone I. Storm Structure" *Mon. Wea. Rev.*, vol. 105, pp. 1119-1135. DOI: [http://dx.doi.org/10.1175/1520-0493\(1977\)105<1119:TSAEOT>2.0.CO;2](http://dx.doi.org/10.1175/1520-0493(1977)105<1119:TSAEOT>2.0.CO;2), 1977.
- 24) https://en.wikipedia.org/wiki/Glossary_of_tropical_cyclone_terms, access time and date: 10.00 P.M., 07 March 2015.
- 25) Merrill R. T., "A comparison of Large and Small Tropical cyclones", *Mon. Wea. Rev.*, vol. 112(7), pp. 1408-1418, DOI: 10.1175.1520-0493(1984)112<1408:ACOLAS>2.0.CO;2.
- 26) www.srh.noaa.gov/srh/jetstream/tropics/tc_structure.html, access time and date: 07 P.M., 08 March 2015.
- 27) https://en.wikipedia.org/wiki/Tropical_cyclone_basins, access time and date: 09 A.M., 10 March 2015.
- 28) <http://www.news18.com/news/india/prehistoric-lost-continent-found-in-the-indian-ocean-592927.html>, access time and date: 06 P.M., 12 March 2015.
- 29) <https://www.britannica.com/place/Bay-of-Bengal>, access time and date: 15 P.M., 20 March 2015.
- 30) Emanuel K., "Tropical Cyclone Energetics and Structure", program in Atmospheres, Oceans, and Climate, Massachusetts Institute of Technology.
- 31) Emanuel K.A. : An Air-Sea Interaction Theory for Tropical Cyclones. Part I: Steady-State Maintenance, *J. Atmos. Sci.*, vol. 43, pp. 585-605, DOI: [http://dx.doi.org/10.1175/15200469\(1986\)043<0585:AASITF>2.0.CO;2](http://dx.doi.org/10.1175/15200469(1986)043<0585:AASITF>2.0.CO;2), 1986.
- 32) Emanuel K.A., "Anthropogenic Effects on Tropical Cyclone Activity." Massachusetts Institute of Technology, 07 May 2009.
- 33) https://en.wikipedia.org/wiki/Glossary_of_NHC/TPC_Terms, access time and date: 11.00 P.M., 30 April 2015.
- 34) <https://www.soest.hawaii.edu/GG/ASK/askanerd.html>, access time and date: 08 P.M., 02 April 2015.
- 35) Annamalai, H.; Slingo, J. M.; Sperber, K. R.; Hodges, K. (1999). "The Mean Evolution and Variability of the Asian Summer Monsoon: Comparison of ECMWF and NCEP–NCAR Reanalyses", *Mon. Wea. Rev.*, vol. 127 (6), pp. 1157–1186. DOI:10.1175/1520-0493(1999)127<1157:TMEAVO>2.0.CO;2.

- 36) Bister M. and Emanuel K.A., "Dissipative heating and hurricane intensity". *Meteorol. Atmos. Phys.* vol. 65, pp. 233-240, DOI: 10.1007/BF01030791, 1998.
- 37) www.aoml.noaa.gov/hrd/tcfaq/D7.html, access time and date: 10.00 P.M., 15 May 2015.
- 38) D'Asaro E.A., and Black P.G., "J8.4 Turbulence in the Ocean Boundary Layer Below Hurricane Dennis (2000)", 24th conference on Hurricanes and Tropical Meteorology and 10th conference on interaction of the sea and atmosphere, 25 May 2000.
- 39) www.aoml.noaa.gov/hrd/tcfaq/A15.html, access time and date: 09.00 P.M., 05 June 2015.
- 40) Kikuchi K., Wang B. and Fudeyasu H., "Genesis of tropical cyclone Nargis revealed by multiple satellite observations" *Geophys. Res. Lett.* vol. 36, DOI:10.1029/2009GL037296, 2009.
- 41) Holland G.J., "Tropical Cyclone Motion: Environmental Interaction Plus a Beta Effect", *J. Atmos. Sci.*, vol. 40, pp. 328–342, DOI: [http://dx.org/10.1175/15200469\(1983\)040<0328:TCMEIP>2.0.CO;2](http://dx.org/10.1175/15200469(1983)040<0328:TCMEIP>2.0.CO;2), 1983.
- 42) www.hurricanezone.net/articles/tropicalcycloneformation.html, access time and date: 09 P.M., 20 July 2015.
- 43) <https://books.google.com.bd/books?hl=en=&lr=&id=dQn>, access time and date: 11.00 P.M., 30 July 2015.
- 44) [ww2010.atoms.uiuc.edu/\(Gh\)/guides/mtr/hurr/def.rxml](http://ww2010.atoms.uiuc.edu/(Gh)/guides/mtr/hurr/def.rxml), access time and date: 11.00 P.M., 15 August 2015.
- 45) Irish J. L., Resio D. T. and Ratcliff J. J., "The Influence of Storm Size on Hurricane Surge", *J. Phys. Oceanogr.*, 38 (9), DOI: 10.1175/2008JPO3727.1, 2008.
- 46) Wei W., Jilong C. and Ronghui H, "Water Budgets of Tropical Cyclones: Three Case Studies", *Adv. Atmos. Sci.* vol. 30, pp. 468–484, DOI: 10.1007/s00376-012-2050-7, 2013.
- 47) Wu L., Su H., Fovell R.G., Wang B., Shen J.T, and Kahn B.H.," "Relationship of environmental relative humidity with North Atlantic tropical cyclone intensity and intensification rate" *Geophys. Res. Lett.*, vol. 39, DOI: 10.1029/2012GL053546, 2012.

- 48) Doswell III C.A. and Rasmussen E.N., "The Effect of Neglecting the Virtual Temperature Correction on CAPE Calculations". *Wea. Forecasting* vol. 9, pp. 625–629, DOI: 10.1175/15200434(1994)009<0625: TEONTV>2.0 CO;2, 1994.
- 49) www.clisap.de/the-role-of-convective-available-potential-energy-for-t, access time and date: 10 P.M., 10 October 2015.
- 50) <https://ams.confex.com/ams/31Hurr/webprogram/Paper244618.html>, access time and date: 08 P.M., 20 October 2015.
- 51) Jr F.P.C., "Convective Inhibition as a Predictor of Convection during AVE-SESAME II", *Mon. Wea. Rev.*, vol. 112, pp. 2239–2252. DOI: 10.1175/15200493(1984)112.2.0.CO;2, 1994.
- 52) <https://en.wikipedia.org/wiki/Vorticity>, access time and date: 09 P.M., 20 November 2015.
- 53) https://en.wikipedia.org/wiki/Moisture_advection, access time and date: 09 P.M., 25 November 2015.
- 54) https://en.wikipedia.org/wiki/Relative_humidity, access time and date: 10 P.M., 25 November 2015.
- 55) J.L.Evans, "Sensitivity of Tropical Cyclone Intensity to Sea Surface Temperature" *J Clim.*, vol. 6, pp. 1133-1140, 1993.
- 56) https://en.wikipedia.org/wiki/Convective_available_potential_energy, access time and date: 08 P.M., 01 December 2015.
- 57) Suranjana S., Shrinivas M., Hua-Lu P., Xingren W., and Jiande W., "The NCEP Climate Forecast System Reanalysis", *Bull. Amer. Meteor. Soc.*, vol. 91.8, pp. 1015-1057, 2010.
- 58) www.wmo.int/tcp/TCP21-OP2007, access time and date: 03 P.M., 02 December 2015.
- 59) https://en.wikipedia.org/wiki/2004_North_Indian_Ocean_cyclone_season, access time and date: 03 P.M., 02 December 2015.
- 60) Colby, Jr., Frank P., "Convective Inhibition as a Predictor of Convection during AVE-SESAME II". *Mon. Wea. Rev.* vol. 112 (11), pp. 2239–2252, DOI: 10.1175/1520-0493(1984)112<2239: CIAAPO> 2.0.CO; 2, 1984.
- 61) https://en.wikipedia.org/wiki/Convective_inhibition, access time and date: 06 P.M., 03 December 2015.
- 62) https://en.wikipedia.org/wiki/Geopotential_height, access time and date: 03.30 P.M., 04 December 2015.

- 63) Pick A.C., "Geopotential Heights and Thickness as prediction of Atlantic Tropical Cyclone motion and intensity", *Mon. Wea. Rev.*, vol. 113, pp. 931-939, DOI: [http://dx.doi.org/10.1175/1520-0493\(1985\)113<0931:GHATAP>2.0.CO;2](http://dx.doi.org/10.1175/1520-0493(1985)113<0931:GHATAP>2.0.CO;2) 1985.
- 64) Atkinson G.D. and Holliday C.R., "Tropical Cyclone Minimum Sea Level Pressure/Maximum Sustained Wind Relationship for the Western North Pacific", *Mon. Wea. Rev.*, vol. 105, pp. 421-427, DOI: [http://dx.doi.org/10.1175/15200493\(1977\)105<0421:TCMSLP>2.0.CO;2](http://dx.doi.org/10.1175/15200493(1977)105<0421:TCMSLP>2.0.CO;2), 1977.
- 65) www.bom.gov.au/cyclone/ref=ftr, access time and date: 07 P.M., 04 December 2015.
- 66) https://en.m.wikipedia.org/wiki/Joint_Typhon_Warning_Center, access time and date: 06 P.M., 05 December 2015.
- 67) Saha, S., and Coauthors, "The NCEP Climate Forecast System Reanalysis", *Bull. Amer. Meteor. Soc.*, vol. 91, pp. 1015-1057, DOI: 10.1175/2010BAMS3001.1, 2006.
- 68) Reynolds R.W., "A Real-Time Global Sea Surface Temperature Analysis", *J. Clim.*, vol. 1, pp. 75-87, DOI: 10.1175/1520-0442(1988)001<0075:ARTGSS>2.0.CO;2, 1988.
- 69) http://en.m.wikipedia.org/wiki/2004_North_Indian_Ocean, access time and date: 06 P.M., 09 December 2015.
- 70) Mazumdar A.B., Lele R.R., and Devi S.S., "Cyclones and depressions over the north Indian Ocean during 2006", *IMD*, vol. 58(3), pp.305-322, 2014.
- 71) "Severe Cyclonic storm "NARGIS" over southwest and adjoining southeast and west central Bay of Bengal", *IMD*, 28 November 2008.
- 72) "Tropical Cyclone 01B Warning April 27, 2008 15z". United States Joint Typhoon Warning Center, 27 April 2008
- 73) "Significant Tropical Weather Advisory for the Indian Ocean 2009-05-21 18z", Joint Typhoon Warning Center, 21 May 2009.
- 74) "Severe Cyclonic Storm Laila Advisory 21", *IMD*, 20 May 2010.
- 75) Australiasevereweather.com/cyclones/2001/summ0012.html, access time and date: 09 P.M., 15 June 2015.
- 76) Steph B., "Severe Cyclone Sidr hurtles towards Bangladesh by Steph Ball", *BBC Weather, BBC World*, 15 November 2007.

- 77) "Cyclonic storm "Giri" over east-central Bay of Bengal". IMD, 21 October 2010.
- 78) "JTWC Tropical Cyclone 06B (Thane) Warning 2011-12-27 03z". United States Navy, United States Air Force, Joint Typhoon Warning Center, 27 December 2011.
- 79) <http://en.m.wikipedia.org/wiki/GrADS>, access time and date: 06 P.M., 15 December 2015.
- 80) Akter N., "Mesoscale Convection and Bimodal Cyclogenesis over the Bay of Bengal", Mon. Wea. Rev, vol. 143, pp 34956-3513, 2015.